A Molecular-Level Investigation of the Interactions Between Organofluorine Compounds and Soil Organic Matter Using Nuclear Magnetic Resonance Spectroscopy

by

James Gregory Longstaffe

A thesis submitted in conformity with the requirements
for the degree of Doctor of Philosophy

Graduate Department of Chemistry
University of Toronto

A Molecular-Level Investigation of the Interactions Between Organofluorine Compounds and Soil Organic Matter Using Nuclear Magnetic Resonance Spectroscopy

James Gregory Longstaffe,

Doctor of Philosophy

Graduate Department of Chemistry
University of Toronto

2013

Abstract

In this dissertation, the intermolecular interactions between soil organic matter (SOM) and organofluorine compounds have been studied at the molecular-level using Nuclear Magnetic Resonance (NMR) spectroscopy. NMR probes the local magnetic environment surrounding atomic nuclei, and is uniquely capable as an analytical tool to probe molecular environments in complex disordered materials, such as soils. Several NMR techniques were employed in this work, including Pulse Field Gradient (PFG)-NMR based diffusion measurements, solid-state cross-polarization (CP), saturation transfer difference (STD) spectroscopy, and reverse-heteronuclear saturation transfer difference (RHSTD) spectroscopy. Using organofluorine compounds as molecular probes, xenobiotic interactions with SOM were studied. Using $^1H\{^{19}F\}$ RHSTD, the interaction sites in humic acid for organofluorine compounds were identified by direct molecular-level methods. Protein and lignin were identified as major binding sites, with different preferences exhibited for these sites by dissimilar organofluorine compounds: aromatic organofluorine compounds display varied preference for aromatic humic

acid sites while perfluorooctanoic acid exhibits near total selectivity for protein-derived binding sites. The mechanisms underlying these preferences were probed in the solution state. Using crucial knowledge from the humic acid studies, a detailed molecular-level investigation of xenobiotic interactions in an intact and unmodified whole soil was made possible. A direct and *in situ* elucidation of the components in soil organic matter that interact with small organofluorine xenobiotic molecules has been presented, allowing, for the first time, resolution of multiple interactions occurring for xenobiotics simultaneously at different sites within a whole soil.

ACKNOWLEDGMENTS

TABLE OF CONTENTS

CHAPTER 2

IDENTIFYING COMPONENTS IN DISSOLVED HUMIC ACID THAT BIND ORGANOFLUORINE XENOBIOTICS USING ^{1}H{^{19}F} REVERSE HETERONUCLEAR SATURATION TRANSFER DIFFERENCE NUCLEAR MAGNETIC RESONANCE SPECTROSCOPY

CHAPTER 5

THE PH-DEPENDENCE OF ORGANOFLUORINE BINDING DOMAIN PREFERENCE IN DISSOLVED HUMIC ACID.......... 148

CHAPTER 6

IN SITU MOLECULAR-LEVEL ELUCIDATION OF ORGANOFLUORINE BINDING SITES IN A WHOLE PEAT SOIL 169

CHAPTER 7

SUMMARY AND FUTURE DIRECTIONS

LIST OF TABLES

LIST OF FIGURES

xvii

LIST OF APPENDICES

LIST OF ABBREVIATIONS AND SYMBOLS USED

γ	Magnetogyric Ratio
ω	Larmor frequency
B_0	External magnetic field
CFC	Chlorofluorocarbon
CMP NMR	Comprehensive Multiphase NMR
CP	Cross-Polarization
CPMAS	Cross-Polarization Magic Angle Spinning
CPMG	Carr-Purcell-Mills-Gill
Da	Dalton
DCP	2,4-dichlorophenol
DDT	Dichlorodiphenyltrichloroethane
DMSO	Dimethylsulfoxide
DOM	Dissolved Organic Matter
DOSY	Diffusion Ordered Spectroscopy
DP	Direct-Polarization
DRM	Distributed Reactivity Model
FA	Fulvic Acid
f_{oc}	The mass fraction of organic carbon in a soil or sediment
HA	Humic Acid

HFB	Hexafluorobenzene
HRMAS	High-Resolution Magic Angle Spinning
HSTD	Heteronuclear Saturation Transfer Difference
HSQC	Heteronuclear Single Quantum Correlation
J	Spin
K_{oc}	Organic carbon normalized sorption coefficient
K_{ow}	The octanol-water partitioning coefficient
K_d	The soil / water distribution coefficient
KPFOS	Potassium Perfluorooctane sulfonate
MAS	Magic Angle Spinning
MFA	Monofluoroacetic Acid
NMR	Nuclear Magnetic Resonance
NOE	Nuclear Overhaüser Effect
NOM	Natural Organic Matter
NQR	Nuclear Quadrupolar Resonance
PAH	Polycyclic Aromatic Hydrocarbon
PFA	Pentafluoroaniline
PFCA	Perfluorocarboxylic Acid
PFG	Pulsed Field Gradient
PFOA	Perfluorooctanoic Acid

PFOS	Perfluorooctanesulfonic Acid
PFP	Pentafluorophenol
POPs	Persistent Organic Pollutants
REDOR	Rotational Echo Double Resonance
RHSTD	Reverse Heteronuclear Saturation Transfer Difference
SEDOR	Spin Echo Double Resonance
SOM	Soil Organic Matter
STD	Saturation Transfer Difference
T	Tesla
T_1	Spin-Lattice relaxation
T_2	Spin-Spin relaxation
TCDD	2,3,7,8-Tetrachlorodibenzodioxin
TRAPDOR	Transfer of Populations by Double Resonance
TMS	Tetramethyl Silane
TNT	Trinitrotoluene

PREFACE

This thesis is based on five original manuscripts that have been published, accepted for publication, or have been prepared for publication in peer-reviewed journals. Consequently, some overlap occurs between chapters within this thesis, particularly in chapter introductions. The studies reported here were designed in collaboration between James G. Longstaffe and André J. Simpson. All data was acquired and interpreted by James G. Longstaffe with advice from Andre J. Simpson. All manuscripts were written by James G. Longstaffe, with critical comments provided by André J. Simpson. The contributions of additional authors are described below.

Chapter 2: Identifying Components in Dissolved Humic Acid that Bind Organofluorine Xenobiotics using ^{1}H{^{19}F} Reverse Heteronuclear Saturation Transfer Difference Nuclear Magnetic Resonance Spectroscopy

The material in this chapter is adapted with permission from

> Longstaffe, J. G.; Simpson, M. J.; Maas, W.; Simpson A. J. Identifying components in dissolved humic acid that bind organofluorine contaminants using ^{1}H{^{19}F} Reverse Heteronuclear Saturation Transfer Difference NMR Spectroscopy. *Environ. Sci. Technol.* **2010**, *40 (14),* 5476-5482.

Copyright (2010) American Chemical Society

The content in this chapter is the same as that of the published text with minor rearrangements, in particular the incorporation of material formerly in the supplementary section.

Author Contributions

JGL conducted sample preparation, experimental work, data analysis, interpretation, and preparation the manuscript under the guidance of AJS. MJS assisted in project design and provided access to an NMR spectrometer. WM provided technical support.

Chapter 3: Understanding Solution-State Non-Covalent Interactions Between Xenobiotics and Natural Organic Matter Using $^{19}F/^{1}H$ Heteronuclear Saturation Transfer Difference NMR Spectroscopy

The material in this chapter has adapted with permission from

> Longstaffe, J. G.; Simpson A. J. Understanding solution-state non-covalent interactions between xenobiotics and natural organic matter using $^{19}F/^{1}H$ heteronuclear saturation transfer difference NMR spectroscopy. *Environ. Toxicol. Chem.* **2011**, *30 (8),* 1745-1753.

The content in this chapter is identical to that of the published text with minor rearrangements, in particular the incorporation of material formerly in the supplementary section.

Author Contributions

JGL conducted sample preparation, experimental work, data analysis, and interpretation, and prepared the manuscript under the guidance of AJS.

Chapter 5: The pH-Dependence of Organofluorine Binding Domain Preference in Dissolved Humic Acid

The material in this chapter has been accepted for publication and has been adapted with permission from

> Longstaffe, J. G.; Courtier-Murias, D.; Simpson A. J. The pH dependence of organofluorine binding domain preference in dissolved humic acid. *Chemosphere* **2012**, (In Press)

The content in this chapter is identical to that of the published text.

Author Contributions

JGL conducted sample preparation, experimental work, data analysis, interpretation, and preparation the manuscript under the guidance of AJS. DCM assisted with data analysis, and paper preparation.

Chapter 6: In Situ Molecular-Level Elucidation of Organofluorine Binding Sites in a Whole Peat Soil

The material in this chapter is adapted with permission from

> Longstaffe, J. G.; Courtier-Murias, D.; Soong, R.; Simpson, M. J.; Maas, W. E.; Fey, M.; Hutchins, H.; Krishnamurthy, S.; Struppe, J.; Alee, M.; Kumar, R.; Monette, M.; Stronks, H. J.; Simpson A. J. In situ molecular-level elucidation of binding sites in a whole peat soil. *Environ. Sci. Technol.* **2012**, *46* (19), 10508-10513.

Copyright (2012) American Chemical Society.

The content in this chapter is the same as that of the published text.

Author Contributions

JGL designed the project, conducted sample preparation, experimental work, data analysis, interpretation, and preparation the manuscript under the guidance of AJS. DC-M assisted in project design, data analysis, and paper preparation. MJS assisted with manuscript preparation. RS provided general technical assistance. WEM, MF, HH, SK, JS, RK, MM, and HJS provided technical assistance with the CMP probe.

CHAPTER 1
INTRODUCTION

1.1 Introduction

The presence of anthropogenic organic pollutants in soils and sediments has long been known to correlate with the presence of naturally occurring organic matter in those systems *(1-3)*. This has lead to the development of many powerful environmental models used to predict contaminant fate and transport in the environment as a whole based on a simple chromatographic analogy in which this organic material acts as a general hydrophobic partitioning medium *(4-6)*. Implicit in this analogy, however, is the macroscopic assumption of chemical and physical homogeneity. While this simplification may be well suited for many studies of environmental fate at global and regional scales where micro- and molecular-scale variability is neither easy to deal with, nor is it necessary given the considerable size of environmental systems *(1)*, the reduction of natural organic matter (NOM) to a simple homogeneous hydrophobic domain fails to account for, or explain, numerous molecular-scale phenomena, such as sequestration or bioaccessibility *(7-9)*. Mechanistic understandings of these phenomena are vital to fully understanding the fate of contamination in the environment and will require, by necessity, consideration of the role the heterogeneous nature of soils plays *(1, 10)*. At the core of these phenomena are the intermolecular interactions between these foreign, anthropogenic compounds, and the different components of soils and sediments, including NOM *(11, 12)*. This dissertation is aimed at probing the nature of these interactions with the intent to assist in the development of a molecular-level understanding of the intermolecular interactions between small organic pollutants, or xenobiotics, and complex environmental matrices, such as NOM. Given their unwelcome and foreign nature in soils, organic pollutant molecules will be referred to as xenobiotics throughout this dissertation, intentionally drawing analogy to the study of contaminant interactions inside biological organisms.

This dissertation explores soil contamination chemistry using a powerful atomic-level analytical probe: nuclear magnetic resonance (NMR) spectroscopy. This is done by employing organofluorine compounds as probes for potential intermolecular interactions by using magnetic

properties of the fluorine-19 nuclei present in these compounds. This work covers a diverse area of research, and as such several different areas of study are combined, each of which will require some introductory coverage. This introductory chapter is thus divided into sections dealing with: the environmental chemistry of soil contamination; the structure of NOM, with emphasis on the natural organic matter found specifically in soils, or soil organic matter (SOM); fluorine in the environment; and nuclear magnetic resonance spectroscopy. At the end of the chapter is a final section reviewing previous NMR studies of NOM-xenobiotic interactions.

1.2   Introduction to the Environmental Chemistry of Soil Contamination

1.2.1 Xenobiotic Contamination of Soils

The release of xenobiotics into the environment is inevitable given current industrial practices and the modern consumer lifestyle. The controlled application of pesticides to agricultural land, for example, represents an intentional release of xenobiotics. This application is widely viewed as necessary to maintain the global food supply as it is estimated that 30% of global food crops are lost each year due to weather, pests, and diseases. In the absence of modern agrochemicals, this loss is predicted to nearly double *(13)*. Nevertheless, the implications of continued introduction of xenobiotic contamination into the environment, whether accidental or intentional, depend on a variety of factors that include not only the toxicology of the compounds themselves *(14)*, but also the processes through which these influences are attenuated by the environment, such as the rates of biodegradation, dispersion, dilution, volatilization, sorption, stabilization, and destruction *(15, 16)*.

Of particular environmental concern are those xenobiotic molecules that do not readily degrade and instead persist long after their initial introduction *(17)*. Such compounds are termed Persistent Organic Pollutants (POPs) and, when identified by environmental chemists, are usually subjected to strong bureaucratic controls or bans, such as the internationally ratified Stockholm Convention on POPs *(18)*. Most recognized POPs can be divided into two categories: organochlorine compounds and polycyclic aromatic hydrocarbons (PAHs). Polyfluorinated organic compounds are an emerging class POPs *(19)* and polybrominated compounds are suspected to exhibit persistent behaviour *(20)*. Due to their persistent nature,

many of these compounds are present in the environment long after their use has been restricted or stopped *(18)*. Interactions with soil are found to play a very significant role in the persistence of many compounds that would otherwise readily degrade *(7, 21)*, however the connection between the mere presence of potentially harmful compounds and actual environmental risk is not simple *(22, 23)*.

For a compound to exhibit harmful effects in the environment, an organism must be exposed to the contaminant, usually by consuming it, and then the contaminant must be able to interfere with the proper functioning of that organism *(24)*. According to Semple *et al. (24)*, in order for an organism to be exposed, a xenobiotic molecule must be accessible to it at some point in space and time (bioaccessible), and then this molecule must also be available to pass into the organism across a cell membrane (bioavailable). It is found that many contaminants sorbed strongly onto soil particles are not bioaccessible, and thus not bioavailable *(24)*, and as such, it has been argued that risk assessments based solely on absolute quantification of xenobiotics are flawed *(23)*. Such assessments can result in an overestimation of the environmental impact of contamination that can lead to economically costly and even environmental destructive site remediation practices that aim for removal of the contaminant far beyond the level where an actual problem exists *(14, 22, 23)*.

In general, the sorption of many organic contaminants by soils and sediments results in two marked changes in the fate of these xenobiotic molecules: a significant increase in the life-time of the contamination, which enhances a preexisting tendency towards a persistence for many compounds, organohalides in particular; but also in a reduction in the apparent ecotoxicity due to reduced bioaccessibility *(24-30)*. For example, a soil contaminated with DDT[1] and Dieldrin[2]

---

[1] DDT - *1,1,1-dichloro-2,2-di(4-chlorophenyl)ethane*, was a popular insecticide until the 1970's, when it was banned in much of the western world after negative effects of its over application were brought to public attention in Rachel Carson's seminal treatise *Silent Spring (31)*, helping to found the modern environmental movement which oversaw the founding of government organizations such as the Environmental Protection Agency in the United States *(32)*. It is still used under WHO restrictions for its powerful mosquito-killing properties, which are key to fighting malaria in tropical and subtropical environments. Its soil half-life can range from 22 days to 30 years. DDT has been linked to diabetes, developmental problems, neurological problems such as Parkinson's diseases, and is a suspected carcinogen *(33)*.

[2] Dieldrin - *(1aR,2R,2aS,3S,6R,6aR,7S,7aS)-3,4,5,6,9,9-hexachloro-1a,2,2a,3,6,6a,7,7a-octahydro-2,7:3,6-dimethanonaphtho[2,3-b]oxirene*, was popular as an insecticide to kill soil pests, such as termites, until the 1970's. Its use is now prohibited on agricultural lands throughout most of the world *(34)*.

was found to exhibit reduced toxicity over time such that after 120 days, the contaminated soil exhibited no toxic properties at all to fruit flies or cockroaches *(26)*. After 270 days the same soil was also no longer toxic to houseflies. This reduction in toxicity occurred even though the soil concentrations of these compounds were relatively constant with time because no natural degradation processes for DDT or Dieldrin occurred; at the end of the experiment nearly all of those compounds could be quantitatively recovered after a vigorous extraction *(26)*. Similar observations have also been reported for rats, which were fed either soil or grain contaminated with TCDD[3] *(35)* and PCBs[4] *(36)*. Both contaminants showed significantly reduced toxicity to the rats when consumed in their soil-bound states, but not when consumed in their grain-bound states indicating reduced bioaccessibility for the soil-bound form. Nevertheless, grazing animals did not exhibit the same effects as rats *(37)*, indicating that biology is important when considering the accessibility of soil-bound contaminants. In general, the full ecological impact of contamination extends beyond the specific toxicity to any given organisms *(38, 39)*. For instance, the production of new biomass can be inhibited by the presence of preexisting contamination as has been observed in soils containing bound residues of metsulfuron-methyl[5] *(39)*. Reduced biomass has a significant impact on the health of the soil by reducing the amount of SOM found in a soil profile *(40)* and has a negative impact on the fertility of a soil due to the role SOM has in nutrient and water retention *(41)*.

The apparent toxicity of a compound typically decreases with time; the longer a contaminated soil ages, the less accessible those xenobiotic molecules often become. The disappearance of ecotoxicity correlates well to the amount and quality of SOM present in the soil *(7)*. This is attributed to the formation of a recalcitrant fraction in which, over time, the xenobiotic molecules become permanently encapsulated in a matrix of organic matter *(45-48)*. The formation of this recalcitrant fraction is thought to be the source of both the increased persistence and the

---

[3] TCDD - 2,3,7,8-Tetrachlorodibenzo-p-dioxin, is a contaminant found in many herbicides, including Agent Orange. It is a potent promoter of cancer caused by other compounds, but does not itself cause cancer. It is most often referred to only as dioxin, although this is not strictly accurate *(42)*.

[4] PCBs – Polychlorinated biphenyls, are used in the production of plastics and electronics but have been banned in much of the world due to their environmental persistence and modes of toxicity that resemble that of dioxins *(43)*.

[5] Metsulfuron-methyl - *2-[[[(4-methoxy-6-methyl-1,3,5-triazin-2-yl)amino]-oxomethyl]sulfamoyl]benzoic acid methyl ester*, is a herbicide designed to kill broadleaf weeds and annual grasses by inhibiting cell division in shoots and roots *(44)*.

reduction in apparent ecotoxicity, as recalcitrant xenobiotics are found to be not only inaccessible for biotic degradation, but are also protected from simple chemical extractions. Understandably, the relationship between aging and ecotoxicity is a topic of much current research in environmental science *(7, 17, 21-23)*. In addition, the formation of a recalcitrant fraction can make the remediation of contaminated soils potentially very difficult *(49)*. At the heart of the sequestration of xenobiotics in soils are the interactions between these compounds and the soil matrices where they reside. Before these interactions can be discussed, however, the structure and nature of soil, in particular the structure of SOM, must first be explored.

1.2.2 The Chemical Composition of Soil

1.2.2.1   Inorganic Components of Soil

For most soils, the primary non-living constituents are inorganic in nature. The inorganic components of soil can be divided into two classes: primary and secondary soil minerals. Primary minerals resemble those of the parent bedrock and exist in soils as sand and silt. Secondary minerals include clays and amorphous oxides, which while derived from the parent rock, have been changed substantially by weathering. Most clays found in soils are layered aluminosilicates and play a key role in the structural integrity of the soil as a whole by slowing the loss of cations, organic material, and water. Clays typically have negatively charged surfaces and are important in the adsorption of positively charged species, particularly metal ions *(50)*.

1.2.2.2   Organic Matter in Soil

Soil organic matter is vital for soil health as it plays important roles in moisture and nutrient retention, and its viability to support most ecosystems *(50)*. This organic matter is concentrated in the uppermost soil horizon, close to the vegetation from which it is derived. SOM is formed from the remains of plant and microbial biopolymers *(2, 51)*. Traditionally, SOM has been divided into two classes of compounds: identifiable biomolecules that have not yet been fully degraded, and humus, which is the degraded fraction of SOM after biotic and abiotic action *(2, 52)*. Humus is then further separated into three distinct classes of compounds based on their

aqueous solubility at different pH values; fulvic acids are compounds soluble at all pH's, humic acids are compounds soluble only at pHs above 2, and humin is insoluble *(2)*. Separation of these classes of material from each other was once viewed as a separation of three distinct classes of compounds, formed through supposed humification processes thought to involve enzymatic couplings and Maillard-type reactions[6] that recombine degraded biopolymers into new macromolecular forms *(52, 53)*. There is little evidence for either the occurrence of these complex humification processes, or for the existence of distinct humic substances as anything more than an operational definition based on differences in aqueous solubilities *(2)*. The modern view of humic substances is more stochastic yet much simpler in form *(51, 54, 55)*, characterizing the whole of SOM as the degraded and partially degraded remnants of former biological materials including biopolymers from plants, including lignin[7] *(56)*, polysaccharides *(59)*, and natural waxes *(60)*, as well as polypeptides primarily from dead and dormant microbes *(61-64)*, with no evidence for the occurrence of distinct 'humic substances' *(51)*.

NMR spectroscopy, which will be discussed in more detail later in this chapter, has been key in developing the modern view of the structure and constitution of humic substances and SOM in general *(65)*. Measurements of the translational motion of dissolved humic substances in solution using diffusion ordered NMR spectroscopy (DOSY) have been used to demonstrate that the constituents of a humic extracts are held together as supramolecular assemblages by weak dispersive and electrostatic forces *(66, 67)*, rather than the covalent linkages assumed in the old view of humic substances. It is this supramolecular nature of SOM extracts that has led to much of the difficulty and confusion in understanding the size, and thus the implied macromolecular nature of these structures *(68-70)*. It is now understood that humic extracts are simply mixtures of smaller molecules *(54, 59, 71)*, and only appear as compounds with excessively large molecular weight molecules due to these intermolecular assemblages. In concentrated solutions of humic acid, where aggregation between constituents results in larger assemblages, large apparent molecular weights have been reported based on self-diffusion measurements *(54, 59)*, while at low concentrations using disaggregating agents it has been shown that the basic

---

[6] Mallaird reactions involve the covalent coupling of amino acids and sugars *(57)*.

[7] Lignin is a biopolymer composed of phenolic and methoxy functionalized aromatic rings joined through ether linkages, and is produced primarily by woody plants *(58)*.

components of humic and fulvic acids, such as alcohols, amino acids, sugars, and lipids, do exist free of each other, and coexist along side some larger biopolymers such as protein/peptides, and carbohydrates, and lignin *(54)*.

The constitution of SOM depends on the types of biological material responsible for its production and the rates of degradation of those materials *(35)*. Figure 1.1 shows the solution-state ^{1}H NMR spectrum of the Pahokee Peat standard humic acid. In the NMR spectrum, every ^{1}H nucleus with a different local chemical environment will give rise to a unique resonance. Due to the complex composition of humic acid, the multitude of different compounds present results in significant convolution hindering identification of each individual resonances directly from the 1D ^{1}H spectrum.

Multi-dimensional NMR spectroscopy helps to reduce the spectral complexity by sorting the ^{1}H resonance from similar structures based on covalent connectivity between ^{1}H and/or ^{13}C nuclei *(51, 55, 56, 59, 63, 72, 73)*. Comparing the 2D NMR patterns to those of representative biopolymers has been useful in demonstrating that these signals arise from structures essentially identical to degraded biopolymers, such as lignin, and polysaccharides *(51)*. Whole, or slightly degraded protein of microbial origin has also been confirmed as a major component of SOM by comparing the ^{1}H NMR profile of plants, microbes, and humic acid *(62)*. It is thought that this protein originates from dead or dormant soil microbes, and is released into solution under the harsh conditions of the extraction. In the unaltered soil, this material may remain encapsulated, either by the intact cell walls *(62, 63)*, or other hydrophobic domains *(61)*. A significant microbial contribution to SOM has also been shown in the form of remnant cell-wall material *(56)*.
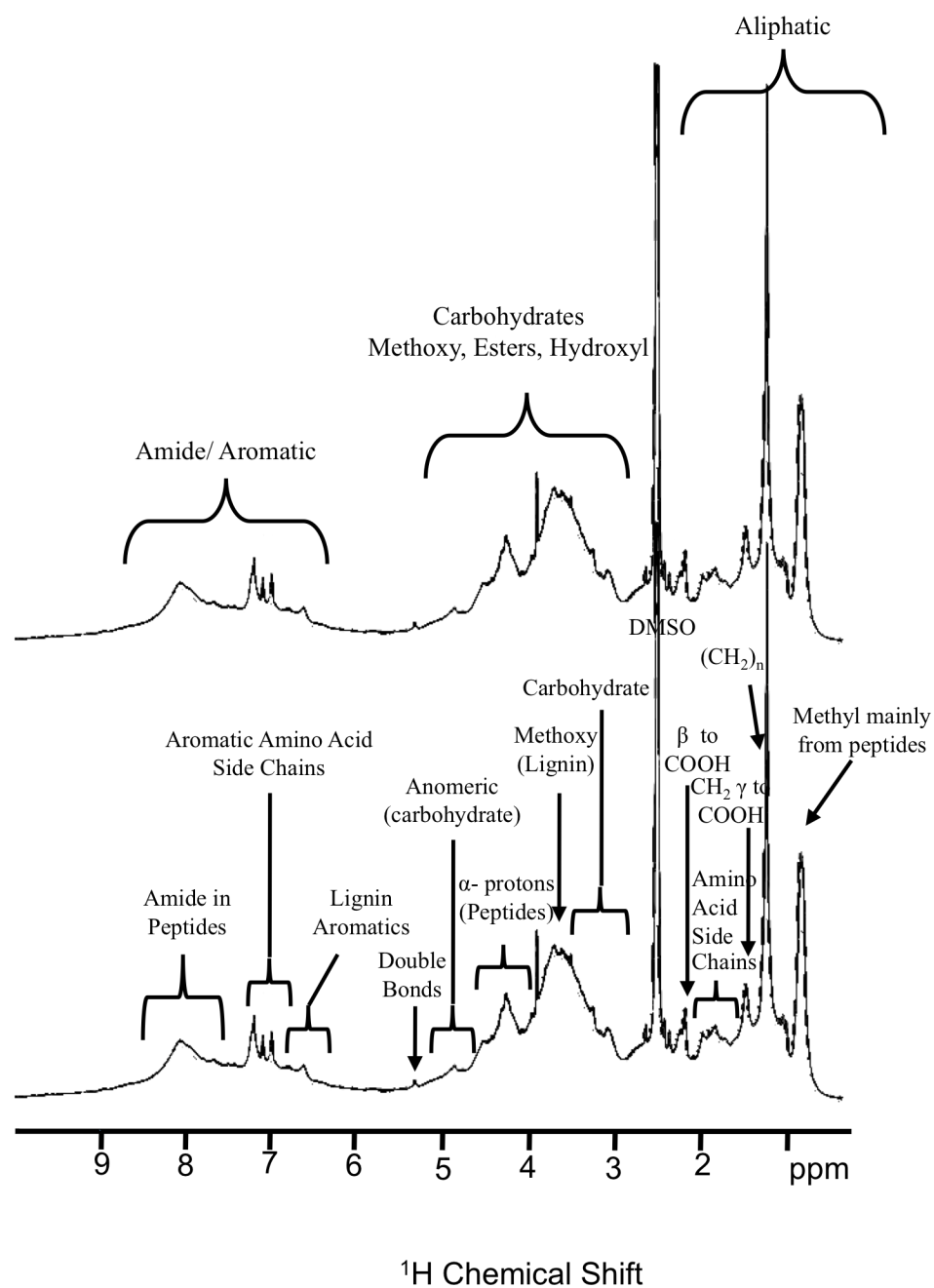
Figure 1.1   1D ^{1}H spectra of the alkali extract of a grasslands soil dissolved in DMSO-d$_6$. On top is the spectrum with the general regions labeled. On bottom is the spectrum with detailed assignments. Modified from reference *(65)*.

For the insoluble fraction of SOM, solid-state NMR experiments based on ^{13}C detection have been very useful for identifying chemical structures *(63)*. ^{1}H$\rightarrow^{13}$C Cross-polarization (CP) and Direct Polarization (DP) under magic angle spinning (MAS) conditions, which are discussed in more detail later in this chapter, have been very useful in verifying the presence of lignin-like structures by explicitly identifying aromatic O-CH$_3$ structures *(56)*. Crystalline and amorphous polymethylene chains have also been identified in whole soils using solid-state NMR as major aliphatic components *(60)*. One significant issue in characterizing the organic matter in whole soils is the presence of ferromagnetic minerals, which generate damaging electric currents inside the high magnetic fields required for NMR spectrometer *(74)*. Furthermore, chelated paramagnetic metals within the organic matter itself strongly couple with the ^{13}C nuclei under observation resulting in broadening of some resonances to the point that they are practically unobservable. In many soils, treatment with hydrofluoric acid and chelating agents is required to remove these metal centres *(75)*. While this does improve quantization by eliminating paramagnetic broadening *(76)*, this process potentially alters the structure of many soil components *(75)*.

1.2.3 Sorption of Xenobiotics into Soils

The implications of soil contamination, such as ecotoxicity and persistence as discussed previously in section 1.2.1, depends intimately upon the associations those xenobiotic compounds form with the environmental matrices in the soil. The molecular theory of the sorption of organic compounds to soils and sediments was largely ignored, or assumed to be simple for much of the 20th century until the early 80's when a period of significant evolution occurred in the field *(7, 22, 24)*. This evolution continues today, as researchers continue to seek evidential support for proposed theories and mechanisms *(77)*. As with any scientific topic that suddenly bursts out of deceivingly simple phenomena, the number of questions and hypotheses in the newly expanded theoretical framework of organic sorption in soil are innumerable. It is here that the new work reported in this dissertation is rooted. In the following sections the evolution of thought on the sorption of organic compounds into soils is discussed, starting with

the simple chromatographic analogy based on structural homogeneity and ending with the modern reductionist approach that looks at the implications of molecular-scale heterogeneity on intermolecular interactions in soils and sediment.

1.2.3.1   *Soil as a Partitioning Medium*

The most commonly used approach to understand xenobiotic interactions with soils and sediments in based on measurements of a soil or sediment's ability to sorb small hydrophobic compounds *(3)*. This approach was developed as an analogy to partitioning chromatography in which soil assumes the role of a stationary phase with water as the mobile phase *(4, 6)*. Measurements of the equilibrium sorbate distribution between soil and water, K_d, provides a simple approach with which to model and predict the fate of organic compounds in aqueous soil environments *(5, 6)*. The chromatographic model assumes reversible two-phase partitioning in which the soil provides a general hydrophobic partitioning domain. Nevertheless, due to the complex and heterogeneous nature of soils and sediments, as discussed previously in section 1.2, the chromatographic approach is meant only as a simple analogy to understand soil sorption at a macroscopic level *(4)*.

For a dissolved organic compound in an aqueous-soil/sediment environment, the distribution between the aqueous and solid domains, K_d, is directly related to the fraction of organic carbon present, f_{oc} *(3)*. This relationship is used to produce in a more versatile distribution coefficient, K_{oc}, normalized to account for the organic carbon fraction and is defined as

$$K_{oc} = K_d \,/\, f_{oc}. \qquad\qquad [1.1]$$

In general, K_{oc} is an experimentally derived factor and can vary depending upon the type of soil. Borrowing from studies of accumulation and biomagnification in which lipids are a dominant partitioning domain, a general predictor for the extent of partitioning into soils or sediments is often used that similarly reduces the organic matter in soils and sediments to a simple uniform hydrophobic substance, most often octanol *(78)*. The octanol–water partitioning coefficient, K_{OW}, is found to be similar to the experimental K_{oc}, typically within a factor of 2 for most nonionic organic compounds *(3)*. Assuming that the equilibrium distribution between the soil

and the aqueous environment is controlled by a simple hydrophobic-based partitioning mechanism, the relationship between K_{oc} and the contaminant concentrations should be linear. At a first approximation this appears to be true *(6)*, however, after further study it became clear that many of the observations supporting linear sorption isotherms were based on equilibrium times that were too short *(3)*, and that extended periods, from days to weeks, are actually required to reach true equilibrium *(8)*. Using these longer periods for equilibration reveals that the sorption of organic compounds into soils may be non-linear, and thus cannot be fully understood as a simple 2-phase partitioning process *(8, 79, 80)*. Further non-ideal sorption behaviours exhibited by soils and sediments not accounted for by pure hydrophobic partitioning have also been observed, including hysteresis *(8)*, competitive binding indicating specific interaction sites *(81, 82)*, and, irreversible binding, which is responsible for the prolonged environmental persistence of numerous compounds *(25, 26)*.

Three standard models are typically used to fit sorption data: partitioning (linear), Langmuir, and Freundlich *(50)*. The partitioning approach, which was described above, assumes a linear relationship between the amount of a compound that is introduced into the system and the amount of that compound that is found in the sorption medium at equilibrium. The Langmuir isotherm assumes that only a finite number of interactions with the sorbent are possible, and that each of these interactions are of equal energy producing a distinctive L-shaped relationship between the initial and equilibrium sorbate concentrations. The Freundlich isotherm differs from the other two models in that it presents an empirical rather than mechanistic analysis of sorption behaviour *(50)*. Mathematically it is similar in form to the linear partitioning isotherms with a built in non-linearity factor to allow for the analysis of sorption behaviour due to multiple simultaneously occurring mechanisms and are useful when a combination of linear and Langmuir-like behaviour is present. The determinations of sorption mechanisms based on the Freundlich isotherm are speculative, however, and should be approached with caution *(50)*.

Analysis of non-linear soil and sediment sorption isotherms using the Freundlich isotherm suggests that at least two distinct sorption processes occur in soils and sediments: one rapid and one slow *(8, 79)*. The underlying mechanism behind the rapid mode of sorption is thought to be similar to a simple partitioning process, thus accounting for the apparent linearity observed in short-term studies *(8)*. The slow mode of sorption is thought to be related to the ability of the

sorbate to diffuse within the soil, and is thus limited by a number of factors, including the composition, density, and porosity of the soil, in addition to properties of the compound itself *(83)*. Mechanisms unrelated to SOM have also been proposed as origins for the apparent non-linear sorption observed in soils, including specific adsorption to mineral surfaces *(10, 84, 85)* or black carbon *(86-88)*. Nevertheless, SOM is itself chemically and physically heterogeneous and the various components found in soil themselves exhibit different sorption behaviour for small xenobiotic compounds *(89, 90)*. As such, the K_{oc} for the same compound in different soils can vary depending upon the composition of the SOM present *(89-91)*. The variation in SOM composition has traditionally been described using factors such as the proportion of aromatic to non aromatic functionality *(91, 92)*, or to the average polarity of the organic matter present based on the amount of oxygen, nitrogen, or aliphatic carbon present *(90, 93)*. In addition to the variability of sorption between different soils, variation is also observed for the same soil under different natural conditions, such as water saturation. This effect has been attributed to the fact that while SOM is a key factor in sorption, in low organic soils minerals may also be involved and at high water concentrations water molecules themselves may outcompete organic molecules for adsorption at mineral surfaces *(84)*. In general, it is often found that simple molecular properties such as K_{OW} or molecular size, which are good predictors for simple hydrophobic-based partitioning, are not necessarily the best predictors for sorption into soils and sediments *(94)*.

Perhaps the first comprehensive model to account for the microscopically heterogeneous nature of soil during the sorption of xenobiotics is the Distributed Reactivity Model (DRM) of Weber Jr. *(11, 85, 96, 97)*. This model suggests that particle-scale heterogeneity, combined with distributed reactivity amongst different components of a soil particle can significantly affect the sorption of contaminants *(11, 12)*. In the DRM, sorption occurs simultaneously at different sites in a soil, and these sites, which may act using different mechanisms, provide a distribution of sorption affinities thus introducing the observed non-linearity. Deconvolution of these competing mechanisms is difficult in practice. Nevertheless, in general it is assumed that there is at least one linear-like mode and one Langmuir-like mode of sorption, with the overall isotherm of the soil exhibiting qualities of both.

1.2.3.2   The Rubbery-Glassy Polymer Model

The degree of non-linearity observed in the sorption isotherms of soils and sediments increases as the concentration of sorbate decreases *(98)*. This has been attributed to stronger sorbate-sorbent interactions at a small number of sites *(85)* that have been suggested to be due to specific, rather than general, interactions *(59)*. The existence of specific interactions is also supported by the observation of competition between hydrophobic compounds for those sites *(81)*. In the distributed reactivity model these specific sites are largely assumed to be at mineral surfaces or black carbon. Pignatello *et al. (99)* argue that most of the available inorganic adsorption sites are likely already occupied by preexisting naturally occurring organic compounds and thus do not contribute much to sorption in soils with moderate levels of organic matter, which are the soils observed to exhibit the highest sorption capacity. Furthermore, non-linear sorption isotherms do not necessarily mean that interactions with specific or preferred sites are occurring, and physically restricted sorption sites, such as that found in porous media, can also produce non-linearity *(86)*. In an effort to provide a cogent mechanism for the non-linearity of soil isotherms that involves only SOM, Pignatello and co-workers, introduced a dual-mode model for sorption based on differences in the physical accessibility of sorption sites in hypothetically dissimilar domains of SOM *(9, 81, 100, 101)*. In this model, the authors develop an analogy between SOM and a mixture of rubbery (i.e. flexible), and glassy (i.e. rigid) polymers. The argument behind this model is that rubbery polymers permit unrestricted and unlimited access to diffusing sorbate molecules, thus producing linear, reversible isotherms. Glassy polymers, conversely, restrict access to a limited number of internal holes thus introducing a Langmuir-like non-ideal quality to the observed sorption isotherms in soils.

In addition to providing a mechanism for non-linear sorption isotherms, the rubbery-glassy model also accounts for several other phenomenological deviations from ideal sorption. The requirement for longer equilibration times to observe the non-linear behaviour is due to the kinetic restrictions on access to the Langmuir-like sites in the glassy material meaning that equilibrium here takes longer to reach than for the partitioning-like processes in the rubbery-material. This process can also account for the increased sequestration typically observed upon aging that has ramifications on ecotoxicity and remediation. Similarly, competitive sorption of hydrophobic compounds is accounted for in the rubbery-glassy model by properties of glassy

polymers. These rigid organic networks contain a finite number of structural holes of various dimensions. It is thermodynamically favorable for a hydrophobic compound with the correct size and shape to occupy those holes, however due to the kinetically-restricted access to those sites it takes time and energy for a small molecule to reach them. Once in place it is even more difficult to for that compound to be extricated from this energetically favorable position *(9)*. Structurally dissimilar sorbate molecules will prefer holes with different spatial dimensions and thus will not compete for these sites while structurally similar sorbate molecules must share the same pool of limited sorption sites *(81)*. The hole-filling model is difficult to prove or disprove, however *(102)*, and the presence of carbonaceous materials in soils, such as black carbon, could also be the origin of non-linear sorption due to their microporous nature *(86-88, 103, 104)*. Nevertheless, it has been shown that the occurrence of non-linearity is practically unaffected by the removal of these mineral phases *(9, 101)*.

While the rubbery-glassy model explains much with respect to sorption phenomenon in soils, it does not consider the chemically heterogeneous nature of SOM focusing instead only on physical heterogeneity *(96)*. Furthermore, because it focuses purely on physical attributes of SOM, the rubbery-glassy model has trouble explaining interactions with dissolved forms of NOM that exhibit similar non-linear binding isotherms to those observed in whole soils *(105, 106)*. It is unlikely that fully dissolved organic matter, which forms hydrophilic supramolecular colloids in aqueous solution *(66)*, would contain the proposed rigid polymer network required by the model to produce non-linear sorption. Nevertheless, while only an analogy, the successes of both the DRM and the rubbery-glassy model in describing many sorption phenomena strongly support the notion that the observed sorption non-linearity results from the simultaneous occurrence of several different types of interactions, at several different types of sites *(96)*.

1.2.4 The Molecular-Level, or Reductionist Approach to Sorption in Soil

In adapting the glassy-rubbery model from a pure polymer-based analogy to real SOM the rubbery phase can be more generally described as loosely ordered organic material, while the glassy phase is tightly packed, or condensed organic matter *(107)*. In general, the loosely ordered domain is rich in aliphatic compounds, such as lipids, while the condensed domain is

rich in aromatic functionality *(95, 104)*. There has been much debate in the literature over whether the role of sorption by aromatic components of SOM *(82, 108)* is more important for sorption than aliphatic components *(104, 109-111)*. Structural changes to SOM, such as the formation of either open or closed conformations affects the rates of sorption *(112)*, and the strengths of the interactions, regardless of the type of organic matter present *(113)*. It is clear, however, that both aromatic and aliphatic components are important, likely contributing to different sorption mechanisms at different sites *(114, 115)*. In addition, not only do aliphatic and aromatic sites potentially act differently in general, but sites with similar base chemical structures do not necessarily act similarly *(116, 117)*.

Conclusions made about the various roles of different constituents of SOM to sorption are based largely on correlations made between the composition of SOM and observations made at the macroscopic–level. A reductionist, or molecular-level approach is needed to fully elucidate chemical processes behind different sorption processes. This will help in clarifying the exact role different components of soil and SOM may play in the sorption of organic contaminants. Investigations into the molecular-level processes behind xenobiotic interactions with SOM are emerging as an important facet in building the understanding of xenobiotic fate in the environment *(77)*. Nevertheless, the chemical complexity inherent in soil makes studying intermolecular-interactions at the molecular-level difficult, and simplified model systems based on the different fractions of soil are often studied as proxies for a whole soil instead. Simplified fractions employed include soluble fractions, such as humic and fulvic acid *(118-120)*, and insoluble constituents such as condensed forms of organic carbon such as char and coals *(121, 122)* or inorganic materials such as clay minerals *(123)*.

Dissolved forms of SOM are particularly well suited to probing the chemical nature of the weak interactions between SOM and xenobiotics because many of the physical attributes that affect contaminant interactions, such as restricted spaces and diffusion through rigid lattices, are absent allowing researchers to focus on the chemical origins of the interactions rather than the physical. Furthermore, in addition to its role in soils and sediments, it is found that naturally dissolved organic matter in the environment itself has a significant effect on the sorption and desorption of contaminants *(119, 120, 123-125)*. Dissolved forms of NOM can increase the solubility of otherwise hydrophobic compounds by as much as eight times *(120)*. Furthermore, it has been

shown that the interactions with dissolved organic matter involve several mechanisms, with both strongly and weakly bound fractions occurring *(119)*.

While there is evidence for the formation of covalently bound xenobiotics when reactive functional groups are present *(126, 127)*, most interactions of xenobiotics with SOM are found to be non-covalent in nature *(77, 128)*, and thus should, in theory, be reversible. In addition to general dispersion interactions, site-specific interactions between xenobiotic molecules and SOM have been proposed based on electrostatics, including dipole-dipole interactions with polar compounds *(129)*, and π-π interactions for aromatic compounds where specific aromatic components of SOM act as a π-electron acceptor with the xenobiotic as a π-electron donor *(118, 130, 131)*. Both simple electrostatic-based quadrupole interactions and charge transfer mechanisms have been proposed for these suggested π-π interactions. For highly polar and charged compounds a connection has been noted between the cation exchange capacity of a soil and sequestration *(132)*, supporting the existence of specific interactions. Others, however, have argued against true specific interactions, suggesting that compound specific factors, such as polarizability, or hydrogen-bond potential can control the strength of the interactions without requiring a specific type of site on SOM for the interaction to occur at *(133)*. Many of these studies proposing specific interactions, nevertheless, are based on correlation to macroscopic measurements and it is difficult to verify their occurrence without some direct means to observe the interactions between xenobiotics and various soil constituents.

The analytical desire for molecular-level probes of xenobiotic interactions in SOM, and NOM in general, forms the heart of this dissertation. There is an emerging literature on this subject, much of it based on observations made using nuclear magnetic resonance spectroscopy, which is perhaps unmatched as an analytical tool for studying the structure of chemical systems at the molecular-level. In this dissertation organofluorine compounds are used in conjunction with NMR spectroscopy to probe molecular-level interactions in NOM. Fluorine-19 is a very sensitive NMR nucleus, and provides a powerful tool to probe inside the local environment around fluorine containing xenobiotics inside NOM. In order that much of the current literature on xenobiotic interactions, and the new work presented in this dissertation be fully discussed, an introduction to both NMR spectroscopy and organofluorine chemistry is helpful. Organofluorine chemistry is discussed in the next section, after which a discussion of NMR is presented.

1.3   Fluorine in the Environment

Organofluorine compounds are of interest to environmental chemists for several reasons. The most obvious is the unique and unusual environmental properties of the compounds themselves that arise from the strong electronegativity of fluorine that makes the carbon-fluorine bond amongst the hardest to break in organic chemistry. Another cause for interest in organofluorine compounds by environmental chemists, as is the case in this dissertation, is for the special physical properties of fluorine itself that allows for the use of fluorine as a powerful probe of the mechanisms behind chemical processes occurring within otherwise opaque environmental matrices. This short section will expand on both of these two points and begin drawing together the two main facets of this dissertation as a whole – the contamination of the environment by xenobiotics, and the development of novel molecular-level analytical approaches to probe the relationships and interactions between xenobiotics and the environment.

1.3.1   Inorganic Fluorine

Nearly all naturally occurring fluorine is inorganic *(134)*. Fluoride, F^-, is highly soluble and is easily taken up by plants and animals, however it is rarely metabolized *(135)*. In animals, F^- readily exchanges with hydroxyl in bones and teeth, stimulating new bone growth that results in painful outgrowths and brittle, mottled teeth *(136)*. Habitually ingested concentrations as low as 2 to 4 mg L^{-1} of F^- in water interfere with can calcium metabolism and lead to fluorosis in individuals with diets that are already low in calcium *(134)*. Naturally high fluoride concentrations are typically found in arid regions with acidic soils. The presence of calcium in soils ameliorates the negative effects of high fluorine by forming CaF_2 precipitates. Anthropogenic sources of inorganic fluoride arise primarily from mining *(137)* and fertilizer pollution *(138, 139)*. The presence of fluorapatite, $Ca_5(PO_4)_3F$, in fertilizers, for example, has been known to causes fluorosis in grazing livestock when this fertilizer has been applied to their pastures *(138, 139)*.

1.3.2 Natural Organofluorine

While rare, naturally occurring organofluorine compounds are not unknown *(135, 140)*. There are approximately 30 known naturally occurring organofluorine compounds, compared to 2150 natural organochlorine and 1850 natural organobromine compounds *(135)*. Some of these organofluorine compounds are produced abiotically, principally from reactions between volcanogenic HF and hydrocarbons *(141)* and are released immediately into the atmosphere. Nevertheless, the release of organofluorine compounds when volcanic rocks are disturbed during mining activity indicates that they may also be stored after their production *(142)*. Abiotically produced compounds are typically small chlorofluorocarbons (CFCs), however fluorobenzenes have also been detected *(135)*. In general, the contribution of CFCs from these natural sources is negligible compared to anthropogenic emissions *(141, 142)*. Although rare, some specialized plants are able to metabolize fluoride to produce organofluorine compounds, such as monofluoroacetic acid (MFA), at high concentrations *(135)*. MFA is one of the most toxic natural compounds known and its presence in plants in South Africa and Australia has been responsible for the death of cattle and other livestock *(143)*. It has been reported that a single leaf of the plant gifblaar (*Dichapetalum cymosum*), contains enough MFA to kill large animals *(143)*. In addition to MFA, the natural production of fluorinated amino acids has been reported *(144)*, as have fatty acids with fluorine bound to the ω carbon *(135)*. It has been suggested that nearly all plants can metabolize inorganic fluorine to some extent producing natural fluoroacetate and fluorocitrate, but that the concentrations are typically too low to exhibit harmful effects. For example, a sample of commercial oatmeal was reported to contain 62 μg g^{-1} of fluoroacetate *(144)*.

1.3.3 Anthropogenic Organofluorine

Practically all environmentally relevant organofluorine is of an anthropogenic source *(135)*. The incorporation of fluorine as a substituent imparts several technologically important properties onto organic compounds and organofluorine compounds have been used for decades without fully understanding their environmental impact. Perhaps best known among organofluorines are the chlorofluorocarbons which were used extensively as refrigerants until their role in

atmospheric ozone depletion became fully realized *(145)*. Also important are long-chain polyfluorinated alkanes, such as perfluoroalkane sulfonyl compounds, which have found numerous uses as the basis for non-stick coatings, emulsifier agents, and surfactants in general *(146)*. Polyfluorinated aromatic compounds, although much rarer, do occur as environmental pollutants from a variety of sources, including as byproducts of the burning of the more common long-chain compounds *(147)*.

Polyfluorinated organic compounds have unique properties arising from the high electronegativity of fluorine, which results in highly polarized carbon-fluorine bonds where the fluorine possess a partial negative charge while the carbon posses a partial positive charge. As a result, long-chain polyfluorinated alkanes are both hydrophobic and oleophobic, in addition to exhibiting weak intermolecular interactions amongst similar molecules *(148)*. A specialized example where polyfluorinated compounds actually exhibit strong intermolecular interactions are polyfluorinated aromatics, which form stable complexes with non-fluorinated aromatics due to opposite, and thus complimentary, quadrupole moments encouraging the formation 1:1 stacked pairs *(149)*.

1.3.4 Physical Properties of Organofluorine Compounds

Polyfluorinated compounds do not follow the same trends with respect to the physical properties observed for polychlorinated or polybrominated compounds *(148)*. For instance, the boiling point of halogenated methanes, CH_nX_{4-n}, initially increases as the number of halogens, be they fluorine, chlorine or bromine, are added. For chlorine and bromine, the boiling point continues to increase up to CX_4, an effect largely explained by increasing molecular weights. For fluorine, however, the increase in boiling point extends only to CH_2X_2, after which the addition of more fluorine results in the boiling point decreasing so that CF_4 ends up with nearly the same boiling point as CH_4 *(148)*. This occurs despite the increase in molecular weight and has been attributed to the weak intermolecular interactions between CF_4 molecules arising from the partial negative charge on each fluorine atom. For long chain polyfluorinated alkyl chains, the boiling point of the fluorocarbon, relative to its hydrocarbon equivalent, decreases as the chain length increases *(148);* this trend is attributed to intermolecular interactions that weaken as the CF_2 chains

become longer due to the repulsion between adjacent CF_2 units producing a more rigid backbone than regular hydrocarbons *(148, 150)*. For halo-benzenes, the boiling point of fluorinated benzene is largely unaffected by the number of substituent fluorine atoms, whereas for chlorine and bromine the boiling point is greatly affected *(148)*.

1.4.5 Organofluorine in the Environment

Due to the strength of the C-F bond, organofluorine compounds are strongly resistant to both biotic and abiotic degradation *(148)*. For compounds that are not fully fluorinated, mechanisms for degradation exist at the C-H bonds, however fully fluorinated compounds are essentially indestructible by natural processes. This startling persistence has made organofluorine compounds a topic of emerging importance in environmental chemistry.

From an environmental vantage, the most important organofluorine compounds are the polyfluorinated alkyl compounds, including carboxylic acids, sulfonates, phosphonates, and telomer alcohols *(151, 152)*. Perfluorooctanoic acid (PFOA) and perfluorooctanesulfonic acid (PFOS) standout as the most environmentally sensitive polyfluorinated alkyl compounds (153) due to the congruence of eight-carbon (C8) polyfluorinated alkyls having the most optimal industrial properties as surfactants *(146)*, thus encouraging their production and emission, and by the fact that C8 compounds, particularly PFOA, are the end degradation product of many other polyfluorinated alky compounds. Perfluorinated alkyl chains longer than 8 are also important environmentally, however their occurrence is rarer, while compounds smaller than C7 are not bio-accumulative and thus not as much of an environmental concern *(154)*.

The presence of fluorine on alkyl acids helps to stabilize the negative charge through induction effects, therein decreasing the pk_a values of these compounds, which, typically occur as charged alkylate species at environmentally relevant pHs *(148)*. Accordingly, compounds such as PFOA and PFOS are found most readily in the environment dissolved in water. Ocean transport is thought to be responsible for the ubiquity of these compounds in even remote regions of the world, such as the high-arctic, far from any emission source *(153, 155)*. These compounds are found nearly everywhere *(156)*, with concentrations typically at the ppt level *(146)*, however ppm levels of perfluoralkyl contamination have been found closer to the source of accidental

emission *(157)*. In domestic sludge, levels of perfluorocarboxylates have been observed in the 5-152 ng g^{-1} range, while those of perfluoroalkyl-sulfonyl-based compounds have been as high as 55-3370 ng g^{-1} *(158)*.

Perfluoroalkyl compounds with chains of 8 carbons or longer have been observed to be bioaccumulative *(159-161)*. The toxicity of these compounds is not fully understood, but it is known that they typically target the liver, affect development and growth, have hormonal effects, and may be weak xenoestrogens *(146)*. PFOS and PFOA are easily absorbed orally, however in accordance with the strong C-F bonds, they are not metabolized. Furthermore, these compounds are poorly eliminated, with PFOA having a half-life of 3.5 years in human serum, where it has been shown to interact strongly with serum albumin *(162)*. Perfluorinated chemicals are now found in nearly all samples of human blood *(154)*.

1.4.6 Organofluorine as an Analytical Probe in Environmental Research

The key analytical advantage to studying organofluorine compounds is that fluorine is very easily observed by way of its nucleus using ^{19}F NMR spectroscopy. This allows for the detection and characterization of organofluorine compounds selectively, without background interference from non-fluorinated compounds *(147, 163)*. The use of organofluorine compounds to probe the interactions between xenobiotics and environmental matrices using ^{19}F NMR spectroscopy is an emerging field of study in analytical environmental chemistry *(162-172)*, and is the main topic of this dissertation as a whole.

1.5   Nuclear Magnetic Resonance Spectroscopy

The work presented in this dissertation makes extensive use of Nuclear Magnetic Resonance spectroscopy to investigate intermolecular interactions between small organic xenobiotic compounds and natural organic matter. As the focus of this dissertation is on the environmental chemistry rather than NMR spectroscopy specifically, an advanced discussion of the theory of magnetic resonance is beyond the scope of this work and textbooks by Keeler *(173)* and Levitt *(174*) recommended for a more through, yet accessible discussion. Some topics in the basic

theory of NMR spectroscopy are covered in this section, including a discussion of the application of NMR as an analytical tool in environmental chemistry.

1.5.1 Introduction to Nuclear Magnetic Resonance

Nuclear magnetic resonance was first suggested as early as 1936 arising from the proposed existence of nuclear degenerate states that would be broken by strong external magnetic fields *(175, 176)*. Degeneracy of the same type had previously been observed for electrons, resulting in the splitting of an electron beam into two when it passes through a magnetic field, an effect called Zeeman splitting. All subatomic particles, including electrons, protons, and neutrons posses a quantum mechanical property called spin. While initially thought of as quantized angular momentum wherein the particle was physically spinning, the modern understanding of spin is best described as intrinsic angular momentum rather than a classical spinning process. In this way, spin differs from other basic properties of subatomic particles, such as mass and charge, in that it does not translate to the macroscopic level and as such has no intuitive meaning to us as macroscopic observers *(74)*.

Most particles, including electrons, protons, and neutrons have a spin value of ½, imparting on them two possible spin states. Inside an atomic nucleus, however, protons and neutrons pair together following a version of the Pauli exclusion principle for nuclear orbitals such that the spin properties of protons and neutrons mostly cancel each other out *(177)*. Nevertheless, when an odd number of protons or neutrons occurs, the nucleus as a whole retains spin as a property. The presence of only a single unpaired proton or neutron produces spin 1/2 nuclei, which include the nuclei of the isotopes ^{1}H, ^{13}C, ^{15}N, ^{19}F, ^{31}P, and ^{29}Si. In the case of multiple unpaired neutrons or protons, the unpaired spin of those particles add to produce nuclei with spins of 3/2, 5/2, 7/2, or 9/2. Examples here include ^{7}Li, ^{23}Na, ^{79}Br, and ^{35}Cl. When there is an even number of protons and neutrons, nuclei are typically structured such that spin 0 is achieved, as is the case for ^{12}C, ^{16}O, and ^{28}Si, however there is a small number of nuclei with unpaired protons and neutrons that have an integer value of spin, including ^{2}D, ^{6}Li, ^{10}B, and ^{14}N.

The spin-state of a particle continually fluctuates between all possible orientations. These transitions require energy to move from lower to higher energy states, but release energy when

moving the other way. The absorption and emission of this energy by spins is called resonance. The first observations of spin-state transitions in atomic nuclei were reported by Isidor Rabi in 1938 using atomic beams of lithium *(178)*. Successful observations of nuclear magnetic resonance in condensed materials were reported nearly simultaneously in 1949 by the groups of Felix Bloch *(179, 180)* and Edward Mills Purcell *(181)*, who both received the Nobel prize for this accomplishment.

1.5.2 Theory

1.5.2.1   Principles of Magnetic Resonance

The base principle of nuclear magnetic resonance is the fact that charged particles with 'spin' (classical and quantum mechanical alike) have a magnetic moment. Spin, J, introduces $2J+1$ degrees of freedom, m_J, on its possessor. This means that nuclei with spin $J=1/2$ posses two different spin states; $m_J = \frac{1}{2}$ and $m_J = -\frac{1}{2}$, with any given nucleus existing in a spin state that is a linear combination of the two. The magnetic moment of a nucleus is proportional to the spin

$$\mu = \gamma \, J \qquad\qquad [1.2]$$

where the proportionality constant, γ, is specific to each type of nucleus and is called the magnetogyric ratio. Spin $\frac{1}{2}$ nuclei only possess magnetic dipole moments while nuclei with spin $> \frac{1}{2}$ also posses higher-order moments due to structural asymmetry. In the presence of an external magnetic field the energy of the nucleus is the scalar product of the vectors of the external field, B_o, and the nuclear magnetic moment

$$E=-\mu \bullet B_o. \qquad\qquad [1.3]$$

This means that nuclear magnetic moments aligned with the external field are lower in energy than those out of alignment, with the energy difference between the $m_J = \frac{1}{2}$ and $m_J = -\frac{1}{2}$ states described by the equation

$$\Delta E=-h\gamma B_o \qquad\qquad [1.4]$$

where h is Planck's constant. This splitting is the origin of the Zeeman effect described above. The energy difference between spin states is proportional to a frequency, ω, using the relationship between the magnetogyric ratio and magnetic field strength:

$$\omega = \gamma B_o \qquad [1.5]$$

resulting in

$$\Delta E = -h\omega \qquad [1.6]$$

where ω can be thought of as the frequency of precession of a nucleus induced by the applied external magnetic field *(74)*. This is called the Larmor frequency and is also the resonance condition for observing nuclear magnetic resonance.

In the absence of an external magnetic field, there is equal probability of either spin-state occurring, and thus the populations of nuclei in either state in a bulk sample are equal as is illustrated in figure 1.2. An external magnetic field breaks the degeneracy between spin states so that in a bulk sample of nuclei, the spin state of lower energy is favoured resulting in a population difference. This can be described using a Boltzmann distribution,

$$n_{upper}/n_{lower} = e^{-\Delta E/kT} \qquad [1.7]$$

where n_{upper} is the population of nuclei in the higher energy spin state, n_{lower} is the population of nuclei in the lower energy spin state, k is Boltzmann's constant and T is the temperature in Kelvin. In a bulk sample of nuclei, when the number of spins in the higher energy state equals the number of spins in the lower energy state, the sum of the nuclear magnetic moments cancel out. However, when a population difference occurs, a small magnetic moment proportional to that population difference can be detected as is illustrated in figure 1.3. This bulk magnetic moment precesses at the Larmor frequency of the individual nuclear magnetic moments that comprise it *(74)*.
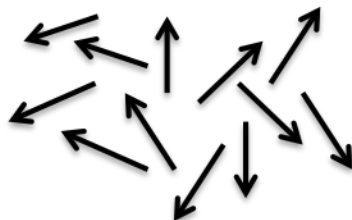
In the absence of external fields, a collection of spins exists with a random distribution of degenerate spins states.
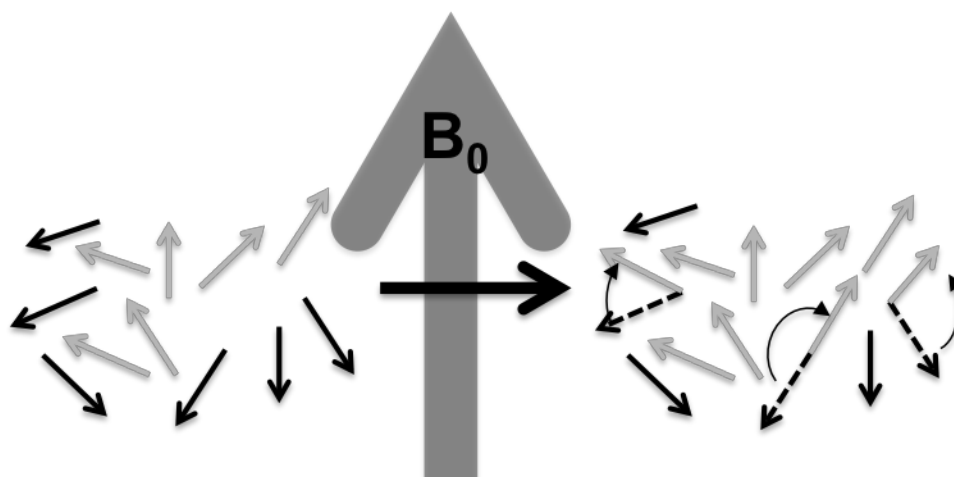
In the presence of an external magnetic field (B_0) degeneracy is broken and spins with magnetic moments aligned with the external field being lower in energy than spins in opposition to this field. There is a preference for spins to align with the external field and a new equilibrium distribution of spin-states is established to reflect this.

Figure 1.2   Breaking the spin-state degeneracy of a collection of spins in the presence of an external magnetic field (see refs *74, 173, 174, 182, 183*).
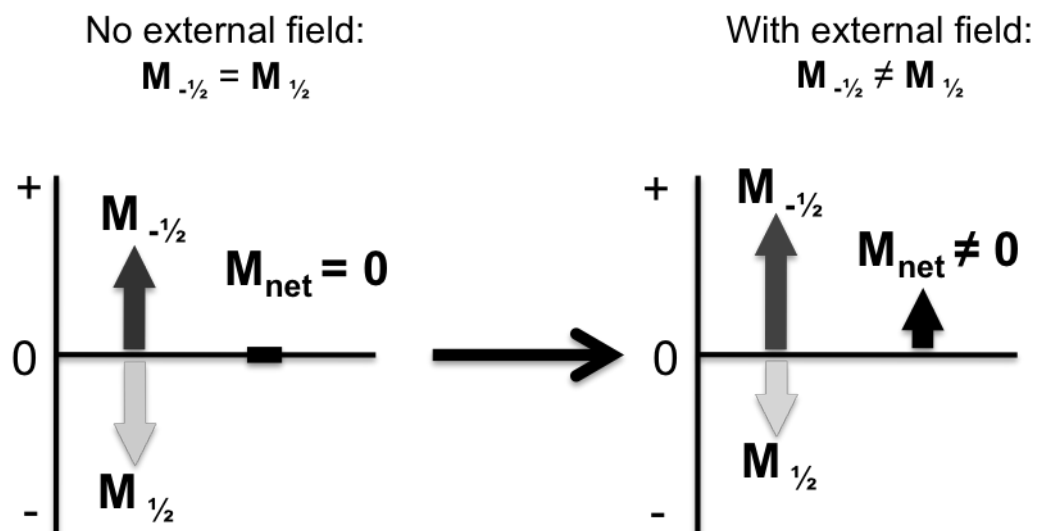
Figure 1.3   The population difference in spin states due to the external magnetic field induces a net magnetic moment in a bulk collection of spins, M_{net}. This is because the individual magnetic moments of the ½ spin state, $M_{½}$, no longer cancels out those of the −½ spin state, $M_{-½}$ (see refs *74, 173, 174, 182, 183*).

The spectroscopic applications of nuclear magnetic resonance lie in manipulating the precession of the spins using a second, applied field created by electromagnetic radiation in the radio-frequency range. This secondary field is applied perpendicular to the original external field, B_0. In the absence of the second field, the bulk magnetic moment is aligned along the same axis as B_0, which is defined as z. In this situation precession of the bulk moment cannot be detected because there is no change in its vector. The simultaneous precession about the two fields, however, shifts the direction of the bulk magnetic moment away from that of B_0. When the second field is turned off, precession about this field also stops, but now the bulk magnetic moment has been reoriented so that it is no longer aligned along z, and precession about B_o is observable in the form of an oscillating field at the Larmor frequency in the XY plane as is illustrated in figure 1.4. This oscillation is recorded as an alternating current (AC) in a nearby inductance coil. The oscillating strength of the AC signal is recorded as a function of time, but is usually converted to the intensity vs. frequency domain using a Fourier transform prior to analysis.

1.5.2.2 *Relaxation*

When the application of a secondary rf field has shifted the bulk magnetization away from the z axis the distribution of nuclear spins is no longer in equilibrium. In order to return to equilibrium, the system must relax. The theory behind spin-relaxation is extraordinarily complex *(173)* and only a basic discussion is necessary here. A system of spins that is out of equilibrium is in a higher energy state than it would be under equilibrium conditions. In general, this excess energy is removed from the spins by coupling to the thermal energy in the system, which is related to molecular motion. The thermal energy in a system due to molecular motion is called the lattice. For a nucleus to release spin energy to the lattice, the motion of the molecule must have a frequency that matches the Larmor frequency corresponding to the transition of spin-states described above. In general, this corresponds to rotational motion and larger molecules will typically have rotational frequencies that are more similar to Larmor frequencies than small molecules, and thus tend to return to equilibrium relatively quickly. Solid materials, which do
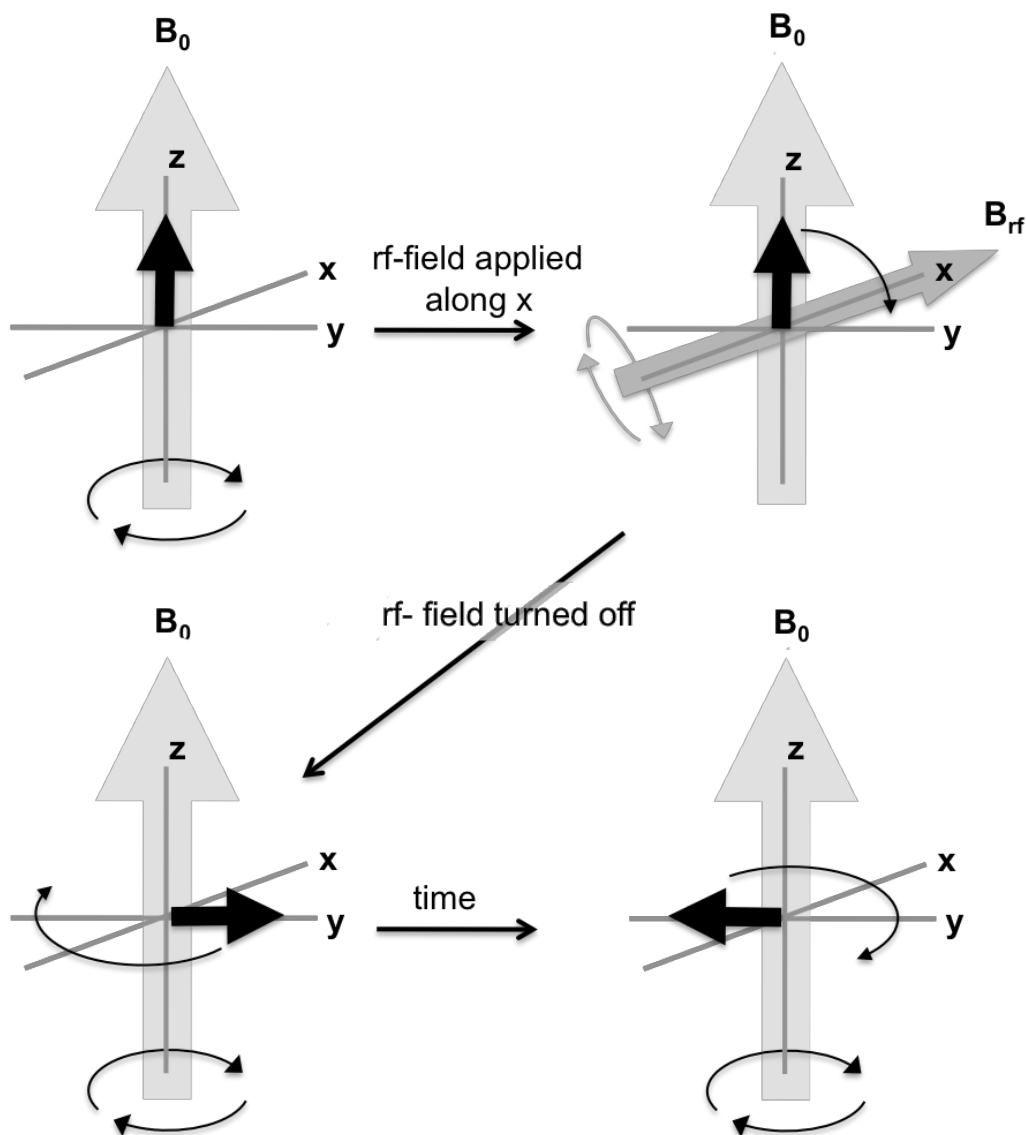
Figure 1.4   The net magnetic moment of a collection of spins precesses about the axis of an externally applied magnetic field, z. When the only field is aligned with the magnetic moment of the spins, this precession is not observable. When an additional field is applied perpendicular to z, precession about this axis moves the net magnetic moment of the spins away from z. Precession about z is now observable in the form of an oscillating magnetic field in the xy plane (see refs *74, 173, 174, 182, 183*).

not have rotational motion, tend to exhibit very long relaxation times. This type of relaxation is often termed spin-lattice relaxation, and occurs with a rate proportional to $1/T_1$, where T_1 is a time period associated with the most probable period required for a nuclear spin to complete spin-lattice relaxation. Spin-lattice relaxation is often called T_1 relaxation, informally. Spin-lattice relaxation limits the sensitivity of an NMR experiment, as typically the experimenter will desire that most of the system has returned to equilibrium before repetition, which, as discussed above, is required to overcome the small population differences inherent in NMR spectroscopy.

While spin-lattice relaxation is required to return a spin system to equilibrium, another mechanism occurs that reduces the energy of the system without a full return to equilibrium. After the application of the secondary rf field that rotates magnetization into the observable xy plane, all of the spins are aligned together and precess with the same phase. Overtime, however, this coherence falls apart due to slight differences in the local spin environment, and the individual spins become distributed randomly about the xy plane. This effect is illustrated in figure 1.5. Because precession is observed for the bulk magnetic moment, the more randomly distributed this spin ensemble become in the xy plane, the weaker the observed signal because the magnetic moment of spins oriented in opposition cancel each other. This type of relaxation is called longitudinal relaxation, and occurs with a rate proportional to $1/T_2$, where T_2 is the average time required for a spin to depart from the grouped coherence. Longitudinal relaxation is also called T_2 relaxation, informally. As mentioned above, T_2 relaxation does not return the system to equilibrium, but it does destroy the observable signal and as such, if T_2 relaxation has occurred, but T_1 relaxation has not, then an experiment may not yet be repeated. While T_2 does not directly influence the sensitivity of an NMR experiment in the way that T_1 does, T_2 relaxation has a significant effect on resolution. The period of time over which an NMR signal may be observed is usually limited by T_2, and as such the longer T_2 is, the longer a signal may be observed. This makes the identification of Larmor frequencies more certain *(173, 182)*. Conversely, a short T_2 limits the observation of precession, and makes the identification of the Larmor frequencies less certain. The more certain a frequency is, the narrower its line width after Fourier transform. In this way short T_2 times lead to broad lines that can obscure finer details in an NMR spectrum.

Transverse Relaxation

Longitudinal Relaxation
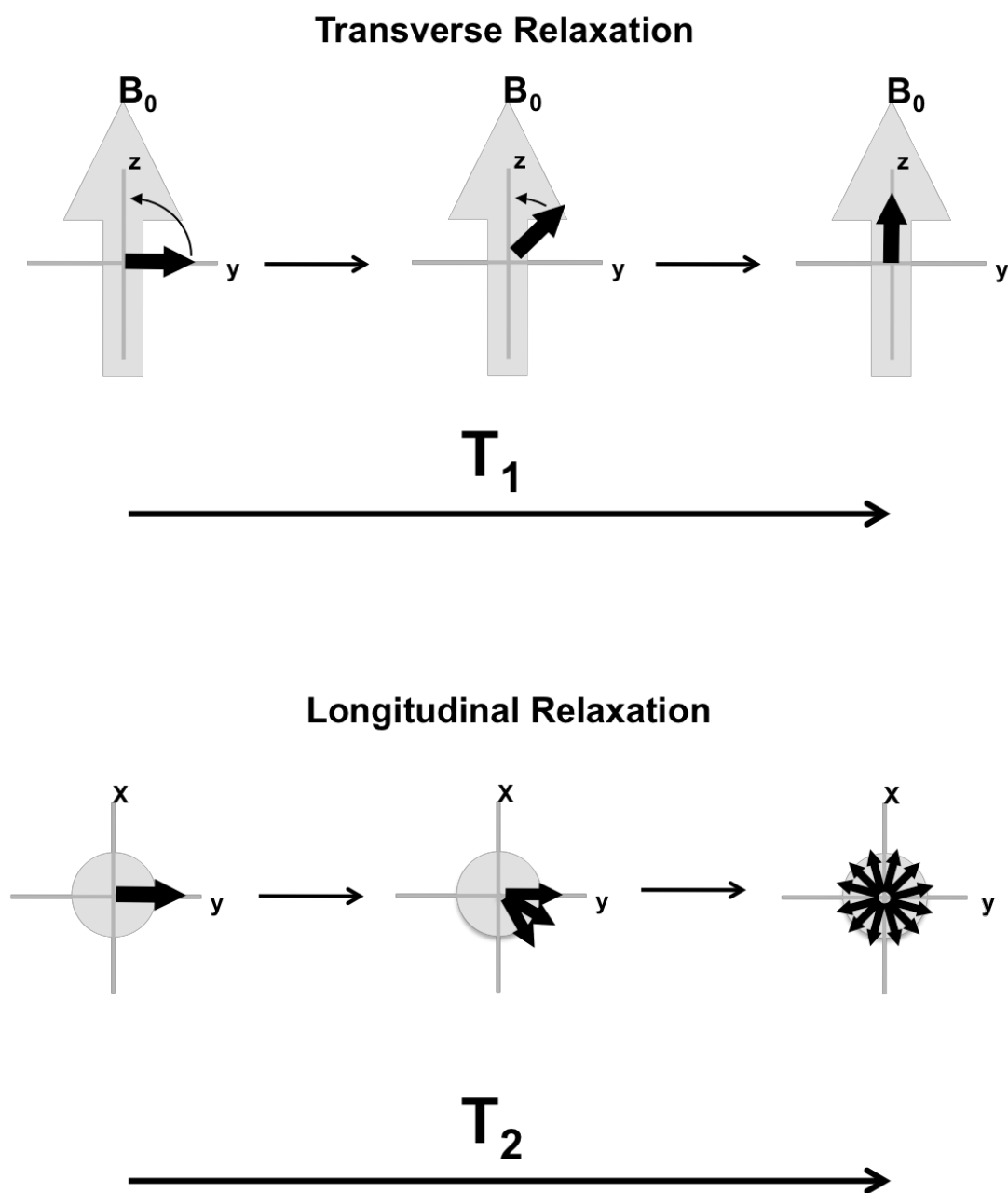
Figure 1.5   Relaxation in NMR. Transverse relaxation returns magnetization to equilibrium aligned with B_0. Longitudinal relaxation scrambles the magnetization about the XY plane, but does not return it to equilibrium. Transverse and longitudinal relaxation occur simultaneously, however longitudinal relaxation is typically much faster with T_2 being much shorter than T_1 (see refs *74, 173, 174, 182, 183*).

1.5.2.3   *The Nuclear Hamiltonian*

The utility of nuclear magnetic resonance spectroscopy as an analytical tool lies in small variations in local magnetic fields due to the local chemical and physical environment surrounding a nucleus. Small differneces in the local magnetic field can have significant influence on the Larmor frequency recorded for nuclei in different physical and chemical environments. The observed Larmor frequency of a nucleus, thus, is proportional to the combination of many perturbations on the nuclear spin Hamiltonian:

$$H = H_{Zeeman} + H_{Chemical\ Shift} + H_{Dipolar\ Coupling} + H_{J\text{-}Coupling} + H_{Quadrupolar\ Coupling} + \ldots \qquad [1.8]$$

where H_{Zeeman} is the contribution from the Zeeman effect due to the strong externally applied field, $H_{Chemical\ shift}$ is caused by the local field of electrons and is related to the chemical environmental surrounding the nucleus, $H_{Dipolar\ coupling}$ is the field felt at one nucleus from the magnetic moment of a nearby nucleus, $H_{J\text{-}Coupling}$ is the field felt at a nucleus from nuclei that are coupled to it through electrons (i.e. covalent bonds), and $H_{Quadrupolar\ coupling}$ is the interaction between the quadrupole moment of an asymmetrical nucleus and its surrounding electric field gradient, which for all spin ½ nuclei is zero *(74, 183)*. Other contributions to the nuclear spin Hamiltonian exist, such as Knight shifts caused by conducting electrons, however these are rarely encountered outside of specialized applications *(74)*.

Perturbations to the Larmor frequency can be both isotropic and anisotropic. The isotropic contributions, which include J-coupling and a portion of the chemical shift perturbation, are independent of the orientation of a given nucleus with respect to its surroundings in the external field. Anisotropic contributions include chemical shift anisotropy (CSA), dipole-dipole coupling, and quadrupole coupling, and are affected by the orientation of the nucleus within its surroundings. Under rapid isotropic motion, such as in a fluid state where molecular tumbling is faster than the NMR time scale (microseconds to milliseconds), anisotropic contributions average to zero and are not observed, limiting the directly observable terms in the spin Hamiltonian to the isotropic chemical shift and J-coupling. In materials where mobility is restricted, such as in a solid or an ordered liquid, anisotropic contributions can be significant, often resulting in broadening of a spectrum due to the myriad possible orientations. In general

this obscures the information from the isotropic contributions, particularly J-coupling. The technique of Magic Angle Spinning (MAS) assists greatly in removing most of the effects of anisotropy by rapidly spinning the sample at 54.7° with respect to the z-axis of the applied static field *(74)*. This angle is the mathematical solution to the orientation dependent term in the first-order anisotropic perturbations to the Hamiltonian, $(1-3\cos^2\theta)$, and represents a node where the time averaged contribution from these terms to the total Hamiltonian is zero. These anisotropic perturbations do not disappear but are simply rendered invisible for an experiment that takes longer than a sample needs to complete a single rotation, which can be quite fast with typical rotational speeds in the 10 to 15 kHz range using standard 4mm diameter sample rotors. Speeds up to 110 kHz are possible with specialized equipment, but with the compromise of much smaller sample volumes. There are many techniques that manipulate these interactions as a means to probe structure and interactions without explicitly requiring their direct observation that will be discussed in the next sub-section.

1.5.3   NMR Spectroscopy as an Analytical Tool

NMR spectroscopy provides a direct probe of the local molecular environment surrounding an atomic nucleus, and in this way it allows for detailed investigations into molecular structure and intermolecular processes in complex systems that are often not accessible using other analytical means. The main limitation to this approach is the insensitivity of NMR spectroscopy that arises from the small population differences between the spin states that is used to generate a signal. The low sensitivity in detecting these small population differences is offset, however, by the non-destructive nature of the technique. Measurements are typically averaged over several hundred, or even thousands of repetitions of the same experiment and many numbers of different experiments may be performed on the same sample without loss or change in the sample.

An NMR spectrum is non-selective within the applied excitation bandwidth, which, in most applications, encompasses the entire range of frequencies possible for a given nucleus. This means that if a compound is present, the signals from its nuclei, ^{1}H or ^{13}C, for example, will be recorded when the spectrometer is tuned for the bandwidth of that nucleus. This makes NMR spectroscopy a powerful tool to scan the composition of a sample without any prior knowledge

of its composition. Table 1-I compares the relative frequency and natural abundance of several NMR active nuclei commonly employed in environmental chemistry. Combined with the information about local molecular structure that may be gleaned from precise measurements of the Larmor frequency, the type of materials present in a given sample can be easily investigated. Chemical shift information provides information about the structure of the electron clouds around nuclei, J coupling has information on how atoms are connected within a molecule, while magnetic dipole couplings contains a wealth of information about intermolecular associations and spatial arrangements. The physical origin of some of these effects, and examples of their application in understanding intermolecular interactions in environmental media are discussed below.

1.5.4 Chemical Shift

Chemical shift is the most common feature of NMR spectroscopy used for chemical analysis. The strong external magnetic field induces motion of the electrons in a sample creating small electric fields felt by nearby atomic nuclei. The strength of these localized fields are proportional to the strength of the external magnetic field meaning that their effect increases as the strength of the applied magnetic field increases *(74)*. Atomic nuclei feel the combined effects of the strong external field and these small fields, shifting the observed Larmor frequency from the common base frequency in accordance with its local electron environment. This effect is called chemical shielding and because of it nuclei with the same base frequency, but in slightly different chemical environments will have different observed Larmor frequencies. As such, different molecules are easily resolvable from each other in an NMR spectrum. The local chemical environment of a nucleus can be inferred from its observed chemical shift using theory supported empirical correlations, aiding in the determination of the structure of a given molecule.

In environmental chemistry, chemical shift is used most frequently to characterize NOM based on analysis of the proportion of nuclei in different chemical environments *(82, 104, 109, 124-127)*. Another use of chemical shift data is to look for the formation of covalent bonds between xenobiotics and NOM *(127, 185, 186)* or the emergence of degradation products *(187-190)* based on changes in the chemical shift or the emergence of resonances from new chemical species.

Table 1-1   Magnetic properties of environmentally relevant NMR nuclei *(184)*.

Nucleus	Spin	Precession frequency under 2.35 T of magnetic inductance, in MHz	Average natural abundance
^{1}H	1/2	100.0	99.9885
^{2}D	1	15.350609	0.0115
^{13}C	1/2	25.145020	1.07
^{14}N	1	7.226317	99.632
^{15}N	1/2	10.136767	0.368
^{17}O	5/2	13.556457	0.038
^{19}F	1/2	94.094011	100
^{27}Al	5/2	26.056859	100
^{29}Si	1/2	19.867187	4.6832
^{31}P	1/2	40.480742	100

1.5.5 Dipole Interactions

Because nuclei posses magnetic dipole moments they are able to feel the presence of each other through-space. The strength of nuclear magnetic dipole-dipole interactions are proportional to the distance between the nuclei in the same manner that the strength of the magnetic field of a bar magnet depends upon distance, although nuclear magnetism is much weaker than ferromagnetism. In general, the dipolar Hamiltonian of a pair of interacting nuclear spins, identified as S and I, is

$$H_{Dipolar\ coupling} = \gamma_S \gamma_I\ h^2\ /r_{SI}^3\ \tfrac{1}{2}\ (3J_{Sz}J_{Iz} - S \bullet I)(1 - 3\cos^2\theta) \qquad [1.9]$$

where r_{SI} is the distance between the nuclei, γ is the magnetogyric ration of the respective nucleus, h is Planck's constant, J_{Sz} and J_{IZ} are the spin quantum numbers specific to two different nuclei, S and I, in the interaction, and θ is the angle between the internuclear vector and the applied field B_0 *(74)*. In a real sample, any given nucleus feels the magnetic dipole of numerous other nuclei in its vicinity and the unique dipole coupling between individual sets of two-nuclei is obscured. Instead, what is measurable is the dipole-dipole second moment, M_2, which is a measure of the distribution of dipolar couplings at a given nucleus *(191, 192)*, and is detailed more thoroughly in reference 193.

In the absence of isotropic motion or fast magic angle spinning to average the myriad dipole-dipole orientations in a sample, the NMR spectrum takes on a characteristic broad pattern, called a Pake powder pattern, which is shown in figure 1.6. The strength of the dipole coupling can be determined from such a pattern, allowing for a direct measurement of the strength of the dipole interactions, and thus the internuclear distance. Pake powder pattern analysis is only practical for isolated spin-pairs, which is a situation unlikely to occur in complex amorphous systems such as those found in the environment. Regardless of whether dipole coupling can be quantified, the relationship between internuclear distance and the strength of nuclear dipole-dipole interactions provides a useful mechanism to probe non-covalent intermolecular interactions. A few NMR techniques employing the through-space dipole-dipole interactions to probe intermolecular interactions are described in the next section.
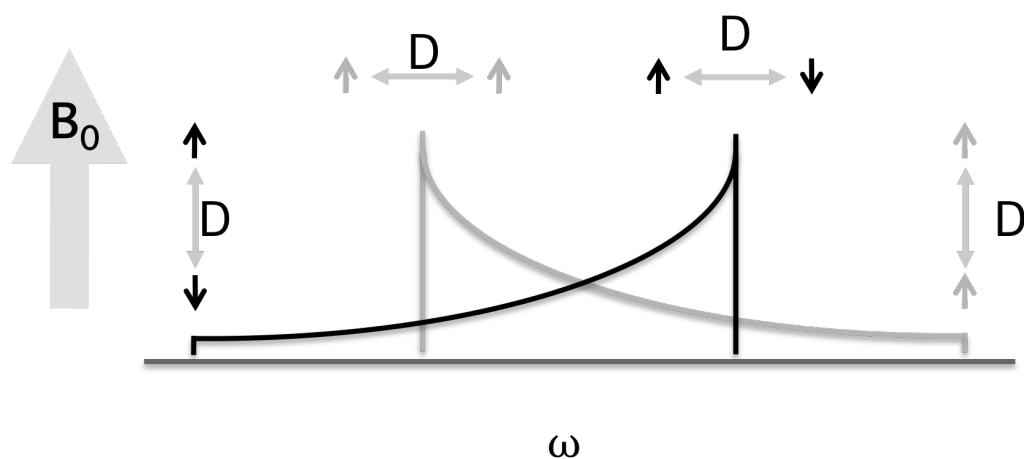
Figure 1.6   The dipole-dipole powder pattern for an isolate spin pair with cylindrical symmetry. Although the strength of the dipole coupling is constant, the orientation of the spin pair with respect to B_0 affects the Larmor frequency, ω, differently. Shown are the individual powder patterns for the cases when the interacting nuclei are in the same or different spin-states, which overlap in the actual observed powder pattern as a doublet. The strength of dipole interaction, D, can be determined by numerical analysis of the powder pattern to determine the tensor values in the dipolar matrix. The signal strength is strongest for the perpendicular orientation because there are an infinite number of distinct orientations possible that still have the same angle with respect to B_0 *(74)*.

1.5.5.1 Cross-Relaxation, the Nuclear Overhaüser Effect, and Saturation Transfer

In addition to coupling with molecular motion as a mechanism for the relaxation of non-equilibrium spin systems, the relaxation of nuclear spins can also be assisted by transferring the excess energy in one spin system to another spin system using dipole-dipole couplings. For the spin system that is out of equilibrium, its rate of relaxation will increase if it can transfer energy to a second spin system, while that second spin system will end up further from equilibrium due to the absorbed energy. This effect is called cross-relaxation *(173)*. Cross-relaxation can be used to identify intermolecular interactions by observing changes in the relaxation rate of a molecule in the presence of a larger macromolecule but can also be used to build up observational magnetization in the second spin system by taking the magnetization from the first spin system. This last effect is called the nuclear Overhaüser effect, or NOE *(194)*. The NOE is very useful in increasing the observable signal of low sensitivity nuclei, such as ^{13}C, by transferring magnetization to ^{13}C nuclei from nearby ^{1}H nuclei, which experience greater polarization due to their stronger magnetogyric ratios. Because the NOE is mediated by dipole-dipole couplings, it is highly sensitive the internuclear distances between ^{1}H and ^{13}C, and thus can be used to probe the presence of intermolecular interactions.

In addition to increasing signal intensity, dipole-dipole couplings can be used to induce a saturated equilibrium state in a selected spin system such that magnetization is no longer observable *(195-197)*. Using constant rf irradiation, a state is created where T_1 relaxation is prevented, but T_2 relaxation still occurs. This makes the spin-system unobservable, but also unable to return to equilibrium. So long as the Larmor frequency of a nucleus is well resolved from its neighbouring nuclei, it is possible to selectively saturate only that nucleus in a sample. In the absence of cross-relaxation, when that nucleus is saturated no signal is recorded for it while signals from other nuclei are unaffected. Cross-relaxation between the saturated nuclei and other nuclei in close proximity will act to transfer saturation from the saturated to the unsaturated nuclei. Saturation is a relatively high-energy state and is far from its desired equilibrium state. Energy is dissipated by transferring saturation to nuclear spins in lower energy states, such as those already in equilibrium. The result of saturation transfer is that signals from nuclei that are in close proximity to the directly saturated nuclei will be attenuated to some extent. In a covalently bonded molecule this is mediated through a process called spin-diffusion

and all nuclei in the system are quickly saturated. For non-covalently bound molecules participating in intermolecular interactions, the transfer of saturation is slower, with the degree of attenuation related to the relative spatial proximity of different nuclei to the directly saturated nuclei, as well as to the period of time over which the intermolecular interaction occurs *(197)*.

1.5.5.2 *Cross-Polarization*

Cross-polarization is a solid-state technique that uses dipole-dipole interactions to alter the Boltzmann distribution of a spin system without changing the applied magnetic field and is similar to the NOE. For a sample containing both ^{1}H and ^{13}C, the different magnetogyric ratios of these nuclei mean that the energy required to induce transitions for ^{1}H are naturally higher than for ^{13}C at the same magnetic field strength. Relative to ^{1}H, the ^{13}C nuclei are in a higher energy state with transitions between $-\frac{1}{2}$ and $+\frac{1}{2}$ states occurring much more rapidly for ^{13}C than for ^{1}H. ^{13}C is said to have a higher spin temperature than ^{1}H *(198)*. This is why at the same magnetic field strength there is a greater population difference for ^{1}H than for ^{13}C. For example, for any magnetic field strength, at the equilibrium population difference between the $+\frac{1}{2}$ and $-\frac{1}{2}$ states for ^{1}H is 4 times that for ^{13}C.

The energy gap between spin transitions is related to the precession frequency of a nucleus, and, in general, ^{1}H spins precess about the external magnetic field 4 times faster than ^{13}C. When a second field is applied to the system in the form of rf radiation (see figure 1.5), the rate at which the spins precess about this field are proportional to the strength of that field. When two different sets of nuclear spins, such as ^{1}H and ^{13}C, are set to precess about two different, but simultaneously applied secondary rf fields at the same rate, the two spin-states mix. This is called the Hartman-Hahn match condition *(199)*. Under the Hartmann-Hahn condition the mixed spin states re-equilibrate in the xy plane with a common spin temperature.

Because ^{1}H accounts for nearly 100% of all hydrogen nuclei, and ^{13}C is only ~1% all carbon nuclei, in a typical hydrocarbon sample the high spin temperature of ^{13}C makes only a small contribution to the equilibrated spin temperature, while ^{1}H makes a very large contribution. The end result is that the equilibrated ^{1}H/^{13}C system will see a slight reduction in the strength of the ^{1}H signal, but the ^{13}C signal will increase nearly 4 times. The efficiency of cross-polarization is

directly related to the strength of the dipole-interaction, however unlike the NOE or saturation transfer, cross-polarization is sensitive to fluctuating dipole interactions, and is most efficient in solid samples where translational and rotational motion is essentially eliminated.

1.5.5.3   *Dipole Mediated Dephasing*

Another powerful method to probe dipole-dipole interactions in solids is to modulate the strength of the dipole interaction to induce controlled attenuations of signal strength proportional to the strength of the dipole interactions. This can be done under non-spinning conditions using experiments such as spin-echo double resonance, SEDOR, *(200)*, but is most commonly done under magic angle spinning conditions using experiments such as rotational-echo double resonance, REDOR *(193, 201, 202)*, or transfer of populations by double resonance, TRAPDOR *(203, 204)*.

Through an experiment such as REDOR, which probes the strength of heteronuclear interactions, quantitative measurements of dipole interactions, and thus internuclear distances, can be measured. This is accomplished by modulating the strength of the dipole interaction between two values in a rotor-synchronized manor[8]. In general, the dipole-dipole contribution to the nuclear spin Hamiltonian is averaged to zero under magic angle spinning conditions because the of the rapid passage of any given dipole-dipole pairing through all possible geometric orientations in a short period. The symmetry of this averaging can be broken if the strength of the dipole interaction is changed half-way through each rotor period. If detection always occurs at the completion of a rotor period, the dipole-dipole interaction will not be fully cancelled out, and attenuation of the signal is observed proportional to the strength of the interaction *(202)*. Dipolar recoupling experiments have been key to providing understanding several structural questions in complex amorphous systems, such as inorganic glasses *(192, 193)*, however these experiments are intolerant of fluctuations of the dipole interaction and are thus extremely sensitive to molecular motion.

---

[8] The rotor is the sample container for a solid-state NMR experiment. During MAS, the rotor is spun about its axis. In NMR terminology, a rotor period is the time required for the rotor to complete one full rotation.

1.5.6 Diffusion

While not relying on a specific property of nuclear magnetic resonance, aside from non-selective detection, NMR spectroscopy is a powerful tool to measure the translational motion of molecules by measuring their rates of self-diffusion. In NMR spectroscopy, diffusion experiments are performed using applied gradient fields that augment the static external field felt at each nucleus. This provides an easy way to encode the position in space of any given nucleus. The spatial encoding given to a nucleus is easily undone using a gradient of the same strength, but with opposite sign to the original, however this will only occur if a nucleus has not moved too far from where it was when it was first encoded *(205)*. The signals from nuclei that move too far will not be recovered, and as a result are not observable in the NMR spectrum. Thus, the sequential application of encoding and decoding gradients attenuates the signals in an NMR spectrum based on the statistical probability that a nucleus has diffused away from its starting position in a given period of time. When a small, fast moving molecule interacts with a slow moving molecule its apparent diffusion rate will slow down. This effect is observable in an NMR diffusion measurement and provides an elegant and direct method to assess the strength of that interaction *(206)*.

1.6 NMR Applications to Xenobiotic Interactions in the Environment

There have been two reviews written specifically on the use of NMR spectroscopy to study interactions between xenobiotics and environmental matrices *(77, 207)*, both written within the last 6 years, demonstrating the relative newness of the application of these techniques in this field. Studies have made use of several NMR active nuclei in addition to ^{1}H, which is most commonly used, including: ^{2}D *(208-212)*, ^{15}N *(189, 190, 213)*, ^{13}C *(127, 128, 185, 187, 188, 214-215)*, ^{31}P *(217)*, and ^{19}F *(164-171)*. The most widely used approach is to employ chemical shift information from either the xenobiotic, which is used to infer significant changes in the local chemical environment such as the formation of covalent bonds or the production of degradation products (*127, 185, 187)*; or of the NOM itself, where NMR is used primarily as a characterization tool *(82, 104, 109, 218-221)*. The second most commonly applied NMR approach is to investigate relaxation properties of xenobiotics in environmental matrices to infer

the presence of interactions between small, slower relaxing xenobiotics and large, fast relaxing macromolecules and surfaces *(128, 164, 165, 208-210, 214, 215)*. Other applications of NMR spectroscopy to studying xenobiotic-NOM interactions include: the application of Saturation Transfer Difference (STD) spectroscopy to develop binding epitope maps for selected xenobiotics *(222, 223)*; micro-imaging to produce macroscopic visual maps of xenobiotic transport through whole soils *(172)*; quadrupole-echo experiments on ^{2}D making use of distinctive quadrupole powder patterns to investigate changes in molecular motion during non-covalent interactions with environmental media *(211)*; diffusion studies using pulsed-field gradients, to quantify changes in molecular self-diffusion due to non-covalent interactions in soils and soil components *(164, 224-226)* and High-Resolution Magic Angle Spinning (HR-MAS), which makes use solution-state NMR experiments under MAS conditions to reduce the line broadening of signals from xenobiotic nuclei bound to surfaces in soils and clays *(186, 222, 227-229)*.

At its most basic application, NMR spectroscopy is useful in quantifying the presence of a xenobiotic in soil by using it as a detection mechanism for NMR active nuclei such as ^{19}F, that are uncommon in soil environments but are found in select xenobiotics *(170)*. However, perhaps the greatest utility of NMR spectroscopy as an analytical tool in environmental chemistry is its ability to probe the nature of the binding mechanisms between those xenobiotics to NOM.

In environmental chemistry, NMR spectroscopy is most often used to correlate sorption phenomenon of different xenobiotics, or different soils, to measureable structural properties of those soils *(219)*. These types of observations have been vital in developing the dual-mode sorption models discussed above and used to explain non-linear sorption behaviour *(77)*. For instance, using NMR spectroscopy as a characterization tool it has been confirmed that not only are the aromatic components of SOM important for sorption *(218)*, which is well established, but that aliphatic components also play key roles that were less well known *(104, 109, 185, 220)*. The evidence provided by NMR spectroscopy that both rigid aromatic and mobile aliphatic domains both contribute to sorption agree with the theory behind multi-mode, non-linear sorption, and provides cogent explanations for the identity of different types of sorption domains. The dual importance of aromatic and aliphatic domains has also been confirmed using relaxation studies. ^{1}H T_2 measurements have been used to show that aromatic domains in humic acid

extracted from compost, peat, and mineral soil are more rigid than aliphatic domains, and that their removal by bleaching results in a more linear sorption behaviour *(82)*. The removal of the mobile domains by hydrolysis, conversely, results in an increase in non-linear sorption behaviour, demonstrating experimentally that considering aliphatic and aromatic domains of SOM as different sorption domains may help explain non-linear sorption in soils *(82)*.

In one of the earliest NMR studies to probe intermolecular interactions in the environment directly at the site of interaction, Hatcher *et al.* used ^{13}C labeled compounds to monitor the formation of covalent bonds between 2,4-dichlorophenol (DCP) and SOM during enzymatic couplings *(127)* by observing changes in the ^{13}C chemical shift of DCP. It has been noted, however, that chemical shift changes of labeled xenobiotics interacting with SOM are not necessarily indicative of covalent bond formation and that often observed changes in chemical shift likely have non-covalent origins *(171, 185)*. The issue of whether the bound state for xenobiotics is actually the product of covalent bonds *(187)*, or is simply entrapment due to non-covalent interactions and steric restrictions is important for the overall study of xenobiotic fate in sub-surface environments *(49)*. Currently, most studies point to a primarily non-covalent origin for these interactions *(77)*.

In their sequestered states, bound xenobiotics cannot be extracted under environmentally relevant conditions, and, as discussed previously, have a reduced availability for both biotic and abiotic degradation processes. For instance, Guthrie *et al.* used solid-state $^{1}H \rightarrow ^{13}C$ CP-MAS experiments of labeled pyrene to show that even in its sequestered state, the structure of this xenobiotic is intact and therefore must be held to the soil through non-covalent processes *(215)*. Similarly, it as has been observed using ^{13}C labeled phenanthrene and fluroanthrene that the residues of the degradation products of these xenobiotics, which are not easily extracted, are bound primarily non-covalently, however some fraction of the bound residues may have been covalently coupled to the SOM *(187)*. When covalently bound fractions do form, it is through specific processes such as enzymatic or oxidative coupling reactions *(127, 187)*. NMR spectroscopy has been key to unraveling these processes. For example, using a novel $^{15}N/^{13}C/^{1}H$ double cross-polarization experiment, Knicker observed ^{15}N-labelled TNT degrade and then become incorporated into the products of rapidly degrading ^{13}C labeled plant materials *(190)*.

NMR spectroscopy has been used to observe multiple types of non-covalent binding sites for hexafluorobenzene (HFB) in soil using ^{19}F MAS solid-state NMR *(168)*. The chemical shift of fluorine is very sensitive to small changes in the local environment, much more so than ^{1}H or ^{13}C *(171)*, and HFB molecules occupying different binding sites produce a wide assortment of apparent chemical shifts. The nature of the multiple types of binding sites observed for HFB can be described based on the mobility these sites afford the xenobiotic. Differences in mobility are manifested in the line-width of each observed resonance such that unbound, weakly bound, and rigidly bound fractions can be identified *(168)*. In a similar study, Khalaf *et al.* physically separated humic acid into fractions based on a gradient of molecular sizes *(169)*. In this study HFB was observed to sit in at least three type of binding sites in the smaller-sized humic acid fractions, which were characterized using ^{1}H$\rightarrow$^{13}C CPMAS as being primarily aromatic, and in at least two types of binding sites in the larger-sized fractions of humic acid, which were characterized as consisting of primarily aliphatic material *(169)*. A similar change in the ^{13}C chemical shifts of labeled xenobiotic compounds was observed in a study by Smernik, indicating again that a range of possible binding sites exist within SOM *(215)*. Here, the strength of binding at these sites was described based on changes in the relaxation of the xenobiotic using the principle that sorbed xenobiotics take on the relaxation properties of the sorbate material they are interacting with.

The use of nuclear relaxation as a tool to probe intermolecular interactions provides a considerable wealth of information regarding the nature of the interactions between xenobiotics and NOM. In general, when a xenobiotic interacts with NOM its relaxation will slow down because it takes on the relaxation characteristics of the much larger molecules it is interacting with. Simpson *et al.* measured ^{13}C relaxation of labeled naphthalene, naphthol, and quinoline in the presence of dissolved humic acid, finding that the rate of relaxation slows down as the humic acid concentration increases, demonstrating that the presence of more humic acid results in more interactions *(128)*. Dixon *et al.* measured both T_1 and T_2 relaxation of ^{19}F nuclei in a fluorine containing xenobiotic to gauge the strength of the non-covalent interactions with fulvic acid *(164)*. From changes in the strength of association at varying pH values they suggest two competing mechanism for xenobiotic-fulvic acid association: hydrophobic effects, and H-bonding. Smejkalova *et al.* used combined ^{1}H and ^{19}F studies of T_1 and T_2 relaxation of fluorinated and chlorinated phenols, to show that increased hydrophobicity of the xenobiotic

increases its interaction with dissolved humic acid *(165)*. They observe an inverse relationship with pH and binding strength that they attribute to a preference for binding of the protonated form of the phenols over the anionic form. Nanny and coworkers used ^{2}D labeled xenobiotics in a relaxation study to compare the interactions with fulvic acid *(208)*, and humic acid *(209)*, of small aromatic compounds. They show fulvic and humic acids from different sources interact with different xenobiotics differently. Phenol, for instance, only interacts with humic acid with a high aromatic component, and then only at low pH values, while benzene interacts with both humic and fulvic acid, but again more strongly to material with a higher aromatic component. Pyridine shows a maximum strength of interaction in the pH 3-8 region, and it is suggested that two modes of interaction may exist for this compound: π-π interactions, and binding through the nitrogen lone pair. Such specific interactions, it should be noted, are not directly observed but only inferred from pH responses. Zhu *et al.* report changes in the binding affinity of perdeuterated pyridine to dissolved humic acid as a function of pH as measured by ^{2}D T_1 measurements *(210)*. They observes a pH value of 6 as being optimal for the interaction, which they attribute to different types of interactions by protonated and non-protonated forms of pyridine and propose that cation-anion interactions occur at lower pH, while hydrophobic-driven interactions occur at higher pH.

Xiong *et al.* also use deuterated xenobiotics to probe interactions, but instead of using relaxation properties, they make use of unique quadrupolar properties of ^{2}D nuclei *(211)*. As mentioned briefly in the discussion on the theory of NMR, quadrupolar nuclei are asymmetrical and thus the nuclear magnetic quadrupole moments couple to the surrounding electric field gradient. Changes in intermolecular interactions may have a profound effect on this coupling, which influences the resulting lineshape by producing characteristic quadrupolar patterns. Xiong *et al.* *(211)* were able to study the influence of intermolecular interactions on by studying the quadrupolar line-shape of ^{2}D as a function of temperature. Through simulation of the characteristic line-shapes of ^{2}D labeled trichloroethylene, acetone, pyridine, and benzene, they were able to describe the local motion of these molecules while sorbed to environmental media. A similar study using ^{2}D was reported by Emery *et al. (212)*.

Changes in molecular mobility can be another important indicator of intermolecular interactions that can be studied using NMR spectroscopy. One common application of NMR to characterize

the mobility of a xenobiotic is high-resolution Magic Angle Spinning (HR-MAS), which uses magic angle spinning to reduce anisotropy in compounds that are unable to undergo isotropic motion *(228)*. The main use of HR-MAS is to distinguish between free xenobiotics, which do not require MAS to be observed; surface bound xenobiotics, which have some motion but still require MAS to fully remove anisotropy; and internally bound xenobiotics, which are difficult to observe by HR-MAS, but are easily resolved using high-powered solid-state NMR spectroscopy *(226-228)*. Another approach to studying the changes in the rates of xenobiotic motion by interactions with environmental matrices is to employed pulsed-field gradient (PFG) NMR to measure molecular self-diffusion. Fomba *et al.* studied the self-diffusion of toluene in Aldrich humic acid and observed a temperature dependent change in toluene diffusion that they attribute to a structural change in humic acid *(224)*. In another study employing PFG-NMR, Fomba *et al.* correlate the molecular motion of aliphatic components of humic acid to the attenuation of xenobiotic self-diffusion. In the solution-state, Dixon *et al.* used ^{19}F diffusion measurements to show that only a small quantity of 4-fluoro-1-aceto-napthene actually binds to fulvic acid in solution and, because there is fast exchange between bound and free forms of the xenobiotic, the bound form cannot be directly observed in the ^{19}F NMR spectrum *(164)*. Using similar approaches, Otto *et al.* showed the affect of the apparent diffusivity of humic acid on the presence of surfactant concentration *(229)*.

Thus far, the use of NMR spectroscopy to probe xenobiotic interactions in NOM, soils, and SOM has progressed from using NMR as a characterization tool used to correlate structure to macroscopic observations of sorption, to a more intensive molecular-level tool to probe how the environmental matrix affects observable properties of the xenobiotic, such as nuclear relaxation properties, or apparent diffusivity. Most of these studies have used NMR spectroscopy to probe how a xenobiotic is affected by its interactions with NOM. Studies of soil sorption directly at the molecular-level using NMR has moved the study of soil sorption phenomena as a whole closer to a reductionist point of view from a purely macroscopic understanding. Thus far, however, these NMR studies have all been undertaken from the vantage point of the xenobiotic with NOM being treated largely as a generic homogeneous, hydrophobic sorption domain. There is a growing wealth of NMR studies showing how various xenobiotics see NOM during their interactions, but almost no investigations on how NOM sees the xenobiotic molecules. NOM is not chemically homogeneous and direct molecular-level studies aimed at probing the interactions between

xenobiotics and NOM from the vantage point of the NOM itself are desperately needed for a truly useful reductionist understanding of xenobiotic-NOM interactions. The work in this dissertation aims to fill this gap. What is the nature of these interactions from the perspective of NOM, in particular SOM? SOM is a complex mixture; do all these components act as equals during soil sorption? It is through answering questions such these, that a full molecular-level picture of xenobiotic-NOM interactions will be prepared, and in doing so provide a framework to probe the molecular-level origin of soil sorption phenomenon, such as sequestration and bioaccessibility.

1.7 Outline of Dissertation

The central research question of this dissertation is '*what do xenobiotic interactions with NOM look like from the vantage of NOM itself?*'. This question is first addressed using the humic acid fraction of a peat soil, and then with the parent peat soil from which this humic acid was extracted. It is proposed here that using NMR spectroscopy, the occurrence of different processes occurring simultaneously at different sites within NOM can be observed directly at the molecular-level. Furthermore, using NMR, the observation of intermolecular interactions at multiple sites within a soil can be made essentially *in situ*, without significant modification or pretreatment of the soil. The general hypothesis that is tested in both humic acid and then the peat soil is that different components of soil-based NOM, will behave as discrete binding sites during interactions with xenobiotics and that these sites act using different mechanisms for dissimilar xenobiotic compounds.

These research goals are addressed here through five interconnected research studies that are in preparation or have been published in peer-reviewed journals in environmental chemistry. Chapter 2 begins by establishing a novel NMR technique to identify binding domains in complex environmental mixtures, Reverse-Heteronuclear Saturation Transfer Difference (RHSTD). Using RHSTD the hypothesis that dissimilar xenobiotic compounds will interact with different components of NOM is tested by comparing the bindings sites in dissolved humic acid for two dissimilar organofluorine compounds, perfluorooctanoic acid and heptafluoronaphthol.

In chapter 3, a preliminary investigation of the mechanistic nature of the apparent distribution of interactions at different domains of NOM is presented. Interactions with humic acid are compared for a suite of structurally similar monoaromatic organofluorine compounds, including the relationship between xenobiotic structure and preferred humic acid binding domain, and the orientation of those xenobiotics during their interaction. Here, differences in the amount of signal produced by the RHSTD experiment, and the distribution of interactions at different domains of humic acid, is related to varying physical properties of those organofluorine compounds.

Chapter 4 focuses on the mechanisms driving the associations between organofluorine xenobiotics and dissolved humic acid and probes the origin of the dissimilar interaction mechanisms proposed in chapter 2. The hypothesis tested is that desolvation by association with humic acid can largely explain the extent of interaction for those xenobiotic compounds that interact in a less-selective manner, driving the formation of associations, whereas for compounds with strong preference for a specific binding sites, desolvation has a minimal influence on the intermolecular-interactions formed.

Chapter 5 probes the mechanisms driving the distribution of interactions at different domains of humic acid for similar aromatic organofluorine compounds. This study investigates the relationship between the conformation of dissolved humic acid and the distribution of organofluorine interactions at different domains and probes the likelihood that specific interactions are necessarily responsible for apparent site selectivity.

Finally, in chapter 6 the same questions and hypothesis studied using humic acid in chapter 2 are studied in the parent peat soil in an attempt to apply the mechanistic knowledge of xenobiotic-NOM interactions gained in the previous chapters in the solution-state to a whole soil. This final research study represents a significant transition away from using humic acid as a proxy for SOM in general, and presents the first direct and *in situ* molecular-level elucidation of the interaction sites for some xenobiotics in a whole unmodified soil after sorption.

1.8 References

(1)   Manahan, S. E. *Environmental Chemistry*; CRC Press: Boca Raton, Fl, USA, 2005.

(2)   Sutton, R.; Sposito, G. Molecular structure in soil humic substances: the new view. *Environ. Sci. Technol.* **2005**, *39* (23), 9009-9015.

(3)   Karickhoff, S. W.; Brown, D. S.; Scott, T. A. Sorption of hydrophobic pollutants on natural sediments. *Water Research* **1979**, *13* (3), 241-248.

(4)   Lambert, S. M.; Porter, P. E.; Schieferstein, R. H. Movement and sorption of chemicals applied to the soil. *Weeds* **1965**, *13*, 185-190.

(5)   Lambert, S. M. Functional relationship between sorption in soil and chemical structure. *J. Agri. Food Chem.* **1966**, *15* (4), 572-576.

(6)   Chiou, C. T.; Peters, L. J.; Freed, V.H. A physical concept of soil-water equilibria for nonionic organic compounds. *Science* **1979**, *206* (4420), 831-832.

(7)   Chung, N.; Alexander, M. Differences in sequestration and bioavailability of organic compounds aged in dissimilar soils. *Environ. Sci. Technol.* **1998**, *32* (7), 855-860.

(8)   Karickhoff, S. W.; Morris, K. R. Sorption dynamics of hydrophobic pollutants in sediment suspensions. *Environ. Toxicol. Chem.* **1985,** *4* (4)*, 469-479.

(9)   Xing, B.; Pignatello, J. J.; Dual-mode sorption of low-polarity compounds in glassy poly(vinyl chloride) and soil organic matter. *Environ. Sci. Technol.* **1997**, *31* (3), 792-799.

(10)   Luthy, R. G.; Aiken, G. R.; Brusseau, M. L.; Cunningham, S. D.; Gschwend, P. M.; Pignatello, J. J.; Reinhard, M.; Traina, S. J.; Weber, W. J.; Westall, J. C. Sequestration of hydrophobic organic contaminants by geosorbants. *Environ. Sci. Technol.* **1997**, *31* (12), 3341-3347.

(11)   Weber, W. J.; McGinley, P. M.; Katz, L. E. A distributed reactivity model for sorption by soils and sediments. 1. Conceptual basis and equilibrium assessments. *Environ. Sci. Technol.* **1992***, 26* (10), 1955-1962.

(12)   Pedit, J. A.; Miller, C. T. Heterogeneous sorption processes in subsurface systems. 1. Model formulations and applications. *Environ. Sci. Technol.* **1994***, 28* (12), 2094-2104.

(13)   Richardson, M. Pesticides – friend or foe?. *Water Sci. Technol.* **1998**, *37* (8), 19-25.

(14)   Alexander, M. How toxic are toxic chemicals in soils?. *Environ. Sci. Technol.* **2005**, *29* (11), 2713-2717.

(15)   Odencrantz, J. E.; Vogl, R. A.; Varljen, M. D. Natural attenuation rate clarifications: The true picture is in the details. *Soil Sedi. Contam.* **2003**, *12* (5), 663-672.

(16)   Semple, K. T.; Morriss, A. W. J.; Paton, G. I. Bioavailability of hydrophobic organic contaminants in soils: fundamental concepts and techniques for analysis. *Euro. J. Soil Sci.* **2003**, *54* (4), 809-818.

(17)   Reid, B. J.; Jones, K. C.; Semple, K. T.; Bioavailability of persistent organic pollutants in soils and sediments – a perspective on mechanisms, consequences and assessment. *Environ. Poll.* **2000**, *108* (1), 103-112.

(18)   Muir, D. C. G.; Howards, P. H. Are there other persistent organic pollutants? A challenge for environmental chemists. *Environ. Sci. Technol.* **2006**, *40* (23), 7157-7166.

(19)   Adams, D. E. C.; Haiden, R. U. Fluorinated chemicals and the impacts of anthropogenic use. IN *Contaminants of Emerging Concern in the Environment: Ecological and Human Health Considerations*, Chapter 27, pp539-560. ACS Symposium Series, 2010.

(20)   Vermeulen, F.; Covaci, A.; D'Havé, H.; Van den Brink, N. W.; Blust, R.; De Coen, W.; Bervoets, L. Accumulation of background levels of persistent organochlorine and organobromine pollutants through the soil-earthworm-hedgehog food chain. *Environ. Inter.* **2010**, *36* (7), 721-727.

(21)   Nash, R. G.; Woolson, E. A.; Persistence of chlorinated hydrocarbon insecticides in soils. *Science* **1967**, *157* (3791), 924-927.

(22)   Dean, J. R.; Scott, W. C. Recent developments in assessing the bioavailability of persistent organic pollutants in the environment. *Trends Anal. Chem.* **2004**, *23* (9), 609-618.

(23)   Alexander, M. Aging, bioavailability, and overestimation of risk from environmental pollutants. *Environ. Sci. Technol.* **2000**, *34* (20), 4259-4265.

(24)   Semple, K. T.; Doick, K. J.; Jones, K. C.; Burauel, P.; Craven, A.; Harms, H. Defining bioavailability and bioaccessibility of contaminated soil and sediment is complicated. *Environ. Sci. Technol.* **2004**, *38* (12), 228a-231a.

(25)   Nam, K.; Alexander, M. Relationship between biodegradation rate and percentage of a compound that becomes sequestered in soil. *Soil Bio. Biochem.* **2001**, *33* (6), 787-792.

(26)   Robertson, B. K.; Alexander, M. Sequestration of DDT and dieldrin in soil: disappearance of acute toxicity but not the compounds. *Environ. Toxicol. Chem.* **1998***, 17* (6), 1034-1038.

(27)   Landrum, P. F.; Eadie, B. J.; Faust, W. R. Variation in the bioavailability of polycyclic aromatic hydrocarbons to the amphipod *Diporeia* (SPP.) with sediment aging. *Environ. Toxicol. Chem.* **1992**, *11* (8), 1197-1208.

(28)   Shu, H.; Teitelbaum, P.; Webb, A. S.; Marple, L.; Brunck, B.; Dei Rossi, D.; Muray, F. J.; Paustenbach, D. Bioavailability of soil-borne TCDD: dermal bioavailability in the rat. *Fund. App. Toxicol.* **1988**, *10* (1), 335-343.

(29)   Chai, Y.; Davis, J. W.; Saghir, S. A.; Qiu, X.; Budinsky, R. A.; Bartels, M. J. Effects of aging and sediment composition to oral bioavailability in rats. *Chemosphere* **2008**, *72* (3), 432-441.

(30)   White, J. C.; Alexander, M. Reduced biodegradability of desorption-resistant fractions of polycyclic aromatic hydrocarbons in soil and aquifer solids. *Environ. Toxicol. Chem.* **1996**, *15* (11), 1973-1978.

(31)   Carson, R. Silent Spring; Houghton Mifflin Company: Boston, 1962.

(32)   www.epa.gov/history accessed on June 2, 2012.

(33)   U.S. Department of Health and Human Services, Public Health Service, Agency for Toxic Substances and Disease Registry, Toxicological profile for DDT, DDE, and DDD, September 2002.

(34)   Hayes, W. The toxicity of dieldrin to man. *Bull. World Health Organ*. **1959**, *20* (5): 891-912.

(35)   Lucier, G. W.; Rumbaugh, R. C.; McCoy, Z.; Hass, R.; Harvan, D.; Albro, P. Ingestion of soil contaminated with 2,3,7,8-Tetrachlorodibenzo-p-dioxin (TCDD) alters hepatic enzyme activities in rats. *Fund. Appl. Toxicol.* **1986**, *6* (2), 364-371.

(36)   Fries, G. F.; Marrow, G. S.; Somich, C. J. Oral bioavailability of aged polychlorinated biphenyl residues contained in soil. *Bull. Environ. Contam. Toxicol.* **1989**, *43* (5), 683-690.

(37)   Fries, G. F. Bioavailability of soil-borne polybrominated biphenyls ingested by farm animals. *J. Toxicol. Environ. Health* **1985**, *16* (3-4), 565-579.

(38)   Moermond, C. T. A; Roessink, I.; Jonker, M. T. O.; Meijer, T.; Koelmans, A. A. Impact of polychlorinated biphenyl and polycyclic aromatic hydrocarbon sequestration in sediment on bioaccumulation in aquatic food webs. *Environ. Toxicol. Chem.* **2007**, *26* (4), 607-615.

(39)   Li, Z-J.; Xu, J-M.; Muhammad A.; Ma, G-R. Effect of bound residues of metsulfuron-methyl in soil on rice growth. *Chemosphere* **2005**, *58* (9), 1177-1183.

(40)   Beyer, W. N. Estimating toxic damage to soil ecosystems from soil organic matter profiles. *Ecotoxicology* **2001**, *10* (5), 273-283.

(41)   Bauhus, J.; Barthel, R. Mechanisms of carbon and nutrient release and retention in beech forest gaps. *Plant Soil.* **1995**, *168-169* (1), 585-592.

(42)   Birnbaum, L. S.; Tuomisto, J. Non-carcinogenic effects of TCDD in animals. *Food. Add. Contam*. **2000**, *17* (4), 275-288.

(43)   Safe, S. H. Polychlorinated biphenyls (PCBs): environmental impact, biochemical and toxic responses, and implications for risk assessment. *Critical Rev. Toxicol.* **1994**, *24* (2), 87-149.

(44)   EXTOXNET Pesticide Information Profile: Metsulfuron-methyl. **1996**.

(45)   Puglisi, E.; Vernile, P.; Bari, G.; Spagnuolo, M.; Trevisan, M.; de Lillo, E.; Ruggiero, P. Bioaccessibility, bioavailability and ecotoxicity of pentachlorophenol in compost amended soils. *Chemosphere* **2009**, *77* (1), 80-86.

(46)   Gevao, B.; Mordaunt, C.; Semple, K. T.; Piearce, T. G.; Jones, K. C. Bioavailability of nonextractable (bound) pesticide residues to earthworms. *Environ. Sci. Technol.* **2001**, *35* (3), 501-507.

(47)   Ahmad, R.; Kookana, R. S.; Megharaj, M.; Alston, A. M. Aging reduces the bioavailability of even a weakly sorbed pesticide (Carbaryl) in soil. *Environ. Toxicol. Chem.* **2004***, 23* (9), 2084-2089.

(48)   Hatzinger, P. B.; Alexander, M. Effect of aging of chemicals in soil on their biodegradability and extractability. *Environ. Sci. Technol.* **1995**, *29* (2), 537-545.

(49)   Gevao, B.; Semple, K. T.; Jones, K. C. Bound pesticide residues in soils: a review. *Environ. Poll.* **2000**, *108* (1), 3-14.

(50)   Sparks, D. L. *Environmental Soil Chemistry*, Second Edition; Elsevier: USA, 2003.

(51)   Kelleher, B. P.; Simpson, A. J. Humic substances in soils: are they really chemically distinct?. *Environ. Sci. Technol.* **2006**, *40* (15), 4605-4611.

(52)   Burdon, J. Are the traditional concepts of the structures of humic substances realistic. *Soil Sci.* **200**1, *166* (11), 752-769.

(53)   Fan, T. W-M.; Lane A. N.; Chekmenev, E.; Wittebort, R. J.; Higashi R. M. Synthesis and physico-chemical properties of peptides in soil humic substances. *J. Pep. Res.* **2004**, 63 (3), 253-264.

(54)   Simpson, A. J.; Kingery, W. L.; Spraul, M.; Humpfer, E.; Dvortsak, R.; Kerssebaum, R. Separation of structural components in soil organic matter by diffusion ordered spectroscopy. *Environ. Sci. Technol.* **2001***, 35* (22), 4421-4425.

(55)   Hertkorn, N.; Permin, A.; Perminova, I.; Kovalevskii, D.; Yudov, M.; Petrosyan, V.; Kettrup, A. Comparative analysis of partial structures of a peat humic and fulvic acid using one- and two-dimensional nuclear magnetic resonance spectroscopy. *J. Environ. Qual.* **2002**, *31* (2), 375-387.

(56)   Mao, J-D.; Xing, B.; Schmidt-Rohr, K. New structural information on a humic acid from two-dimensional ^{1}H-^{13}C Correlation solid-state nuclear magnetic resonance. *Environ. Sci. Technol.* **2001**, *35* (10), 1928-1934.

(57)   Jokic, A.; Wang, M. C.; Liu, C.; Frenkel, A. I.; Huang, P. M. Integration of the polyphenol and Maillard reactions into a unified abiotic pathway for humification in nature: The role of δ-MnO_2. *Org. Geochem. 35* (6), 747-762.

(58)   Ralph, J.; Lapierre, C.; Marita, J. M.; Kim, H.; Lu, F.; Hatfield, R. D.; Ralph, S.; Chapple, C.; Franke, R.; Hemm, M. R.; Van Doorsselaere, J.; Sederoff, R. R.; O'Malley, D. M.; Scott, J. T.; MacKay, J. J.; Yahiaoui, N.; Boudet, A-M.; Peani, M.; Pilate, G.; Jouanin, L.; Boerjan, W. Elucidation of new structures in lignins of CAD- and COMT-deficient plants by NMR. *Phytochem.* **2001**, *57* (6), 993-1003.

(59)   Simpson, A. J.; Kingery, W. L.; Hayes, M. H. B.; Spraul, M.; Humpfer, E.; Dvortsak, P.; Kerssebaum, R.; Godejohann, M.; Hofmann, M. Molecular structures and associations of humic substances in the terrestrial environment. *Naturwissenschaften* **2002**, *89* (2), 84-88.

(60)   Hu, W-G.; Mao, J-D.; Xing, B.; Schmidt-Rohr, K. Poly(methylene) crystallites in humic substances detected by nuclear magnetic resonance. *Environ. Sci. Technol.* **2000**, *34* (3), 530-534.

(61)   Zang, X.; van Heemst, J. D. H.; Dria, K. J.; Hatcher, P. G. Encapsulation of protein in humic acid from a histosol as an explanation for the occurrence of organic nitrogen in soil and sediment. *Org. Geochem.* **2000**, *31* (7-8), 679-695.

(62)   Simpson, A. J.; Simpson, M. J.; Smith, E.; Kelleher, B. P. Microbially derived inputs to soil organic matter: are current estimates too low?. *Environ. Sci. Technol.* **2007**, *41* (23), 8070-8076.

(63)   Mao, J-D.; Tremblay, L.; Gagné, J-P.; Kohl, S.; Rice, J.; Schmidt-Rohr, K. Humic acids from particulate organic matter in the Saguenay Fjord and the St. Lawrence Estuary investigated by advanced solid-state NMR. *Geochim. Cosmochim. Acta* **2007**, *71* (22), 5483-5499.

(64)   Fan, T. W-M.; Higashi R. M.; Lane A. N. Chemical characterization of a chelator-treated soil humate by solution-state multinuclear two-dimensional NMR with FTIR and pyrolysis-GCMS. *Environ. Sci. Technol.* **2000**, *34* (9), 1636-1646.

(65)   Simpson, A. J.; McNally, D. J.; Simpson, M. J. NMR spectroscopy in environmental research: From molecular interactions to global processes. *Prog. Magn. Reson. Spect.* **2010**, *58* (3), 97-175.

(66)   Piccolo, A. The supramolecular structure of humic substances. *Soil Sci.* **2001**, *116* (11), 810-832.

(67)   Engebretson, R. R.; Von Wandruszka, R. The effect of molecular size on humic acid associations. *Org. Geochem.* **1997**, *26* (11-12), 759-767.

(68)   Piccolo, A.; Spiteller M. Electrospray ionization mass spectrometry of terrestrial humic substances and their size fractions. *Anal. Bioan. Chem.* **2003**, *377* (6), 1047-1059.

(69)   Stenson, A. C.; Landing, W. M.; Marshall, A. G.; Copper, W. T. Ionization and fragmentation of humic substances in electrospray ionization Fourier transform-ion cyclotron resonance mass spectrometry. Anal. *Chem.* **2002**, *74* (17), 4397-4409.

(70)   Leenheer, J. A.; Rostad, C. E.; Gates, P. M.; Furlong, E. T.; Ferrer, I. Molecular resolution and fragmentation of fulvic acid by electrospray ionization/multistage tandem mass spectrometry. *Anal. Chem.* **2001**, *73* (7), 1461-1471.

(71)   Simpson, A. J. Determining the molecular-weight, aggregation, structures and interactions of natural organic matter using diffusion ordered spectroscopy. *Magn. Reson. Chem.* **2002**, *40* (13), S72-S82.

(72)   Cook, R. L.; McIntyre, D. D.; Langford, C. H.; Vogel, H. J. A comprehensive liquid-state heteronuclear and multidimensional NMR study of Laurentian fulvic acid. *Environ. Sci. Technol.* **2003,** *37* (17), 3935-3944.

(73)   Simpson, A. J.; Burdon, J.; Graham, C. L.; Hayes, M. H. B.; Spencer, N.; Kingery, W. L. Interpretation of heteronuclear and multidimensional NMR spectroscopy of humic substances. *Euro. J. Soil Sci.* **2001**, *52* (3), 495-509.

(74)   Slichter, C. P. *Principles of Magnetic Resonance, Third Enlarged and Updated Edition*; Springer-Verlag: New York, 1989.

(75)   Rumpel, C.; Rabia, N.; Derenne, S.; Quenea, K.; Eusterhues, K.; Kögel-Knabner, I.; Mariotti, A. Alteration of soil organic matter following treatment with hydrofluoric acid (HF). Org. Geochem. **2006**, *37* (11), 1437-1451.

(76)   Keeler, C.; Maciel, G. E. Quantitation in the solid-state ^{13}C NMR analysis of soil and organic soil fractions. *Anal. Chem.* **2003**, *75* (10), 2421-2432.

(77)   Simpson, M. J. Nuclear Magnetic Resonance Based Investigations of Contaminant Interactions with Soil Organic Matter. *Soil Sci. Soc. Am. J.* **2006**, 70 (3), 995-1004.

(78) Schwarzenbach, R. P.; Gschwend, P. M.; Imboden, D. M. *Environmental Organic Chemistry, Second Edition.* Wiley Interscience, Hoboken, USA. **2003**.

(79) Weber, W. J.; Miller, C. T. Modeling the sorption of hydrophobic contaminants by aquifer materials – I. *Water Res.* **1988**, *22* (4), 457-464.

(80) Spurlock, F. C.; Biggar, J. W. Thermodynamics of organic chemical partition in soils. 2. Nonlinear partition of substituted phenylureas from aqueous solution. *Environ. Sci. Technol.* **1994**, *28* (6), 996-1002.

(81) Xing, B.; Pignatello, J. J.; Gigliotti, B. Competitive sorption between atrazine and other organic compounds in soils and model sorbents. *Environ. Sci. Technol.* **1996**, *30* (8), 2432-2440.

(82) Gunasekara, A. S.; Simpson, M. J.; Xing, B. Identification and characterization of sorption domains in soil organic matter using structurally modified humic acids. *Environ. Sci. Technol.* **2003**, *37* (5), 852-858.

(83) Wu, S-C.; Gschwend, P. M. Sorption kinetics of hydrophobic organic compounds to natural sediments and soils. *Environ. Sci. Technol.* **1986**, *20* (7), 717-725.

(84) Rutherford, D. W.; Chiou, C. T. Effect of water saturation in soil organic matter on the partition of organic compounds. *Environ. Sci. Technol.* **1992**, *26* (50), 965-970.

(85) McGinley, P. M.; Katz, L. E.; Weber, W. J. A distributed reactivity model for sorption by soils and sediments. 2. Multicomponents systems and competitive effects. *Environ. Sci. Technol.* **1993**, *27* (8), 1524-1531.

(86) Endo, S.; Grathwohl, P.; Haderlein, S. B.; Schmidt, T. C. Characterization of sorbent properties of soil organic matter and carbonaceous geosorbents using n-Alkanes and cycloalkanes as molecular probes. *Environ. Sci. Technol.* **2009**, *43* (2), 393-400.

(87) Accardi-Dey, A.; Gschwend, P. M. Assessing the combined roles of natural organic matter and black carbon as sorbents in sediments. *Environ. Sci. Technol.* **2002**, *36* (1), 21-29.

(88)   Cornelissen, G.; Gustfsson, O. **2004**. Sorption of phenanthrene to environmental black carbon in sediment with and without organic matter and native sorbates. *Environ. Sci. Technol.* **2004***, 38* (1), 148-155.

(89)   Garbarini, D. R.; Lion, L. W. Influence of the nature of soil organics on the sorption of toluene and trichloroethylene. *Environ. Sci. Technol.* **1986**, *20* (12), 1263-1269.

(90)   Rutherford, D. W.; Chiou, C. T.; Kile ,D. E. Influence of soil organic matter composition on the partition of organic compounds. *Environ. Sci. Technol.* **1992**, *26* (2), 336-340.

(91)   Gauthier, T. D.; Seltz, W. R.; Grant, C. L. Effects of structural and compositional variations of dissolved humic materials on pyrene K_{OC} values. *Environ. Sci. Technol.* **1987**, *21* (3), 243-248.

(92)   Xing, B.; McGill, W. B.; Dudas, M. J. Sorption of α-naphthol onto organic varying in polarity and aromaticity. *Chemosphere* **1994**, *28* (1), 145-153.

(93)   Kile, D. E.; Chiou, C. T.; Zhou, H.; Li, H.; Xu, O. Partition of nonpolar organic pollutants from water to soil and sediment organic matters. *Environ. Sci. Technol.* **1995**, *29* (5), 1401-1406.

(94)   Kottler, B. D.; Alexander, M. Relationship of properties of polycyclic aromatic hydrocarbons to sequestration in soil. *Environ. Poll.* **2001**, *113* (3), 293-298.

(95)   Weber, W. J. Jr.; Huang, W. A distributed reactivity model for sorption by soils and sediments. 4. Intraparticle heterogeneity and phase-distribution relationships under nonequilibrium conditions. *Environ. Sci. Technol.* **1996**, *30* (3), 881-888.

(96)   LeBoeuf, E. J.; Weber, W. J. Jr. A distributed reactivity model for sorption by soils and sediments. 8. Sorbent organic domains: discovery of a humic acid glass transition and an argument for a polymer-based model. *Environ. Sci. Technol.* **1997**, *31* (6), 1697-1702.

(97)   Huang, W.; Weber, W. J. Jr. A distributed reactivity model for sorption by soils and sediments. 10. Desorption, hysteresis, and the chemical characteristics of organic domains. *Environ. Sci. Technol.* **1997**, *31* (9), 2562-2569.

(98) Endo, S.; Grathwohl, P.; Haderlein, S. B.; Schmidt, T. C. LFERs for soil organic carbon-water distribution coefficients (K_{OC}) at environmentally relevant sorbate concentrations. *Environ. Sci. Technol.* **2009**, *43* (9), 3094-3100.

(99) Sander, M.; Pignatello, J. J. On the reversibility of sorption to black carbon: distinguishing true hysteresis from artificial hysteresis caused by dilution of a competing adsorbate. *Environ. Sci. Technol.* **2007**, *41* (3), 843-849.

(100) Pignatello, J. J. **1998**. Soil organic matter as a nanoporous sorbent of organic pollutants. *Adv. Coll. Inter. Sci.* **1998**, *76-77*, 445-467.

(101) Xia, G.; Pignatello, J. J. Detailed sorption isotherms of polar and apolar compounds in high-organic soil. *Environ. Sci. Technol.* **2001**, *35* (1), 84-94.

(102) Chiou, C. T.; Kile, D. E. Deviations from sorption linearity on soils of polar and nonpolar organic compounds at low relative concentrations. *Environ. Sci. Technol.* **1998***, 32* (3), 338-343.

(103) Xiao, B.; Yu, Z.; Huang, W.; Song, J.; Peng, P. Black carbon and kerogen in soils and sediments. 2. Their roles in equilibrium sorption of less-polar organic pollutants. *Environ. Sci. Technol.* **2004**, *38* (22), 5842-5852.

(104) Ran, Y.; Sun, K.; Yang, Y.; Xing, B.; Zeng, E. Strong sorption of phenanthrene by condensed organic matter in soils and sediments. *Environ. Sci. Technol.* **2007**, *41* (11), 3952-3958.

(105) Laor, Y.; Rebhun, M. Evidence for nonlinear binding of PAHs to dissolved humic acids. *Environ. Sci. Technol.* **2002**, *36* (5), 955-961.

(106) Pan, B.; Ghosh, S.; Xing, B. Nonideal binding between dissolved humic acids and polyaromatic hydrocarbons. *Environ. Sci. Technol.* **2007**, *41* (18), 6472-6478.

(107) Lueking, A. D.; Huang, W.; Soderstrom-Schwarz, S.; Kim, M.; Weber, W. J. Jr. Relationship of soil organic matter characteristics to organic contaminant sequestration and bioavailability. *J. Environ. Qual.* **2000**, *29* (1), 317-323.

(108) Perminova, I. V.; Grechishcheva, N. Y.; Petrosyan, V. S. Relationships between structure and binding affinity of humic substances for polycyclic aromatic hydrocarbons: relevance of molecular descriptors. *Environ. Sci. Technol.* **1999**, *33* (21), 3781-3787.

(109) Chefetz, B.; Deshmukh, A. P.; Hatcher, P. G.; Guthrie, E. A. Pyrene sorption by natural organic matter. *Environ. Sci. Technol.* **2000**, *34* (14), 2925-2930.

(110) Stimler, K.; Xing, B.; Chefetz, B. Transformation of plant cuticles in soil: effect on their sorptive capabilities. *Soil Sci. Am. J.* **2006**, *70*, 1101-1109.

(111) Chen, B.; Johnson, E. J.; Chefetz, B.; Zhu, L.; Xing, B. Sorption of polar and nonpolar aromatic organic contaminants by plant cuticular materials: role of polarity and accessibility. *Environ. Sci. Technol.* **2005**, *39* (16), 6138-6146.

(112) Flogeac, K.; Guillon, E.; Aplincourt, M. Effect of metallic cations on the sorption of pesticides on soil. *Environ, Chem. Lett.* **2005**, *3* (2), 86-90.

(113) Murphy, E. M.; Zachara, J. M.; Smith, S. C.; Phillips, J. L.; Wietsma, T. W. Interaction of hydrophobic organic compounds with mineral-bound humic substances. *Environ. Sci. Technol.* **1994**, *28* (7), 1291-1299.

(114) Wang, X.; Xing, B. Importance of structural makeup of biopolymers for organic contaminant sorption. *Environ. Sci. Technol.* **2007**, *41* (10), 3559-3565.

(115) Chefetz, B.; Xing, B. Relative role of aliphatic and aromatic moieties as sorption domains for organic compounds: a review. *Environ. Sci. Technol.* **2009**, *43* (6), 1680-1688.

(116) Golding, C. J.; Smernik, R. J.; Birch, G. F. Investigation of the role of structural domains identified in sedimentary organic matter in sorption of hydrophobic organic compounds. *Environ. Sci. Technol.* **2005**, *39* (11), 3925-3932.

(117) Mao, J. D.; Hundal, L. S.; Thompson, M. L.; Schmidt-Rohr, K. Correlation of Poly(methylene)-rich amorphous aliphatic domains in humic substances with sorption of nonpolar organic contaminant, phenanthrene. *Environ. Sci. Technol.* **2002**, *36* (5), 929-936.

(118) Wijnja, H.; Pignatello, J. J.; Malekani, K. Formation of π-π complexes between phenanthrene and model π-acceptor humic subunits. *J. Environ. Qual.* **2004**, *33* (1), 25-275.

(119) Akkanen, J.; Tuikka, A.; Kukkonen, J. V. Comparative sorption and desorption of benzo[a]pyrene and 3,4,3',4'-Tetraclhorobiphenyl in natural lake water containing dissolved organic matter. *Environ. Sci. Technol.*, **2005**, *39* (19), 7529-7534.

(120) Chiou, C. T.; Malcom, R. L.; Brinton, T. I.; Kile, D. E. Water solubility enhancement of some organic pollutants and pesticides by dissolved humic and fulvic acids. *Environ. Sci. Technol.* **1986**, *20* (5) 502-508.

(121) Shi, X.; Fu, H.; Li, Y.; Mao, J.; Zheng, S.; Zhu, D. Impact of coal structural heterogeneity on the nonideal sorption of organic contaminants. *Environ. Toxicol. Chem.* **2011**, *30* (6), 1310-1319.

(122) Sander, M.; Pignatello, J. J. Characterization of charcoal adsorption sites for aromatic compounds: Insights drawn from single solute and bi-solute competitive experiments *Environ. Sci. Technol.* **2005**, *39* (6), 1606-1615.

(123) Luo, L.; Zhang, S.; Ma, Y. Evaluation of impacts of soil fractions on phenanthrene sorption. *Chemosphere* **2008**, *72* (6), 891-896.

(124) Smith, K. E. C.; Thullner, M.; Wick, L. Y.; Harms, H. Sorption to humic acids enhances polycyclic aromatic hydrocarbon biodegradation. *Environ. Sci. Technol.* **2009**, *43* (19), 7205-7211.

(125) Ter Laak, T. L.; Ter Bekke, M. A.; Hermens, J. L. M. Dissolved organic matter enhances transport of PAHs to aquatic organisms. *Environ. Sci. Technol.* **2009**, *43* (19), 7212-7217.

(126) Barriuso, E.; Benoit, P.; Dubus, I. G. Formation of pesticide nonextractable (Bound) residues in soil: magnitude, controlling factors and reversibility. *Environ. Sci. Technol.* **2008,** *42* (6), 1845-1854.

(127) Hatcher, P. G.; Bortiatynski, J. M.; Minard, R. D.; Dec, J.; Bollag, J-M. Use of high-resolution ^{13}C NMR to examine the enzymatic covalent binding of ^{13}C-labelled 2,4-dichlorophenol to humic substances. *Environ. Sci. Technol.* **1993**, *27* (10), 2098-2103.

(128) Simpson, M. J.; Simpson, A. J.; Hatcher, P. G. Noncovalent interactions between aromatic compounds and dissolved humic acid examined by nuclear magnetic resonance spectroscopy. *Environ. Toxicol. Chem.* **2004**, *23* (2) 334-362.

(129) Chiou, C. T.; Kile, D. E.; Rutherford, D. W. Sorption of selected organic compound from water to a peat soil and its humic-acid and humin fractions: potential source of the sorption nonlinearity. *Environ. Sci. Technol.* **2000**, *34* (7), 1254-1258.

(130) Zhu, D.; Hyun, S.; Pignatello, J. J.; Lee. L. S. Evidence for π-π donor-acceptor interactions between π-donor aromatic compounds and π-acceptor sites in soil organic matter through pH effects on sorption. *Environ. Sci. Technol.* **2004**, *38* (16), 4361-4368.

(131) Keiluweit, M.; Kleber, M. Molecular-level interactions in soils and sediments: the role of aromatic π-Systems. *Environ. Sci. Technol.* **2009**, *43* (10). 3421-3429.

(132) Chung, N.; Alexander, M. Effect of soil properties on bioavailability of phenanthrene and atrazine sequestration in soil. *Chemosphere* **2002**, *48* (1), 109-115.

(133) Endo, S.; Grathwohl, P.; Haderlein, S. B.; Schmidt, T. C. Compound-specific factors influencing sorption nonlinearity in natural organic matter. *Environ. Sci. Technol.* **2008**, *42* (16), 5897-5903.

(134) Oliver, M. A. Soil and human health: a review. *Euro. J. Soil Sci.* **1997**, 48 (4), 573-592.

(135) Gribble G.W. Naturally occurring organofluorines, Chapter 5, *The Handbook of Environmental Chemistry Vol.3, Part N: Organofluorine,* Springer-Verlag, Berlin, 2002. pp122-136.

(136) Singh, A.; Jolly, S. S.; Bansal, B. C.; Mathur, C. C. Endemic fluorosis: epidemiological, clinical and biochemical study of chronic fluorine intoxication in Panjaei (India). *Medicine* **1963**, 42 (3), 229-246.

(137) Arnesen, A. K. M.; Abrahamsen, G.; Sandvik, G.; Krogstad, T. Aluminum-smelters and fluoride pollution of soil and soil solution in Norway. *Sci. Tot. Environ,* **1995**, *163* (1-3), 39-53.

(138) Cronin, S. J.; Manoharan, V.; Hedley, M. J.; Loganathan, P. Fluoride: A review of its fate, bioavailability, and risks of fluorosis in grazed-pasture systems in New Zealand. *New Zea. J. Agri. Res.* **2000***,* 43 (3), 295-321.

(139) Loganathan, P.; Hedley, M. J.; Grace, N. D.; Lee, J.; Grace, N. D.; Bolan, N. S.; Zanders, J. M. Fertiliser contaminants in New Zealand grazed-pasture with special reference to cadmium and fluorine: a review. *Austra. J. Soil Res.* **2003**, *41* (3), 501-532.

(140) O'Hagen D.; Harper D. B. Fluorine-containing natural products. *J. Fluor. Chem.* **1999**, *100* (1-2), 127-133.

(141) Jordan, A.; Harnisch, J.; Borchers, R.; Le Guerm, F.; Shonohara, H. Volcanogenic halocarbons. *Environ. Sci. Technol. 34* (6), 1122-1124.

(142) Isidorov, V. A.; Prilepsky, E. B.; Povarov, V. G. Photochemically and optically active components of minerals and gas emissions of mining plants. *J. Ecolog. Chem.* **1993**, *2-3*, 201-207.

(143) Marois, J. S. C. Monofluoroacetic acid, the toxic principle of "gifblaar", *Dichapetalum cymosum*. *Onderstepoort J. Vet. Sci. Anim. Ind.* **1943***, 20*, 67-73.

(144) Peters, R. A.; Shorthouse, M. Fluorocitrate in plants and food stuffs. *Phytochem.* 1972, *11*, 1337-1338.

(145) Manzer, L. E. The CFC-ozone issue: Progress on the development of alternatives to CFCs. *Science*, *249* (4964), 31-35.

(146) Lau, C.; Anitole, K.; Hodes, C.; Lai, D.; Pfahles-Hutchens, A.; Seed, J. Perfluoroalkyl Acids: A review of Monitoring and Toxicological Findings. *Toxicol. Sci.* **2007**, *99* (2), 366-394.

(147) Murphy, C. D. The application of ^{19}F nuclear magnetic resonance to investigate microbial biotransformations of Organofluorine Compounds. *OMICS: J. Integra. Bio*. **2007**, *11* (3), 314-324.

(148) Ellis, D. A.; Cahill T. M.; Mabury S. A.; Cousins I. T.; Mackay D. Chapter 2: Partitioning of Organofluorine compounds in the Environment IN: *The Handbook of Environmental Chemistry Vol.3, part N Organofluorines*. **2002**, pp.64-83.

(149) Collings, J. C.; Batsanov, A. S.; Howard, J. A. K.; Marder, T. B. Arene-perfluoroarene interactions in crystal engineering. Part 14. 1:1 Complexes of octafluoronaphthalene with fluorine and 9,10-dihydrophenanthrene. *Can. J. Chem.*, **2006**, *84*, 238-242.

(150) Ellis, D. A.; Denkenberger, K. A.; Burrow, T. E.; Mabury, S. A. The use of ^{19}F NMR to interpret the structural properties of perfluorocarboxylate acids: a possible correlation with their environmental disposition. *J. Phys. Chem. A*. **2004**, *108* (46), 10099-10106.

(151) Liu, J.; Lee, L. S. Effect of fluorotelomer alcohol chain length on aqueous solubility and sorption by soils. *Environ. Sci. Technol.* **2007**, *41* (15), 5357-5362.

(152) D'Eon, J. C.; Hurley, M. D.; Wallington, T. J.; Mabury, S. A. Atmospheric chemistry of N-methyl perfluorobutane sulfonamidoethanol, $C_4F_9SO_2N(CH_3)CH_2CH_2OH$: Kinetics and mechanism of reaction with OH. *Environ. Sci. Technol.* **2006**, *40* (6), 1862-1868.

(153) Prevedouros, K.; Cousins, I. T.; Buck, R. C.; Korzeniowski, S. H. Sources, fate and transport of perfluorocarboxylates. *Environ. Sci. Technol.* **2006**, *40* (1), 32-44.

(154) Condor, J. W.; Hoke, R. A.; De Wolf, W.; Russell, M. H.; Buck, R. C. Are PFCA's bioaccumulative? A Critical review and comparison with regulatory criteria and persistent lipophilic compounds. *Environ. Sci. Technol.* **2008**, *42* (4), 995-1003.

(155) Wania, F. A global mass balance analysis of the source of perfluorocarboxylic acids in the arctic ocean. *Environ. Sci. Technol.* **2007**, *41* (13), 4529-4535.

(156) Langer, V.; Dreyer, A.; Ebinghaus, R. Polyfluorinated compounds in residential and nonresidential indoor air. *Environ. Sci. Technol.* **2010**, *44* (21), 8075-8081.

(157) Moody, C. A.; Martin, J. W.; Kwan, W. C.; Muir, D. C. G.; Mabury, S. A. Monitoring perfluorinated surfactants in biota and surface water samples following an accidental release of fire-fighting foam into Etobicoke Creek. *Environ. Sci. Technol.* **2002**, *36* (4), 545-551.

(158) Higgins, C. P.; Field, J. A.; Criddle, C. S.; Luthy, R. G. Quantitative determination of perfluorochemicals in sediments and domestic sludge. *Environ. Sci. Technol.* **2005**, *39* (11), 3946-3956.

(159) Giesy, J. P.; Kannan, K. Global distribution of perfluorooctane Sulfonate in wildlife. *Environ. Sci. Technol.* **2001**, *35* (7), 1339-1342.

(160) Martin, J. W.; Whittle, D. M.; Muir, D. C. G.; Mabury, S. A. Perfluoroalkyl contaminants in food web from Lake Ontario. *Environ. Sci. Technol.* **2004**, *38* (20), 5379-5385.

(161) Martin, J. W.; Smithwick, M. W.; Braune, B. M.; Hoekstra, P. F.; Muir, D. C. G.; Mabury, S. A. Identification of long-chain perflourinated acids in biota from the Canadian arctic. *Environ. Sci. Technol.* **2004**, *38* (2), 373-380.

(162) D'Eon, J. C.; Simpson, A. J.; Kumar, R.; Baer, A. J.; Mabury, S. A. Determining the molecular interactions of perfluorinated carboxylic acids with human sera and isolated human serum albumin using nuclear magnetic resonance spectroscopy. *Environ. Toxicol. Chem.* **2010**, *29* (8), 1678-1688.

(163) Ellis, D. A.; Martin, J. W.; Muir, D. C. G.; Mabury, S. A. Development of an ^{19}F NMR method for the analysis of fluorinated acids in environmental water samples. *Anal. Chem.* **2000**, *72* (4), 726-731.

(164) Dixon, A. M.; Mai, M. A.; Larive, C. K. NMR investigation of the interactions between 4'-Fluoro-1'acetonaphtone and the Suwannee river fulvic acid. *Environ. Sci. Technol.* **1999**, *33* (6), 958-964.

(165) Smejkalová, D.; Spaccini, R.; Fontaine, B.; Piccolo, A. Binding of phenol and differently halogenated phenols to dissolved humic matter as measured by NMR spectroscopy. *Environ. Sci. Technol.* **2009**, *43* (14), 5377-5382.

(166) Longstaffe, J. G.; Simpson, A. J. Understanding solution-state noncovalent interactions between xenobiotics and natural organic matter using ^{19}F/^{1}H heteronuclear saturation transfer difference nuclear magnetic resonance spectroscopy. *Environ. Toxicol. Chem*. **2011**, *30* (8), 1745-1753.

(167) Longstaffe, J. G.; Simpson, M. J.; Maas, W.; Simpson, A. J. Identifying components in dissolved humic acid that bind organofluorine contaminants using [1]H{[19]F} reverse heteronuclear saturation transfer difference NMR spectroscopy. *Environ. Sci. Technol.* **2010**, *44* (14), 5476-5482.

(168) Kohl, S. D.; Toscano, P. J.; Hou, W.; Rice, J. A. Solid-state ^{19}F NMR investigation of hexafluorobenzene sorption to soil organic matter. *Environ. Sci. Technol.* **2000**, *34* (1), 204-210.

(169) Khalaf, M.; Kohl, S. D.; Klumpp, E.; Rice, J. A.; Tombacz, E. Comparison of sorption domains in molecular weight fractions of a soil humic acid using solid-state ^{19}F NMR. *Environ. Sci. Technol.* **2003**, *37* (13), 2855-2860.

(170) Strynar, M.; Dec, J.; Benesi, A.; Jones, A. D.; Fry, R. A.; Bollag, J. M. Using ^{19}F NMR spectroscopy to determine trifluralin binding to soil. *Environ. Sci. Technol.*, **2004**, *38* (24), 6645-6656.

(171) Nanny, M.A. Proton and ^{19}F NMR spectroscopy of pesticide intermolecular interactions. IN *Nuclear Magnetic Resonance Spectroscopy in Environmental Chemistry*. **1997**, Oxford University Press: New York.

(172) Simpson, M. J.; Simpson, A. J.; Gross, D.; Spraul, M.; Kingery, W. L. [1]H and ^{19}F nuclear magnetic resonance microimaging of water and chemical distribution in soil columns. *Environ. Toxicol. Chem.* **2007**, *26* (7), 1340-1348.

(173) Keeler, J. *Understanding NMR Spectroscopy*; John Wiley & Sons Ltd: England, 2005.

(174) Levitt, M. H, *Spin Dynamics, Second Edition*; John Wiley & Sons Ltd: England, 2008.

(175) Gorter, C. J. Negative results in an attempt to detect nuclear magnetic spins. *Physica* **1936**, *3*, 995-998.

(176) Gorter, C. J.; Broer, L. J. F. Negative result of an attempt to observe nuclear magnetic resonance in solids. *Physica* **1942**, *9*, 591-596.

(177) Cohen, B.L. *Concepts of Nuclear Physics*; McGraw-Hill Book Company: New York, 1971.

(178) Rabi, I. I.; Zacharias, J. R.; Millman, S.; Kusch, P. A new method of measuring nuclear magnetic moment. *Phys. Rev.* **1938**, *53*, 318.

(179) Bloch, F.; Hansen, W. W.; Packard, M. The nuclear induction experiment. *Phys. Rev.* **1946**, *70* (7-8), 474-485.

(180) Bloch, F. Nuclear induction. *Phys. Rev.* **1946**, *70* (7-8), 460-474.

(181) Purcell, E. M.; Torrey, H. C.; Pound, R. V. Resonance absorption by nuclear magnetic moments in a solid. *Phys. Rev.* **1946**, *69*, 37-38.

(182) Pavia, D. L.; Lampman, G. M.; Kriz, S. G. *Introduction to spectroscopy, 3rd Edition*; Brooks-Cole: Belmont, CA, USA, 2001.

(183) Abragham, A. *The Principles of Nuclear Magnetism*; Oxford University Press: Great Britain, 1961.

(184) Harris, R. K. IN *Encyclopedia of Nuclear Magnetic Resonance*, D.M. Granty and R.K. Harris, (eds.), vol. 5, John Wiley & Sons, Chichester, UK, 1996.

(185) Witte, E. G.; Philipp, H.; Vereecken, H. Binding of ^{13}C-labelled 2-aminobenzothiazoles to humic acid as derived from ^{13}C NMR spectroscopy. *Org. Geochem.* **1999**, *29* (5-7), 1829-1835.

(186) Chamignon C.; Haroune N.; Forano C.; Delort A.M.; Besse-Hoggan P.; Combourieu B. Mobility of organic pollutants in soil components. What role can magic angle spinning NMR play?. *Euro. J. Soil Sci.* **2008**, 59 (3), 572-583.

(187) Käcker, T.; Haupt, E. T. K.; Garms, C.; Francke, W.; Steinhart, H. Structural characterization of humic acid-bound PAH residues in soil by ^{13}C-CPMAS-NMR-spectroscopy: evidence of covalent bonds. *Chemosphere* **2002**, *48* (1), 117-131.

(188) Tao, T.; Maciel, G. E. Interactions of methyl bromide with soil. *Environ. Sci. Technol.* **2002**, *36* (4), 603-607.

(189) Thorn, K. A.; Kennedy, K. R. ^{15}N NMR investigation of the covalent binding of reduced TNT amines to soil humic acid, model compounds, and lignocellulose. *Environ. Sci. Technol.* **2002**, *36* (17), 3787-3796.

(188) Knicker, H. Incorporation of ^{15}N-TNT transformation products into humifying plant organic matter as revealed by one- and two-dimensional solid state NMR Spectroscopy. *Sci. Tot. Environ.* **2003**, *308* (1-3), 211-220.

(189) Reynhardt, E. C. A nuclear magnetic resonance study of H-1, Na-23, and P-31 relaxation and molecular dynamics in the sodium-salts of some pyrophosphates. *Can. J. Phys.* **1989**, 67, 592-598.

(190) Longstaffe, J. G.; Werner-Zwanziger, U.; Schneider, J. F.; Nascimento, M. L. F.; Zanotto, E. D.; Zwanziger, J. W. Intermediate-range order of alkali disilicate glasses and its relation to the devitrification mechanisms. *J. Phys. Chem. C* **2008**, *112* (15), 6151-6159.

(193) Longstaffe, J. G. A solid-state NMR study of the intermediate-range order of alkali disilicate glasses and its relationship to crystallization behaviour. MSc Thesis, Department of Chemistry, Dalhousie University, Halifax, Nova Scotia, Canada

(194) Slichter, C. P. Concept of temperature and the overhauser nuclear polarization effect. Phys. Rev. 1955, *99* (6), 1822-1823.

(195) Mayer, M.; Meyer, B. Characterization of ligand binding by saturation transfer difference NMR spectroscopy. *Angew. Chem. Int. Ed.* **1999**, *38* (12)*, 1784-1788.

(196)   Diercks, T.; Riberio, J.P.; Canada, F. J.; André. S.; Jiménez-Barbero, J.; Gabius, H-J. Fluorinated carbohydrates as lectin ligands: Versatile Sensors in ^{19}F-detected saturation transfer difference NMR spectroscopy. *Chem. Eur. J.* **2009,** *15* (23), 5666-5668.

(197)   Mayer, M.; Meyer, B. Group epitope mapping by saturation transfer difference NMR to identify segments of a ligand in direct contact with a protein receptor. *J. Am. Chem. Soc.* **2001**, *123* (25)*,* 6108-6117.

(198)   Bloembergen, N.; Purcell, E. M.; Pound, R. V. Relaxation effects in nuclear magnetic resonance absorption. *Phys. Rev.* 1948, *73* (7), 679-712.

(199)   Duer, M. J. *Introduction to Solid-State NMR Spectroscopy*; Blackwell Publishing: Oxford, UK, 2004.

(200)   Herzog, B.; Hahn E. L. Transition nuclear induction and double nuclear resonance in solids. *Phys. Rev.* **1956**, *103* (1), 148-166.

(201)   Gullion, T.; Schaefer, J. Rotational-echo double-resonance NMR. *J. Mag. Reson.* **1989**, *81* (1)*,* 196-200.

(202)   Marshall, G. R.; Beusen, D. D.; Kociolek, K.; Redlinski, A. S.; Leplawy, M. T.; Pan, Y.; Schaefer J. Determination of precise interatomic distance in helical peptide by REDOR NMR. *J. Am. Chem. Soc.* **1990**, *112* (3), 936-966.

(203)   Longstaffe, J. G.; Chen, B.; Huang, Y. Characterization of the amorphous phases formed during the synthesis of microporous material $AlPO_4$-5. *Micro. Meso. Mater.* **2007**, *98* (1-3), 21-28.

(204)   Grey, C. P.; Veeman, W. S. The detection of weak heteronuclear coupling between spin 1 and spin ½ nuclei in MAS NMR; ^{14}N/^{13}C/^{1}H triple resonance experiments. *Chem. Phys. Lett.* **1992**, *192* (4), 379-385.

(205)   Wu, D.; Chen, A.; Johnson, C. S.; An improved diffusion-ordered spectroscopy experiment incorporating bipolar-gradient pulses. *J. Magn. Reson., Ser. A*, **1995**, *115* (2), 260-264.

(206) Derrick, T. S.; Lucas, L. H.; Dimicoli, J-L.; Larive, C. K. ^{19}F diffusion NMR analysis of enzyme-inhibitor bindings. *Magn. Reson. Chem.* **2002***, 40* (13), S98-S105.

(207) Delort, A-M.; Combourieu, B.; Haroune, N. Nuclear magnetic resonance studies of interactions between organic pollutants and soil components, a review. *Environ. Chem. Lett.* **2004**, *1* (4), 209-213.

(208) Nanny, M. A. Deuterium NMR characterization of noncovalent interactions between monoaromatic compounds and fulvic acid. *Org. Geochem.* **1999**, *30* (8), 901-909.

(209) Nanny ,M. A.; Maza J. P. Noncovalent interactions between monoaromatic compounds and dissolved humic acids: a deuterium NMR T_1 relaxation study. *Environ. Sci. Technol.* **2001**, *35* (2), 379-384.

(210) Zhu, D.; Herbert, B. E.; Schlautman, M. A. Sorption of pyridine to suspended soil particles studied by deuterium nuclear magnetic resonance. *Soil Sci. Soc. Am. J.* **2003**, *67* (5), 1370-1377.

(211) Xiong, J.; Lock, H.; Chuang, I.; Keeler, C.; Maciel, G. E. Local motions of organic pollutants in soil components, as studied by ^{2}H NMR. *Environ. Sci. Technol.*, **1999**, *33* (13), 2224-2233.

(212) Emery, E. F.; Junk, T.; Ferrell, R. E.; De Hon, R.; Butler, L.G. Solid-state ^{2}H MAS NMR Studies of TNT absorption in soil and clays. *Environ. Sci. Technol.* **2001**, *35* (14) 2973-2978.

(213) Bruns-Nagel, D.; Knicker, H.; Drzyga, O.; Butehorn, U.; Steinbach, K.; Gemsa, D.; Von Low, E. Characterization of ^{15}N-TNT residues after and anaerobic/aerobic treatment of soil/Molasses mixtures by solid-state ^{15}N NMR spectroscopy. 2. Systematic investigation of whole soil and different humic fractions. *Environ. Sci. Technol.* **2000**, *34* (8), 1549-1556.

(214) Sachleben, J. R.; Chefetz, B.; Deshmukh, A.; Hatcher, P. G. Solid-State NMR characterization of pyrene-cuticular matter interactions. *Environ. Sci. Technol.* **2004**, *38* (16), 4369-4376.

(215) Smernik, R.J. A new way to use solid-state carbon-13 nuclear magnetic resonance spectroscopy to study the sorption of organic compounds to soil organic matter. *J. Environ. Qual.* **2005**, *34* (4), 1194-1204.

(216) Guthrie, E. A.; Bortiatynski, J .M.; Van Heemst, J. D. H.; Richman, J. E.; Hardy, K. S.; Kovach, E. M.; Hatcher, P. G. Determination of [^{13}C]pyrene sequestration in sediment mircrosms using flash pyrolysis-GC-MS and ^{13}C NMR. *Environ. Sci. Technol.* **1999**, *33* (1), 119-125.

(217) Vestergren, J.; Vincent, A. G.; Jansson, M.; Persson, P.; Ilstedt, U.; Gröbner, G.; Giesler, R.; Schleucher, J. High-resolution characterization of organic phosphorus in soil extracts using 2D ^{1}H-^{31}P NMR correlation spectroscopy. Environ. Sci. Technol. **2012**, *46* (7), 3950-3956.

(218) Ahmad, R.; Kookana, R. S.; Alston, A. M.; Skjemstad, J. O. The nature of soil organic matter affects sorption of pesticides. 1. Relationships with carbon chemistry as determined by ^{13}C CPMAS NMR Spectroscopy. *Environ. Sci. Technol.* **2001**, *35* (5), 878-884.

(219) Kulikova, N. A.; Perminova, I. V. Binding of atrazine to humic substances from soil, peat, and coal related to their structure. *Environ. Sci. Technol.* **2002**, *36* (17), 3720-3724.

(220) Salloum, M. J.; Chefetz, B.; Hatcher, P. G. Phenanthrene sorption by aliphatic-rich natural organic matter. *Environ. Sci. Technol.* **2002**, *36* (9), 1953-1958.

(221) Simpson, M. J.; Johnson, P. C. E. Identification of mobile aliphatic sorptive domains in soil humin by solid-state ^{13}C nuclear magnetic resonance. *Environ. Toxicol. Chem.* **2006**, *25* (1), 52-57.

(222) Shirzadi, A.; Simpson, M. J.; Kumar, R.; Baer, A.; Xu, Y.; Simpson, A. J. Molecular interactions at the soil-water interface. *Environ. Sci. Technol.* **2008**, *42* (15), 5514-5520.

(223) Shirzadi, A.; Simpson, M. J.; Xu, Y.; Simpson, A. J. Application of saturation transfer double difference NMR to elucidate the mechanistic interactions of pesticides with humic acid. *Environ. Sci. Technol.* **2008**, *42* (4)*,* 1084-1090.

(224) Fomba, K. W.; Galvosas, P.; Roland, U.; Kärger, J.; Kopinke, F. New options for characterizing the mobility of organic compounds in humic acids *Environ. Sci. Technol.* **2009**, *43* (21), 8264-8269.

(225) Fomba, K.W.; Galvosas, P.; Roland, U.; Kärger, J.; Kopinke, F. Mobile aliphatic domains in humic substances and their impact on contaminant mobility in the matrix. *Environ. Sci. Technol.* **2011**, *45* (12), 5164-5169.

(226) Combourieu, B.; Inacio, J.; Delort, A.; Forano, C. Differentiation of Mobile and Immobile Pesticides on Anionic Clays by ^{1}H HR MAS NMR Spectroscopy. *Chem. Comm.* **2001**, *21*, 2214-2215.

(227) Simpson, A. J.; Simpson, M. J.; Kingery, W. L.; Lefebvre, B. A.; Moser, A.; Williams, A. J.; Kvasha, M.; Kelleher, B. P. The application of ^{1}H high-resolution magic-angle spinning NMR for the study of clay-organic associations in natural and synthetic complexes. *Langmuir* **2006**, *22* (10), 4498-4503.

(228) Simpson, A. J.; Kingery, W. L.; Shaw, D. R.; Spraul, M.; Humpfer, E.; Dvortsak, P. The application of ^{1}H HR-MAS NMR spectroscopy for the study of structures and associations of organic components at the solid-aqueous interface of a whole soil. *Environ. Sci. Technol.* **2001**, 35 (16), 3321-3325.

(229) Otto, W. H.; Britten, D. J.; Larive, C. K. NMR diffusion analysis of surfactant-humic substance interactions. *J. Coll. Interface Sci.* **2003**, *261* (2), 508-513.

CHAPTER 2

IDENTIFYING COMPONENTS IN DISSOLVED HUMIC ACID THAT BIND ORGANOFLUORINE XENOBIOTICS USING ^{1}H{^{19}F} REVERSE HETERONUCLEAR SATURATION TRANSFER DIFFERENCE NUCLEAR MAGNETIC RESONANCE SPECTROSCOPY

2.0   Abstract

In this study, the interactions between dissolved peat humic acid and two structurally dissimilar organofluorine compounds, heptafluoro-2-naphthol and perfluorooctanoic acid, are probed using a novel ^{1}H{^{19}F} Nuclear Magnetic Resonance (NMR) spectroscopy technique based on the Saturation Transfer Difference (STD) experiment. This technique is used here to show selectively only those regions of the ^{1}H NMR spectrum of humic acid that arise from chemical constituents interacting with perfluorinated organic compounds. This approach provides a tool for high-resolution analysis of interactions between contaminants and natural organic matter (NOM), directly at the molecular level. NOM is a chemically heterogeneous mixture and traditional techniques used to study sorption or binding phenomenon are unable to resolve multiple processes occurring simultaneously at distinct chemical moieties. Here, multiple interaction domains are identified in humic acid, a fraction of soil-based NOM, based on known chemical constituents of humic acid, most notably from lignin- and protein-derived material. Specifically, heptafluoro-2-naphthol is shown to interact with lignin, protein, and aliphatic

material, however, preference is exhibited for lignin-derived domains, while perfluorooctanoic acid exhibits near exclusive preference for the protein-derived domains of humic acid.

2.1   Introduction

Soils and sediments are recognized as a major environmental sink for a large number of anthropogenic compounds *(1, 2)*.   The nature of the molecular associations and interactions influencing the retention of these compounds is a topic of significant research interest *(2-12)*. Evidence suggests that the natural organic matter (NOM) found in soils, or soil organic matter (SOM) is the most important component involved in sorption interactions with organic contaminants *(13-15)*.   Nevertheless, SOM is itself a complex heterogeneous mixture of decomposed and chemically altered biogenic material from a variety of sources *(16)*, including lignin, protein, carbohydrates, and cuticular material. It has been demonstrated that SOM does not behave as a physically homogeneous entity during sorption phenomenon *(3, 17-19)*, in contrast with commonly applied 'black box' approaches that treat SOM as a homogeneous, generic organic phase *(20)*. It is often hypothesized that dissimilar components of SOM will exhibit varying affinities for different types of organic contaminants *(15, 21, 22)*; however, the nature of the interactions involved remains unresolved. Current approaches to studying these interactions often rely on indirect methods that correlate changes in some property of a contaminant molecule, such as its apparent mobility or its NMR chemical shift, with an interaction *(4)*. Smejkalova *et al. (5)* used NMR measurements of the ^{19}F T_1 relaxation time of fluorinated phenols to show that protonated forms interacts more strongly with dissolved humic acid than the ionic forms.   Kohl *et al. (6)* used solid-state ^{19}F NMR to show that hexafluorobenzene interacts simultaneously and independently with mobile and rigid domains of SOM. Shirzadi *et al. (7, 8)* used ^{1}H STD NMR experiments to reveal the binding orientation of contaminants when they interact with various forms of SOM.

Studying sorption solely from the vantage of the contaminant means that the chemical nature of the binding sites is obscured. A common approach to overcome this limitation is to correlate macroscopic sorption properties, such as K_{OCS}, to the chemical composition of SOM *(4)*, or to isolated biomolecules *(9, 15)*. Khalaf *et al. (10)* separated components of humic acid based on

their size, and found that small, predominately aromatic fractions, show several binding sites for hexafluorobenzene, whereas large, predominately aliphatic, fractions show less clearly defined binding sites. Golding and Smernik *(11, 12)* present an interesting solution to this problem by editing the ^{13}C CPMAS NMR spectra of SOM based on its T_1 relaxation properties and then using difference spectroscopy to identify different domains that ^{13}C labeled compounds are more associated with.

In this chapter, molecular-level interactions between a dissolved peat humic acid and selected organofluorine compounds are probed using nuclear magnetic resonance (NMR) spectroscopy by employing a novel heteronuclear [1]H{[19]F} saturation transfer difference (STD) technique. This approach, termed Reversed Heteronuclear Saturation Transfer Difference (RHSTD), makes use of the through-space magnetic dipole-dipole interactions between the ^{19}F nuclei of an organofluorine molecule and the ^{1}H nuclei in the humic acid. Dipole-dipole interactions act independently of atomic bonding and provide a useful mechanism for probing non-covalent interactions between organic compounds in solution. Saturation transfer has been used extensively for the elucidation of binding configuration between small organic compounds and large macromolecular assemblages, such as proteins *(23, 24)*, as well as in humic acid *(8)*. RHSTD represents an experimental inversion of the conventional STD experiment: STD NMR is used to observe interactions from the vantage of the small compound, revealing its binding orientation, or epitope map *(23, 24)*. This approach, however, reveals nothing directly about the macromolecular site where the interaction occurs *(7, 8)*. RHSTD instead observes binding interactions from the vantage of the larger receptor molecules, revealing the presence of interactions at different types of sites in a mixture. In RHSTD, magnetic saturation is transferred from the ^{19}F nuclei in the target organofluorine compound to the ^{1}H nuclei in the components of humic acid with which it is interacting. By subtracting a saturated spectrum from an unaffected reference spectrum, the resultant ^{1}H NMR spectrum shows only those components of humic acid where interactions with an organofluorine molecule occur. Figure 2.1 illustrates this experiment conceptually.
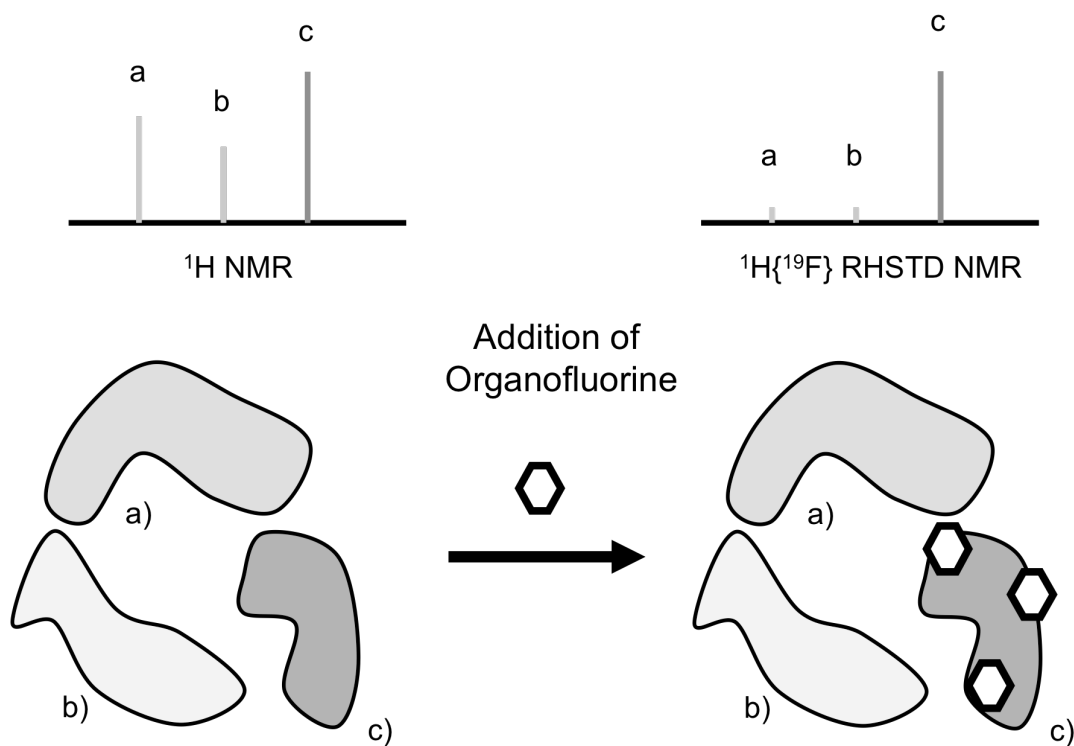
Figure 2.1   A conceptual diagram of the ^{1}H$\{^{19}$F$\}$ RHSTD experiment.   Shown is a hypothetical mixture of three components along with the corresponding ^{1}H NMR spectrum, which shows three peaks. In this hypothetical scenario, an added organofluorine compound only interacts with one of the components, and saturation is transferred between ^{19}F and ^{1}H nuclei here, and only here. The resultant ^{1}H$\{^{19}$F$\}$ RHSTD spectrum shows only the signal from the component that participates in the interaction.

The goal of this work is to reveal explicitly different binding domains in humic acid without either prior physical separation, or indirect property-composition correlations. Identifying the actual binding domains in humic acid, and SOM or NOM in general, is a vital step towards elucidating the mechanisms of interactions between xenobiotics and NOM. Two structurally dissimilar organofluorine compounds are selected as probes for these humic acid binding domains: heptafluoro-2-naphthol (HFNap) and perfluorooctanoic acid (PFOA). By contrasting how different organic compounds interact with humic acid, different binding domains can be revealed. In addition to being persistent organic pollutants, perfluorinated organic compounds are ideal probes for identifying binding domains in a complex environmental matrix because the fluorine-19 nucleus is both an excellent NMR nucleus, *(5, 6, 10)*, and because it does not occur naturally in soil organic matter *(25)*. It should be noted that perfluorinated compounds are not necessarily simple analogs for their non-fluorinated counterparts; perfluorooctanoic acid differs significantly from octanoic acid in that it is simultaneously hydrophobic and lipophobic, whereas octanoic acid is hydrophobic but lipophyllic. Perfluorinated aromatic compounds can be thought of as highly substituted arenes *(26)*.

2.2 Materials & Methods

2.2.1 Sample Preparation

Humic acid samples were prepared using the same batch of International Humic Substances Society (IHSS) Pahokee peat humic acid. Alkali lignin (CAS 8068-05-1) and albumin (ovalbumin from chicken egg white, grade V, 98%) were purchased from Aldrich and used as is. Pentadecafluoro-octanoic acid (perfluorooctanoic acid) (99%) and heptafluoro-2-naphthol (perfluoronaphthol) (97%) were purchased from Synquest Labs, Inc. Deuterium Oxide (99.9%), NaOD (99.5%D, 30% in D_2O), and DCl (99.5%D, 35% in D_2O) were purchased from Cambridge Isotope Laboratories. Humic acid samples were prepared by mixing 50 mg humic acid and the stated loading of organofluorine in a glass vial, and then fully dissolving it in 1.0 ml D_2O with the pH set to 6.60 ± 0.05 using minimal quantities of NaOD and DCl. After correction for the isotope effect, pH 6.6 corresponds to a pD of 7.0 *(27)*. Samples were allowed to equilibrate for a week before analysis and repeated analysis after periods of several weeks to

months showed no changes in experimental results. Lignin and albumin samples were prepared using 25 mg of the respective material; lignin-albumin mixtures were prepared using 25 mg of each material, for a combined mass of 50 mg. All lignin/albumin solutions were prepared with 10 mg organofluorine using the same method described for humic acid.

2.2.2 NMR Spectroscopy

NMR experiments were performed on a Bruker Avance 500 MHz Spectrometer using a QXI probe. Water suppression in all spectra was achieved using presaturation. The pulse sequence for the RHSTD experiment is identical to that described in the original STD paper by Mayer and Meyer *(24)*, with the exception that band selective saturation is applied to the heteronuclei, ^{19}F, with detection of ^{1}H, and that the relaxation based filter is removed. This pulse sequence is illustrated in appendix F. The on-resonance irradiation of perfluorooctanoic acid was carried out at -57300 Hz, while heptafluoro-2-naphthol was irradiated at -70700 Hz. Off resonance irradiation was set at +1,000,000 Hz, where signals from ^{19}F are not present. Saturation was achieved using a train of 18 Gaussian shaped pulses of 50 ms length. The spectra were subtracted internally via phase cycling after every scan to produce a difference spectrum. All experiments were performed with 16384 time domain points, 64 dummy scans, and 8192 scans and a recycle delay of 2 s. Spectra were apodized through multiplication with an exponential decay corresponding to 20 Hz line broadening in the transformed spectrum and zero filled to 32,768 points.

2.3 Results & Discussion

2.3.1 Direct Observation of Humic Acid-Organofluorine Interactions

For comparative purposes, the ^{1}H NMR spectrum of the IHSS Pahokee Peat humic acid is shown in figure 2.2 with the general assignments for lignin, protein, carbohydrates, and aliphatics labeled. Figure 2.3(a-e) shows the ^{1}H{^{19}F} RHSTD spectra for the organofluorine-humic acid mixtures using HFNap, while figure 2.3(f-j) shows ^{1}H{^{19}F} RHSTD spectra for mixtures using PFOA.
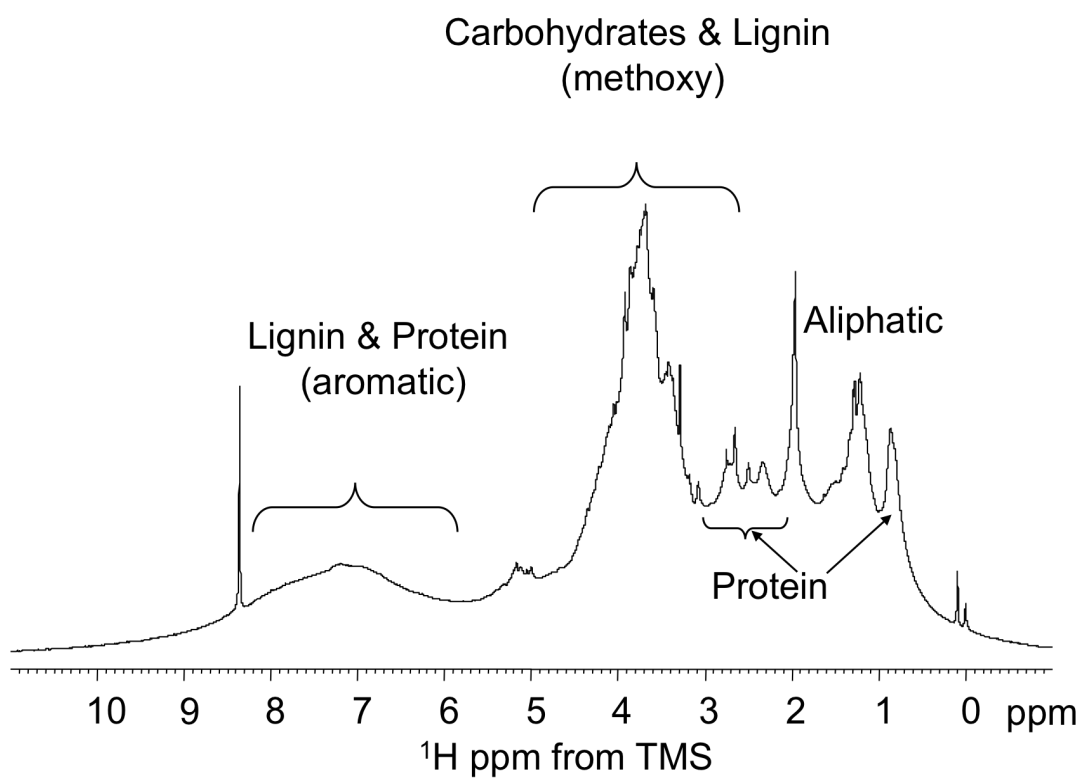
Figure 2.2   The ^{1}H NMR spectrum of the IHSS peat humic acid with major spectral features corresponding to the key humic acid biopolymers highlighted.

Figure 2.3 $^1H\{^{19}F\}$ RHSTD Spectra of IHSS peat humic acid mixed with different loading ratios of: (a-e) Heptafluoronaphthol, and (f-j) Perfluorooctanoic acid. Loading ratios, LR, are reported as the mass ratio of organofluorine to humic acid in solution. Major spectral features corresponding to the key humic acid biopolymers are highlighted: lignin (L), aliphatics (A), and protein (P).

Theoretically, in the case that no components of humic acid are preferred over others for interaction, the resultant RHSTD spectra should not differ significantly from the total ^{1}H spectrum. The deviations in the RHSTD spectra from the total ^{1}H NMR spectrum observed here suggest that both organofluorine compounds are selecting some components of humic acid for interaction preferentially over others. Furthermore, visible differences between the ^{1}H{^{19}F} RHSTD spectra observed for the two compounds suggest that PFOA and HFNap are interacting with different components of humic acid.

Traditional sorption or binding studies make use of concentration-interaction relationships *(3, 22, 28-31)*; unfortunately, most analytical techniques are only able to resolve interactions with soil organic matter, or humic acid, as a whole. The ^{1}H NMR spectrum resolves different components of humic acid internally quantitatively (i.e. the signal intensity is proportional to the concentration of the components producing those signals within the same sample, but not necessarily between different samples), while the ^{1}H{^{19}F} RHSTD spectrum shows signal attenuations due to proximal interactions with organofluorine compounds. Those signals resulting from ^{1}H relatively distant from ^{19}F are less affected than those signals resulting from ^{1}H relatively close to ^{19}F. We surmise, therefore, that the amount of ^{1}H{^{19}F} signal recorded at any given site should be related to the occurrences of interactions at the component giving rise to those signals. If multiple sites of interaction exist in humic acid, and if those sites exhibit different affinities for associations with organofluorine compounds, then those differences will be evident in changes in the ^{1}H{^{19}F} RHSTD spectra as the concentration of organofluorine compound changes.

The constituents of the humic acid extract of a soil are derived from complex biomolecules. The ^{1}H NMR spectra of those components, even in their isolated forms, are similarly complex, with signals typically spread across the entire chemical shift range. This means that simple deconvolutions are not easily performed because the signals in any chemical shift region arise from multiple components. The considerable overlap between different components in the RHSTD spectra makes absolute quantification of changes in different regions challenging, and thus much of the discussion presented here is limited to qualitative and semi-quantitative analysis by necessity. In cases where a single constituent dominates the signal in any one region a semi-quantitative analysis may be performed by focusing on that peak or spectral region. This

is the case for lignin and lignin-derived material in peat humic acid, which gives rise to most of the aromatic signal in the ^{1}H spectra. Protein is not as easily separated out from a total humic acid spectra, however the peak at 0.8 ppm is likely due to methyl groups from proteins. In the HFNap spectra, complete isolation of this peak from the neighboring aliphatic peak is not possible because of overlap. Furthermore, lignin also contributes some signals to the spectrum in the 'protein' region. Nevertheless, integration and comparison of the RHSTD spectra in terms of the total signal, and contributions from aromatic and aliphatic regions may be informative and has been attempted here.

Figure 2.4 shows changes in the integrations of the total RHSTD spectra as the organofluorine loading increases and demonstrates that both organofluorine compounds exhibit a strong initial rise in total RHSTD signal. For perfluorooctanoic acid, the rise in signal increase eventually levels off. Recall from the PFOA RHSTD spectra (fig. 2.2), this loading concentration corresponds to a point where subsequent spectra recorded at higher concentrations are indistinguishable from each other. For HFNap, conversely, the initial rise is followed by a more gradual rise that continues as concentrations increase. Recall that the HFNap RHSTD spectra continue to change with increasing loading.
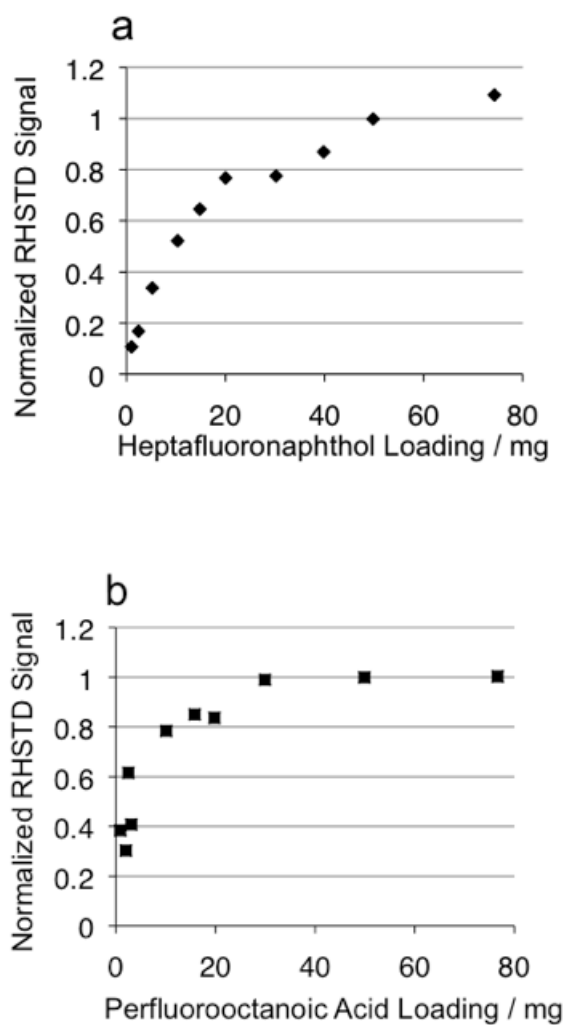
Figure 2.4   Integrations of the total RHSTD signal of humic acid as a function of different loading concentrations of (a) heptafluoronaphthol, and (b) perfluorooctanoic acid. Integrations are scaled to the 50 mg loading of each compound, respectively.

Figure 2.5 shows a more detailed integrative analysis of the RHSTD spectra for the HFNap-humic acid mixtures based on rough deconvolutions. Figure 2.5a shows integration of the isolated aromatic or aliphatic regions in the HFNap RHSTD spectra and reveals that the aromatic signal does not continue to increase indefinitely, signifying a saturation of available interaction sites or sorption capacity beyond a certain loading. The aliphatic region, however, continues to increase in intensity as the concentration of HFNap increases. For the initial concentrations, the signal in the aromatic region increases at a faster rate than in the aliphatic region, suggesting that interactions with aromatic material are preferred over those of aliphatic material. Because the integration of the aliphatic material, which includes signals from protein, aliphatics, and lignin, is not as domain specific as the integration of the aromatic material, which is mostly lignin, some of the rise here is very likely due to interactions not specifically at aliphatic sites. This means that the slope shown is a maximum, and that the true extent of interaction at aliphatic and protein-derived components is less than that suggested by the integrations.

Figure 2.5b compares changes in the RHSTD spectra of the HFNap mixtures to quantitative reference spectra of the same mixtures. The relative contribution of aromatic or aliphatic signals to the total signal is calculated using

$$\text{Relative contribution} = (S - S_o)/S_o, \qquad [2.1]$$

where S is the % contribution of the spectral region of interest relative to the total RHSTD spectrum and S_o is the same value for a quantitative reference ^{1}H spectrum.

Overall, the aromatic region gives a positive result, signifying that this region contributes more to the RHSTD spectrum than it does in the reference spectrum. The aliphatic region, however, generally gives a negative relative contribution, signifying that this region contributes less to the total RHSTD spectrum than it does to the same region in the reference spectrum. The aliphatic region gradually increases its contribution to the spectra as the HFNap concentration increases, signifying that interactions at these domains gradually become more important, whereas the relative contribution of interactions at aromatic region increases slightly at low concentrations, then holds steady, after which it starts to decline, signifying that interactions at other regions are becoming more important.
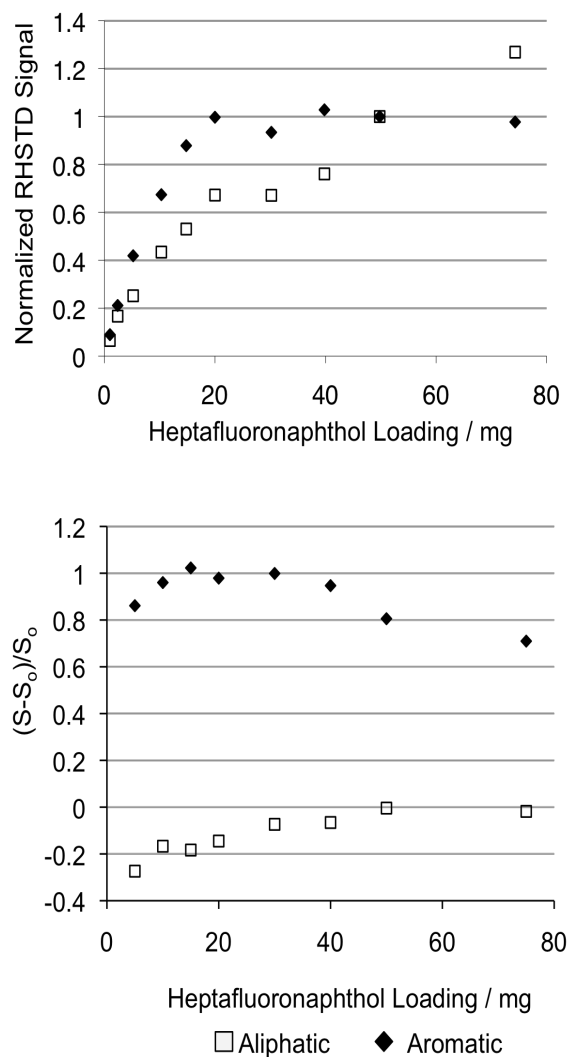
Figure 2.5 Semi-quantitative deconvolution of the RHSTD spectra as a function of the loading of heptafluoronaphthol. (a) Normalized signal intensity at aromatic and aliphatic domains. (b) Signal area of aromatic and aliphatic signal regions relative to the same signals in a quantitative reference spectrum.

From observations of changes in the ^{1}H{^{19}F} RHSTD spectra with increasing organofluorine loading ratios, it is evident that HFNap engages in a more complex binding scenario than does perfluorooctanoic acid. Initially, for HFNap the main signal increases are located in the aromatic and methoxy region. Eventually signal increases at these sites stop, however, and instead signals in the methyl region become relatively more important as they continue to increase. This observation suggests the presence of at least two distinct modes of interaction for HFNap with humic acid: a primary mechanism dominated by aromatic material, and a secondary mechanism dominated by aliphatic material, nevertheless both mechanisms occur simultaneously. In contrast, the ^{1}H{^{19}F} RHSTD spectra of PFOA does not change appreciably with higher loadings; when the primary binding sites become saturated, no secondary binding sites emerge.

Many models designed to account for non-ideality in the binding of organic compounds have suggested multiple binding domains *(2, 3, 8 18, 32)*, however, these domains are typically based on physical differences rather than chemical, such as sorption into dense vs. diffuse SOM *(3, 8)*. Because this study is conducted using a dissolved form of SOM where the humic material is likely more accessible for binding than in the solid state, we suggest that the observation of non-ideality, or preferential binding, here is rooted primarily in the chemically heterogeneous nature of SOM rather than the physical heterogeneity that is prevalent in a true whole soil. The limit in binding capacity at the aromatic sites agrees with observations that aromatic material, such as lignin, exhibits non-linear sorption, which is often explained in the solid-state as a specific mode of interaction (9). The continued increase in binding interactions at aliphatic material observed for HFNap, but not by PFOA suggests different mechanisms for interactions at aliphatic material for these two compounds. For HFNap, the observations that interactions with the relatively non-polar aliphatic moieties continue to increase at higher loadings suggests a general partitioning mechanism (32, 34), however the absence of an increase in interaction for PFOA at higher concentrations suggests a more specific interaction.

2.3.2 Characterization of Binding Sites

The identities of the major humic acid components involved in binding interactions are determined here using assignments from previous multidimensional NMR experiments *(16, 35-*

40). NMR spectroscopy has been used to demonstrate that the vast majority of SOM can be described as mixtures of biologically derived molecules, specifically lignin, protein, cellulose, aliphatics, and their respective degradation products. Furthermore, unique humic structures do no exist in significant amounts, if they exist at all *(41)*. Protein-derived fractions of SOM have been shown to arise from microbial cells lysed during the extraction of both humic acid and humin *(35, 37)*. Lignin resonances have been assigned using a range of ^{1}H-^{1}H and ^{1}H-^{13}C NMR correlation experiments *(38, 39)*, and aliphatic components by 3D NMR spectroscopy *(40)*. In addition, these major resonances have been identified in the specific humic acid studied here by both ^{1}H-^{1}H TOCSY and ^{1}H-^{13}C HSQC, which, when combined, demonstrate that the humic acid used here is predominately composed of lignin, protein, carbohydrate, and long-chain aliphatics. For simplicity the key assignments pertinent to this study are shown above on figure 2.2.

For HFNap, two dominant spectral features in figure 2.3 suggest the presence of interactions with lignin-derived components: the observed relative enhancement of the aromatic and methoxy signals. These resonances dominate the overall ^{1}H{^{19}F} RHSTD spectra at low HFNap loading ratios (fig. 2.3a-c), suggesting that lignin-derived components provide the primary binding sites for this compound. As the loading ratio increases, signals characteristic of protein side chains become more apparent (fig. 2.3d), suggesting that secondary binding sites for HFNap are associated with protein-derived components. At very high loading ratios (fig. 2.3d-e), a sharp resonance from long chain aliphatic species emerges from the protein background suggesting that aliphatic domains may continue to contribute to the binding of HFNap after the lignin and protein sites become saturated.

For PFOA, the ^{1}H{^{19}F} RHSTD spectra (fig. 2.3f-j) are dominated by signals known to be from protein-derived material *(16)*. It has been shown that the IHSS soil humic acid extract studied here contains a significant contribution from microbial proteins *(37)*, many of which are lipid-binding proteins *(35, 37, 42)*, similar to albumins for which PFOA is known to have specific binding sites *(43)*. These proteins are extracted into soil humic substances during the chemical extraction process when dead or dormant biological cells are lysed *(37)*. There appears, also, a strong contribution from aliphatic species at 1.2 ppm most easily explained as being from aliphatic components that are interacting with PFOA. This hypothesis disagrees, however, with observations that perfluorinated carboxylic acids generally avoid associative interactions with

long chain hydrocarbons (*44*). Nevertheless, this does not preclude the possibility of interactions with aliphatic components derived from plant cuticles, which are a major component of humic acid (*40*). An alternate explanation, however, is that the aliphatic signals are occurring as the result of an indirect interaction through the protein rather than as the result of a direct interaction between aliphatic species and PFOA. During the ^{1}H{^{19}F} RHSTD experiment, saturation from PFOA is passed to its humic acid-binding site, which, if that site is a lipoprotein, will then quickly permeate the entire protein-lipid complex via spin-diffusion regardless of whether the contaminant is specifically interacting with the lipid component (*45*). This explanation is supported by the ^{1}H{^{19}F} RHSTD spectra of humic acid with different PFOA loading ratios (fig. 2.3f-j); any change observed in the aliphatic signal at 1.2 ppm is matched by an equal change in the protein signal at 0.8 ppm. This correlation agrees with the hypothesis that the aliphatic component of humic acid giving rise to the signal at 1.2 ppm is strongly associated with the protein-derived material producing the signal at 0.8 ppm and thus strongly suggests that these protein and aliphatic signals represent a single effective chemical component in the solution.

The hypothesis presented here that HFNap interacts with both protein and lignin, while PFOA only interacts with protein, is tested using ^{1}H{^{19}F} RHSTD experiments of the organofluorine compounds mixed with representative biopolymers. Both lignin and protein are available in soluble forms, however, to the authors knowledge all representative cuticular materials are insoluble in water precluding their examination in the present study and the exact role of the aliphatic species in contaminant binding to humic acid will require future investigations. Figures 2.6a and 2.6b show the ^{1}H{^{19}F} RHSTD spectra of alkali extracted lignin in the presence of either HFNap or PFOA, respectively. Strong signals are seen for the HFNap mixture, demonstrating that lignin has a strong affinity for this compound. For PFOA, however, essentially no signals are observed in the ^{1}H{^{19}F} RHSTD spectrum indicating the absence of significant interactions with lignin. Figures 2.6c and 2.6d show the ^{1}H{^{19}F} RHSTD spectra obtained of albumin mixed with HFNap or PFOA, respectively. Both spectra exhibit strong signals, indicating that both compounds associate strongly with the protein. Given that the ^{1}H{^{19}F} RHSTD spectra will be slightly biased towards those ^{1}H nuclei physically closer to the organofluorine compound, subtle differences in the shape and line-width of the two spectra suggest that the two organofluorine compounds interact with protein in slightly different manners. PFOA, for instance, has been shown previously to prefer specific 'fatty-acid' binding
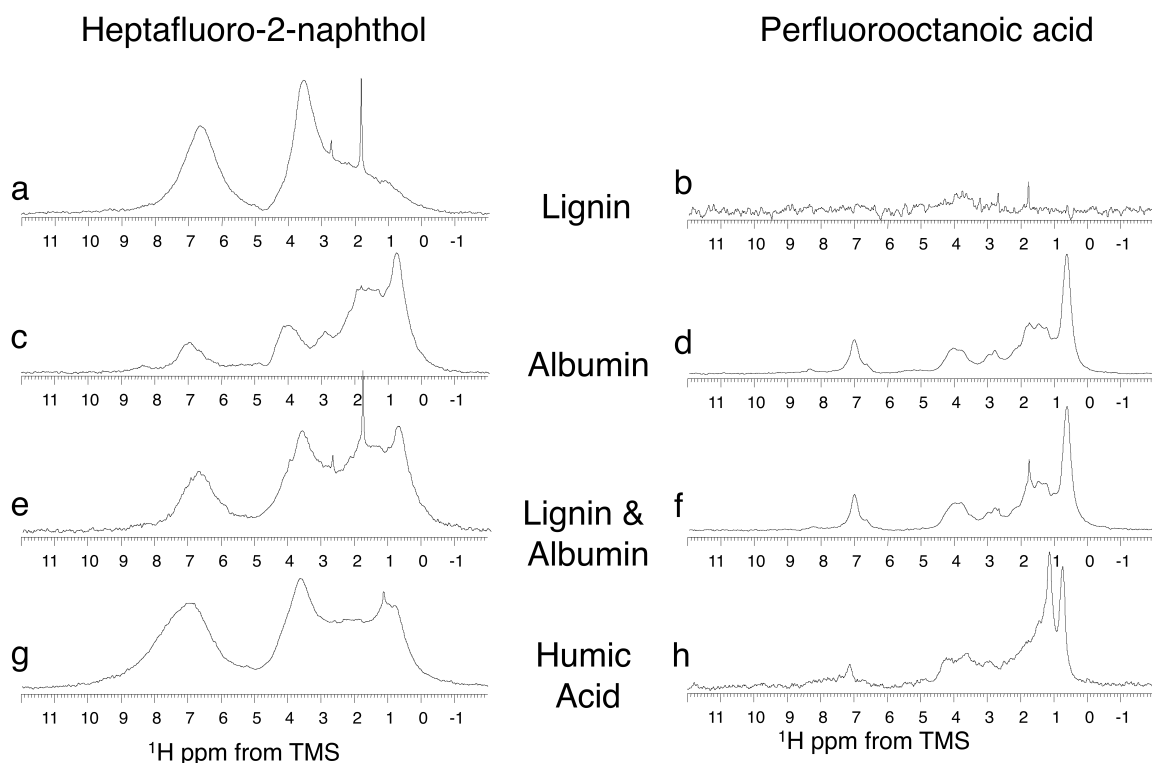
Figure 2.6 ^{1}H{^{19}F} RHSTD spectra of representative biomolecules mixed with heptafluoronaphthol (HFNap) or perfluorooctanoic acid (PFOA). (a) HFNap with lignin, (b) PFOA with lignin, (c) HFNap with albumin, (d) PFOA with albumin, (e) a mixture of albumin and lignin with HFNap, and (f) a mixture of albumin and lignin with PFOA, (g) HFNap with humic acid, (h) PFOA with humic acid. All spectra were obtained using identical acquisition parameters, including number of transients and recycle delay.

sites in proteins *(43)*, which may be different than the binding sites for the HFNap molecules. Figures 2.6e and 2.6f show the ^{1}H{^{19}F} RHSTD spectra obtained for mixtures of both protein and lignin with HFNap or PFOA, respectively. Comparison of these spectra to the individual components (fig. 2.6a-d) shows clearly that PFOA interacts selectively with protein-derived components, whereas HFNap interacts readily with both biopolymers and that interactions with a mixture of material similar to lignin and protein can, at a qualitatively level, account for the RHSTD spectra of humic acid as a whole (fig. 2.6g-h).

2.4   Conclusions

The separation of the humic acid ^{1}H NMR spectrum based on interactions with different organofluorine compounds into spectra that closely resembling the biomolecules from which humic acid is formed is, to the best of the author's knowledge, the first direct and *in situ* characterization of distinct binding domains in dissolved humic acid. This new information complements the existing literature showing multiple sorption modes in soil *(3, 17, 21),* and the literature showing that the chemical constitution of SOM is important in binding or sorption capacity (*15*) by explicitly showing the chemical domains where interactions occur. Lignin has been used previously as a model for studying sorption to SOM based on the knowledge that as an isolated compound, lignin has a higher sorption capacity than other constituent biopolymers from which humic substances are derived *(9, 15, 46).* While this application may work well for those compounds that do interact with lignin, the use of lignin alone to represent SOM does not account for the interactions with SOM for compounds that do not interact with lignin, such as PFOA.

In the present work humic acid is studied in the dissolved state, which makes its components more accessible to contaminants than they would be in a whole soil, where the preferred sites for contaminant interactions may not be the most accessible. Physical conformation may block favorable binding sites, or sites may be unreachable to contaminants, such as the proteins that are locked inside microbial cells or sites that are previously occupied by other compounds *(9).* Furthermore, while humic acid is a major fraction of SOM, it is not fully representative of the whole; a significant quantity of SOM is insoluble and therefore cannot be studied by solution-

state experiments. To fully understand the molecular-level binding of contaminants to soils a whole soil will need to be considered in the future.

2.5 References

(1)   Alexander, M. How toxic are toxic chemicals in soil? *Environ. Sci. Technol.* **1995**, *29* (11)*,* 2713-2717.

(2)   Luthy, R. G.; Aiken, G. R.; Brusseau, M. L.; Cunningham, S. D.; Gschwend, P. M.; Pignatello, J. J.; Reinhard, M.; Traina, S. J.; Weber, W. J. Jr.; Westall, J. C. Sequestration of hydrophobic organic contaminants by geosorbents. *Environ. Sci. Technol.* **1997**, *31* (12)*,* 3341-3347.

(3)   Xing, B.; Pignatello, J. J. Dual-mode sorption of low-polarity compounds in glassy poly(vinyl chloride) and soil organic matter. *Environ. Sci. Technol.* **1997**, *31* (3)*,* 792-799.

(4)   Delort, A-M.; Combourieu, B.; Haroune, N. Nuclear magnetic resonance studies of interactions between organic pollutants and soil components, a review. *Environ. Chem. Lett.* **2004**, *1* (4), 209-213.

(5)   Smejkalova, D.; Spaccini, R.; Fontaine, B.; Piccolo, A. Binding of phenol and differently halogenated phenols to dissolved humic acid as measured by NMR spectroscopy. *Environ. Sci. Technol.* **2009**, *43* (14), 5377-5382.

(6)   Kohl, S. D.; Toscano, P. J.; Hou, W.; Rice, J. A. Solid-State ^{19}F NMR Investigation of hexafluorobenzene Sorption to Soil Organic Matter. *Environ. Sci. Technol.* **2000**, *34* (1), 204-210.

(7)   Shirzadi, A.; Simpson, M. J.; Kumar, R.; Baer, A. J.; Xu, Y.; Simpson, A. J. Molecular interactions of pesticides at the soil-water interface. *Environ. Sci. Technol.* **2008**, *42* (15)*,* 5514-5520.

(8)   Shirzadi, A.; Simpson, M. J.; Xu, Y.; Simpson, A. J. Application of saturation transfer double difference NMR to elucidate the mechanistic interactions of pesticides with humic acid. *Environ. Sci. Technol.* **2008**, *42* (4)*,* 1084-1090.

(9)   Wang, X.; Cook, R.; Tao, S.; Xing. B. Sorption of organic contaminants by biopolymers: Role of polarity, structure and domain spatial arrangement. *Chemosphere* **2007**, *66* (8), 1476-1484.

(10)   Khalaf, M.; Kohl, S. D.; Klumpp, E.; Rice, J. A.; Tombacz, E. Comparison of sorption domains in molecular weight fractions of a soil humic acid using solid-state ^{19}F NMR. *Environ. Sci. Technol.* **2003**, *37* (13), 2855-2860.

(11)   Golding, C. J.; Smernik, R. J.; Birch, G. F. Investigation of the role of structural domains identified in sedimentary organic matter in sorption of hydrophobic organic compounds. *Environ. Sci. Technol.* **2005**, *39* (11), 3925-3932.

(12)   Smernik, R. J. A new way to use solid-state carbon-13 nuclear magnetic resonance spectroscopy to study the sorption of organic compounds to soil organic matter. *J. Environ. Qual.* **2005**, *34* (4), 1194-1204.

(13)   Karickhoff, S. W.; Brown, D. S.; Scott, T. A. Sorption of hydrophobic pollutants on natural sediments. *Water Res.* **1979**, *13* (3)*,* 241-248.

(14)   Karickhoff, S. W.; Morris, K. R. Sorption dynamics of hydrophobic pollutants in sediment suspensions. *Environ. Toxicol. Chem.* **1985**, *4* (4)*,* 469-479.

(15)   Garbarini, D. R.; Lion, L. W. Influence of the nature of soil organics on the sorption of toluene and trichloroethylene. *Environ. Sci. Technol.* **1986**, *20* (12)*,* 1263-1269.

(16)   Kelleher, B. P.; Simpson, A. J. Humic substances in soils: are they really chemically distinct? *Environ. Sci. Technol.* **2006**, *40* (15)*,* 4605-4611.

(17)   Weber Jr., W. J.; McGinley, P. M.; Katz, L. E. A distributed reactivity model for sorption by soils and sediments. 1. Conceptual basis and equilibrium assessments. *Environ. Sci. Technol.* **1992**, *26* (10)*,* 1955-1962.

(18) Huang, W.; Weber Jr., W. J. A distributed reactivity model for sorption by soils and sediments. 10. Relationships between desorption, hysteresis, and the chemical characteristics of organic domains. *Environ. Sci. Technol.* **1997**, *31* (9)*,* 2562-2569.

(19) Xing, B.; Pignatello, J. J.; Gigliotti, B. Competitive sorption between atrazine and other organic compounds in soils and model sorbents. *Environ. Sci. Technol.* **1996**, *30* (8)*,* 2432-2440.

(20) Lambert, S. M.; Porter, P. E.; Schieferstein, R. H. Movement and sorption of chemicals applied to the soil. *Weeds* **1965**, *13*, 185-190.

(21) Chefetz, B.; Xing, B. Relative role of aliphatic and aromatic moieties as sorption domains for organic compounds: A review. *Environ. Sci. Technol.* **2009**, *43* (6)*,* 1680-1688.

(22) Endo, S.; Grathwohl, P.; Haderlein, S. B.; Schmidt, T. C. Compound-specific factors influencing sorption nonlinearity in natural organic matter. *Environ. Sci. Technol.* **2008**, *42* (16)*,* 5897-5903.

(23) Mayer, M.; Meyer, B. Group epitope mapping by saturation transfer difference NMR to identify segments of a ligand in direct contact with a protein receptor. *J. Am. Chem. Soc.* **2001**, *123* (25)*,* 6108-6117.

(24) Mayer, M.; Meyer, B. Characterization of ligand binding by saturation transfer difference NMR spectroscopy. *Angew. Chem. Int. Ed.* **1999**, *38* (12)*,* 1784-1788.

(25) Larsen, S.; Widdowson, A.E. Soil fluorine. *J. Soil Sci.* **1971**, *22* (2)*,* 210-221.

(26) Ellis, D. A.; Cahill, T. M.; Mabury, S. A.; Cousins, I. T.; Mackay, D. Partitioning of organofluorine compounds in the environment. The handbook of environmental chemistry, Vol . 3, Part N ed. A.H. Neilson, Springer-Verlag, Berlin, **2002**. pp 63-83.

(27) Krezel, A.; Bal, W. A formula for correlating pKa values determined in D_2O and H_2O. *J. Inorg. Biochem.* **2004**, *98* (1), 161-166.

(28)   Wang, X.; Xing, B. Importance of structural makeup of biopolymers for organic contaminant sorption. *Environ. Sci. Technol.* **2007**, *41* (10)*,* 3559-3565.

(29)   Chen, B.; Johnson, E. J.; Chefetz, B.; Zhu, L.; Xing, B. Sorption of polar and nonpolar aromatic organic contaminants by plant cuticular materials: Role of polarity and accessibility. *Environ. Sci. Technol.* **2005**, *39* (16)*,* 6138-6146.

(30)   Chiou, C. T.; Kile, D. E.; Rutherford, D. W.; Sheng, G.; Boyd, S. A. Sorption of selected organic compounds from water to a peat soil and its humic-acid and humin fractions: potential sources of the sorption nonlinearity. *Environ. Sci. Technol.* **2000**, *34* (7)*,* 1254-1258.

(31)   Chiou, C. T.; Kile, D. E. Deviations from sorption linearity on soils of polar and nonpolar organic compounds at low relative concentrations. *Environ. Sci. Technol.* **1998**, *32* (3)*,* 338-343.

(32)   Pedit, J. A.; Miller, C. T. Heterogeneous sorption processes in subsurface systems. 1. Model formulations and applications. *Environ. Sci. Technol.* **1994**, *28* (12)*,* 2094-2104.

(33)   Mao, J. D.; Hundal, L. S.; Thompson, M. L.; Schmidt-Rohr, K. Correlation of Poly(methylene)-rich amorphous aliphatic domains in humic substances with sorption of nonpolar organic contaminant, phenanthrene. *Environ. Sci. Technol.* **2002**, *36* (5), 929-936.

(34)   Sun, H.; Zhu, D.; Mao, J. Sorption of polar and nonpolar aromatic compounds to two humic acids with varied structural heterogeneity. *Environ. Toxicol. Chem.* **2008**, *27* (12), 2449-2456.

(35)   Simpson, A. J.; Song, G.; Smith, E.; Lam, B.; Novotny, E. H.; Hayes, M. H. B. Unraveling the structural components of soil humin by use of solution-state nuclear magnetic resonance spectroscopy. *Environ. Sci. Technol.* **2007**, *41* (3)*,* 876-883.

(36)   Simpson, A. J.; Kingery, W. L.; Shaw, D. R.; Spraul, M.; Humpfer, E.; Dvortsak, P. The application of ^{1}H HR-MAS NMR spectroscopy for the study of structures and

associations of organic components at the solid-aqueous interface of a whole soil. *Environ. Sci. Technol.* **2001**, *35* (16)*,* 3321-3325.

(37) Simpson, A. J.; Simpson, M. J.; Smith, E.; Kelleher, B. P. Microbially derived inputs to soil organic matter: are current estimates too low? *Environ. Sci. Technol.* **2007**, *41* (23)*,* 8070-8076.

(38) Simpson, A. J.; Lefebvre, B.; Moser, A.; Williams, A.; Larin, N.; Kvasha, M.; Kingery, W. L.; Kelleher, B., Identifying residues in natural organic matter through spectral prediction and pattern matching of 2D NMR datasets. *Mag. Reson. Chem.* **2004**, *42* (1), 14-22.

(39) Simpson, A. J. Multidimensional solution state NMR of humic substances: a practical guide and review. *Soil Sci.* **2001**, *166* (11), 795-809.

(40) Simpson, A. J.; Kingery, W. L.; Hatcher, P. G. The identification of plant derived structures in humic materials using three-dimensional NMR spectroscopy. *Environ. Sci. Technol.* **2003**, *37* (2)*,* 337-342.

(41) Nelson, P. N.; Baldock, J. A., Estimating the molecular composition of a diverse range of natural organic materials from solid-state C-13 NMR and elemental analyses. *Biogeochemistry* **2005**, *72* (1), 1-34.

(42) Mao, J. D.; Tremblay, L.; Gagne, J. P.; Kohl, S.; Rice, J.; Schmidt-Rohr, K. Humic acids from particulate organic matter in the Saguenay fjords and the St. Lawrence estuary investigated by advanced solid-state NMR. *Geochim. Cosmochim. Acta* **2007**, *71* (22), 5483-5499.

(43) Han, X.; Snow, T. A.; Kemper, R. A.; Jepson, G. W. Binding of perfluorooctanoic acid to rat and human plasma proteins. *Chem. Res. Toxicol.* **2003**, *16* (6)*,* 775-781.

(44) Dunitz, J. D.; Gavezzotti, A.; Schweizer, W.B. Molecular shape and intermolecular liaison: hydrocarbons and fluorocarbons. *Helv. Chim. Acta* **2003**, *86* (12)*,* 4073-4092.

(45) Simpson, A. J.; Woods, G.; Mehrzad, O. Spectral editing of organic mixtures into pure components using NMR spectroscopy and ultraviscous solvents. *Anal. Chem.* **2008**, *80* (1)*,* 186-194.

(46) Van Beinum, W.; Beulke, S.; Brown, C. D. Pesticide sorption and desorption by lignin described by an intraparticle diffusion model. *Environ. Sci. Technol.* **2006**, *40* (2)*,* 494-500.

CHAPTER 3
UNDERSTANDING SOLUTION-STATE NON-COVALENT INTERACTIONS BETWEEN XENOBIOTICS AND NATURAL ORGANIC MATTER USING ^{19}F/^{1}H HETERONUCLEAR SATURATION TRANSFER DIFFERENCE NUCLEAR MAGNETIC RESONANCE SPECTROSCOPY

The material in this chapter is adapted with permission from

3.0 Abstract

A combination of forward and reverse heteronuclear (^{19}F/^{1}H) saturation transfer difference (STD) nuclear magnetic resonance (NMR) spectroscopic techniques are applied to characterize the non-covalent interactions between perfluorinated aromatic xenobiotics and dissolved humic acid. These NMR techniques produce detailed molecular-level descriptions of weak non-covalent associations between components in complex environmental mixtures, thereby allowing for the mechanisms underlying these interactions to be explored. ^{19}F observe Heteronuclear STD (HSTD) is used to describe the average molecular orientation of the xenobiotics during their interactions with humic acid, while ^{1}H observe Reverse-Heteronuclear STD (RHSTD) is used to identify and quantify preferences exhibited by xenobiotics for interactions at different types of humic acid moieties. First, using HSTD it is shown that selected aromatic organofluorides orient with their non-fluorine functional groups (OH, NH$_2$, and COOH) directed away from humic acid during the interactions, suggesting that these functional groups are not specifically involved.

Second, the RHSTD experiment is shown to be sensitive to subtle differences in preferred interaction sites in humic acid, and is used here to demonstrate preferential interactions at aromatic humic acid sites for selected aromatic xenobiotics, $C_{10}F_7OH$, and $C_6F_4X_2$, (where X = F, OH, NH_2, NO_2, or COOH), that can be predicted in general using simple solubility and partitioning factors, as well as the electrostatic potential maps of the xenobiotic.

3.1   Introduction

Interactions with natural organic matter (NOM) are known to influence the fate, transport, and toxicity of anthropogenic organic compounds in the environment *(1-3)*. Organic matter in soils, or soil organic matter (SOM) is key to sorption and sequestration *(2-5)*, while interactions with colloidal and dissolved organic matter (DOM) influence the solubility, desorption, and transport of xenobiotics in the environment. For instance, the solubility of hydrophobic compounds in the aquatic environment is enhanced when these compounds interact with DOM *(2, 3)*, which can facilitate transport and increase bioavailability to plants and aquatic organisms *(6, 7)*. Alternatively, strong interactions with SOM can be environmentally ameliorating; desorption of organic contamination is slowed, or stopped *(8)*, effectively keeping organic contamination out of the watersheds during runoff events. Furthermore, it has been argued that the reduced bioaccessibility of sequestered xenobiotics, responsible in part for the enhanced longevity of many persistent organic pollutants *(8, 9)*, also limits the actual toxicity of many of these compounds *(1, 4, 5, 8, 9)*. Nevertheless, gradual buildup of potentially toxic chemicals in soils, over time, results in uncertain toxicity in the future and the possibility of catastrophic release during times of environmental change or disturbance.

Consequent to the importance of xenobiotic interactions with natural organic matter as an interface between the natural and man-made chemical worlds, understanding the nature and mechanism of these interactions is a topic of considerable research *(10-22)*. Knowledge of the molecular-level interactions between xenobiotics and NOM, in general, has the potential to lead to more efficient and targeted remediation strategies. In general, these interactions are known to be non-covalent in nature, even when the contaminants appear to be bound irreversibly *(23)*. In the solid-state, non-ideal sorption into SOM is well documented and is often described in

physical terms, usually based on a multi-domain model comprising flexible domains, where fast reversible diffusion occurs, and rigid domains, where slow, irreversible diffusion occurs *(19)*. Non-ideal binding has also been documented in dissolved organic matter, suggesting a complex mode of interaction beyond simple hydrophobic desolvation effects, influenced by the types of non-covalent interactions that may occur between organic contaminants and different chemical constituents of NOM *(11-18, 24)*.

Nuclear Magnetic Resonance (NMR) spectroscopy has emerged as a powerful tool for characterizing the interactions between organic compounds in complex environmental media *(10, 11, 21, 25)*. Techniques based on the Saturation Transfer Difference (STD) NMR experiment have recently been applied in environmental research. The more-traditional 'forward' STD experiment has been used to illustrate the binding epitope of several environmentally important xenobiotics during their interactions with natural organic matter *(15, 25)*. Longstaffe *et al.* (see chapter 2) recently introduced reverse heteronuclear saturation transfer difference (RHSTD) as a novel experiment to identify binding sites in a humic acid mixture *(11)*. By comparing organofluorine compounds with strongly contrasting interaction behaviour in humic acid, distinct binding domains in humic acid were clearly observed, notably lignin- and protein-derived moieties *(11)*. The utility of the RHSTD technique to reveal more subtle differences in interaction sites for structurally similar xenobiotics has not yet been explored. In addition, there have not been any studies that have yet utilized the combination of STD, used to describe molecular orientation of the smaller xenobiotic molecule, and RHSTD, which identifies the component of the binding mixture where the interactions occur, in environmental research *(26)*. Combined, these techniques have the potential to describe in detail, how, why, and where, contaminants interact with natural organic matter, directly at the molecular-level.

Here, the combination of both forward and reverse heteronuclear STD experiments is used to investigate the binding interactions between perfluorinated organic compounds, which are used as proxies for xenobiotic compounds, and dissolved humic acid, which is used in this study as a proxy for a complex mixture of natural organic matter similar to that found in soil and aquatic environments. Humic acid is the alkali extracted fraction of natural organic matter and is often used to investigate xenobiotic interactions with NOM because of its ready availability and a

diverse chemical constitution that reflects many, albeit not all, of the types of chemical moieties found in NOM *(10, 11, 13-15)*. Humic acid may be altered from its natural state during the extraction process and therefore caution should be employed when using this material in environmental studies as a direct proxy *(27, 28)*. Nevertheless, while humic acid is extremely complex, it is simpler than whole soils and thus provides an excellent medium for the application and development of the NMR experiments described herein, where humic acid is used simply to simulate a complex mixture of organic compounds, of the type found in the environment. High humic acid concentrations are used in this study primarily to reduce experimental time. While it is common to employ low concentrations of humic acid in solution to simulate aquatic humic acid levels, the humic acid used here originates from a peat soil and high concentrations may be a more realistic proxy for soil organic matter in its natural state, where aggregation plays a key role in its physico-chemical properties.

The purpose of this study is to demonstrate the utility of combining forward and reverse STD experiments to provide key molecular-level information for environmental research. As such, this study explores interactions in the solution-state, focusing on the development of the NMR experiments and the type of information that can be extracted from these methods. Future applications will move towards more environmentally relevant systems, such as whole soils, rather than operational extracts like humic acid. Molecular-level investigations of real-world systems are exceedingly complicated and as such it is imperative that the NMR experiments themselves are established first in simpler systems.

Here, the nature of the interactions, including orientation and interaction site specificity, between dissolved humic acid and a series of differently substituted aromatic organofluorine compounds, ($C_{10}F_7OH$, and $C_6F_4X_2$, X= F, OH, NH_2, NO_2, COOH) is investigated. The compounds used in this study and selected properties are listed in table 3-1. $^{19}F\{^1H\}$ Heteronuclear Saturation Transfer Difference (HSTD) spectroscopy provides information as to the average molecular orientation of the organofluorine compound during their interactions *(25, 29-31)*, while $^1H\{^{19}F\}$ Reverse Heteronuclear Saturation Difference (RHSTD) spectroscopy is used to investigate the distribution of the chemical moieties of humic acid where interactions occur *(11, 29)*. To reduce the complexity of the system being studied, and thereby increasing the analytical feasibility of

Table 3-1 Properties of organofluorine compounds used.

Organofluorine Compound	Melting Point/ °C	Log H_2O Solubility	Log K_{OW}	pK_a	pK_b	Q_{zz} / Debeye Å
Heptafluoro – 2-naphthol	120-124	-6.08	4.67	5.11	*NA*	*NA*
Tetrafluoro-1,3-aminobenzene	131-132	-2.89	1.54	21.10	-0.34	-11.247
Pentafluoroaniline	36-37	-4.03	3.14	20.24	-0.16	2.3603
Tetrafluoro-1,3-hydroxybenzene	95	-3.58	2.05	5.81, 7.32	*NA*	3.307
Tetrafluoro-1,4-hydroxy benzene	172-174	-4.05	2.34	5.93, 7.30	*NA*	3.347
Pentafluorophenol	34-36	-4.09	3.00	5.27	*NA*	9.193
Pentafluorobenzoic acid	100-102	-4.58	4.33	1.46	*NA*	11.78
Pentafluoro-nitrobenzene	*NA*	-5.34	3.93	*NA*	*NA*	18.79
Tetrafluoro-1,2-phthalic acid	152-154	-4.9	3.5	1.58, 3.50	*NA*	20.66
Tetrafluoro-1,4-terephthalic acid	275-277	-5.52	3.89	1.42, 1.73	*NA*	32.2

* Solubility and K_{OW} factors were calculated using the SPARC on-line calculator. Q_{zz} values were calculated using SPARTAN, employing quantum mechanical methods. Pentafluoronitrobenzene is liquid at room temperature.

investigating such weak interactions directly at the molecular-level, this study limits its scope to investigating how changes in the organofluorine chemistry influences the interactions, and makes no strong attempt to include the roles different physical attributes of dissolved humic acid, such as colloidal conformation, have in governing these interactions, which has been studied previously *(12, 32,)* and will be the primary topics of chapters 4 and 5 in this dissertation. Perfluorinated compounds were employed in this study in order to segregate the pertinent NMR active nuclei into either the humic acid (^{1}H) or xenobiotic (^{19}F) components, thereby removing ambiguities in the analysis, such as transfer of saturation between ^{19}F and ^{1}H on the same molecule, and spurious ^{1}H signals in the RHSTD spectra arising from the xenobiotic itself *(11)*. Perfluorinated aromatic compounds have unique physico-chemical properties compared to standard hydrocarbon, chlorinated, or brominated aromatics. Fluorinated and non-fluorinated analogues should therefore not be expected to exhibit the same behaviours *(33, 34)*. Nevertheless, the knowledge of the effects of different functional groups on the interaction behavior of an organic compound is transferable to non-fluorinated compounds.

3.2 Materials & Methods

3.2.1 Sample Preparation

Heptafluoro-2-naphthol (CAS 727-49-1), tetrafluoro-1,3-amino benzene (CAS 1198-49-1), pentafluoroaniline (CAS 771-60-8), tetrafluoro-1,3-hydroxy benzene (CAS 16840-25-8), tetrafluoro-1,4-hydroxy benzene (CAS 771-63-1), pentafluorophenol (CAS 771-61-9), pentafluorobenzoic acid (CAS 602-94-5), tetrafluorophthalic acid (CAS 652-03-9), tetrafluoroterephthalic acid (CAS 652-32-8), and pentafluoronitrobenzene (CAS 880-78-4) were purchased from Synquest Chemical Laboratories (Alachua, Florida, USA) and used as is. The International Humic Substance Society (IHSS) Pahokee peat standard humic acid was used throughout. Due to the low sensitivity of these experiments, and, as Dixon *et al.* have reported *(33)*, the reality that only a small number of xenobiotics molecules may actually be associating with the dissolved humic acid at any given moment, much higher solute concentrations than are typically found in the environment are required to ensure the presence of a large enough number of interactions for observation. Mechanistic studies on non-covalent interactions using direct

NMR methods, such as those routinely employed in molecular biology, often need to employ model systems where the conditions are optimized for the analytical technique rather than for their direct relevance to the real world *(35)*. The NMR experiments used here provide unique information about the xenobiotic interactions that cannot be obtained directly through other analytical means, and while the experiments are conducted under less than ideal conditions, the type of information obtained is invaluable in developing a fuller molecular-level understanding of the processes influencing contaminant fate in the environment.

The samples for the ^{1}H observe RHSTD experiments were prepared by mixing 100 mg humic acid with 10 mg organofluorine in 1.00 ml D_2O (Cambridge Isotope Laboratories, 99.9%D) in glass vials. The pH was set to 6.6 ±0.1 using minimal quantities of NaOD (99.5 %D, 30% in D_2O) and DCl (99.5 %D, 35% in D_2O), corresponding to an actual pD of 7.0 *(36)*. Samples were allowed to equilibrate for 1 week and were visibly dissolved at the time of analysis. Samples for the ^{19}F observed HSTD experiments were prepared using 50 mg humic acid and 10 mg organofluorine in 1.00 ml D_2O. The pH was set using NaOD and DCl to values between 3 and 10.

3.2.2 Electrostatic Potential Calculations

Electrostatic potential maps were calculated for the neutral forms of the organofluorine compounds and selected lignin monomers using the Spartan computational software employing the Hartree-Fock quantum mechanical method and the 6-311+G** basis set *(37)*. Quadrupole moments were calculated using these electrostatic potential maps. Previous studies have suggested that the neutral forms of many aromatic molecules dominate the interactions with humic acid *(14, 38)*, and so all organofluorine molecules were assumed to be neutral for the calculations. At the pH employed (~7), however, most of the acidic compounds should be largely deprotonated.

Some of these compounds, pentafluorophenol in particular, exhibit a strong relationship between the ^{19}F chemical shift and the equilibrium dynamics between the neutral and anionic forms. All three peaks in the ^{19}F spectrum of pentafluorophenol are shifted to higher chemical shift values the closer the equilibrium is to the ionized form, with the resonance from the fluorine nucleus

para to the hydroxyl being the most sensitive to this effect. The % ionization of 10 mg pentafluorophenol in 1.00 ml D_2O as calculated from the pk_a and measured pH. For measurements in pure D_2O, the pk_a has been converted to the pk_a* using the equation

$$pK_a* = (pk_a - 0.42)/ 0.929 \qquad [3.1]$$

accounting for the differences in ionization potential in D_2O versus H_2O *(36)*. The pH was converted to pD using

$$pD = pH + 0.4 \qquad [3.2]$$

which accounts for isotopic effects at the pH electrode *(36)*. The % ionization is calculated as

$$\% \text{ ionization} = 100\ \% \ \textbf{x}\ k_a{}^*/[(D_3O^+) + k_a]. \qquad [3.3]$$

The ^{19}F chemical shift of pentafluorophenol as a function of ionization is shown in figure 3.1. The data in figure 3.1a is fit to a logarithmic curve. A plot of the chemical shift versus the double log of the % ionization, shown in figure 3.2b, give linear fits, with R^2 values ranging from 0.9913 to 0.9891 for the three ^{19}F resonances. The correlation between ^{19}F chemical shift and the % ionization of pentafluorophenol provides a rough gauge of the effective pk_a of this compound in the humic acid solution.

Table 3-2 compares the % ionization of pentafluorophenol expected from measurements of the solution's pD, assuming standard $pk_a{}^*$s, and that calculated from the chemical shift of the para fluorine for four samples of pentafluorophenol mixed with humic acid. For all of these samples, the ^{19}F chemical shifts suggests a much lower % ionization for this compound when it interacts with humic acid than what would be expected in pure aqueous solution. This effect may be the result of a favorable interaction between humic acid and the protonated form of the molecule that shifts the apparent pK_a away from that expected in a pure aqueous environment.
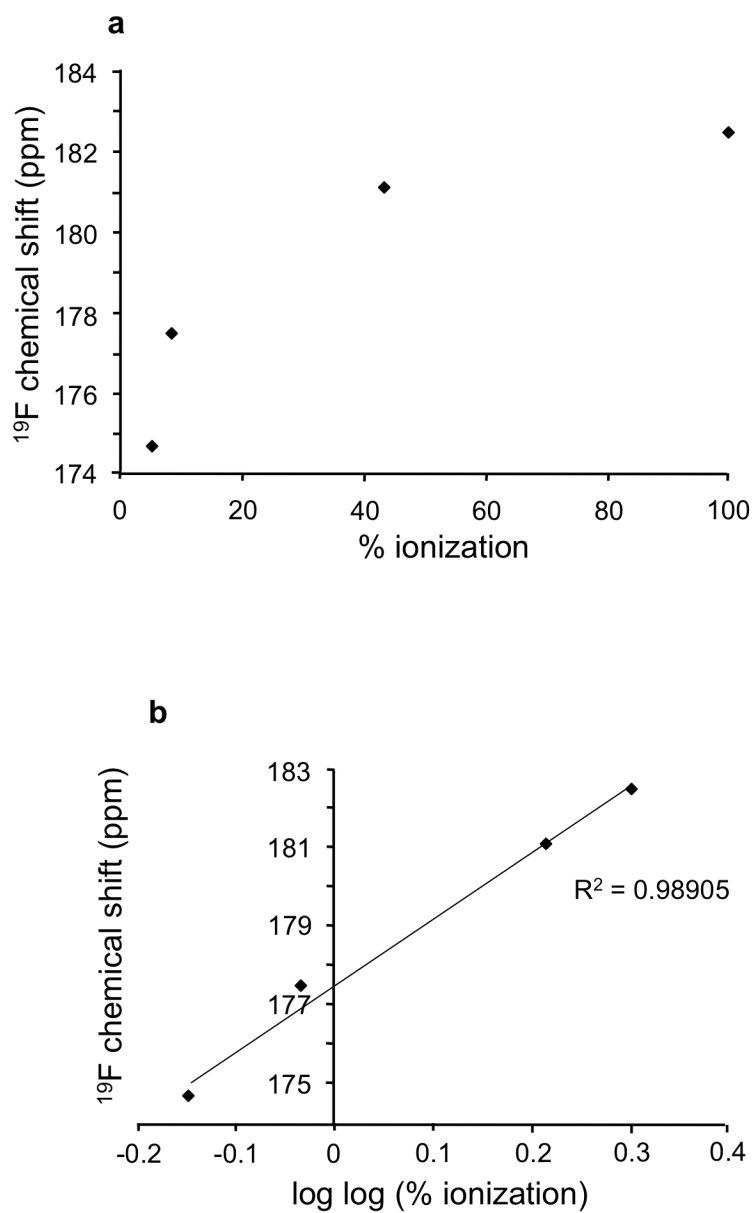
Figure 3.1 Chemical shift of the para ^{19}F resonance of pentafluorophenol as a function of the % ionization of the OH group (**a**). Chemical shift of the para ^{19}F resonance as a function of the loglog(% ionization) of pentafluorophenol (**b**).

Table 3-2   Para ^{19}F chemical shifts of pentafluorophenol compared to theoretical and actual % ionizations in humic acid solutions.

Measured pD	Para ^{19}F shift	% ionization calculated from pk_a/pD	% ionization calculated from chemical shift
4.27	170.80	5.96	2.48
6.23	176.20	85.25	6.73
7.01	178.77	96.70	15.13
9.75	182.65	99.99	103.6

3.2.2 NMR Spectroscopy

3.2.3.1 Experimentation

^{19}F{^{1}H} HSTD spectra were performed using a Bruker Avance III 500 MHz Nuclear Magnetic Resonance Spectrometer employing a ^{19}F optimized SEF probe. The pulse sequence is similar to the STD experiment reported by Mayer *(11, 30, 31)*, except with the saturation frequency tuned to ^{1}H with detection on ^{19}F, the exclusion of relaxation filters, and the solvent suppression turned off. This pulse sequence is illustrated in appendix F. Between 2048 and 4096 transients, 64 dummy scans and recycle delays of 2 s were employed. Spectra were acquired and processed using 32768 data points and apodized using an exponential multiplication function corresponding to 20 Hz line broadening. Separate experiments were conducted with selective saturation using 0.2414 W of saturation power of the ^{1}H spectrum, tuned to +400 Hz (corresponding to aliphatic protons) or +3600 Hz (corresponding to aromatic protons), resulting in only minimal differences. ^{1}H off-resonance was set at +1,000,000 Hz.

The ^{1}H{^{19}F} RHSTD experiments were performed on a Bruker Avance 500 MHz Nuclear Magnetic Resonance spectrometer employing a 5 mm QXI probe. The same pulse sequence as for the ^{1}H detect experiments was used, except with the saturation frequency tuned to ^{19}F with detection on ^{1}H (see appendix F). Water suppression was achieved using presaturation. All experiments were performed using 8192 transients, 64 dummy scans, and recycle delays of 2 s. Spectra were acquired and processed using 16384 time domain points and apodized using an exponential multiplication function corresponding to 20 Hz line broadening. Saturation on ^{19}F was produced using a train of 18 Gaussian shaped pulses of 50 ms length at 26 W of power performed on resonance; off-resonance saturation was set to +1,000,000 Hz. Difference spectra were produced via internal phase cycling.

3.2.3.2 Overview of STD NMR spectroscopy

The Saturation Transfer Difference NMR approaches used here have been described previously *(11, 25, 29-31)*. Saturation is a relatively high-energy state where transitions between spin states is rapid so that the system is not in the observable equilibrium state. To return to equilibrium, a

saturated spin system will transfer some of this energy, and thus saturation, to nearby spin systems with which it is coupled. Where covalent bonds exist, spin diffusion occurs and saturation is rapidly transferred throughout the molecule via scalar spin-spin coupling *(30, 31)*. In the absence of covalent bonds, the transfer of saturation between molecules is limited to through-space dipole coupling, which is strongly correlated with internuclear distances. In heteronuclear STD spectroscopy, saturation is produced selectively in the spin set of one nucleus while an NMR spectrum is recorded in another. The more efficient the transfer of saturation is between spin sets, the greater the loss of signal is in the observed set of nuclei. For non-covalent interactions, the relationship between spatial distances and dipole coupling means that unsaturated nuclei that spend more time closer to the saturated nuclei experience more efficient saturation transfer *(30)*. To highlight the resonances at nuclei where saturation is transferred most efficiently a difference spectrum is recorded by subtraction of the saturated spectrum from an unaffected quantitative spectrum via alternating phase cycling (i.e. alternating spectra are of opposite phase and thus when summed together an overall subtraction occurs). In the traditional STD experiment, the direction of transfer saturation is from a larger macromolecule, such as a protein, to a small probe molecule. In this study, experiments are employed that reverse the direction of saturation transfer so that saturation originates in the small probe molecule and is transferred to the larger binding molecules. For clarifying purposes, we refer to the standard approach, where saturation moves from the big molecule to the probe molecule as the forward direction, while saturation transfer from the probe molecule to the larger binding molecule is the reverse direction.

3.3 Results & Discussion

3.3.1 Molecular Orientation of Organofluorine with Respect to Humic Acid

$^{19}F\{^{1}H\}$ HSTD spectra were recorded for four organofluorine compounds: pentafluoroaniline, pentafluorophenol, tetrafluoro-1,3-hydroxy benzene, and pentafluorobenzoic acid using identical concentrations but at a variety of pH values. In the forward $^{19}F\{^{1}H\}$ Heteronuclear Saturation Transfer Difference (HSTD) experiment, saturation is transferred from ^{1}H nuclei in the macromolecular humic acid to ^{19}F nuclei on the organofluorine compounds while a ^{19}F NMR

spectrum is recorded *(29, 31)*. Here, the relative strength of the observed resonances is related to the predominant molecular orientation of the organofluorine compounds *(30)*. In the resultant difference spectrum, signals from ^{19}F nuclei that are closer to ^{1}H nuclei in humic acid during the interaction are favored *(15)*. Integration of the signals relative to the para fluorine peak, which is assigned a nominal value of 100%, and comparison to similar integrations of a quantitative, non-STD ^{19}F spectrum, allows epitope maps to be created showing which fluorine nuclei experience the strongest interaction with humic acid. Figure 3.2 shows epitope maps for four of the organofluorine compounds studied here. In these maps, circles of different sizes and associated percentages correspond to the relative change in signal strength from a reference spectrum due to interaction with ^{1}H at each ^{19}F in the molecule *(29)*.

These epitope maps demonstrate that on average the para and meta positions on the benzene rings are closer to the humic acid than the ortho positions, suggesting that for these compounds the non-fluorine functional groups, OH, NH_2, or COOH, are oriented away from humic acid during the interaction. Two independent regions of the ^{1}H humic acid spectrum were selectively saturated, aromatic and aliphatic protons, with nearly the same results observed regardless of the type of humic acid component where the saturation originates, indicating that the average orientation of the organofluoride does not noticeably vary at different domains of humic acid to a degree that can be measured using this approach.

At the pH values used here, some of the organofluorine compounds studied exist in equilibrium between protonated and unprotonated forms, such as pentafluorophenol ($pK_a= 5.27$), while others are not, such as pentafluoroaniline, which is neutral at all pHs used ($pK_a = 20.24$) *(39)*. To evaluate the effect of ionization equilibrium on the orientation, HSTD experiments were run at different pHs for pentafluorophenol and pentafluoroaniline. Figure 3.3 shows that the ratio of the ortho to meta fluorine signal strength decreases with increasing pH for both pentafluoroaniline and pentafluorophenol. This suggests that as the pH increases the organofluorine molecules are undergoing faster exchange between bound and unbound states, thereby slowing the rate of saturation transfer to fluorine nuclei further from humic acid.
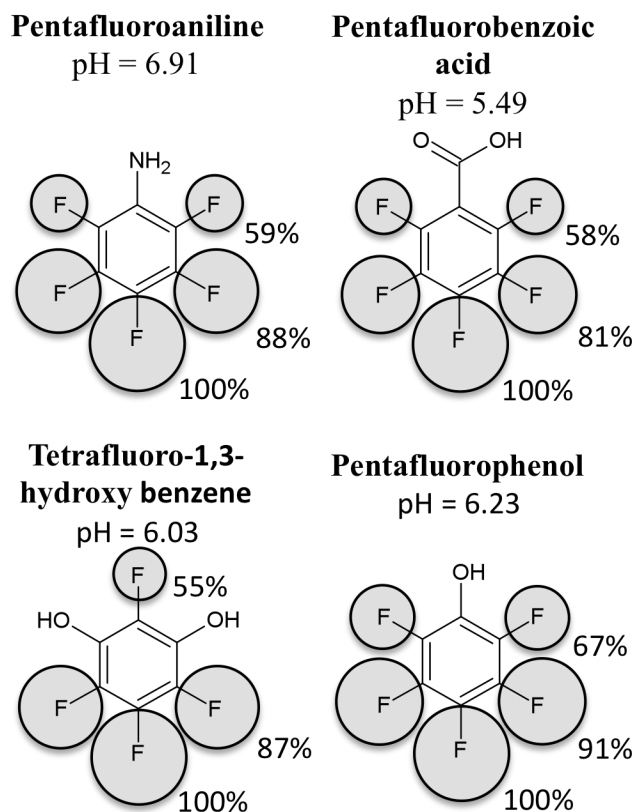
Figure 3.2   Epitope maps of 4 aromatic organofluorine compounds interacting with humic acid as determined using $^{19}F\{^1H\}$ HSTD NMR spectroscopy.   The size of the circle encompassing each fluorine atom is scaled to the relative signal intensity of those fluorine nuclei in the STD spectrum compared to a quantitative reference spectrum with the para site assigned a value of 100%. The larger the circle, the closer the proximity of that fluorine nucleus to humic acid.
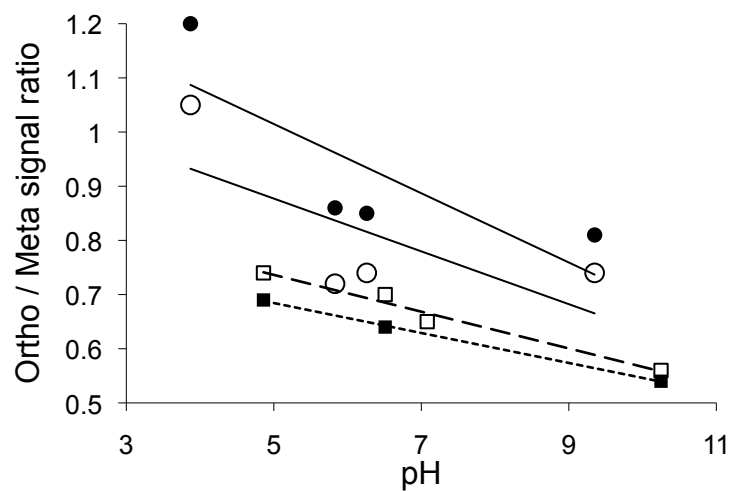
Figure 3.3   The ratio between the ortho and meta fluorine signals in the $^{19}F\{^1H\}$ HSTD spectra as a function of pH for pentafluorophenol (circles) and pentafluoroaniline (squares). Open points are for measurements made irradiating the aliphatic region of the humic acid ^1H spectrum, while closed points are for measurements made irradiating the aromatic region of the humic acid ^1H spectrum.

Pentafluoroaniline does not ionize at the pH values used, suggesting that the decrease in interaction is likely associated with pH-related changes in the humic acid, which contains numerous phenoxy and carboxylic functional groups. Pentafluorophenol, which does ionize at the relevant pH values, exhibits a greater response to pH than pentafluoroaniline, suggesting that the unprotonated form does not interact with humic acid as strongly as does the protonated form, in agreement with previous observations *(14, 38)*. This effect is explored in further detail in chapter 5.

Because the mode of interaction for these compounds is not directly through the OH, NH_2, or COOH functional groups, these observations support a model where neither hydrogen bonding nor cation-anion interactions are prevalent between these aromatic organofluorine compounds and humic acid, suggesting that these functional groups are more engaged in interactions with the surrounding water than with humic acid. While not observed for the compounds studied here, interactions with humic acid through the functional group have been suggested before, such as for the N: lone pair on pyridine *(38)* or, similarly, cation-anion interactions with pyridine N^+ at the appropriate pH *(40)*, indicating that the mode of interaction with humic acid can be highly xenobiotic specific. None of the compounds studied here are cationic at the pHs employed and further research would be required to address these types of interactions.

3.3.2 Distribution of Organofluorine Compounds in Proximity to Humic Acid Moieties

In the ^{1}H observe RHSTD experiment the efficiency of saturation transfer is directly related to the strength of the ^{19}F-^{1}H dipole interactions at a given humic acid moiety, which is controlled by the spatial proximity of organofluorine molecules interacting with the larger humic acid molecules and aggregates, and by the prevalence of the interactions. Dynamics is thought to have a reduced role in saturation efficiency here relative to the forward HSTD experiments discussed above. The strength of magnetic dipole interactions decrease rapidly with increasing distance, thereby nearly eliminating the possibility of both false positive and false negative results: saturation will be transferred if, and only if, an interaction between organofluorine compound and humic acid occurs. It has been demonstrated previously that when no interaction

occurs, no signals are observed in the RHSTD spectrum *(11)*. Therefore, if an interaction does occur, the observed degree of saturation transfer is governed largely by the prevalence of the interaction as dictated by its duration and frequency *(11, 30)*. Comparison of the ^{1}H observed RHSTD spectrum with a standard ^{1}H NMR spectrum, which shows the components of humic acid quantitatively, reveals two things: 1) those components of humic acid that are interacting with an organofluorine; and 2) based on deviations from the reference spectrum, governed by the prevalence of interaction, the relative affinity for associations at some humic acid moieties over others *(11)*.

[1]H{[19]F} RHSTD spectra were recorded for 10 different aromatic organofluorine compounds mixed with humic acid in a 1:10 organofluorine to humic acid mass ratio under uniform concentration and pH conditions. The RHSTD spectra of humic acid mixed with three selected organofluorine compounds are shown in figure 3.4 overlaying their respective reference humic acid spectra, scaled such that signals in the aromatic region are at the same intensity. Qualitatively, the RHSTD spectrum using pentafluorobenzoic acid overlaps the reference humic acid spectrum almost completely, whereas for tetrafluoro-1,3-amino benzene the RHSTD spectrum is reduced in the non-aromatic region of humic acid relative to the reference. Pentafluorophenol produces a result intermediate between the other two. The close similarity between the reference spectrum and the [1]H{[19]F} RHSTD spectrum of the pentafluorobenzoic acid experiment suggests that this compound interacts with the different chemical moieties of humic acid more or less indiscriminately under these conditions. Tetrafluoro-1,3-amino benzene, and to a lesser extent pentafluorophenol, both exhibit a greater proportion of aromatic signal in their respective RHSTD humic acid spectra than is found in the reference ^{1}H spectra, suggesting a preference for interactions at aromatic moieties over non-aromatic moieties of humic acid.
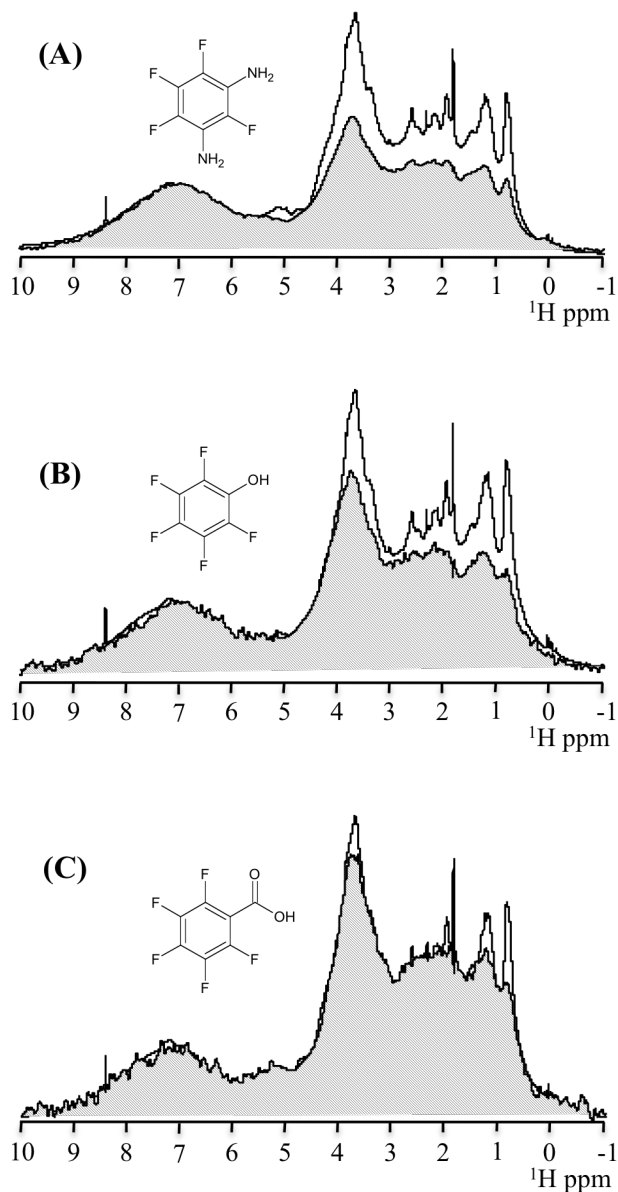
Figure 3.4 $^{1}H\{^{19}F\}$ RHSTD spectra of peat humic acid mixed with different aromatic organofluorine xenobiotics (striped region), scaled to the aromatic signal region (9 to 5.5 ppm) and overlaid on quantitative, non-STD, reference spectra of the same sample. (A) tetrafluoro-1,3-amino benzene, (B) pentafluorophenol, (C) pentafluorobenzoic acid.

In chapter 2, binding domains in humic acid were identified based on the type of component actually involved *(11)*. In that study such clear distinction was possible because the xenobiotics used exhibited wide variation in their binding profiles; heptafluoronaphthol interacted with all components while perfluorooctanoic acid, interacted nearly exclusively with protein-derived humic acid moieties. Here, the organofluorine compounds selected for study are structurally very similar to one another and as such do not show strong differentiation between their binding profiles with humic acid, exhibiting instead only the subtle differences illustrated above. As such, the binding profiles are not analyzed based on the actual component of humic acid where each ^{1}H resonance originates, but instead on the chemical nature of those sites, specifically aromatic or non-aromatic moieties. Figure 3.5A compares the total signal recorded in the various ^{1}H{^{19}F} RHSTD spectra, relative to the strongest spectra (heptafluoro-2-naphthol), divided into their absolute contributions from aromatic and non-aromatic resonances for each spectra. Figure 3.5B shows the difference in the ratio of aromatic to non-aromatic signal between the RHSTD spectrum and the quantitative non-STD reference spectrum using the equation

$$\Delta(\text{aro/non-aro}) = (\text{aro/non-aro})_{\text{RHSTD}} - (\text{aro/non-aro})_{\text{reference}}, \qquad [3.4]$$

such that a positive value indicates a greater weighting towards aromatic signal than is found in the reference spectrum. The further this value is from zero, the further the distribution of xenobiotics interacting with humic acid is from a homogeneous distribution, signifying greater specificity in the humic acid moieties where the interactions occur. All compounds studied show at least some excess of aromatic signal in the RHSTD spectra, however some show a much clearer preference for aromatic humic acid moieties than others.

The differences in substitution on the aromatic organofluorine rings influence the molecule's character in two ways: specific functionality, such as acid/base, or H-bonding properties; and the overall electron distribution in the molecule due to withdrawing/donating effects. The organofluorine compounds used here have a variety of functional groups ranging from electron-donating (NH_2 and OH) to electron withdrawing (COOH, NO_2, and F itself). The ^{19}F observe HSTD experiments discussed above indicate that the aromatic organofluorine compounds studied here orient with the functional group directed away from humic acid indicating that their
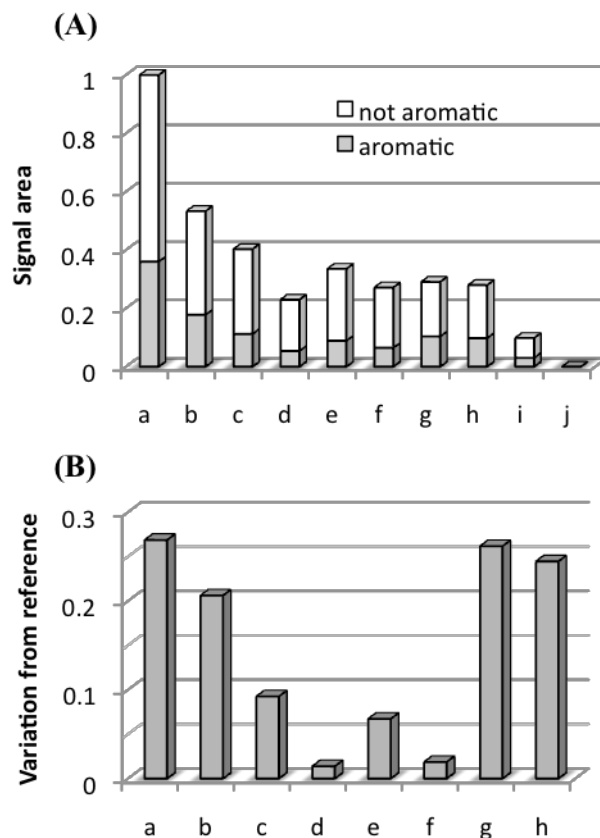
Figure 3.5 (A): Relative integrated signal areas of the $^1H\{^{19}F\}$ RHSTD spectra. (B): Difference in the aromatic/non-aromatic signal ratio between the RHSTD spectra and a quantitative non-STD reference. Legend: a: heptafluoro-2-naphthol; b: tetrafluoro-1,3-amino benzene; c: pentafluoroaniline; d: pentafluoronitrobenzene; e: pentafluorophenol; f: pentafluorobenzoic acid; g: tetrafluoro-1,3-hydroxy benzene; h: tetrafluoro-1,4-hydroxy benzene; i: tetrafluoro-1,2-phthalic acid; j: tetrafluoro-1,4-terephthalic acid.

specific functionality may not be directly responsible for the humic acid-organofluorine interactions at the molecular-level. The apparent trend in the data here is instead that the compounds with the more electron-donating substituents (e.g. tetrafluoro-1,3-amino benzene) interact with the humic acid more strongly and selectively than those with more electron-withdrawing constituents (e.g. tetrafluorophthalic acid), which interact weakly and non-selectively.

Presented in figure 3.6 are electrostatic potential maps for selected organofluorine compounds, ranging from those that exhibit the strongest to the least preference for aromatic humic acid. The origin of the general observation reported here of aromatic xenobiotics interacting strongly with aromatic rich organic matter is often explained invoking π-π interactions *(16, 21, 41)*, which are actually interactions between compatible quadrupole moments of the aromatic xenobiotic and the aromatic components of natural organic matter *(41, 42)*. Also shown in figure 3.6 are the electrostatic potential maps of three common lignin monomers; much of the aromatic content of humic acid is lignin-derived suggesting that the interactions between the xenobiotics and aromatic humic acid is with structures similar to these *(11)*. Qualitatively, the closer the organofluorine compound resembles the lignin monomers, the greater preference is exhibited for associations with aromatic humic acid under these conditions. Aromatic rings with similar electrostatic density maps do not possess compatible quadrupole moments for stacking interactions, and if such organized structures were predominant, the opposite result to what is observed here would be expected; perfluorinated aromatic xenobiotics that are electrostatically least similar to humic acid would interact most strongly with aromatic humic acid *(42)*.
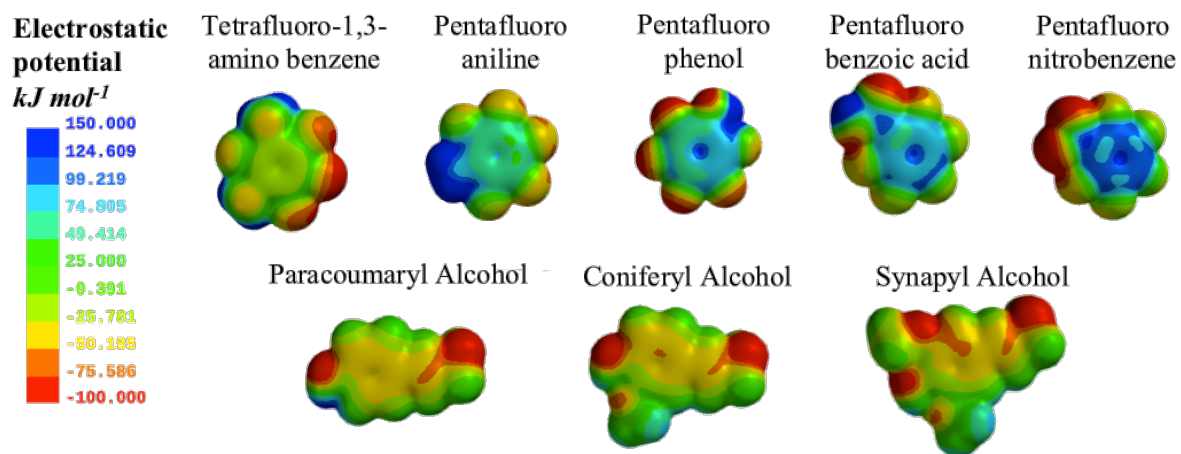
Figure 3.6   Electrostatic potential maps (kJ mol^{-1}) of selected aromatic organofluorine compounds and representative lignin monomers: synapyl alcohol, coniferyl alcohol, and paracoumaryl alcohol.

Quadrupole moments, nevertheless, are very useful measures of the surface electrostatic properties of aromatic compounds and consequently influence the polarity of these compounds. This in turn affects their bulk properties, such as aqueous solubility and partitioning equilibria between polar and non-polar domains. As a direct property of a molecule, quadrupole moments are very useful in understanding intermolecular interactions, while solubility and partitioning factors, which are measureable only for bulk samples, are routinely used for understanding macroscopic observations, such as the environmental fate of xenobiotics. When dissolved in water, humic acid forms a homogeneous single phase with the solvent. Associations between xenobiotics and dissolved humic acid, however, may be thought of as pseudo-partitioning between the free aqueous environment and the hydrophilic colloids of humic acid. In addition to observing associations with humic acid in general, here we observe preferred distribution for association between different types of humic acid moieties. Continuing the partitioning analogy, this observation is in essence an *in situ* observation of partitioning within the primary partitioning medium, humic acid itself.

To model the molecular-level observation of a phenomenon that is traditionally observed only at the macroscopic level, the total amount of signal recorded in the aromatic and non-aromatic compartments of the humic acid RHSTD spectra is compared to aqueous solubility, the octanol-water partitioning factor, K_{OW}, which were both calculated using the SPARC on-line calculator *(39)*, and to the molecular quadrupole moments, Q_{zz}, which were calculated from the electrostatic potential maps of each organofluorine compound using Spartan *(37)*. The total amount of RHSTD signal in each region of the spectrum, aromatic or non-aromatic humic acid, is a deterministic measurement of where molecules are located during the observation. These comparisons are shown in figures 3.7A, 3.7B, and 3.7C, respectively and reflect the observation of independent processes occurring simultaneously at different components of the same system.

The amount of aromatic signal in the RHSTD spectra is linearly correlated to all three factors, with log K_{OW} providing the poorest correlation (R^2=0.6499), and the quadrupole moment, Q_{zz}, providing the best correlation (R^2=0.9743). A similar result is observed for the non-aromatic contribution to the RHSTD spectra, with the data appearing much more scattered for the log K_{OW} and log (solubility) than for the Q_{zz} correlations. Overall, the correlations for the aromatic
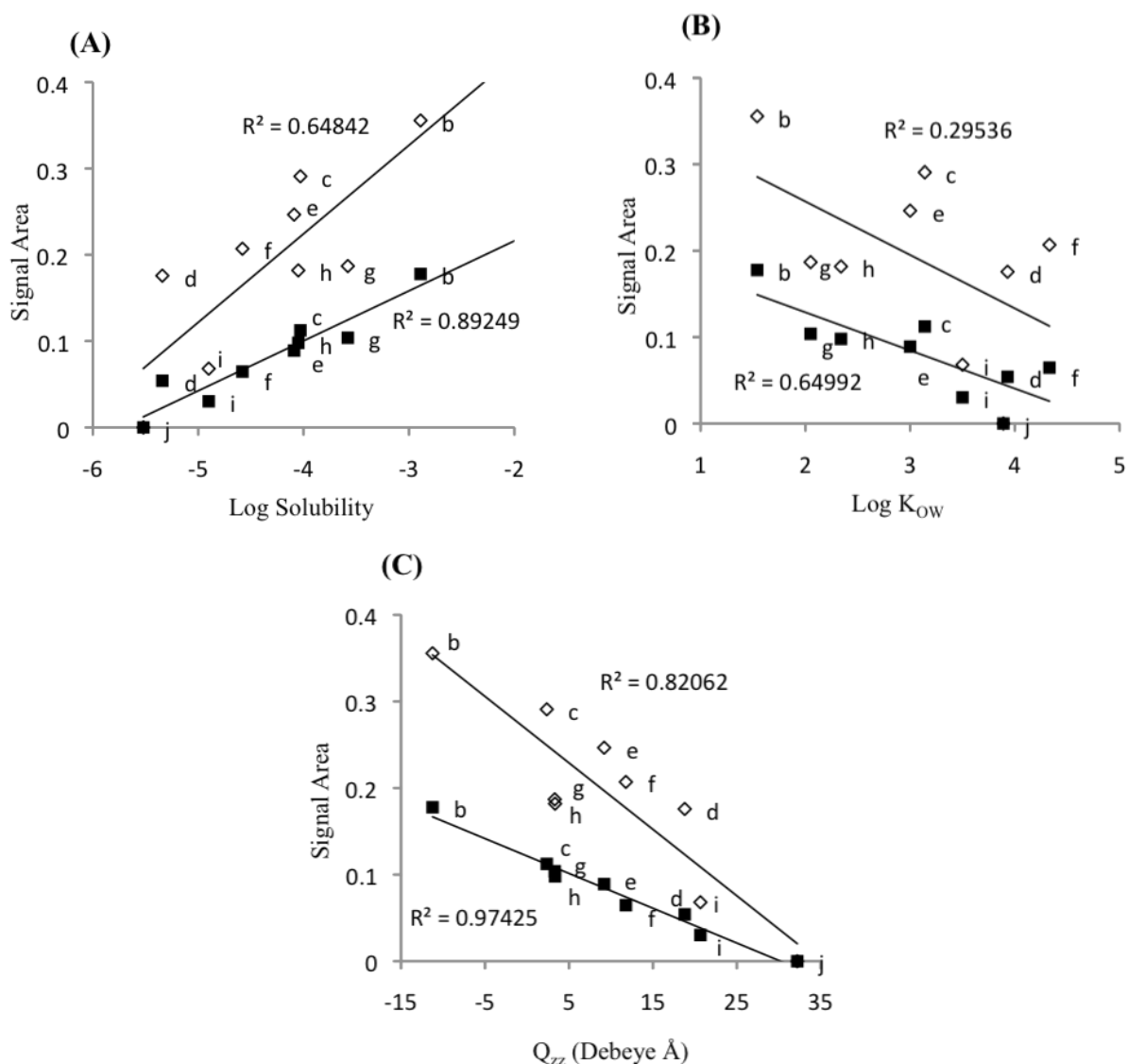
Figure 3.7 Comparison of relative aromatic and non-aromatic signal area with (A) Log solubility, (B) Log K_{OW}, and (C) the molecular quadrupole, Q_{zz}.

Legend: b: tetrafluoro-1,3-amino benzene; c: pentafluoroaniline; d: pentafluoronitrobenzene; e: pentafluorophenol; f: pentafluorobenzoic acid; g: tetrafluoro-1,3-hydroxy benzene; h: tetrafluoro-1,4-hydroxy benzene; i: tetrafluoro-1,2-phthalic acid; j: tetrafluoro-1,4-terephthalic acid.

contributions are better than for the non-aromatic contributions for all three comparisons, however, it should be noted that for the comparison for the non-aromatic contribution there appears to be a bimodal distribution, with the two dihydroxy benzenes and phthalic acid comprising one set, and the remaining compounds comprising a second set. This is most apparent on the Q_{zz} plot (fig. 3.7C). These observations suggest a number of things. The first is that differences in molecular polarity are useful in explaining the extent of interaction between the organofluorine compounds and different components of humic acid studied here. The second is that interactions at aromatic components of humic acid fit these correlations better than the non-aromatic components. The third is that Q_{zz} is a better parameter to model these observations, which are a direct observation of intermolecular interactions, than solubility or K_{OW}, which is the least reliable parameter. The weakened correlations with solubility may be the result of unreliable solubility data, the fact that solubility is highly system dependent, or that some factors influencing solubility are not as important in governing these interactions as molecular polarity. The poor correlation with the octanol-water partitioning factor may also be the result of unreliable K_{OW} factors, or may be demonstrative of the fact that octanol is not an ideal analogue for soil organic matter.

To further explore the differences in the distributions between the aromatic and non-aromatic moieties of humic acid, the ratio of aromatic to non-aromatic signal in the RHSTD spectra are compared again to the same xenobiotic properties as above. Here, comparing distributions between domains rather than the extent of intermolecular interactions directly, as was shown in figure 3.7, moves the analysis here towards a stochastic observation, where intermolecular interactions occur simultaneously at different humic acid domains, but are not necessarily independent of one another, from the above discussion of a deterministic model where intermolecular interactions at different domains were accounted for individually. The resultant plots are shown in figure 3.8. All three plots clearly show a bimodal distribution, with the two dihydroxy benzenes and phthalic acid forming one set, and diaminobenzene, aniline, phenol, benzoic acid, and nitrobenzene forming the second set. Tetrafluoroerephthalic acid was left out of the comparisons because the weak interaction here produced poor signal to noise preventing deconvolution. Good correlations are observed for all comparisons, however this time the solubility comparisons have the weakest correlations while
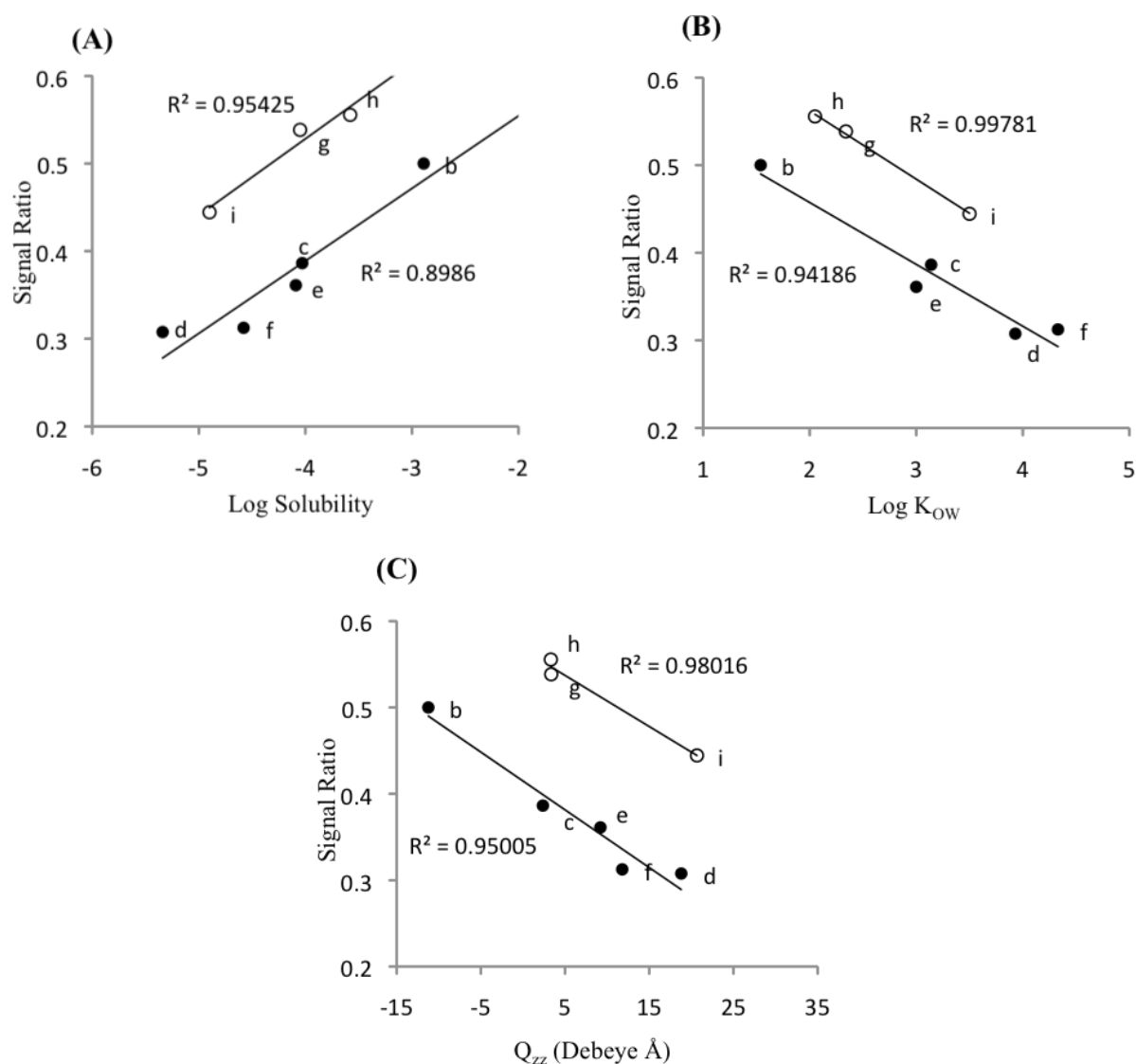
Figure 3.8 Comparison of the ratio of the aromatic and non-aromatic signal: (A) Log solubility, (B) Log K_{OW}, and (C) Q_{zz}.

Legend: b: tetrafluoro-1,3-amino benzene; c: pentafluoroaniline; d: pentafluoronitrobenzene; e: pentafluorophenol; f: pentafluorobenzoic acid; g: tetrafluoro-1,3-hydroxy benzene; h: tetrafluoro-1,4-hydroxy benzene; i: tetrafluoro-1,2-phthalic acid.

those for log K_{OW}, which were by far the weakest before, are as good as those for Q_{zz}. The fact that all three parameters give essentially the same correlations when the stochastic distribution of organofluorine between different components of humic acid is considered, but the molecular-level property Q_{zz} produces the best correlations when looking at the presence of interactions directly at different components of humic acid directly, suggests that molecular-level properties are better than bulk properties of xenobiotics for understanding the independent molecular-level associations between xenobiotics and different domains of humic acid, but that the bulk properties, particularly partitioning factors, in addition to the underlying molecular properties, are good for describing interdependent distributions between components of natural organic matter.

Regarding the origin of the two sets of xenobiotics that emerge in the aromatic/non-aromatic distribution plots, all compounds fit the same trend for the number of interactions at aromatic sites very well, but less so for the non-aromatic contribution (see fig 3.7). This suggests that these compounds have the same type of attractive interaction with the aromatic components of humic acid, but the dihydroxy benzenes and phthalic acid have an additional repulsive factor at the non-aromatic components of humic acid not exhibited by the other organofluorine compounds studied. These three compounds are di-acids and potentially exist in equilibrium with highly anionic forms, whereas for the other compounds, even those that are ionizable, such as pentafluorophenol, interact with humic acid as though they are neutral, as discussed above. It is possible that electrostatic repulsion prevents the di-acidic compounds from interacting as strongly with non-aromatic humic acid domains.

3.4 Conclusions

It is shown here that the Reverse-Heteronuclear Saturation Transfer Difference NMR experiment is very sensitive to subtle differences in the binding pattern of structurally similar xenobiotics interacting with dissolved humic acid. In combination with the forward HSTD experiment, which reveals the binding orientation of the xenobiotic compound during its interaction, a detailed picture of the interactions between xenobiotics and a complex mixture of environmentally relevant organic matter is possible. Current limitations of this approach include

the requirement of perfluorinated xenobiotics and high concentrations of both dissolved natural organic matter and xenobiotic compounds. Further work is necessary to reduce the need for such high xenobiotic concentrations. The research in this chapter further shows that the type of non-covalent interactions that occur in environmental systems are highly complex and are a promising area for future study that will require a variety of different analytical and theoretical approaches to be fully understood. Nevertheless, the analytical approaches to the problem of contaminant interactions in the environment presented here show great promise in providing a detailed molecular-level picture of environmental phenomenon such as sorption and desorption that is needed to fully understand the transport and fate of environmental organic contaminants.

3.5 References

(1)   Alexander, M. How toxic are toxic chemicals in soil? *Environ. Sci. Technol.* **1995**, *29* (11)*,* 2713-2717.

(2)   Gauthier, T. D.; Selz, W. R.; Grant, C. L. Effects of structural and compositional variations of dissolved humic materials on pyrene Koc values. *Environ. Sci. Technol.* **1987**, *21* (3), 243-248.

(3)   Chiou, G. T.; Malcom, R. L.; Brinton, T. I.; Kile, D. E. Water solubility enhancement of some organic pollutants and pesticides by dissolved humic and fulvic acids. *Environ. Sci. Technol.* **1986**, *20* (5), 502-508.

(4)   Robertson, B. K.; Alexander, M. Sequestration of DDT and dieldrin in soil: disappearance of acute toxicity but not the compounds. *Environ. Toxicol. Chem.* **1998**, *17* (6), 1034-1038.

(5)   Chung, N.; Alexander, M. Differences in sequestration and bioavailability of organic compounds aged in dissimilar soils. *Environ. Sci. Technol.* **1998**, *32* (7), 855-860.

(6)   Ter Laak, T. L.; Ter Bekke, M. A.; Hermens, J. L. M. Dissolved organic matter enhances transport of PAHs to aquatic organisms. *Environ. Sci. Technol.* **2009**, *43* (19), 7212-7217.

(7)   Smith, K. E. C.; Thullner, M.; Wick, L. Y.; Harms, H. Sorption to humic acids enhances polycyclic aromatic hydrocarbon biodegradation. *Environ. Sci. Technol.* **2009**, *43* (19), 7205-7211.

(8)   Alexander, M. Aging, bioavailability, and overestimation of risk from environmental pollutants. *Environ. Sci. Technol.* **2000**, *34* (20), 4259-4265.

(9)   Semple, K. T.; Morriss, A. W. J.; Patton, G. I. Bioavailability of hydrophobic organic contaminants in soils: fundamental concepts and techniques for analysis. *Euro. .J Soil Sci.* **2009***, 54* (4), 809-818.

(10)   Khalaf, M.; Kohl, S. D.; Klumpp, E.; Rice, J. A.; Tombácz, E. Comparison of sorption domains in molecular weight fractions of a soil humic acid using solid-state ^{19}F NMR. *Environ. Sci. Technol.* **2003***, 37* (13), 2855-2860.

(11)   Longstaffe, J. G.; Simpson, M. J.; Maas, W.; Simpson, A. J. Identifying components in dissolved humic acid that bind organofluorine contaminants using ^{1}H{^{19}F} reverse heteronuclear saturation transfer difference NMR spectroscopy. *Environ. Sci. Technol.* **2010**, *44* (14), 5476-5482.

(*12*)   Pan, B.; Ghosh, S.; Xing, B. Dissolved organic matter conformation and its interaction with pyrene as affected by water chemistry and concentration. *Environ. Sci. Technol.* **2008**, *42* (5), 1594-1599.

(13)   Pan, B.; Ghosh, S.; Xing, B. Nonideal binding between dissolved humic acids and polyaromatic hydrocarbons. *Environ. Sci. Technol.* **2007**, *41* (18), 6472-6478.

(14)   Smejkalova, D.; Spaccini, R.; Fontaine, B.; Piccolo, A. Binding of phenol and differently halogenated phenols to dissolved humic acid as measured by NMR spectroscopy. *Environ. Sci. Technol.* **2009**, *43* (14), 5377-5382.

(15)   Shirzadi, A.; Simpson, M. J.; Xu, Y.; Simpson, A. J. Application of saturation transfer double difference NMR to elucidate the mechanistic interactions of pesticides with humic acid. *Environ. Sci. Technol.* **2008**, *42* (4)*,* 1084-1090.

(16)   Zhu, D.; Hyun, S.; Pignatello, J. J.; Lee, L. S. Evidence for π-π electron donor-acceptor interactions between π-donor aromatic compounds and π-acceptor sites in soil organic matter through pH effects on sorption. *Environ. Sci. Technol.* **2004***, 38* (16), 4361-4368.

(17)   Wang, X.; Xing, B. Importance of structural makeup of biopolymers for organic contaminant sorption. *Environ. Sci. Technol.* **2007**, *41* (10)*,* 3559-3565.

(18)   Laor. Y.; Rebhun, M. Evidence for nonlinear binding of PAHs to dissolved humic acids. *Environ. Sci. Technol.* 2002, *36* (5), 955-961.

(19)   Xing, B.; Pignatello, J.J. Dual-mode sorption of low-polarity compounds in glassy poly(vinyl chloride) and soil organic matter. *Environ. Sci. Technol.* **1997**, *31* (3)*,* 792-799.

(20) Chefetz, B.; Xing, B. Relative role of aliphatic and aromatic moieties as sorption domains for organic compounds: A review. *Environ. Sci. Technol.* **2009**, *43* (6)*,* 1680-1688.

(21) Keiluweit, M.; Kleber, M. Molecular-level interactions in soils and sediments: the role of aromatic π-Systems. *Environ. Sci. Technol.* **2009**, *43* (10), 3421-3429.

(22) Tülip, H.G.; Fenner, K.; Schwarzenbach, R. P.; Goss, K-U. pH-dependent sorption of acidic organic chemicals to soil organic matter. *Environ. Sci. Technol.* **2009**, *43* (24), 9189-9195.

(23) Barriuso, E.; Benoit, P.; Dubus, I. Formation of pesticide nonextractable (bound) residues in soil: magnitude, controlling factors and reversibility. *Environ. Sci. Technol.* **2008**, *42* (6)*,* 1845-1854.

(24) Xing, B.; Pignatello, J. J.; Gigliotti, B. Competitive sorption between atrazine and other organic compounds in soils and model sorbents. *Environ. Sci. Technol.* **1996**, *30* (8)*,* 2432-2440.

(25) Shirzadi, A.; Simpson, M. J.; Kumar, R.; Baer, A. J.; Xu, Y.; Simpson, A. J. Molecular interactions of pesticides at the soil-water interface. *Environ. Sci. Technol.* **2008**, *42* (15)*,* 5514-5520.

(26) Simpson, A. J.; McNally, D. J.; Simpson, M. J. NMR spectroscopy in environmental research: From molecular interactions to global processes. *Prog. Magn. Reson. Spect.* **2010**, *58* (3), 97-175.

(27) Kelleher, B. P.; Simpson, A. J. Humic substances in soils: are they really chemically distinct? *Environ. Sci. Technol.* **2006**, *40* (15)*,* 4605-4611.

(28) Sutton, R.; Sposito, G. Molecular structure in soil humic substances: the new view. *Environ. Sci. Technol.* **2005**, *39* (23), 9009-9015.

(29) D'eon. J. C.; Simpson, A. J.; Kumar, R.; Baer, A. J.; Mabury, S. A. Determining the molecular interactions of perfluorinated carboxylic acids with human sera and isolated human serum albumin using nuclear magnetic resonance spectroscopy. *Environ. Toxicol. Chem.* **2010***, 29* (8), 1678-1688.

(30) Mayer, M.; Meyer, B. Characterization of ligand binding by saturation transfer difference NMR spectroscopy. *Angew. Chem. Int. Ed.* **1999**, *38* (12)*,* 1784-1788.

(31) Diercks, T.; Riberio, J.P.; Canada, F. J.; André. S.; Jiménez-Barbero, J.; Gabius, H-J. Fluorinated carbohydrates as lectin ligands: Versatile Sensors in ^{19}F-detected saturation transfer difference NMR spectroscopy. *Chem. Eur. J.* **2009,** *15* (23), 5666-5668.

(32) De Paolis, F.; Kukkonen, J. Binding of organic pollutants to humic and fulvic acids: influence of pH and the structure of humic material. *Chemosphere* **1997**, *34* (8), 1693-1704.

(33) Dixon, A. M.; Mai, M. A.; Larive, C. K. NMR investigation of the interactions between 4'-fluoro-1'-acetonaphthone and the Suwannee river fulvic acid. *Environ. Sci. Technol.* **1999**, *33* (6), 958-964.

(34) Ellis, D. A.; Cahill, T. M.; Mabury, S. A.; Cousins, I. T.; Mackay, D. Partitioning of organofluorine compounds in the environment. The handbook of environmental chemistry, Vol . 3, Part N ed. A.H. Neilson, Springer-Verlag, Berlin, **2002**. pp 63-83.

(35) Soong, R.; Smith, P. E. S.; Xu, J.; Yamamoto, K.; Im, S-C.; Waskell, L.; Ramamoorthy, A. **2010**. Proton-evolved local-field solid-state NMR studies of cytochrome b$_5$ embedded in bicelles, revealing both structural and dynamical information. *J. Am. Chem. Soc.* **2010**, 132, 5779-5788.

(36) Krezel, A.; Bal, W. A formula for correlating pKa values determined in D$_2$O and H$_2$O. *J. Inorg. Biochem.* **2004**, *98* (1), 161-166.

(37) Wavefunction, SPARTAN (Wavefunction, Irvine, CA), 2009, Version 4.11.

(38) Nanny, M. A.; Maza, J. P. Noncovalent interactions between monoaromatic compounds and dissolved humic acids: A deuterium NMR T$_1$ relaxation study. *Environ. Sci. Technol.* **2001**, *35* (2), 379-384.

(39) SPARC On-line Generator. http://sparc.chem.uga.edu/sparc/ Accessed on March 5 2011.

(40) Zhu, D.; Herbert, B. E.; Schlautman, M. A. Sorption of pyridine to suspended soil particles studied by deuterium nuclear magnetic resonance. *Soil Sci. Soc. Am. J.* **2003**, *67* (5), 1370-1377.

(41) Wijnja, H.; Pignatello, J. J.; Malekani, K. Formation of π-π complexes between phenanthrene and model π-acceptor humic subunits. *J. Environ. Qual.* **2004**, *33* (1), 265-275.

(42) Dunitz, J. D.; Gavezzotti, A.; Schweizer, W. B. Molecular shape and intermolecular liaison: hydrocarbons and fluorocarbons. *Helv. Chim. Acta* **2003**, *86* (12), 4073-4092.

CHAPTER 4
TEMPERATURE EFFECTS ON SOLUTION-STATE ORGANOFLUORINE-HUMIC ACID ASSOCIATIONS

4.0   Abstract

Natural organic matter (NOM) plays an important role as a mediator in the fate and transport of many anthropogenic organic contaminants in aquatic and soil environments. There is a growing body of knowledge regarding the components of humic acid, the alkali soluble fraction of NOM, where polyfluorinated organic compounds may interact. Both general and site-specific modes of interaction having been suggested, however a more quantitative understanding of the strengths of these interactions is needed to fully understand the underlying mechanisms. The equilibrium between free and humic acid-bound organofluorine is studied here using Pulsed Field Gradient (PFG) Nuclear Magnetic Resonance (NMR) spectroscopy. Detection of ^{19}F is used to quantify the attenuation of the apparent diffusivity of organofluorine with and without humic acid present, while ^{1}H detection is used to account for motion of the humic acid aggregates. From these measurements, the equilibrium between free and bound organofluorine is estimated. Four selected compounds with known divergence in their humic acid interaction mechanisms are investigated; pentafluoroaniline (PFA), pentafluorophenol (PFP), perfluorooctanoic acid (PFOA), and potassium perfluorooctane sulfonate (KPFOS). Under the conditions employed here, it is shown for PFA, PFP, and KPFOS that the extent of association with humic acid association increases as temperature decreases, supporting a general interaction mechanism controlled largely by desolvation effects. PFOA exhibits divergent behavior, with a marked non-linear decrease in the extent of interaction as temperature decreases, suggesting a specific mode of interaction independent of desolvation effects in agreement with previous studies.

4.1   Introduction

Interactions between natural organic matter (NOM) and anthropogenic organic contaminants, or xenobiotics, influence numerous processes that control the fate and transport of xenobiotics in the environment. The strong sorption or sequestration of contaminants by soil-bound NOM, *(1, 2)* reduces bioaccessibility *(3, 4)*, in turn increasing the environmental persistence of organic contaminants *(4, 5)* but reducing their immediate ecotoxicological impact *(6)*. Interactions with dissolved forms of NOM increase the solubility of otherwise hydrophobic xenobiotics *(7)*, aiding in their desorption and facilitating transport *(8, 9)* that can extend the environmental impact over a larger area than the site of the initial spill or application, as well as increasing the bioaccessibility of hydrophobic xenobiotics to various organisms in the ecosystem *(8, 10)*. Elucidating these interactions is key to developing a full understanding of the role NOM plays in the lifecycle of anthropogenic organic contamination and subsequently their potential impact on the environment *(11)*.

Nuclear Magnetic Resonance (NMR) spectroscopy is emerging as a key tool in environmental science for probing the molecular nature of xenobiotic interactions with natural organic matter *(12-15)*. Recently, environmental applications of the saturation transfer NMR technique have been used to probe intermolecular interactions between xenobiotics and dissolved forms of NOM *(16-18)*. These studies have been useful in producing qualitative molecular-level understandings of the interactions between xenobiotics and NOM, specifically the distribution of xenobiotic interactions at different components of humic acid *(17, 18)*, the identity of those sites *(17)*, and the orientation of the xenobiotics during their interactions *(16, 18)*. It is known that the mode of interaction between these xenobiotics and NOM are primarily weak and non-covalent, and as such there is rapid exchange between the bound and unbound forms in solution *(15, 18)*. It has been observed that aromatic organofluorine compounds interact with all components of humic acid *(18)* while perfluorooctanoic acid (PFOA) interacts selectively with protein-derived components *(17)*. At a first approximation, the mechanism for interactions between aromatic organofluorine compounds and dissolved humic acid resembles partitioning into humic acid aggregates and can be modeled to a degree using measures of solubility and hydrophobicity *(18)*. Less is known about the mechanisms of interaction for PFOA, aside from the proteinaceous nature of its selective binding domain *(17)*.

In the present study, NMR-based diffusion measurements are used to probe the dynamics of interaction between dissolved humic acid and several organofluorine compounds: pentafluoroaniline (PFA), pentafluorophenol (PFP), perfluorooctanoic acid (PFOA), and potassium perfluorooctane sulfonate (KPFOS). The aromatic compounds used here are not known specifically as environmental pollutants, but are used instead because their interactions with dissolved humic acid have been well studied *(18)*. PFA and PFP interact primarily non-specifically with humic acid, however, both can exhibit a preference for associations at aromatic components of humic acid under certain conditions. These interactions are hypothesized to be largely non-specific in origin, arising primarily from hydrophobic desolvation effects *(18)*. PFOA and KPFOS are known persistent organic pollutants *(19-21)* that have industrial use as surfactants *(22)* in addition to their environmental introduction as bi-products of the production and use of polyfluorinated non-stick coatings *(23)*. For PFOA, it is known that the interaction with humic acid occurs selectively at protein-like components *(17)*, whereas the sites of interaction for KPFOS at humic acid have yet to be determined.

For this study, the use of perfluorinated organic compounds as xenobiotics provides an easy method to observe NMR signals independently from both the xenobiotics and from the humic acid by using ^{19}F Nuclear Magnetic Resonance (NMR) spectroscopy to selectively observe the xenobiotic and ^{1}H NMR spectroscopy to selectively observe the humic acid. The diffusion of both the xenobiotic and the aggregated humic acid are determined using pulsed-field gradient (PFG)-based NMR spectroscopy *(24)*, which acts by encoding the position of a set of molecules along the z-axis, and then measuring the movement of molecules away from this starting position after a set period for diffusion *(25)*. The proportion of free vs. humic acid-associated organofluorine can be determined by measuring the attenuation of the apparent organofluorine diffusivity in the presence of humic acid *(26)*. Weak interactions with a macromolecule, or supramolecular assemblage, such as that formed by humic acid *(27, 28)*, result in the organofluorine compounds spending some period of time in free solution, diffusing at a rate determined by the molecules hydrodynamic size, and a period of time bound to the aggregate, moving at a slower rate determined by the motion of humic acid. The measured self-diffusion coefficient of a quickly exchanging molecule in solution is a weighted average of the two rates of diffusion *(27)*. The self-diffusion of the free organofluorine compound is determined by measurements in the absence of humic acid, while the rate of diffusion of the bound xenobiotic is

the same as that of humic acid, and is estimated from ^{1}H diffusion measurements. This general approach for measuring association equilibrium is well established *(27, 28)* and has been applied previously to understand environmental xenobiotic interactions by Dixon *et al.*, where the authors used it to estimate the extent of association between humic acid and 4'-fluoro-1'-acetonaphtone *(26)*.

In this study, association equilibria are estimated at various temperatures in order to extract thermodynamic information about the interactions using the van't Hoff relationship between equilibrium and temperature.   In doing so, the previously developed hypotheses for the mechanisms of interaction between these xenobiotics and humic acid are tested, specifically that PFA and PFP are driven to interact with dissolved humic acid primarily by general desolvation effects *(15, 18)*, while perfluorooctanoic acid interacts through a more specific mechanism *(17)*. The interactions between KPFOS and humic acid have not previously been studied; here, comparison of the interaction strength of KPFOS to other organofluorine compounds are used to predict the type of interactions expected for this compound and humic acid, which are then tested using the ^{1}H$\{^{19}$F$\}$ reverse-heteronuclear saturation transfer difference (RHSTD) NMR experiment *(17, 29)*.

4.2 Materials & Methods

4.2.1 Sample Preparation

All solutions of humic acid were prepared using the International Humic Substance Society (IHSS) standard Pahokee Peat Humic Acid. Organofluorine compounds were purchased from Synquest Chemical Laboratories (Alachua Florida, USA) and used as is. For the diffusion experiments, organofluorine/humic acid mixtures were prepared using humic acid concentrations of 0, 5, 10, and 20 mg ml^{-1} and, individually, organofluorine concentrations of 0.03 mmol ml^{-1} for pentafluoroaniline (CAS 771-60-8), and pentafluorophenol (CAS 771-61-9), and 0.003 mmol ml^{-1} for perfluorooctanoic acid (CAS 68141-02-6), and potassium perfluorooctane sulfonate (CAS 2795-39-3). The pH of each sample was set to 6.8 using minimal quantities of NaOD (99.5% D, 30% in D$_2$O) and DCl (99.5% D, 35% in D$_2$O), which corresponds to an actual pD of about 7.2 due to isotope effects at the electrode *(30)*.   At this pH, pentafluorophenol and

perfluorooctanoic acid should be fully anionic. For the RHSTD experiments, the samples were prepared by mixing 50 mg IHSS peat humic acid with 10 mg organofluorine in D_2O with the pH set to 6.8 (pD=7.2). Higher humic acid concentrations are required for the RHSTD experiments than for the diffusion experiments in order to reduce experimental time, as RHSTD experiments are less sensitive than diffusion measurements.

4.2.2 NMR Spectroscopy

4.2.3.1 Diffusion Measurements

Diffusion NMR experiments were preformed on a Bruker Avance III 500 MHz NMR spectrometer utilizing a ^{19}F optimized SEF probe with actively shielded Z-gradients. The stimulated echo experiment employing bipolar gradients and longitudinal eddy current delays was used for diffusion measurements. The probe gradient was calibrated to 52.8 Gauss cm^{-1} at full power. 50 ms diffusion time was employed for the ^{19}F diffusion measurements and 180 ms for the ^{1}H humic acid measurements. Gradient pulse lengths of 3.6 ms and an eddy current delay of 0.5 ms were applied. Diffusion measurements were performed by incrementing the gradient strength over 32 values until the signal is attenuated to 10% of the original signal strength. For the ^{19}F measurements, 90° pulse lengths of 8.15 to 8.63 μs were used and spectra were acquired after 128 dummy scans using 16 transients per gradient strength for pentafluoroaniline and pentafluorophenol, and 128 transients for PFOA and KPFOS. Recycle delays of 5 s were used throughout. For the ^{1}H measurements, 90° pulse lengths of 11.50 to 11.60 μs were used and spectra were acquired using 128 scans at each gradient power level, with recycle delays of 2 s. Spectra were apodized using an exponential multiplication factor corresponding to 20 Hz line broadening for the ^{19}F spectra and 50 Hz line broadening for the ^{1}H spectra. Apparent diffusivity was determined from 2D DOSY plots created using Bruker Topspin™ version 2.1 using monoexponential fittings, a noise-sensitivity factor of 4, and a spike-suppression factor of 1. 32 slices were processed with 32728 points in the F2 dimension and the diffusion axis was created with 512 points in the F1 dimension.

All experiments were performed at 300 K, except for the variable temperature experiments, which were run sequentially at temperatures between 278 K and 313 K. Temperatures were

calibrated using neat methanol *(31)*. On select samples, experiments were performed incrementing the temperature from high to low values, and then back to high temperature to check for hysteresis and to verify that equilibrium was reestablished after each temperature adjustment. No hysteresis was observed.

4.2.3.2 Reverse Heteronuclear Saturation Difference Spectroscopy

The $^1H\{^{19}F\}$ RHSTD NMR experiment was performed on a mixtures of organofluorine and humic acid using a 500 MHz Bruker Avance NMR spectrometer employing a 5 mm QXI probe. The RHSTD experiment has been described previously *(17, 18, 29)*. Saturation was produced in the ^{19}F nuclei of each organofluorine using a train of 18 on resonance Gaussian shaped pulses at 0.6866 W power and 50 ms length, while a ^1H spectrum of humic acid was acquired. This spectrum was subtracted using phase cycling from the equivalent spectrum obtained with the ^{19}F saturation set to + 1,000,000 Hz, where no ^{19}F resonances occur. The resultant difference spectrum reveals those signals in the ^1H spectrum that receive saturation from ^{19}F nuclei by way of an intermolecular interaction. ^1H 90° pulses were between 10.5 and 11.5 µs. 12288 transients were acquired using 8192 points and 2s recycle delays. Spectra were processed using 16384 points and apodized using an exponential function corresponding to 50 Hz line broadening. Water signals were suppressed using presaturation. All RHSTD spectra were acquired at 298 K.

4.3 Results & Discussion

For the PFG-NMR diffusion experiments used here, molecular diffusivity, D, can be determined by the loss of signal intensity as a function of the gradient strength, G, and the period allowed for diffusion, Δ, using

$$I = I_0 \exp [-(\gamma G\delta)^2 (\Delta - \delta/3 - \tau/2)D] \qquad [4.1]$$

where I is the recorded signal strength, I_o is the signal strength in the absence of any diffusion, γ is the magnetogyric ratio of the nucleus, δ is the duration of the gradient pulse, and τ is the delay for the electronics to recover from eddy currents induced by changes in gradients *(24)*.

Figure 4.1 compares organofluorine diffusivity in the presence of humic acid, $D_{X(obs)}$, with that of a standard solution free from humic acid, $D_{X(free)}$, over a range of humic acid concentrations at 298 K. A marked attenuation of the organofluorine diffusivity is observed in the presence of humic acid. This effect is due to weak associations between the small, fast moving organofluorine compounds and the larger, slow moving humic acid aggregates, with the degree of attenuation controlled by the dynamics of the equilibrium between free and bound organofluorine compounds. The attenuation as a function of humic acid concentration appears to be linear for all compounds over the range studied. Equilibrium dynamics should be affected by a change in mechanism: the lack of such a change here demonstrates that over the concentration range tested, an increase in the humic acid concentration provides more material for organofluorine associations without influencing the mechanism behind the interaction. This suggests that even at very dilute humic acid concentrations, where the attenuation of self-diffusion would be hardly noticeable, and thus difficult to study by this method, the same association dynamics between these organofluorine compounds and humic acid should be present.

The apparent rate of diffusion of a small molecule in rapid equilibrium between a free state and a colloid-bound state is the weighted average of its rates of diffusion in those two states *(27)*. Therefore, quantitative analysis of the dynamic equilibrium between free and bound organofluorine can be made by comparison of the degree of attenuation of the apparent organofluorine diffusion relative to its rate of self-diffusion in the absence of humic acid and to that of the humic acid aggregates themselves *(28)*. Here, the rate of free diffusion is taken to be the measured rate of diffusion in a solution without humic acid, while the rate of bound diffusion is taken to be the same as that of the humic acid. Humic acid is fully soluble at moderate to high pH values, where it forms fully solvated supramolecular aggregates, the structure of which has been well studied *(32, 33)*. In general, there is a distribution of apparent diffusion rates amongst the different components *(32)*, which are structurally similar to the biopolymers, such as lignin, protein, carbohydrates, and lipids from which the humic acid is derived (*34-36*). Diffusion experiments do not show directly at which type of humic acid material the organofluorine compounds interact and, for the purposes here, the median diffusion rate of humic acid is used throughout. While this introduces some error in the knowledge of the exact diffusivity of the humic acid aggregates, and thus the diffusivity of the bound organofluorine, the spread between
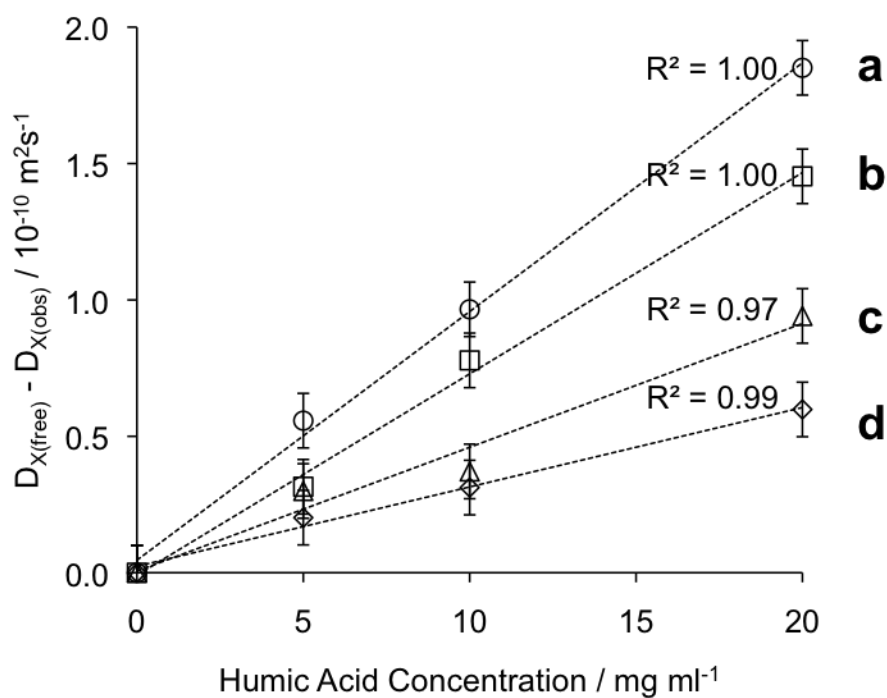
Figure 4.1 Plots of $D_{X(free)} - D_{X(obs)}$ vs. humic acid concentration for selected organofluorine compounds at 298 K. **a**: pentafluoroaniline; **b**: potassium perfluorooctane sulfonate; **c**: perfluorooctanoic acid; **d**: pentafluorophenol.

the fastest and slowest humic acid components is small relative to the observed attenuation of the apparent organofluorine diffusion.

Assuming the attenuation of the measured organofluorine diffusion rates is proportional to the average extent of interaction with humic acid at equilibrium, under the conditions employed here the extent of the humic acid associations for these compounds is found to follow the order PFA > KPFOS > PFOA > PFP. Presuming that the primary driving force for associations with humic acid is the energy cost of full solvation of these molecules in the aqueous environment, differences in time spent associating with humic acid for different compounds should be comparable to differences in the energy requirement for the solvation for these compounds *(37)*: the least soluble compound would form the strongest associations with humic acid, and the most soluble the weakest.

As a measure for this effect, the solubility of these compounds at the appropriate pH (i.e. pD in D_2O), as well as log K_{OC}, were calculate using ACD/Labs physical property calculator and are compared in table 4-1 *(38)*. In pure H_2O, KPFOS has a much lower solubility than PFOS, which has a solubility of 7.55 mg ml^{-1}, and without knowledge of the speciation in our samples the exact solubility here is unknown. Both PFP and PFOA are essentially fully anionic at the pH studied *(38)*. The ordering of the aqueous solubilities (KPFOS < PFA < PFP < PFOA) differs from the ordering observed for the humic association equilibria with PFOA interacting much more strongly than its relative solubility would suggest, and the ordering of PFA and KPFOS being switched, however the solubility of KPFOS is uncertain. The ordering of the log K_{OC} values, (PFA > KPFOS > PFOA =PFP), provides a closer match to the relative humic acid association equilibria, however here PFP and PFOA should be expected to exhibit similar equilibria, which they do not. A hydrophobic-driven desolvation model accounts for the ordering of the extent of humic acid association for KPFOS, PFA, and PFP, however PFOA interacts with humic acid more strongly under this set of conditions than would be expected if simple desolvation was the primary mechanism driving the PFOA associations.

Table 4-1   Solubility and hydrophobicity parameters for selected organofluorine compounds at pH 7.2 and 298 K.

Compound	Solubility (mg mL^{-1})	Log K$_{OC}$
Potassium perfluorooctane sulfonate	Barely soluble	1.70
Perfluorooctanoic acid	3.4	1.13
Pentafluoroaniline	0.023	2.82
Pentafluorophenol	0.84	1.18

Figure 4.2 shows the apparent diffusivity for the free organofluorine, the attenuated organofluorine and humic acid as a function of temperature for the four organofluorine compounds studied. For all three sets of diffusion measurements, PFA (fig. 4.2a) and PFP (fig. 4.2b) exhibit similar curves to each other. For PFOA (fig. 4.2d), the free and apparent curves converge at lower temperatures while the humic acid curve is essentially the same as that observed for PFA and PFP. The similarity in the humic acid curves for these three compounds which are themselves each affected differently by the presence of humic acid (see fig. 4.1) indicate that the interactions have minimal effect on the structure of the humic acid aggregates. For KPFOS (fig. 4.2c), however, the rate of diffusion of humic acid increases in the presence of this xenobiotic. It has been reported previously that surfactants, such as KPFOS, can have a significant effect on the rate of diffusion of humic substances *(39)*. PFOA, which also has surfactant properties, does not seem to have the same influence on humic acid; however, this may reflect the greater solubility, and thus greater extent of free PFOA under the same conditions.
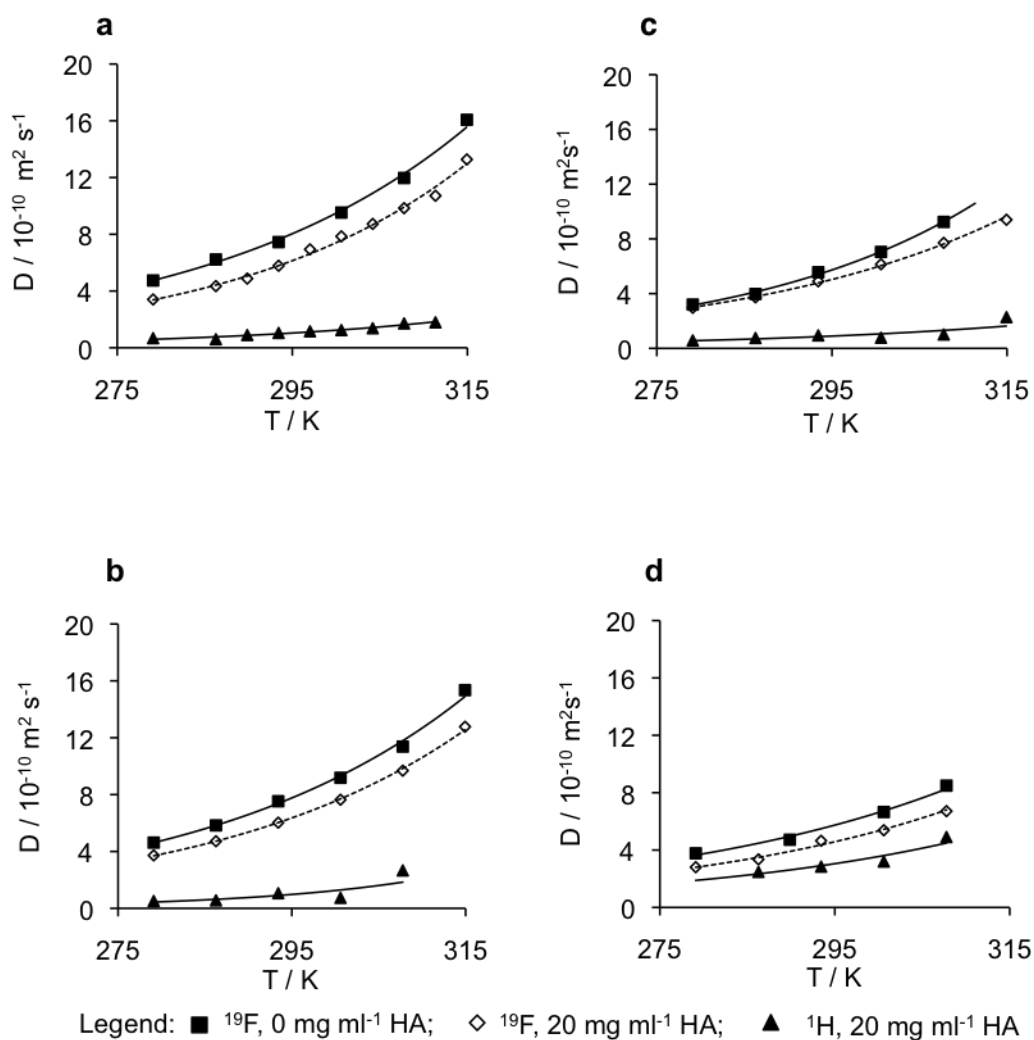
Figure 4.2 Changes in the apparent diffusivity of the components in the humic acid / organofluorine mixtures as a function of temperature. Shown are the rates of the organofluorine compound in the 0 mg ml^{-1} humic acid reference, the organofluorine in the 20 mg ml^{-1} humic acid sample, and the average rate of diffusion of the humic acid components. **a**: PFA; **b**: PFP; **c**: PFOA; **d**: KPFOS. The error in these measurements is smaller than the data points.

The equilibrium for the association between organofluorine xenobiotics and humic acid is estimated here as a partitioning operation between the hydrophilic humic acid aggregates and water:

$$k_{HA\text{-}aq} = f_{HA} / f_{aq} \qquad\qquad [4.2]$$

where f_{HA} and f_{aq} are the fraction of xenobiotic present in each of the humic acid and aqueous domains at any given time. The fractional amount of xenobiotic in the bound humic acid state at a given moment is

$$f_{HA} = (D_{X(free)} - D_{HA}) / (D_{X(free)} - D_{X(obs)}), \qquad\qquad [4.3]$$

with the equivalent fraction in the free state given as

$$f_{aq} = 1 - f_{HA}, \qquad\qquad [4.4]$$

where D_{HA}, $D_{X(free)}$, and $D_{X(obs)}$ are the measured self-diffusion rates of humic acid in the presence of organofluorine, the organofluorine in pure D_2O, and the organofluorine in the presence of humic acid, respectively, under identical temperature, concentration, and pH conditions (27).

Association equilibria for each organofluorine system is calculated here based on exponential fittings to the diffusion data in figure 4.2 and equations 2, 3 and 4. These $k_{HA\text{-}aq}$ equilibria are presented as van't Hoff plots in figure 4.3 to illustrate the temperature dependence on the measured associations. For PFA and PFP, which exhibited similar diffusion-temperature trends in figure 4.2, both compounds show an increase in humic acid association as the temperature, and thus aqueous solubility, decreases. This increased association is more marked for PFA, suggesting that these interactions are largely driven by solubility, with PFA having a lower aqueous solubility, and thus exhibiting a more significant change in its equilibrium dynamics upon changes in temperature than PFP, which is formally anionic at the studied pH and thus highly soluble.
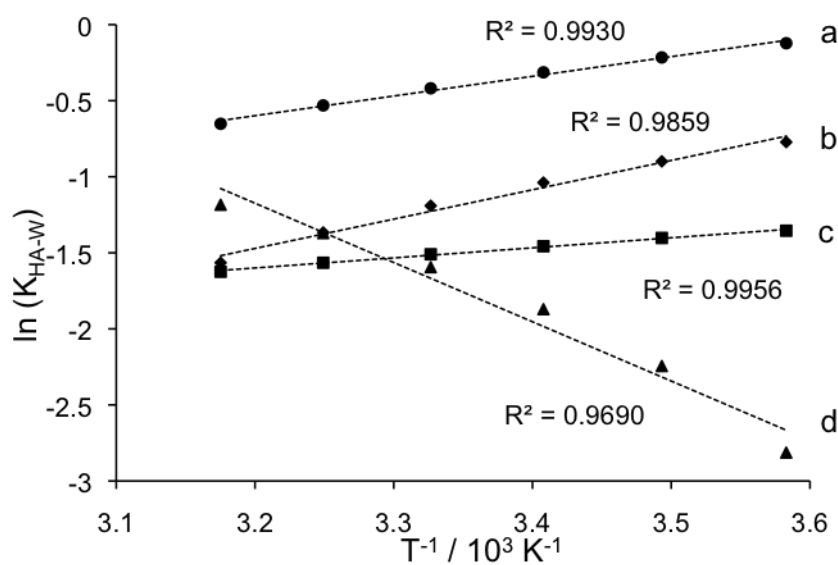
Figure 4.3   Van't Hoff plots using the calculated association equilibrium constants, K_{HA-W}, for organofluorine compounds in humic acid solutions. **a**: KPFOS; **b**: PFA; **c**: PFP; **d**: PFOA. The error in these measurements is smaller than the data points.

At the higher temperatures, where aqueous solubility of the organofluorine compounds is increased, PFA and PDP exhibit similarly low degrees of associations with humic acid. KPFOS, which has much lower aqueous solubility than the other organofluorine compounds, associates much more strongly with humic acid than either PFA or PFP, with the extent of association also increasing as the temperature decreases. The greater the extent of association for KPFOS in general may explain the strong effect this xenobiotic has on the structure, and thus rate of diffusion, of humic acid itself. PFOA exhibits divergent behavior from the other compounds studied here, with the extent of interaction increasing at higher temperatures and only minimal association observed at lower temperatures where the other compounds showed their strongest interactions.

Following from the van't Hoff equation

$$d \ln K / d (T^{-1}) = - \Delta H° / R, \qquad\qquad [4.5]$$

where K is the equilibrium coefficient, T is the temperature in an absolute scale, and R is the ideal gas constant; the change in equilibrium with temperature is linear only if the change in enthalpy, $\Delta H°$, is independent of temperature *(40)*. The van't Hoff plots for KPFOS, and PFP, support this assumption, with linear correlation factors of 0.9930 and 0.9956, respectively. PFA exhibits some divergence from linearity with a correlation factor of 0.9859, and PFOA exhibits marked divergence from linearity over the temperature range tested with a correlation factor of 0.9690 and is visibly curved, suggesting that the enthalpy change for the interaction here is not independent with temperature. It was shown previously that PFA and PFP interact with dissolved humic acid primarily through a polarity driven mechanism, roughly proportional to their solubility and measures of their hydrophobicity *(18)*. A general interaction such as this would be expected to exhibit temperature independent enthalpy changes since the functionality of the binding sites, which are essentially any and all of humic acid, should not significantly change their mode of operation with temperature. The slight non-linearity observed for PFA suggests that under these conditions PFA may have a less uniform distribution profile than PFP, both of which are known to exhibit small preferences for interactions at aromatic humic acid sites. PFOA, however, has been shown to interact selectively with protein-derived components of humic acid *(17)*. This selectivity was suggested to arise from a specific interaction

mechanism independent of hydrophobic or solubility driven processes. If the only sites available for PFOA interaction are at protein-like structures, this suggests stericlly restricted sites, the nature and accessibility of which is likely temperature dependent. It is possible that at lower temperatures, the PFOA binding sites in humic acid become inaccessible due to conformational changes from changes in the dynamics of the inter- and intra-molecular responsible for the secondary structure of protein-like structures. Changes such as this explain the observed decrease in association strength as the temperature decreases.

The binding sites for KPFOS in dissolved humic acid have not yet been determined. From the similarity between the van't Hoff plots of KPFOS and PFA and PFP, it is predicted that this compound also interacts with the components of humic acid primarily in a non-specific manner, driven by hydrophobic effects rather than through a specific interaction as is observed for PFOA. To test this hypothesis, ^{1}H{^{19}F} RHSTD NMR experiments of mixtures of humic acid and the four organofluorine compounds were acquired in order to elucidate their humic acid binding sites. The resultant RHSTD spectra are shown in figure 4.4. Comparing the RHSTD spectrum of the KPFOS mixture to a quantitative reference ^{1}H spectrum of the humic acid, which is also shown as an overlay on the RHSTD spectra, it is clear that KPFOS interacts with all components of humic acid, nearly proportional to their occurrence in the mixture. This confirms the hypothesis that KPFOS interacts with humic acid via a general mechanism similar to that for PFA and PFP. It is also observed that under the conditions applied here, PFA exhibits greater preference for aromatic humic acid sites while PFP does not. This may account for the slight deviation from linearity observed for PFA in the van't Hoff plot, as the interactions influencing this aromatic preference may have temperature dependent changes in enthalpy, possibly due to conformational changes.

4.4 Conclusions

Using changes in the apparent self-diffusion of organofluorine compounds in solutions of humic acid, quantitative measurements of the equilibrium dynamics of the association between dissolved humic acid and organofluorine compounds were made to test hypothesis regarding the mechanisms driving these interactions. It was confirmed that pentafluorophenol and
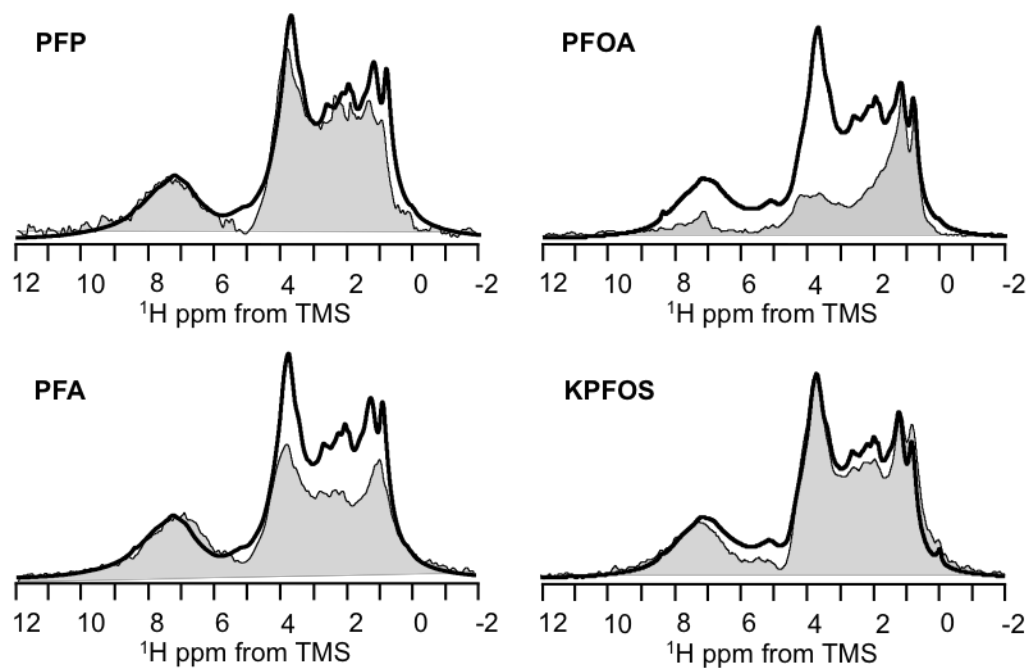
Figure 4.4 ^{1}H{^{19}F} RHSTD NMR spectra for mixtures of organofluorine and humic acid at 298 K. Quantitative spectra without ^{19}F saturation are shown in bold lines overlaid on the spectra with ^{19}F saturation, which are shaded.

pentafluoroaniline both interact with dissolved humic acid primarily via desolvation effects. Potassium perfluorooctane sulfonate was shown to form association equilibria with humic acid in a manner similar to pentafluoroaniline and pentafluorophenol, which was confirmed using the $^1H\{^{19}F\}$ RHSTD NMR experiment, which shows that this compound does not exhibit any preference for the type of humic acid moiety where interaction occurs. Perfluorooctanoic acid exhibits deviant behavior from the other three compounds studied here. A specific mechanism for interaction with humic acid is supported, agreeing with previous observations that this compound interacts solely with protein-derived components of humic acid. The accessibility of protein-like binding sites for this compound are highly temperature dependent.

4.5   References

(1)   Weber, W. J.; McGinley, P. M.; Katz, L. E. A distributed reactivity model for sorption by soils and sediments. 1. Conceptual basis and equilibrium assessments. *Environ. Sci. Technol.* **1992***, 26* (10), 1955-1962.

(2)   Karickhoff, S. W.; Brown, D. S.; Scott, T. A. Sorption of hydrophobic pollutants on natural sediments. *Water Res.* **1979**, *13* (3)*,* 241-248.

(3)   Chung, N.; Alexander, M. Differences in sequestration and bioavailability of organic compounds aged in dissimilar soils. *Environ. Sci. Technol.* **1998**, *32* (7), 855-860.

(4)   Robertson, B. K.; Alexander, M. Sequestration of DDT and Dieldrin in soil: disappearance of acute toxicity but not the compounds. *Environ. Toxicol. Chem.* **1998**, *17* (6), 1034-1038.

(5)   Semple, K. T.; Morriss, A. W. J.; Patton, G. I. Bioavailability of hydrophobic organic contaminants in soils: fundamental concepts and techniques for analysis. *Euro. .J Soil Sci.* **2009***, 54* (4), 809-818.

(6)   Alexander M. How toxic are toxic chemicals in soils?. *Environ. Sci. Technol.* **2005**, *29* (11), 2713-2717.

(7) Chiou C. T.; Malcom R. L.; Brinton T. I.; Kile D. E. Water solubility enhancement of some organic pollutants and pesticides by dissolved humic and fulvic acids. *Environ. Sci. Technol.* **1986***, 20* (5) 502-508.

(8) Ter Laak T. L.; Ter Bekke M. A.; Hermens J. L. M. Dissolved organic matter enhances transport of PAHs to aquatic organisms. *Environ. Sci. Technol.* **2009**, *43* (19), 7212-7217.

(9) Smit, M. P. J.; Grotenhuis, T.; Bruning, H.; Rulkens, W. H. Desorption of dieldrin from field aged sediments: simulating flood events. *J. Soils Sed.* **2004**, *8* (2), 80-85.

(10) Smith K. E. C.; Thullner M.; Wick L. Y.; Harms H. Sorption to humic acids enhances polycyclic aromatic hydrocarbon biodegradation. *Environ. Sci. Technol.* **2009**, *43* (19), 7205-7211.

(11) Bertsch, P. M.; Seaman, J. C. Characterization of complex mineral assemblages: Implications for contaminant transport and environmental remediation. *PNAS* **1999**, *96* (7), 3350-3357.

(12) Simpson M. J.; Simpson A. J.; Hatcher P. G. Noncovalent interactions between aromatic compounds and dissolved humic Acid examined by nuclear magnetic resonance spectroscopy. *Environ. Toxicol. Chem.* **2004**, *23* (2) 334-362.

(13) Delort, A-M.; Combourieu, B.; Haroune, N. Nuclear magnetic resonance studies of interactions between organic pollutants and soil components, a review. *Environ. Chem. Lett.* **2004**, *1* (4), 209-213.

(14) Simpson, M. J. Nuclear magnetic resonance based investigations of contaminant interactions with soil organic matter. *Soil Sci. Soc. Am. J.* **2006**, *70* (3), 995-1004.

(15) Smejkalová D.; Spaccini R.; Fontaine B.; Piccolo A. Binding of phenol and differently halogenated phenols to dissolved humic matter as measured by NMR spectroscopy. *Environ. Sci. Technol.* **2009**, *43* (14), 5377-5382.

(16) Shirzadi A.; Simpson M. J.; Xu Y.; Simpson A. J. Application of saturation transfer double difference NMR to elucidate the mechanistic interactions of pesticides with humic acid. *Environ. Sci. Technol.* **2008**, *42* (4), 1084-1090.

(17) Longstaffe, J. G.; Simpson, M. J.; Maas, W.; Simpson, A. J. Identifying components in dissolved humic acid that bind organofluorine contaminants using ^{1}H{^{19}F} reverse heteronuclear saturation transfer difference NMR spectroscopy. *Environ. Sci. Technol.* **2010**, *44* (14), 5476-5482.

(18) Longstaffe, J. G.; Simpson, A. J. Understanding solution-state noncovalent interaction between xenobiotics and natural organic matter using ^{19}F/^{1}H heteronuclear saturation transfer difference nuclear magnetic resonance spectroscopy. *Environ. Toxicol. Chem.* **2011**, *30* (8), 1745-1753.

(19) Giesy J. P.; Kannan K. Global distribution of perfluorooctane Sulfonate in wildlife. *Environ. Sci. Technol.* **2001**, *35* (7), 1339-1342.

(20) Calafat, A. M.; Needham, L. L.; Kuklenyik, Z, Reidy, J. A; Tully, J. S.; Aguilar-Villalobos, M.; Naeher, L.P. Perfluorinated chemicals in selected residents of the American continent. *Chemosphere* **2006**, *63* (3), 490-496.

(21) Martin, J. W.; Smithwick, M. W.; Braune, B.M.; Hoekstra, P. F.; Muir, D. C. G.; Mabury, S. A. Identification of long-chain perfluorinated acids in biota from the Canadian arctic. *Environ. Sci. Technol.* **2004**, *38* (2), 373-380

(22) Lau, C.; Anitole, K.; Hodes, C.; Lai, D.; Pfahles-Hutchens, A.; Seed, J. Perfluoroalkyl acids: a review of monitoring and toxicological findings. *Toxicol. Sci.* **2007**, *99* (2), 366-394.

(23) D'Eon, J. C.; Mabury, S. A. Production of perfluorinated carboxylic acids (PFCAs) from the biotransformation of polyfluoroalkyl phosphate surfactants (PAPS): exploring routes of human contamination. *Environ. Sci. Technol.* **2007,** *41* (13), 4799-4805.

(24) Wu, D.; Chen, A.; Johnson, C. S.; An improved diffusion-ordered spectroscopy experiment incorporating bipolar-gradient pulses. *J. Magn. Reson., Ser. A*, **1995**, *115* (2), 260-264.

(25) Johnson C. S. Jr. Diffusion ordered nuclear magnetic resonance spectroscopy: principles and applications. *Prog. Nucl. Magn. Reson. Spectrosc.* **1999,** *34* (3-4), 203-.256

(26) Dixon A. M.; Mai M. A.; Larive C. K. NMR investigation of the interactions between 4'-Fluoro-1'acetonaphtone and the Suwannee river fulvic acid. *Environ. Sci. Technol.* **1999**, *33* (6), 958-964.

(27) Derrick, T. S.; Lucas, L. H.; Dimicoli, J-L.; Larive, C. K. ^{19}F diffusion NMR analysis of enzyme-inhibitor bindings. *Magn. Reson. Chem.* **2002***, 40* (13), S98-S105.

(28) Morris, K. F.; Becker, B. A.; Valle, B. C.; Warner. I. M.; Larive, C. K. 2006. Use of NMR binding interaction mapping techniques to examine interactions of chiral molecules with molecular micelles. *J. Phys. Chem. B* **2006**, *110* (35), 17359-17369.

(29) D'eon. J. C.; Simpson, A. J.; Kumar, R.; Baer, A. J.; Mabury, S. A. Determining the molecular interactions of perfluorinated carboxylic acids with human sera and isolated human serum albumin using nuclear magnetic resonance spectroscopy. *Environ. Toxicol. Chem.* **2010***, 29* (8), 1678-1688.

(30) Krezel, A.; Bal, W. A formula for correlating pKa values determined in D_2O and H_2O. *J. Inorg. Biochem.* **2004**, *98* (1), 161-166.

(31) Amman, C.; Meier, P.; Merbach, A. E. A simple multinuclear NMR thermometer. *J. Magn. Reson.* **1982**, *46* (2), 319-321.

(32) Simpson, A. J.; Kingery, W. L.; Spraul, M.; Humpfer, E.; Dvortsak, R.; Kerssebaum, R. Separation of structural components in soil organic matter by diffusion ordered spectroscopy. *Environ. Sci. Technol.* **2001***, 35* (22), 4421-4425.

(33) Piccolo A. The supramolecular structure of humic substances. *Soil Sci.* **2001**, *116* (11), 810-832.

(34)   Simpson, A. J.; Simpson, M. J.; Smith, E.; Kelleher, B. P. Microbially derived inputs to soil organic matter: are current estimates too low? *Environ. Sci. Technol.* **2007**, *41* (23)*,* 8070-8076.

(35)   Sutton, R.; Sposito, G. Molecular structure in soil humic substances: the new view. *Environ. Sci. Technol.* **2005**, *39* (23), 9009-9015.

(36)   Kelleher, B. P.; Simpson, A. J. Humic substances in soils: are they really chemically distinct? *Environ. Sci. Technol.* **2006**, *40* (15)*,* 4605-4611.

(37)   Schwarzenbach, R. P.; Gschwend, P. M.; Imboden, D. M. *Environmental Organic Chemistry, Second Edition.* Wiley Interscience, Hoboken, USA. **2003**.

(38)   ACD/Labs, Advanced Chemistry Development, Physical Properties Calculator (ACD/Labs, Toronto, Canada). Database accessed on October 5 2011.

(39)   Otto, W. H.; Britten, D. J.; Larive, C. K. NMR diffusion analysis of surfactant-humic substance interactions. *J. Coll. Interface Sci.* **2003**, *261* (2), 508-513.

(40)   Ragone, R.; Colonna, G. Reliability of the van't Hoff plots. *J. Phys. Chem.* **1995**, *99* (34), 13050-13050

CHAPTER 5
THE PH-DEPENDENCE OF ORGANOFLUORINE BINDING DOMAIN PREFERENCE IN DISSOLVED HUMIC ACID

The material in this chapter has been reproduced with permission from

5.0   Abstract

In this study, the relationship between solution pH and the distribution of the binding interactions at different domains of a dissolved humic acid is explored for three organofluorine xenobiotics: pentafluoroaniline (PFA), pentafluorophenol (PFP), and hexafluorobenzene (HFB).   The components of humic acid where xenobiotic interactions occur are identified using the $^{1}H\{^{19}F\}$ Reverse Heteronuclear Saturation Transfer Difference (RHSTD) Nuclear Magnetic Resonance (NMR) spectroscopy experiment. At low pH, PFA and PFP interact preferentially with aromatic components of humic acid. Increasing pH reduces this preference. Conversely, HFB interacts with all components of humic acid equally, across the entire pH range. The possible roles of both aromatic-specific interactions and conformational changes of humic acid behind these observations are explored. It is shown that T-oriented π-π interactions at π-electron accepting humic acid structures are slightly stronger for PFA and PFP than for HFB. Using DOSY NMR it is shown that the pH-dependence of the interactions is correlated with changes in the conformation of the carbohydrate components of humic acid rather than with the aromatic components. It is argued that the observed preference for aromatic humic acid is caused by restricted access to the non-aromatic components of humic acid at low pH. These humic acid components form tightly bound hydrophobic domains due to strong inter- and intra-molecular

hydrogen bonds. At high pH, these structures open up, making them more accessible for interactions with polar compounds.

5.1   Introduction

Natural organic matter (NOM) is an important mediator in the environmental fate of numerous anthropogenic organic pollutants *(1, 2)*. This organic matter, which is a major constituent of most soils and sediments, is most often considered in global fate models as an ideal hydrophobic partitioning domain *(3)*. While seemingly applicable at the macroscopic-level, many of the assumptions inherent in the partitioning approach fail when studied at the molecular-level, including non-linear sorption isotherms *(1, 4)*, desorption hysteresis *(4)*, competitive binding *(5, 6)*, site-specific interactions *(7)*, and the formation of non-covalently bound sequestered states *(8)*.

While the soil-partitioning factors used in fate models are often derived from easily measured hydrophobic parameters, such as K_{OW}, Xing *et al. (9)* have shown that these predictions are prone to error without some description of the chemistry of the organic matter acting as a sorbent. A molecular-level understanding of the interactions between the natural organic matter found in soils, or soil organic matter (SOM) and xenobiotic molecules is imperative for a full understanding of the role(s) SOM plays in the lifecycles of anthropogenic compounds. In soils and sediments, for example, interactions with SOM lead to enhanced persistence due to sequestration *(8)*. In aquatic environments, interactions with dissolved and particulate forms of NOM can markedly increase the solubility of otherwise hydrophobic compounds *(2)*.

SOM is a mixture of compounds derived from the degraded and partially degraded remnants of plants *(10)* and microbes *(11, 12)*. On a physical level, SOM possess both rigid and flexible domains, accounting for at least two different modes of sorption *(13, 14)*. In addition, the chemical components of SOM, such as lignin, chitin, cellulose, and aliphatic structures exhibit varied sorption behaviour *(9, 15, 16)*. In general, it has been shown that both aromatic *(17)* and aliphatic components *(18, 19)* of SOM are important in governing the interactions between xenobiotics and SOM, but that these types of structures likely participate in different types of interactions *(6, 20)*.

Recent studies have identified the components of humic acid where intermolecular interactions of organofluorine xenobiotics occur using direct approaches based on Nuclear Magnetic Resonance (NMR). Using the Reverse-Heteronuclear Saturation Transfer Difference (RHSTD) NMR experiment, aromatic organofluorine compounds have been shown to exhibit varied preference for interactions at aromatic moieties over non-aromatic moieties in a peat humic acid *(7, 21)*.

In this study, the apparent preference for aromatic humic acid sites for some organofluorine compounds is examined further by probing the response of these interactions to changes in solution pH. Using the ^{1}H$\{^{19}$F$\}$ RHSTD NMR experiment, the distribution of interactions at different components of the humic acid are compared for pentafluorophenol (PFP), pentafluoroaniline (PFA), and hexafluorobenzene (HFB) over a pH range of 3 to 12. These changes are compared to molecular properties of the organofluorine compounds, and to conformational changes in the humic acid itself.

5.2 Materials & Methods

5.2.1 Sample Preparation

Humic acid samples were prepared using the International Humic Substance Society standard Pahokee peat humic acid. Hexafluorobenzene (CAS 392-56-3) was purchased from Sigma Aldrich; pentafluoroaniline (CAS 771-60-8) and pentafluorophenol (CAS 771-61-9) from SynQuest Chemical Laboratories, and used as is. Solutions were prepared using D_2O (99.9% D), NaOD (99.5% D, 30% in D_2O), and DCl (99.5% D, 35% in D_2O), all from Cambridge Isotope Laboratories. The RHSTD NMR experiment is insensitive and requires high concentrations to produce usable spectra. Solutions were prepared by dissolving 250 mg of humic acid in 5.0 ml of D_2O using a minimal quantity of NaOD. 150 mg of hexafluorobenzene, pentafluoroaniline, or pentafluorophenol was added to the humic acid solutions and then divided into 7 parts, each set to pH values between 3 and 12 using minimal quantities of DCl and NaOD. Measured pH values were corrected to account for isotope effects at the electrode arising from the use of D_2O *(22)*.

5.2.2 NMR Spectroscopy

NMR experiments were performed on a Bruker Avance III 500 MHz NMR spectrometer employing a 5 mm QXI probe doubly tuned to ^{1}H and ^{19}F at 298 K. ^{19}F NMR spectra were acquired using a 90° pulse of 17.5 μs and 128 transients following 8 dummy scans with a recycle delay of 5 s. In the ^{1}H{^{19}F} RHSTD experiments, a ^{1}H spectrum was acquired with ^{19}F saturation applied on alternating scans using a train of 18 on-resonance Gaussian-shaped pulses at a power level of 0.6866 W. Alternating phase cycling was used to subtract signals acquired with ^{19}F saturation from signals acquired without ^{19}F saturation. Water signals were removed using presaturation. For each RHSTD spectrum, 32 dummy scans and 16384 transients were acquired with a recycle delay of 1 s. Each FID was apodized with an exponential multiplication factor equivalent to 50 Hz line broadening.

^{1}H DOSY experiments were performed on select samples using the stimulated echo with bipolar gradients method *(23, 24)*. The gradient power was varied from 2% to 95% of its maximum strength over 32 graduations with ^{1}H spectra was acquired using 256 transients and 32 dummy scans with recycle delays of 2 s for each gradient power. The maximum gradient strength here was 52.8 Gauss cm^{-1}, the diffusion period was 180 ms, and the gradient pulse lengths were 3.6 ms. Apparent diffusivity for components in humic acid were determined from 2D DOSY plots created using Bruker Topspin™ version 2.1 using monoexponential fittings, a noise-sensitivity factor of 4, and a spike-suppression factor of 1. 32 slices were processed with 32728 points in the F2 dimension and the diffusion axis was created with 512 points in the F1 dimension.

2.3 Quantum Mechanical Calculations

The GAMESS computational chemistry package *(25)* was used for theoretical calculations of intermolecular interactions between organofluorine compounds and model humic acid aromatic structures. The structures of three organofluorine and two idealized aromatic humic acid proxies, 1,3,5-trihydroxybenzene, and benzene-1,3,5-tricarboxylic acid, were fully optimized at the MP2(full) level using the 6-31+G** basis set. Interaction energies were calculated for face-edge and face-face arrangements of organofluorine and the humic acid proxy compounds using the counterpoise correction method to correct for the basis set superposition error *(26)* at the

MP2(full) 6-31+G** level of theory, which has been shown to be adequate to gage relative differences in the gas-phase intermolecular interactions between aromatic compounds *(27)*. A higher level of theory is needed for absolute interaction energies, which is beyond the scope of the present study. For each orientation, the vertical distance between monomers was varied to identify the energy minimum. The method for calculating intermolecular interactions is described in further detail in appendix D, along with examples of GAMESS inputs.

5.3　Results

5.3.1　^{1}H{^{19}F} Reverse Heteronuclear Saturation Transfer Difference

Figure 5.1 displays ^{1}H{^{19}F} RHSTD NMR spectra for selected mixtures across the pH range studied. For each mixture, a shaded spectrum is shown for RHSTD experiments. This is superimposed onto quantitative ^{1}H spectra acquired using the same sequence but with the addition of all scans and without applied ^{19}F saturation. In RHSTD spectra only those ^{1}H resonances of humic acid that receive spin saturation from the organofluorine compound will show signals, the intensity of which has been shown to be relative to the extent of the interaction *(21)*. For the reference ^{1}H spectra, all components in the mixture produce signals proportional to their concentration. Differences between the RHSTD and reference spectra represent deviations from a random distribution of interactions at all components of humic acid, which is assumed for non-selective behaviour *(21)*.

For pentafluoroaniline (PFA), the RHSTD spectra are diminished in the non-aromatic region relative to the reference spectra across all pH values. This signifies a preferential interaction at aromatic humic acid structures over non-aromatic structures. For pentafluorophenol (PFP), the measurements made at low pH resemble those of PFA, however as the pH increases preference for aromatic sites disappears and PFP interacts with all components of humic acid equally. Hexafluorobenzene (HFB) exhibits no preference in the site of interaction across all pH levels studied.
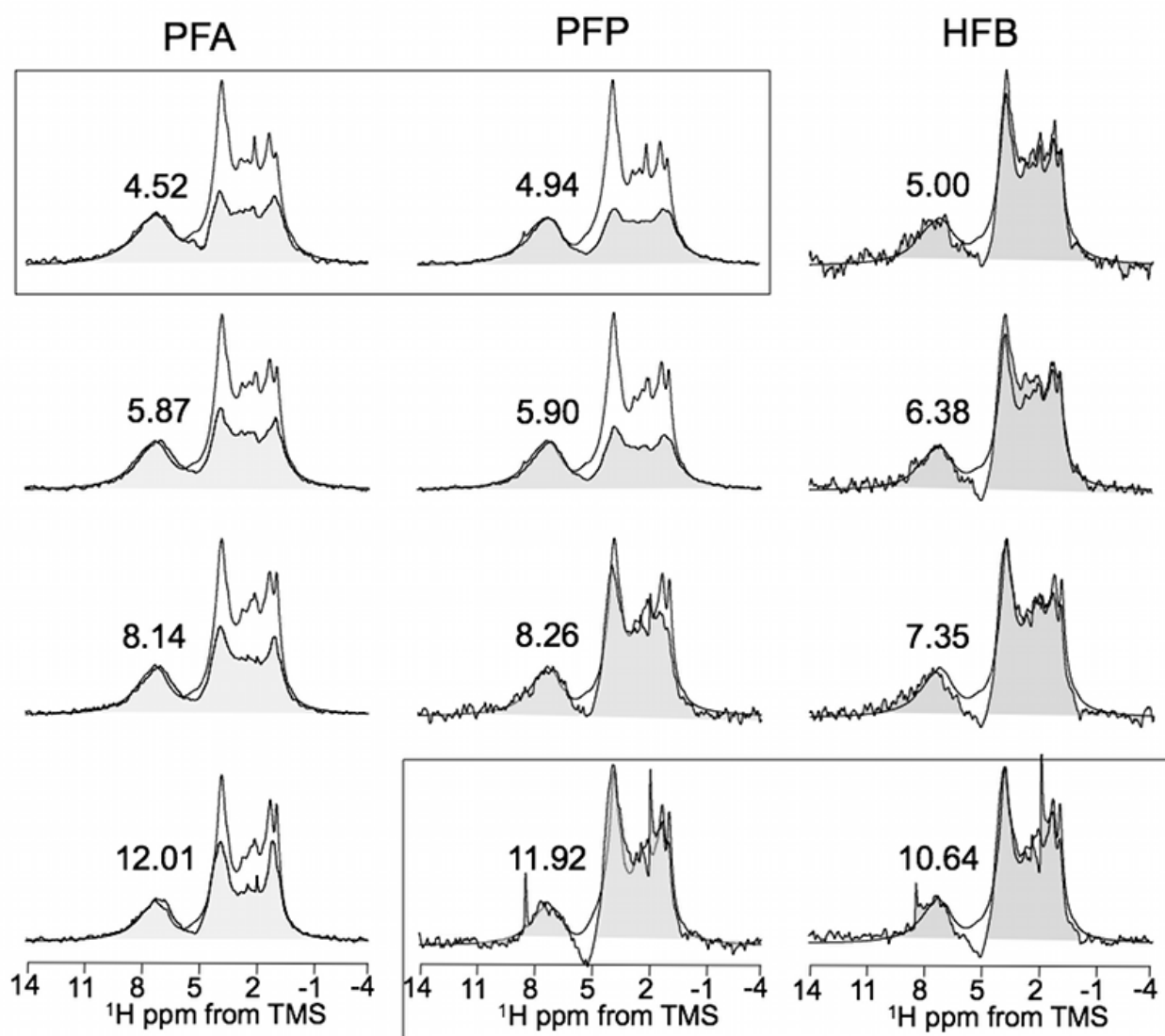
Figure 5.1 Overlays $^1H\{^{19}F\}$ RHSTD spectra (shaded) and the corresponding reference spectra for samples of humic acid mixed with either PFA, PFP, or HFB at selected pH values, which are given. The reference spectra are scaled to the same size while RHSTD spectra are scaled to the same intensity in the aromatic region as the reference spectra.

A more quantitative analysis of changes in the RHSTD spectra with pH is presented in figure 5.2, which compares changes in the RHSTD signal strength relative to the reference spectrum for three distinct regions of the ^{1}H NMR spectrum. The regions selected for study are aromatics (10 to 5.7 ppm), carbohydrates (5 to 2.9 ppm), and aliphatics (1.7 to 0 ppm). The region from 5.7 to 5 ppm was excluded due to distortions arising from water suppression, while the region from 2.9 to 1.7 ppm was excluded due to the convoluted nature of resonances arising from a variety of complex structures. For each mixture, the RHSTD spectra were integrated with respect to the same scale such that the amount of signal is proportional to the relative extent of organofluorine interaction. The reference spectra were integrated in a similar manner. To produce the plots in figure 5.2, the amount of RHSTD signal from each region was divided by the amount of signal in the reference spectra for the same region. The resulting ratio has an arbitrary value, but is scaled the same for each organofluorine allowing for direct comparisons between PFA, PFP and HFB. Also shown is the ratio of the total RHSTD signal intensity to the total reference signal allowing for a means to compare the total amount of interaction of each organofluorine compound regardless of the site of interaction. Both PFA and PFP show a decrease in interaction strength with increasing pH while HFB shows an increase. PFP interacts more strongly than PFA at low pH, however PFP exhibits a marked decrease in signal strength from pH 6 to 7 so that at high pH, PFA interacts with humic acid more strongly than PFP. The interaction strength of HFB is about one third that of PFA at low pH, but at high pH the two compounds interact with nearly equal strength.

For PFA, relative to the total RHSTD signal intensity the aromatic signal is overrepresented at low pH while the carbohydrate signal is underrepresented. As the pH increases, the aromatic signal declines while the carbohydrate signal increases. For the aliphatic region, changes in signal strength correlate to changes in the total amount of RHSTD signal across the entire pH range. Observations for PFP are similar to those of PFA, however, instead of a gradual decrease of aromatic signal, the change is rapid, beginning at pH 6 with the marked loss in total signal. Initially, the carbohydrate region increases in signal strength with increasing pH, however this signal also decreases at pH 6. Similar to PFA, the signal recorded for PFP in the aliphatic region correlates to the total signal intensity. Above pH 7, PFP exhibits essentially no preference for different components of humic acid. HFB interacts with all components of humic acid equally, independent of solution pH.
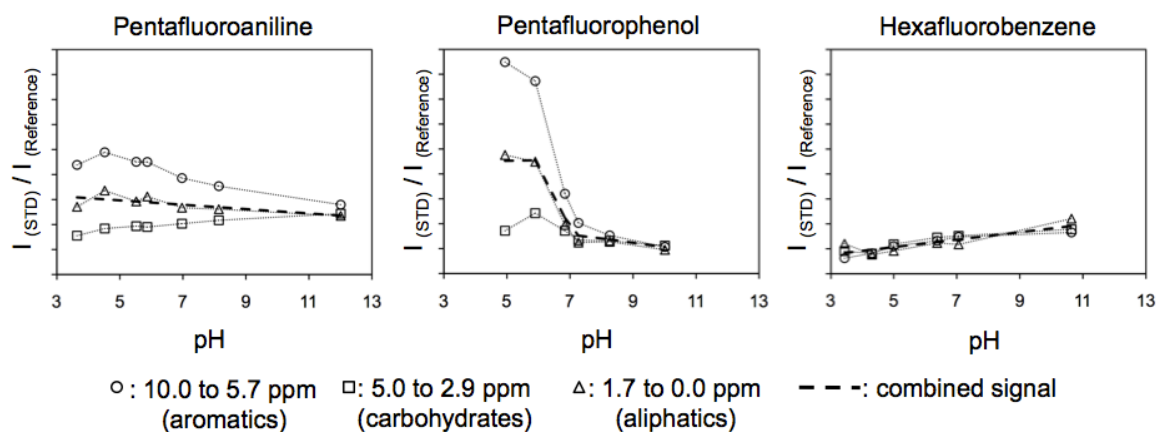
Figure 5.2 Changes in signal intensity of selected regions of the $^1H\{^{19}F\}$ RHSTD spectra of humic acid relative to the same regions in the reference spectra for mixtures with PFA, PFP, and HFB as a function of pH. The ratios reported are of the same arbitrary scale, permitting direct comparisons in interaction strength between compounds. The error in these measurements is estimated to be smaller than the data points.

5.3.2 ^{19}F NMR

The ^{19}F chemical shift values of fluorine nuclei on a benzene ring are sensitive to the equilibrium between protonated and unprotonated forms of OH and NH$_2$ groups on the same ring. Figure 5.3 compares changes in pH to changes in the ^{19}F chemical shift of the para ^{19}F resonance for all three organofluorine compounds in the humic acid mixtures. PFP exhibits a marked change in the ^{19}F chemical shift with changes in pH, while HFB and PFA do not. For PFP, this indicates that the rapid decrease in RHSTD signal is concurrent with formation of the anion, which does not interact with humic acid as strongly as the protonated form. For PFA, however, this shows that its structure does not change over the pH range studied indicating that the small loss of signal, and corresponding decrease in aromatic preference, is due to changes in humic acid itself.

5.4 Discussion

For hexafluorobenzene, the interactions with humic acid are random, and while increasing the pH does result in more signal, due to either more frequent or stronger interactions, this does not correspond to changes in where these interactions occur. For pentafluorophenol and pentafluoroaniline, observations here indicate a pH-dependent preference for interactions at aromatic domains of humic acid at the expense of interactions at carbohydrates. For both of these compounds, interactions at aliphatics are independent of pH. For PFA, as the pH increases, the distribution of interactions shifts away from the aromatic domains towards the carbohydrates, however carbohydrates never dominate the overall distribution. The slight decrease in PFA RHSTD signal with increasing pH may be due to either fewer overall interactions or to a greater proportion of weaker interactions. For PFP, at low pH this compound interacts in a manner similar to that of PFA, however at high pH its interaction profile is more similar to that of HFB. Smejkalová *et al. (28)* also observed a decrease in interaction for PFP as pH increases, which they attributed to stronger interactions of the protonated form of the phenol than the anionic phenolate form. Overall, some humic acid-based mechanism acts at low pH to induce aromatic site-selectivity for PFA and PFP, but not for HFB.
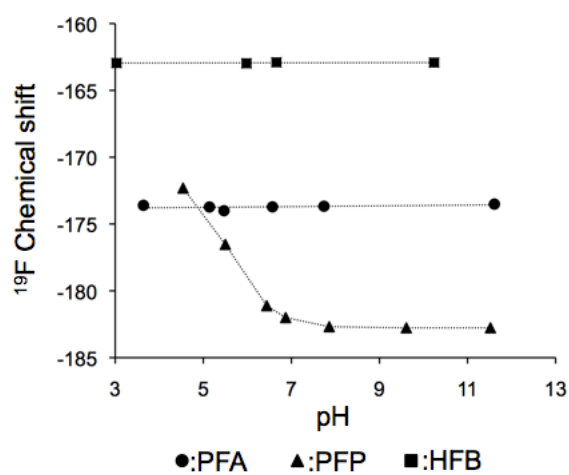
Figure 5.3   Changes in the ^{19}F NMR Chemical shift as a function of pH for PFA, PFP, and HFB. For PFA and PFP, the chemical shift is that of the para ^{19}F.

5.4.1 Aromatic Interactions

Non-ideal binding with natural organic matter is often explained by invoking specific interactions *(29)*. Zhu *et al. (30)* report evidence for pH-dependent face-face π interactions between π-donor xenobiotics and carboxyl-rich π–acceptor sites in SOM that lead to enhanced sorption at lower pH. Aromatic organofluorine compounds are poor π-donors, however, and are unlikely to engage in face-face π-π interactions with π-acceptor sites in humic acid but may form face–edge π complexes instead *(31)*. Mao *et al. (32)* report, however, that while carboxyl-rich aromatic material does occur in humic acid, most aromatic acidic functionality is in the form of phenolic groups, which are not π-acceptors but π-donors and would form face-face π complexes with the organofluorine compounds used here. In either scenario, increases in pH would deprotonated these groups, significantly altering their electrostatics and thus the strength of these hypothetical complexes.

Table 5-1 compares the calculated strength of the intermolecular interactions between model humic acid structures and the three organofluorine compounds studied here. The goal here is to test if differences in the strength of these interactions can account for the aromatic preference observed for PFA and PFP at low pH, but not for HFB. The two model humic acid aromatic structures are benzene-1,3,5-carboxylic acid, which is a π-electron acceptor, and should only form face-edge complexes with aromatic organofluorine compounds; and 1,3-5-trihydroxyl benzene, which is a π-electron donor and will form face-face complexes with all aromatic organofluorine compounds, and face-edge complexes for PFA and PFP when the OH or NH_2 group is directed into the complex. Figure 5.4 shows examples of face-face and face-edge complexes between pentafluoroaniline and 1,3,5-trihydroxybenzene.

Table 5-1 Calculated interaction energies (E_h) between organofluorine compounds and model humic acid aromatic structures using the MP2(full) 6-31+G** level of theory. For face-edge complexes, the orientation of the organofluorine is noted.

	Orientation	PFA	PFP	HFB
1,3,5-trihydroxy benzene *(π-donor)*	*face-face*	-6.39589	-8.16701	-6.57141
	face-edge	-3.75209 *(via NH₂)*	-1.766759 *(via OH)*	-0.87727 *(via F)*
Benzene-1,3,5-tricarboxylic acid *(π-acceptor)*	*face-edge*	-3.95816 *(via F)*	-3.50638 *(via F)*	-2.61258 *(via F)*
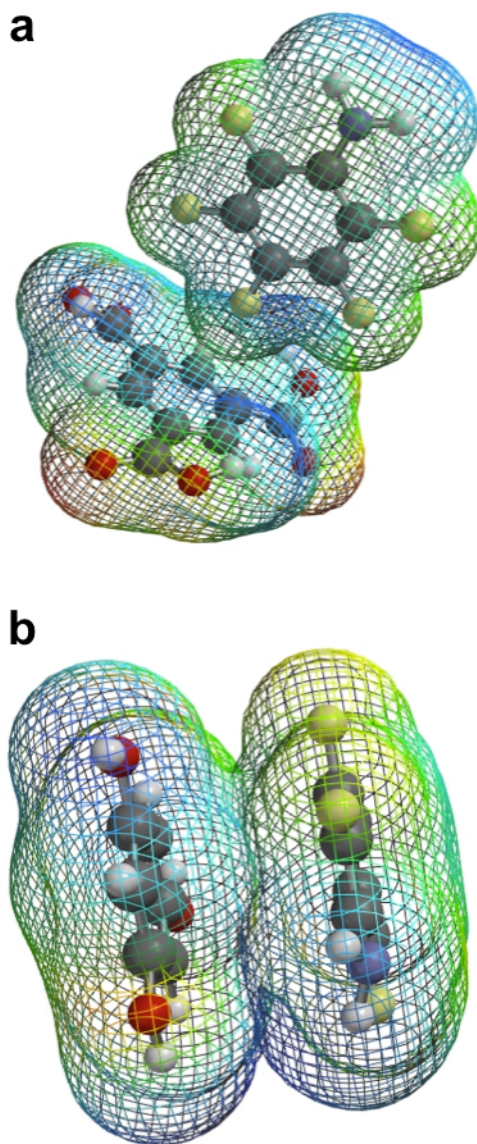
Figure 5.4   Example T-shaped face-edge (a) and stacked face-face (b) dimer complexes between pentafluoroaniline and 1,3,5-trihydroxy benzene.

The most favorable complexes formed for all three organofluorine compounds are through face-face interactions with 1,3,5-trihydroxy benzene. The interactions with PFA and HFB are nearly identical in strength, while PFP forms a slightly stronger complex. Because the strengths of these three complexes are similar, it is unlikely that their formation could account for the differences observed experimentally, wherein HFB does not show any aromatic preference but PFA and PFP do. For face-edge complexes using 1,3,5-trihydroxyl benzene where the NH_2 or OH groups of PFA and PFP are directed inwards, the strengths of the interactions are much stronger than for HFB. Here, the differences in the relative strength of interaction may account for the experimental differences observed here, as HFB does not exhibit a strong interaction while PFA and PFP do. However, the RHSTD measurements (see fig. 5.2) indicate that PFP exhibits a stronger aromatic preference than PFA, which is not supported by these calculations. Regardless, the face-face interactions are shown to be much stronger overall than the face-edge interactions, suggesting that their formation would be favored here. Thus, any differences found between the three organofluorine compounds in the strength of face-edge complexes would be negated by the preference for face-face complexes, which are all of similar strength.

For benzene-1,3,5-tricarboxylic acid, the face-edge interactions are weaker than the face-face interactions calculated for 1,3,5-trihydroxyl benzene. In this scenario however, HFB exhibits an interaction that is 35 and 25 % weaker than that for PFA and PFP, respectively. Experimental evidence has shown that both PFA and PFP interact with humic acid with their NH_2 or OH group directed outwards on average *(21)*, supporting the presence of these complexes, however it is not clear if the modest difference in interaction strength alone is enough to account for the clear lack of aromatic preference observed for HFB.

5.4.2 Conformational Changes

Alternative explanations for pH-dependent effects in the interactions between xenobiotics and SOM are based on pH-induced changes in the physical conformation of humic substances. In solution, humic acid forms dynamic supramolecular structures held together by intra- and inter molecular interactions *(33)*. At low pH these structures are stabilized by H-bonds, forming smaller but more stable structures than at high-pH where the influence of H-bonding is reduced

by the deprotonation of acidic sites *(33, 34)*. The role of the supramolecular structure of humic acid in xenobiotic binding as been explored by Pan *et al. (4)*, who attribute both the enhanced binding of hydrophobic compounds to dissolved humic acid at low pH and non-ideal sorption behaviour, to the formation of humic acid structures with hydrophobic cores. Similarly, Sun *et al. (35)* attribute pH changes in sorption behaviour to the formation of more hydrophobic domains at low pH. It has been reported that the degree of aggregation influences binding to dissolved humic acid, with larger binding domains (i.e. more aggregated structures) having a negative influence on the extent of interaction *(35, 36)*.

Figure 5.5 shows the apparent diffusivity of aromatic, carbohydrate, and aliphatic components of the humic acid used here as measured using ^{1}H DOSY NMR. The measured diffusivity for the aromatic components is unaffected by pH, while the carbohydrates, and, to a lesser extent the aliphatic components, are affected by pH, with the apparent rate of diffusivity decreasing with increasing pH. In the supramolecular model, these observations are accounted for by the removal of strong H-bonds holding aggregates together that results in the formation of larger, more diffuse, but less-stable structures. These larger structures are less hydrophobic than the smaller aggregates formed at low pH *(33)*. The decrease in aromatic site preference exhibited by PFA in the RHSTD NMR spectra as pH increases does not correlate to any strong conformational change in aromatic sites, but instead to an opening up of the carbohydrate sites. This correlation agrees with the supramolecular model of dissolved humic acid: at low pH, tightly bound hydrophobic aggregates will be less accessible to the polar PFA and PFP molecules, however HFB, which is non-polar, will not experience the same restrictions. At high pH, the hydrophobic regions of humic acid open up and become more accessible to PFA and PFP explaining why the observed interaction profiles in the RHSTD experiments become more homogeneous.

Rather than exhibiting a preference for interactions at aromatic sites at low pH, which may be explained by specific π-π interactions, it is more likely that at low pH non-aromatic structures, particularly carbohydrates are simply less accessible. At high pH there are fewer restrictions on where interactions are likely to occur, altering the distribution of interactions sites by increasing the number of interactions at carbohydrate sites and reducing the relative number of aromatic interactions accordingly.
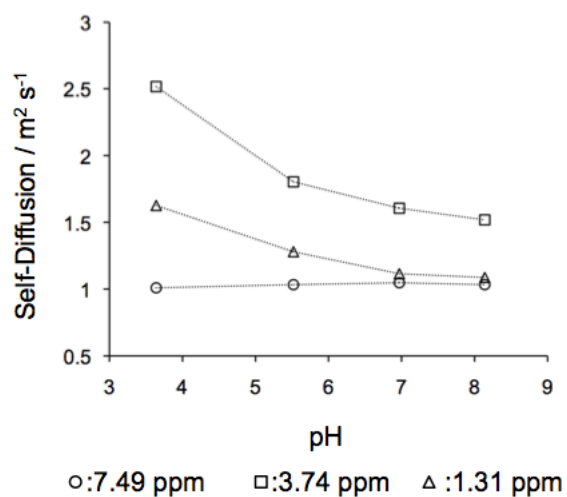
Figure 5.5   Changes in the apparent rate of self-diffusion measured at different resonances in the ^{1}H NMR spectrum of humic acid as a function of pH using ^{1}H DOSY NMR. The error of these measurements is smaller than the data points.

5.5   Conclusions

Polar compounds, pentafluoroaniline and pentafluorophenol, exhibit pH-dependent preference for their interaction domains in dissolved humic acid while the non-polar hexafluorobenzene does not. For the pH dependent compounds, at low pH aromatic binding sites are preferred over non-aromatic binding sites, but as the pH increases, this preference decreases. A more marked decrease is observed for pentafluorophenol than pentafluoroaniline, which is attributed to the formation of the phenoxide anion. The structure of pentafluoroaniline is unaffected by pH over the range studied here and any changes observed here are due to changes in the humic acid binding sites. A decrease in preference for aromatic sites is accompanied by an increase in preference for carbohydrate sites, but these sites never dominate the overall interaction profile for pentafluoroaniline. Face-edge π-π complexes with carboxyl-rich aromatic sites may account for the greater affinity for aromatic sites observed for pentafluoroaniline and pentafluorophenol over hexafluorobenzene at low pH, however theoretical calculations show only a slight advantage for the two polar compounds. Instead, the decrease in aromatic preference as pH increases is more likely attributed to conformational changes in different humic acid binding domains. The supramolecular conformation of carbohydrate sites are strongly affected by changes in pH, whereas aromatic sites are not. At low pH carbohydrates form tight hydrophobic domains held together by strong inter- and intra-molecular bonds that are broken at higher pH. These low-pH domains restrict access to pentafluorophenol and pentafluoroaniline, but not hexafluorobenzene, thus driving a disproportionate number of interactions to aromatic sites. When carbohydrate sites become more available for interactions with polar compounds, a more uniform distribution of interactions sites is observed.

5.6   References

(1)   Karickhoff, S. W.; Morris, K. R. Sorption dynamics of hydrophobic pollutants in sediment suspensions. *Environ. Toxicol. Chem.* **1985,** *4* (4)*,* 469-479.

(2)   Chiou, G. T.; Malcom, R. L.; Brinton, T. I.; Kile, D. E. Water solubility enhancement of some organic pollutants and pesticides by dissolved humic and fulvic acids. *Environ. Sci. Technol.* **1986**, *20* (5), 502-508.

(3)   Karickhoff, S. W.; Brown, D. S.; Scott, T. A. Sorption of hydrophobic pollutants on natural sediments. *Water Res.* **1979**, *13* (3)*,* 241-248.

(4)   Pan, B.; Ghosh, S.; Xing, B. Nonideal binding between dissolved humic acids and polyaromatic hydrocarbons. *Environ. Sci. Technol.* **2007**, *41* (18), 6472-6478.

(5)   Xing B.; Pignatello J. J.; Gigliotti B. Competitive sorption between atrazine and other organic compounds in soils and model sorbents. *Environ. Sci. Technol.* **1996**, *30* (8), 2432-2440.

(6)   Gunasekara, A. S.; Simpson, M. J.; Xing, B. Identification and characterization of sorption domains in soil organic matter using structurally modified humic acids. *Environ. Sci. Technol.* **2003**, *37* (5), 852-858.

(7)   Longstaffe, J. G.; Simpson, M. J.; Maas, W.; Simpson, A. J. Identifying components in dissolved humic acid that bind organofluorine contaminants using $^1H\{^{19}F\}$ reverse heteronuclear saturation transfer difference NMR spectroscopy. *Environ. Sci. Technol.* **2010**, *44* (14), 5476-5482.

(8)   Robertson, B. K.; Alexander, M. Sequestration of DDT and Dieldrin in soil: disappearance of acute toxicity but not the compounds. *Environ. Toxicol. Chem.* **1998**, 17 (6), 1034-1038.

(9)   Xing, B.; McGill, W. B.; Dudas, M. J. Sorption of α-naphthol onto organic sorbents varying in polarity and aromaticity. *Chemosphere*. **1994**, *28* (1), 145-153.

(10)   Kelleher, B. P.; Simpson, A. J. Humic substances in soils: are they really chemically distinct? *Environ. Sci. Technol.* **2006**, *40* (15)*,* 4605-4611.

(11) Simpson, A. J.; Simpson, M. J.; Smith, E.; Kelleher, B. P. Microbially derived inputs to soil organic matter: are current estimates too low? *Environ. Sci. Technol.* **2007**, *41* (23)*,* 8070-8076.

(12) Mao J-D.; Tremblay L.; Gagné J-P.; Kohl S.; Rice J.; Schmidt-Rohr K. Humic acids from particulate organic matter in the Saguenay Fjord and the St. Lawrence Estuary investigated by advanced solid-state NMR. *Geochim. Cosmochim. Acta* **2007**, *71* (22), 5483-5499.

(13) Xing, B.; Pignatello, J. J. Dual-mode sorption of low-polarity compounds in glassy poly(vinyl chloride) and soil organic matter. *Environ. Sci. Technol.* **1997**, *31* (3)*,* 792-799.

(14) Kohl S. D.; Toscano P. J.; Hou W.; Rice J. A. Solid-state ^{19}F NMR investigation of hexafluorobenzene sorption to soil organic matter. *Environ. Sci. Technol.* **2000**, *34* (1), 204-210.

(15) Garbarini D. R.; Lion L. W. Influence of the nature of soil organics on the sorption of toluene and trichloroethylene. *Environ. Sci. Technol.* **1986**, *20* (12), 1263-1269.

(16) Wang, X.; Cook, R.; Tao, S.; Xing. B. Sorption of organic contaminants by biopolymers: Role of polarity, structure and domain spatial arrangement. *Chemosphere* **2007**, *66* (8), 1476-1484.

(17) Chin, Y. -P.; Aiken, G. R.; Danielsen, K. M. Binding of pyrene to aquatic and commercial humic substances: the role of molecular weight and aromaticity. *Environ. Sci. Technol*. **1997**, *31* (6), 1630-1635.

(18) Chefetz B.; Deshmukh A. P.; Hatcher P. G.; Guthrie E. A. Pyrene sorption by natural organic matter. *Environ. Sci. Technol.* **2000**, *34* (14), 2925-2930.

(19) Golding, C. J.; Smernik, R. J.; Birch, G. F. Investigation of the role of structural domains identified in sedimentary organic matter in the sorption of hydrophobic organic compounds. *Environ. Sci. Technol*. **2005**, *39* (11), 3925-3932.

(20)   Chefetz, B.; Xing, B. Relative role of aliphatic and aromatic moieties as sorption domains for organic compounds: A review. *Environ. Sci. Technol.* **2009,** *43* (6)*,* 1680-1688.

(21)   Longstaffe, J. G.; Simpson, A. J. Understanding solution-state noncovalent interaction between xenobiotics and natural organic matter using ^{19}F/^{1}H heteronuclear saturation transfer difference nuclear magnetic resonance spectroscopy. *Environ. Toxicol. Chem.* **2011**, *30* (8), 1745-1753.

(22)   Krezel, A.; Bal, W. A formula for correlating pKa values determined in D_2O and H_2O. *J. Inorg. Biochem.* **2004**, *98* (1), 161-166.

(23)   Wu, D.; Chen, A.; Johnson, C. S.; An improved diffusion-ordered spectroscopy experiment incorporating bipolar-gradient pulses. *J. Magn. Reson., Ser. A*, **1995**, *115* (2), 260-264.

(24)   Simpson A. J.; Kingery W. L.; Spraul M.; Humpfer E.; Dvortsak R.; Kerssebaum R. Separation of structural components in soil organic matter by diffusion ordered spectroscopy. *Environ. Sci. Technol.* **2001***, 35* (22), 4421-4425.

(25)   Schmidt, M. W.; Baldridge, K. K.; Boatz, J. A.; Elbert, S. T.; Gordon, M. S.; Jensen, J. H.; Koseki, J. A.; Matsunaga, N.; Nguyen, K. A.; Su, S. J.; Windus, T. L.; Dupuis, M.; Montgomery, J. A. General atomic and molecular electronic structure system. J. *Comput. Chem.* **1993**, *14* (11), 1347-1363.

(26)   Boys, S. F.; Bernardi, R. The calculation of small molecular interactions by the differences of separate total energies. Some procedures with reduced errors. *Mol. Phys*. **1970**, *19* (4), 553-566.

(27)   Gung, B. W.; Amicangelo, J. C. Substituent effects in $C_6F_6 - C_6H_5X$ stacking interactions. *J. Org. Chem.* **2006**, *71* (25), 9261-9270.

(28)   Smejkalová D.; Spaccini R.; Fontaine B.; Piccolo A. Binding of phenol and differently halogenated phenols to dissolved humic matter as measured by NMR spectroscopy. *Environ. Sci. Technol.* **2009**, *43* (14), 5377-5382.

(29)   Nanny M. A.; Maza J. P. Noncovalent interactions between monoaromatic compounds and dissolved humic acids: a deuterium NMR T_1 relaxation study. *Environ. Sci. Technol.* **2001**, *35* (2), 379-384.

(30)   Zhu, D.; Hyun, S.; Pignatello, J. J.; Lee, L. S. Evidence for π-π electron donor-acceptor interactions between π-donor aromatic compounds and π-acceptor sites in soil organic matter through pH effects on sorption. *Environ. Sci. Technol.* **2004**, *38* (16), 4361-4368.

(31)   Sinnokrot, M. O.; Sherrill, C. D. Substituent effects in π-π interactions: sandwich and T-shaped configurations. *J. Am. Chem. Soc.* **2004**, *126* (124), 7690-7697.

(32)   Mao, J.-D.; Xing, B.; Schmidt-Rohr, K. New structural information on a humic acid from two-dimensional ^{1}H-^{13}C correlation solid-state nuclear magnetic resonance. *Environ. Sci. Technol.* **2001**, *35* (10), 1928-1934.

(33)   Piccolo, A.; Conte, P.; Spaccini, R.; Chiarella, M. Effects of some dicarboxylic acids on the association of dissolved humic substances. *Biol. Fertil. Soils.* **2003**, *37* (4), 255-259.

(34)   Smejkalová, D.; Piccolo, A. Aggregation and disaggregation of humic supramolecular assemblies by NMR diffusion ordered spectroscopy (DOSY-NMR). *Environ. Sci. Technol.* **2008**, *42* (3), 699-706.

(35)   Sun, H.; Zhu, D.; Mao, J. Sorption of polar and nonpolar aromatic compounds to two humic acids with varied structural heterogeneity. *Environ. Toxicol. Chem.* **2008**, *27* (12), 2449-2456.

(36)   Pan, B.; Ghosh, S.; Xing, B. Dissolved organic matter conformation and its interaction with pyrene as affected by water chemistry and concentration. *Environ. Sci. Technol.* **2008**, *42* (5), 1594-1599.

CHAPTER 6
IN SITU MOLECULAR-LEVEL ELUCIDATION OF ORGANOFLUORINE BINDING SITES IN A WHOLE PEAT SOIL

The material in this chapter is adapted with permission from

6.0   Abstract

The chemical nature of xenobiotic binding sites in soils is of vital importance to environmental biogeochemistry.   Interactions between xenobiotics and the naturally occurring organic constituents of soils are strongly correlated to environmental persistence, bioaccessibility, and ecotoxicity.   Nevertheless, because of the complex structural and chemical heterogeneity of soils, studies of these interactions are most commonly performed indirectly, using correlative methods, fractionation, or chemical modification.   Here we identify the organic components of an unmodified peat soil where some organofluorine xenobiotic compounds interact using direct molecular-level methods.   Using $^{19}F \rightarrow ^{1}H$ Cross-Polarization Magical Angle Spinning (CP-MAS) Nuclear Magnetic Resonance (NMR) spectroscopy, the ^{19}F nuclei of organofluorine compounds are used to induce observable transverse magnetization in the ^{1}H nuclei of organic components of the soil with which they are located near after their sorption.   The observed $^{19}F \rightarrow ^{1}H$ CP-MAS spectra and dynamics are compared to those produced using model soil organic compounds, lignin and albumin.   It is found that lignin-like components can account for the interactions observed in this soil for heptafluoronaphthol while protein structures can account for the interactions observed for perfluorooctanoic acid.

6.1   Introduction

Soils and sediments are a major environmental sink for numerous anthropogenic organic compounds *(1)*. At a macroscopic-level, the sorption into soils and sediments can be modeled using a simple partitioning analogy *(2, 3)*.   While useful in many applications, such as understanding fate on a global-scale, this approach is unable to account for numerous known sorption phenomenon in soils including non-ideal isotherms *(4, 5)*, competitive binding *(6)*, enhanced persistence *(7)*, and reduced bioavailability *(8)*. Models have been developed to account for the phenomenological deviations from ideal sorption behaviour based on physical differences in various domains of the natural organic matter occurring in soils, or soil organic matter (SOM) *(9, 10)*. In addition, it has long been known that various forms of organic matter found in soil have different sorption potentials for different contaminants *(11)*, however these preferences have always been observed using fractionated or modified SOM *(13)*, or isolated biopolymers, such as lignin and cellulose *(13)*.

Studying the interactions between small xenobiotic organic compounds and the various components of SOM is most commonly performed using correlative approaches *(14-16)*, as direct methods are made difficult due to the largely amorphous nature of the material. Nevertheless, studies based on direct observations of intermolecular interactions between SOM and xenobiotics have become more common *(17, 18)*. Nuclear magnetic resonance (NMR) spectroscopy, which is capable of resolving distinct chemical moieties at the atomic-level, such that discrete signals can be recorded for compounds with slightly different chemical structures, has shown great utility in resolving intermolecular interactions in SOM and its fractions *(14)*. Nevertheless, the use of NMR spectroscopy in these studies often still requires significant modification *(19)* or fractionation, such as into humin, humic acid, and fulvic acid *(17, 18)*, in order that environmental interactions may be probed at the molecular-level. Studies that have directly resolved different binding sites in a whole soil have thus far focused solely on physical differences between those sites, such as their degree of rigidity *(20)*, typically in line with the dual-mode models for sorption *(9, 10)*.

In addition to their physical differences, the chemical structure of the biopolymers that make up SOM is also known to be a factor in the sorption behavior of xenobiotics *(11, 13)*.   Recent advances have been made to identify the components of a humic acid where interactions occur

with small organofluorine compounds *(17)*. Caution has been made in the analysis of intermolecular interactions in humic acid, however, as these extracts are not fully representative of the entirety of SOM, and that the organizational structure of the various constituents has been altered from the natural state, which may have an effect on the availability of different sites to small xenobiotics.

In this study we bridge observations of preferred interaction sites for organofluorine compounds in humic acid to the behaviour of those same compounds in the parent peat soil. Here, the organofluorine compounds perfluorooctanoic acid (PFOA), heptafluoronaphthol (HFNap), pentafluorophenol, and pentafluorobenzoic acid are mixed with a peat soil using D_2O. These compounds were selected based on previous knowledge of their interactions of the humic acid extracted from this peat (see chapters 2, 3, 4, and 5). Using NMR spectroscopy, cross-polarization (CP) from ^{19}F nuclei on the organofluorine compounds to ^1H nuclei in the soil is used to produce ^1H spectra of the soil showing only signals from constituents of SOM where organofluorine compounds interact. The resulting $^{19}F{\rightarrow}^1H$ CP spectra, as well as the CP dynamic behaviour is compared between peat, lignin, and albumin to identify preferred binding domains hypothesized from observations made previously in humic acid, namely that aromatic organofluorine compounds exhibit preference for lignin-derived components of SOM, and that PFOA prefers protein-derived components, which was discussed in chapter 2 *(17)*.

6.2   Methods & Materials

6.3.1 NMR Spectroscopy

All NMR experiments were performed with a Bruker Avance III 500 MHz spectrometer employing a $^1H/^{19}F/^{13}C/^2H$ Comprehensive Multiphase (CMP) MAS probe designed specifically for multiphase environmental materials equipped with gradients along the magic angle and a ^2H lock channel *(21)*. Samples were prepared in 4mm zirconium oxide rotors and spun at 7000 Hz under MAS conditions, using the ^2D signal from D_2O as a spectrometer lock. The $^{19}F{\rightarrow}^1H$ CP experiment was optimized using polyvinylidene fluoride (Sigma-Aldrich, CAS 24937-79-9) using a 90° ^{19}F flip pulse of 4.5 μs. The CP contact time was varied for each organofluorine compound to produce a buildup curve. The number of scans acquired were as follows: 20480

scans for peat samples and 4096 scans for the lignin and albumin samples. All CP experiments employed a recycle delay of 1 s. The CP spectra were processed using 4096 points and apodized with an exponential multiplication factor equivalent to 50 Hz line broadening. Water signals were subtracted from the spectra using a qfil function equivalent to a line width of 1 ppm centered at 4.7 ppm.

[19]F pulsed-field gradient (PFG) diffusion experiments were used here to verify translational motion of unbound organofluorine compounds in peat and were performed using the stimulated echo experiment employing bipolar gradients and longitudinal eddy current delays *(22)*. The diffusion time was set to 50 ms, gradient pulse lengths were 3.6 ms, and 5 ms was allowed for an eddy current delay following the gradient pulses. 128 scans were acquired following 32 dummy scans for 32 incremented gradient power levels. Recycle delays of 5 s were employed. Relative diffusion rates were calculated from the two-dimensional DOSY spectrum created by monoexponential fitting of the chemical shift decay assuming a gradient strength of 52.8 G cm^{-1} at full power.

6.3.2 Sample Preparation

The soil used here is the Pahokee peat provided by the International Humic Substance Society (IHSS). In order to reduce the interference of strong H_2O signals in the ^{1}H NMR spectra, this soil was ground and soaked in D_2O (Cambridge Isotope Laboratories, 99.9% D) for two weeks and then dried in an oven at 40°C for one week. Albumin samples were prepared using ovalbumin extracted from chicken egg whites (grade V, 98%) purchased from Sigma Aldrich. The lignin samples were prepared using alkali lignin (CAS 8068-05-1) from Sigma Aldrich, Pentafluorophenol (CAS 771-61-9) and pentafluorobenzoic acid (CAS 602-94-8) were purchased from Synquest Laboratories (Alachua Florida, USA) and used as is. Heptafluoro-2-naphthol (CAS 727-49-1) and perfluorooctanoic acid (CAS 335-67-1) were purchased from Synquest Laboratories and converted to deuterated forms prior to use by dissolving in D_2O using minimal quantities of NaOD (Cambridge Isotope Laboratories, 99.5% D, 30% in D_2O) and then precipitated using DCl (Cambridge Isotope Laboratories, 99.5% D, 35% in D_2O).

Heptafluoronaphthol-d was extracted using Chloroform-d (Aldrich, 99.98 % D), which was then evaporated off. Perfluorooctanoic acid-d was filtered and air-dried.

Peat samples were prepared by loading 40 mg of peat into a 4 mm NMR rotor with 60 µl D_2O. A separate sample was prepared for each organofluorine compound by mixing in 0.038 ± 0.005 mmol of perfluorooctanoic acid, pentafluorophenol, pentafluorobenzoic acid, or heptafluoro-2-naphthol. Albumin samples were prepared using 40 mg ovalbumin, 60 µL D_2O, and 0.05 mmol of either perfluorooctanoic acid or heptafluoronaphthol. Lignin samples were prepared using 20 mg alkali lignin, 40 µl D_2O, and 0.05 mmol of either perfluorooctanoic acid or heptafluoronaphthol. For the lignin samples, a Kel-F bottom insert was placed in the rotor prior to sample preparation to allow for a smaller sample volume, which was required due to dielectric effects hindering proper probe tuning. Kel-F top inserts were placed above all mixtures to prevent leaking under magic angle spinning conditions. Samples were allowed to equilibrate for at least 2 days prior to analysis and were rerun after several weeks with no noticeable changes observed in the resulting spectra.

6.3   Results & Discussion

Figure 6.1 shows the $^{19}F \rightarrow {}^{1}H$ CP MAS spectra of peat mixed with either perfluorooctanoic acid or heptafluoronaphthol. The resultant spectra are broad and amorphous, spanning the normal ^{1}H spectral range. Despite the lack of spectral resolution, PFOA and HFNap produce qualitatively different spectra from each other. This indicates that the ^{19}F spin-baths provided by these samples are exciting the ^{1}H nuclei in different components of the soil organic matter and thus that these two compounds are situated near different types of SOM structures in the soil after sorption. For HFNap, the peat spectrum is uniformly distributed from 10 to -2 ppm, while for PFOA the spectrum is more heavily weighted towards signals in the 4 to -2 ppm region.
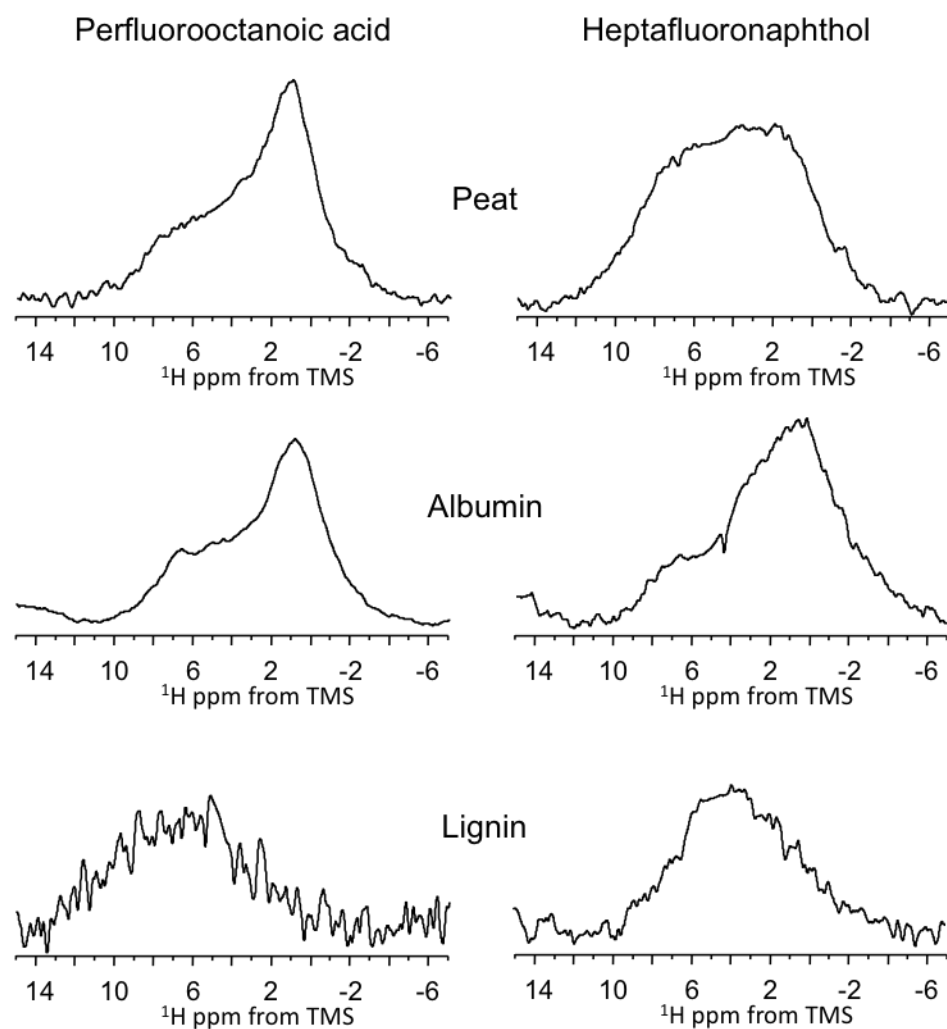
Figure 6.1 $^{19}F{\rightarrow}^1H$ CP MAS NMR spectra of mixtures of peat, albumin, or lignin with perfluorooctanoic acid (left) and heptafluoronaphthol (right).

In a previous study (see chapter 2), Longstaffe *et al. (17)* used the dissolved humic acid extract from this peat soil to study the binding sites of these organofluorine compounds in a fraction of SOM. In the dissolved-state, the anisotropic effects producing the broad solid-state ^{1}H spectra seen here are reduced, allowing for a considerably more detailed analysis of the interaction sites in the previous humic acid study than is permitted here in the whole soil *(17)*. Through comparisons of the spectral profiles of representative biopolymers, it was shown that HFNap interacts with all of the components of humic acid, whereas PFOA interacts only with protein-derived material. While such a clear analysis is precluded here by the broad nature of ^{1}H resonances in the solid-state, following from the previous humic acid work, these organofluorine compounds were mixed with lignin or albumin and ^{19}F→^{1}H CP spectra were acquired and are shown in figure 6.1. In general, it is clear that lignin and albumin produce dissimilar spectra to each other regardless of whether PFOA or HFNap is used as the xenobiotic. For albumin, the two spectra are similar for both organofluorine compounds, however it is difficult to qualitatively compare the two lignin spectra due to the apparent low signal to noise ratio of the PFOA-lignin spectrum. Owing to the similarities between the two albumin spectra, and the differences between the albumin and lignin spectra, these observations suggest that the profile of the ^{19}F→^{1}H CP-MAS spectra depends upon the type of organic matter that the organofluorine compounds are interacting with, rather than the type of organofluorine compound being used as a probe.

For the two albumin spectra, the HFNap-albumin mixture appears slightly noisier given the same scaling as the PFOA-albumin mixture. This suggests that under identical conditions, PFOA interacts slightly more strongly with albumin than does HFNap. For the two lignin spectra, however, the HFNap-lignin mixture clearly has a much higher signal to noise ratio than the PFOA-lignin mixture, suggesting that not only does HFNap interact more strongly with lignin than does PFOA, but that relatively, PFOA hardly interacts with this biopolymer at all under these conditions. In the previous study it was shown that in solution PFOA exhibits nearly no interactions with lignin when in solution *(17)*. These differences in signal strength are discussed with further detail later in this chapter.

Comparing the peat spectra to those of the biopolymers shows that the ^{19}F→^{1}H CP spectrum of the PFOA-albumin mixture is qualitatively similar to the CP spectra of the PFOA-peat mixture while the PFOA-lignin mixture differs markedly from the PFOA-peat mixture. The ^{19}F→^{1}H CP

spectrum of the HFNap-albumin mixture differs from the CP spectrum of the HFNap-peat mixture, however when mixed with lignin, HFNap produces a broad ^{19}F→^{1}H CP spectrum similar to that observed for the HFNap-Peat mixture. The HFNap-lignin spectrum appears to be slightly weighted towards the downfield resonances relative to the HFNap-peat spectrum, which is in accordance with the primarily aromatic composition of lignin *(23)*. A combination of the HFNap-lignin and HFNap-albumin spectra may produce the spectrum observed for HFNap-peat, as was found to be the case for humic acid *(17)*.

From the qualitative shape of the ^{19}F→^{1}H CP spectra of peat, albumin, and lignin mixed with either PFOA or HFNap, the presence of interactions similar to those observed in the isolated humic acid fraction seem to be confirmed in the whole, unmodified soil; PFOA interacts mostly with protein-derived materials found in the soil, while HFNap interacts with components similar in structure to lignin in addition to protein-derived components. Nevertheless, the broad nature of the ^{1}H resonances observed here impact the reliability of these qualitative comparisons. To further support the presence of these binding sites, the dynamics of ^{19}F→^{1}H cross-polarization was studied for these organofluorine compounds in peat, albumin, and lignin. The amount of ^{1}H transverse magnetization produced by cross-polarization depends upon how long the ^{1}H and ^{19}F spin baths are in contact. A plot of signal intensity versus this contact time, which is controlled experimentally, follows a curve that can be fit to two exponential terms reflecting two competing processes: the rate of polarization transfer from ^{19}F to ^{1}H, which increases ^{1}H transverse magnetization with longer contact time and depends upon the nature of the ^{19}F spin bath surrounding ^{1}H; and the rate of relaxation of ^{19}F nuclear spins, which decreases ^{1}H transverse magnetization with increasing contact time and depends upon the relaxation properties of the organofluorine compound during its interaction with SOM. Quantitative analyses of these dynamics are difficult to make using the broad ^{1}H solid-state NMR spectra presented here, which represent all organic sites in SOM and preclude the isolation of discrete signals from distinct chemical sites. Nevertheless, qualitative comparisons of these dynamics are still useful in addressing the main research goal of this chapter and dissertation; the elucidation of preferred xenobiotic SOM binding domains in an unmodified whole soil.

In figure 6.2, the buildup of ^{1}H transverse magnetization as a function of contact time is shown for peat mixed with PFOA and HFNap, as well as for PFP and PFBA. Figure 6.2a shows CP
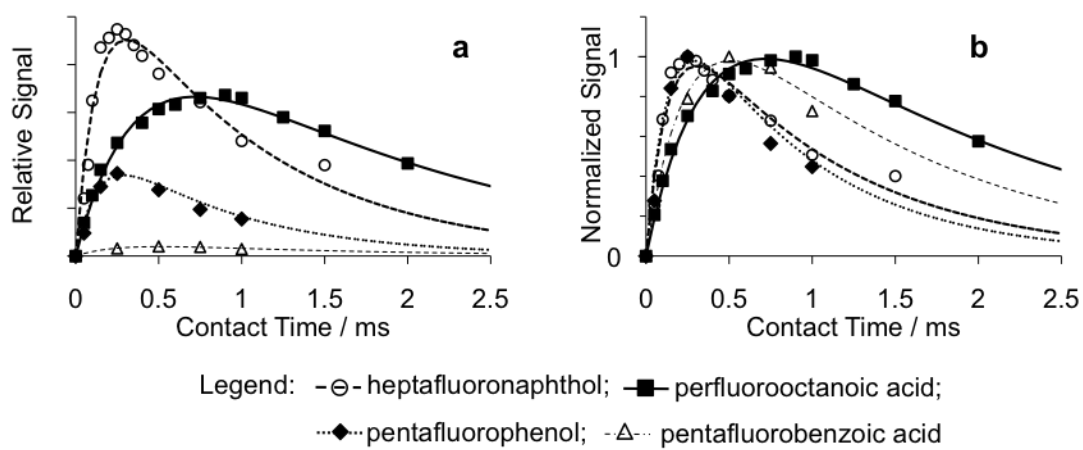
Figure 6.2 $^{19}F \rightarrow {}^{1}H$ CP MAS buildup curves of mixtures for four organofluorine compounds in Pahokee peat soil using the relative signal intensity for each mixture (a), and signals normalized with respect to the strongest signal for each mixture (b).

buildup curves using the same relative scale for all samples. For similar mixtures under similar conditions the amount of signal recorded is related to the degree of interaction between peat and organofluorine, allowing for comparisons in the relative strength of interaction in general. HFNap produces the most CP signal, followed by PFOA and PFP. PFBA produces essentially no CP signal, indicating that this compound is not strongly bound to the soil organic matter. The presence of free organofluorine was verified in the PFOA, PFP, and PFBA samples using a simple ^{19}F PFG-MAS diffusion experiment to measure apparent rates of translational motion *(22)*.

To easily compare the different CP buildup curves, the data points were normalized to the strongest observed signal for that mixture and are shown in figure 6.2b. It is clear that HFNap and PFOA produce very different curves from each other, suggesting again that these two compounds are interacting with the peat through differing mechanisms. PFBA produces a curve intermediate between HFNap and PFOA. It was shown previously (chapter 3) that PFBA interacts with all components of dissolved humic acid without preference *(24)*. PFP produces a curve that is essentially identical to that of HFNap despite exhibiting a much weaker interaction as evident in figure 6.2a. It was shown previously (chapter 3) that the humic acid sites PFP interacts with in dissolved humic acid are similar to those for HFNap, but with PFP exhibiting a much weaker interaction at these sites *(24)*. Extrapolating from the humic acid studies, the similarity in the CP-MAS curves between the strongly bound HFNap and the weakly bound PFP observed here in whole peat, suggests that the profile of the curve is not greatly influenced by the dynamics of the interactions, which differ between these two compounds, but rather by the nature of the site(s) where the interaction occurs, which are likely the same.

The ^{19}F$\rightarrow$^{1}H CP curves are shown for lignin or albumin mixtures using PFOA or HFNap are shown in figure 6.3. For albumin, the CP signal rises more rapidly and decays faster for HFNap than for PFOA. For lignin, the buildup and decay is similar for both organofluorine compounds. Comparing albumin to lignin, the maximum signal intensity occurs at a shorter contact time in the lignin mixtures than the albumin mixtures. The differences between albumin and lignin, and PFOA and HFNap indicate that the rate of cross-polarization is dependent upon both the type of organofluorine compound, and the form of the organic matter with which it is interacting
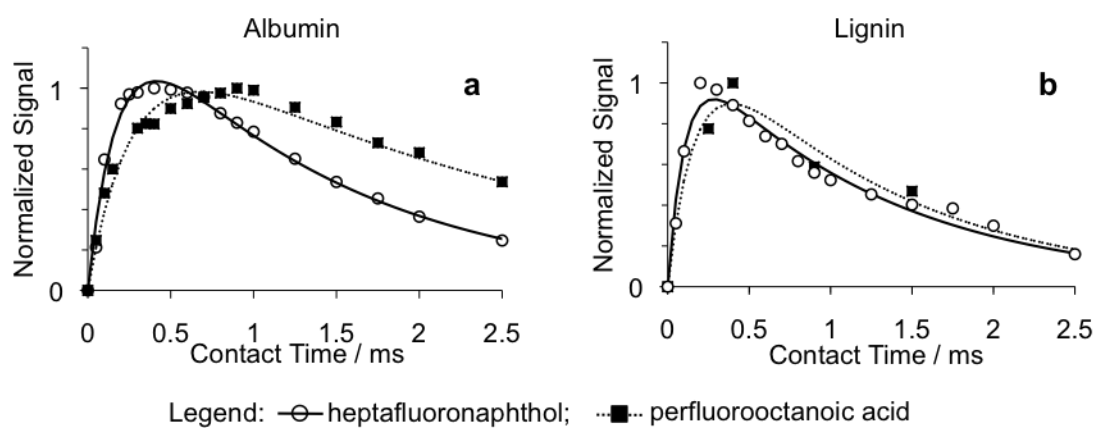
Figure 6.3 $^{19}F\rightarrow{}^{1}H$ CP MAS buildup curves of mixtures for perfluorooctanoic acid and heptafluoronaphthol with albumin (a) and lignin (b).

supporting the argument that the CP curves observed in whole soil reflect the nature of the organic matter where organofluorine compounds are bound.

In figure 6.4 the $^{19}F \rightarrow {}^{1}H$ CP curves of peat are compared with those of albumin and lignin. For PFOA the CP curve of the peat matches that observed for albumin, but is markedly different from that observed for lignin. For HFNap, the CP curve of peat matches that for lignin, but differs from the curve for albumin. These results confirm that the type of organofluorine-SOM interactions producing the ^{1}H signals in the PFOA-peat mixture are similar to PFOA-albumin, while the ^{1}H signals in the HFNap-peat mixture are arising primarily from interactions similar to HFNap-lignin. The observations made here agree with those observed using the dissolved humic acid of the same soil *(17, 24)*.

Previous studies have shown strong correlations between the amount of aliphatic or aromatic material found in soils and their propensity to sorb different types of small xenobiotic compounds *(16, 25-27)*. Methods through which these conclusions were made include correlating sorption behaviour to the relative contribution of aliphatic and aromatic signals in a ^{13}C CPMAS NMR spectrum, comparing the sorption behaviour of a soil before and after it is has been chemically altered to remove certain types of structures *(27)*, and by comparing the sorption behaviour of a soil to the sorption behaviour of representative biopolymers *(11, 13, 28)*. Here, we have shown directly where in an unmodified soil two dissimilar compounds are located after their sorption. Specific knowledge of the chemical nature of the sorption sites, as presented here, complements other studies that have demonstrated the physical nature of these sites in whole soils *(10, 19, 20, 29, 30)*. The results of this study confirm that a variety of different structures of SOM can be important in the sorption of xenobiotic compounds and that a uniform distribution of xenobiotics throughout all components of SOM cannot be taken for granted. PFOA, for example, is shown to interact nearly exclusively with protein-derived components of this soil. While protein is not normally considered as an important sorption domain in soils and sediments, microbial biomass, which is rich in protein, accounts for a significant fraction of the organic material found in many soils *(31)*. For compounds such as PFOA, which are known to accumulate in protein-rich organs in biological systems *(32)*, soil bound protein should be considered when developing fate models for compounds such as PFOA.
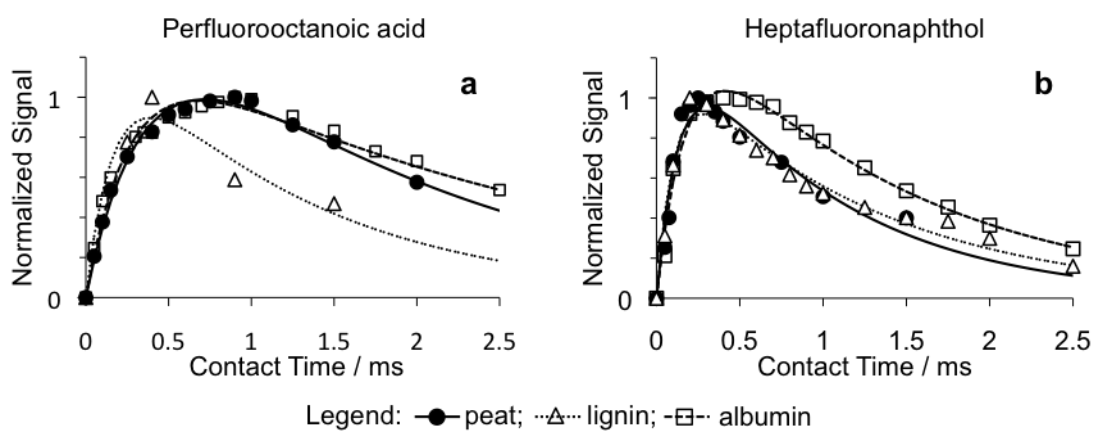
Figure 6.4   Overlaid $^{19}F \rightarrow {}^{1}H$ CP MAS buildup curves of mixtures of Pahokee peat, albumin, and lignin for perfluorooctanoic acid (a) and heptafluoronaphthol (b).

Humic acid is often used as a simplified proxy to study intermolecular interactions between small xenobiotics and SOM, however the analyses presented in these studies are always restrained because the structures found in humic acid are modified from their natural state, and that the soluble fractions of soil organic matter only represent a fraction of the molecular structures found in soils and sediments. Using an unmodified whole peat soil, we have demonstrated differences in the types of organic material where different organofluorine compounds interact when they have been sorbed. These results agree with those observed using the dissolved humic acid of the same peat soil *(17, 24)*, namely that PFOA interacts nearly exclusively with protein-like structures while HFNap interacts preferentially with lignin-like structures. These observations present a direct and clear elucidation of the sorption sites for these compounds in a soil, knowledge of which is vital for improving our understanding of the roles soils and sediments play as an environmental matrix in the lifecycle of many important environmental compounds *(33)*. Furthermore, the similarity in the results observed in the whole soil to those found previously in humic acid alone *(15, 17-19, 24, 27, 34-36)*, strengthen the relevance of conclusions made about the nature of environmental xenobiotic interactions from studies using simpler fractions of SOM, which in most instances are more accessible for molecular-level studies.

6.4   Conclusions

It was shown that observations made with regards to the site of interaction for organofluorine xenobiotics in dissolved humic acid made in chapter 1 *(17)*, correspond to similar associations in the unmodified whole peat soil from which that humic acid was extracted. This observation lends credence to other conclusions made about binding interactions made using the simplified humic acid fraction in chapters 2, 3, 4, and 5 of this dissertation.

The peat soil studied here is primarily organic in content and the various roles that inorganic components of a soil may play in the sorption of xenobiotics have been largely avoided. In the absence of inorganic components, the analysis here has been able to focus entirely upon the chemistry of the organic-organic interactions that may occur and as such this study represents a first step towards a full molecular-level elucidation of soil-xenobiotic interactions in intact whole

soils. Future work is needed to expand this line of inquiry into more chemically diverse soils, as well as into other classes of xenobiotics.

6.5   References

(1)   Luthy, R. G.; Aiken, G. R.; Brusseau, M. L.; Cunningham, S. D.; Gschwend, P. M.; Pignatello, J. J.; Reinhard, M.; Traina, S. J.; Weber, W. J.; Westall, J. C. Sequestration of hydrophobic organic contaminants by geosorbents. *Environ. Sci. Technol.* **1997,** *31* (12)*,* 3341-3347.

(2)   Lambert, S. M.; Porter, P. E.; Schieferstein, R. H. Movement and sorption of chemicals applied to the soil. *Weeds* **1965,** 185-190.

(3)   Karickhoff, S. W.; Brown, D. S.; Scott, T. A. Sorption of hydrophobic pollutants on natural sediments. *Water Res.* **1979,** *13* (3)*,* 241-248.

(4)   Karickhoff, S. W.; Morris, K. R. Sorption dynamics of hydrophobic pollutants in sediment suspensions. *Environ. Toxicol. Chem.* **1985,** *4* (4)*,* 469-479.

(5)   Chiou, C. T.; Kile, D. E. Deviations from sorption linearity on soils of polar and nonpolar organic compounds at low relative concentrations. *Environ. Sci. Technol.* **1998,** *32* (3)*,* 338-343.

(6)   Xing, B.; Pignatello, J. J.; Gigliotti, B. Competitive sorption between atrazine and other organic compounds in soils and model sorbents. *Environ. Sci. Technol.* **1996,** *30* (8)*,* 2432-2440.

(7)   Barriuso, E.; Benoit, P.; Dubus, I. G. Formation of pesticide nonextractable (bound) residues in soil: Magnitude, controlling factors and reversibility. *Environ. Sci. Technol.* **2008**, *42* (6), 1845-1854.

(8)   Robertson, B. K.; Alexander, M. Sequestration of DDT and Dieldrin in soil: disappearance of acute toxicity but not the compounds. *Environ. Toxicol. Chem.* **1998**, *17* (6), 1034-1038.

(9)   Weber, W. J.; McGinley, P. M.; Katz, L. E. A distributed reactivity model for sorption by soils and sediments. 1. Conceptual basis and equilibrium assessments. *Environ. Sci. Technol.* **1992***, 26* (10), 1955-1962.

(10)   Xing, B.; Pignatello, J. J. Dual-mode sorption of low-polarity compounds in glassy poly(vinyl chloride) and soil organic matter. *Environ. Sci. Technol.* **1997,** *31* (3)*,* 792-799.

(11)   Wang, X.; Xing, B. Importance of structural makeup of biopolymers for organic contaminant sorption. *Environ. Sci. Technol.* **2007,** *41* (10)*,* 3559-3565.

(12)   Chiou, C. T.; Kile, D. E.; Rutherford, D. W.; Sheng, G.; Boyd, S. A. Sorption of selected organic compounds from water to a peat soil and its humic-acid and humin fractions: potential sources of the sorption nonlinearity. *Environ. Sci. Technol.* **2000,** *34* (7)*,* 1254-1258.

(13)   Garbarini, D. R.; Lion, L. W. Influence of the nature of soil organics on the sorption of toluene and trichloroethylene. *Environ. Sci. Technol.* **1986,** *20* (12)*,* 1263-1269.

(14)   Simpson, M. J. Nuclear magnetic resonance based investigations of contaminant interactions with soil organic matter. *Soil Sci. Soc. Am. J.* **2006**, *70* (3), 995-1004.

(15)   Sun, H.; Zhu, D.; Mao, J. Sorption of polar and nonpolar aromatic compounds to two humic acids with varied structural heterogeneity. *Environ. Tox. Chem.* **2008**, *27* (12), 2449-2456.

(16)   Mao, J-D.; Hundal, L. S.; Thompson, M. L.; Schmidt-Rohr, K. Correlation of Poly(methylene)-rich amorphous aliphatic domains in humic substances with sorption of nonpolar organic contaminant, phenanthrene. *Environ. Sci. Technol.* **2002**, *36* (5)*,* 929-936.

(17)   Longstaffe, J. G.; Simpson, M. J.; Maas, W.; Simpson, A. J. Identifying components in dissolved humic acid that bind organofluorine contaminants using $^{1}H\{^{19}F\}$ reverse heteronuclear saturation transfer difference NMR spectroscopy. *Environ. Sci. Technol.* **2010**, *44* (14), 5476-5482.

(18) Smejkalova, D.; Spaccini, R.; Fontaine, B.; Piccolo, A. Binding of phenol and differently halogenated phenols to dissolved humic acid as measured by NMR spectroscopy. *Environ. Sci. Technol.* **2009**, *43* (14), 5377-5382.

(19) Khalaf, M.; Kohl, S. D.; Klumpp, E.; Rice, J. A.; Tombacz, E. Comparison of sorption domains in molecular weight fractions of a soil humic acid using solid-state ^{19}F NMR. *Environ. Sci. Technol.* **2003**, *37* (13), 2855-2860.

(20) Golding, C. J.; Smernik, R. J.; Birch, G. F. Investigation of the role of structural domains identified in sedimentary organic matter in sorption of hydrophobic organic compounds. *Environ. Sci. Technol.* **2005**, *39* (11), 3925-3932.

(21) Courtier-Murias, D.; Farooq, H.; Masoom, H.; Botana, A.; Soong R.; Longstaffe, J. G.; Simpson M. J.; Maas, W. E.; Fey M.; Andrews, B.; Struppe, J.; Hutchins, H.; Krishnamurthy S.; Kumar, R.; Monette, M. J.; Stronks, H. J.; Hume, A.; Simpson, A. J. Comprehensive multiphase NMR spectroscopy: basic experimental approaches to differentiate phases in heterogeneous samples. *J. Mag. Reson.* **2012**, *217*, 61-76.

(22) Wu, D.; Chen, A.; Johnson, C. S. An improved diffusion-ordered spectroscopy experiment incorporating bipolar-gradient pulses. *J. Magn. Reson., Ser. A* **1995**, *115* (2), 260-264.

(23) Mao, J.-D.; Xing, B.; Schmidt-Rohr, K. New structural information on a humic acid from two-dimensional [1]H-^{13}C correlation solid-state nuclear magnetic resonance. *Environ. Sci. Technol.* **2001**, *35* (10), 1928-1934.

(24) Longstaffe, J. G.; Simpson, A. J. Understanding solution-state noncovalent interaction between xenobiotics and natural organic matter using ^{19}F/^{1}H heteronuclear saturation transfer difference nuclear magnetic resonance spectroscopy. *Environ. Toxicol. Chem.* **2011**, *30* (8), 1745-1753.

(25) Delort, A-M.; Combourieu, B.; Haroune, N. Nuclear magnetic resonance studies of interactions between organic pollutants and soil components, a review. *Environ. Chem. Lett.* **2004**, *1* (4), 209-213.

(26) Chefetz, B.; Xing, B. Relative role of aliphatic and aromatic moieties as sorption domains for organic compounds: A review. *Environ. Sci. Technol.* **2009,** *43* (6)*,* 1680-1688.

(27) Gunasekara, A. S.; Simpson, M. J.; Xing, B. Identification and characterization of sorption domains in soil organic matter using structurally modified humic acids. *Environ. Sci. Technol.* **2003**, 37 (5), 852-858.

(28) Wang, X.; Cook, R.; Tao, S.; Xing. B. Sorption of organic contaminants by biopolymers: Role of polarity, structure and domain spatial arrangement. *Chemosphere* **2007**, *66* (8), 1476-1484.

(29) Smernik, R. J. A new way to use solid-state carbon-13 nuclear magnetic resonance spectroscopy to study the sorption of organic compounds to soil organic matter. *J. Environ. Qual.* **2005**, *34* (4), 1194-1204.

(30) Kohl, S. D.; Toscano, P. J.; Hou, W.; Rice, J. A. Solid-State ^{19}F NMR Investigation of hexafluorobenzene Sorption to Soil Organic Matter. *Environ. Sci. Technol.* **2000**, *34* (1), 204-210.

(31) Simpson, A. J.; Simpson, M. J.; Smith, E.; Kelleher, B. P. Microbially derived inputs to soil organic matter: are current estimates too low? *Environ. Sci. Technol.* **2007,** *41* (23)*,* 8070-8076.

(32) D'Eon, J. C.; Simpson, A. J.; Kumar, R.; Baer, A. J.; Mabury, S. A. Determining the molecular interactions of perfluorinated carboxylic acids with human sera and isolated human serum albumin using nuclear magnetic resonance spectroscopy. *Environ. Toxicol. Chem.* **2010**, *29* (8), 1678-1688.

(33) Chung, N.; Alexander, M. Differences in sequestration and bioavailability of organic compounds aged in dissimilar soils. *Environ. Sci. Technol.* **1998**, 32 (7), 855-860.

(34) Pan, B.; Ghosh, S.; Xing, B. Nonideal binding between dissolved humic acids and polyaromatic hydrocarbons. *Environ. Sci. Technol.* **2007**, *41* (18), 6472-6478.

(35)   Laor, Y.; Rebhun, M. Evidence for nonlinear binding of PAHs to dissolved humic acids. *Environ. Sci. Technol.* **2002**, *36* (5), 955-961.

(36)   Nanny, M. A.; Maza, J. P. Noncovalent interaction between monoaromatic compounds and dissolved humic acids: a deuterium NMR T_1 relaxation study. *Environ. Sci. Technol.* **2001**, *35* (2), 379-384.

CHAPTER 7
SUMMARY AND FUTURE DIRECTIONS

7.1 Summary

The central research question of this dissertation has been '*what do xenobiotic interactions with Natural Organic Matter (NOM) look like from the vantage of NOM itself?*'. The general hypothesis here was that different components of NOM interact with different types of xenobiotic compounds independently and simultaneously through similar and dissimilar mechanisms, a like. The research goal of this dissertation was to study this hypothesis as directly as possible by using molecular-level analysis and as completely as possible by modifying the system under study as minimally as possible, if modified at all. The hypothesis that different chemical components of NOM behave differently in regards to their interactions with xenobiotics is not new, however it has never before been addressed by observing these proposed interactions directly without significant modification of the system being studied. Understanding the interactions between xenobiotics and NOM, particularly in soils and sediments, has implications for improving our understanding of the molecular origins for many phenomena governing the fate and impact of anthropogenic contamination in the environment.

To answer the central question posed above, the intermolecular interactions between soil-based NOM, or soil organic matter (SOM) and organofluorine compounds were studied at the molecular-level using Nuclear Magnetic Resonance (NMR) spectroscopy. Several NMR techniques were employed in this work, including Pulse Field Gradient (PFG)-NMR based diffusion measurements, solid-state cross-polarization (CP), saturation transfer difference (STD) spectroscopy, and reverse-heteronuclear saturation transfer difference (RHSTD) spectroscopy, which was introduced here as a technique specifically for the study of molecular-level processes occurring within complex environmental matrices.

The use of organofluorine xenobiotics provided an unambiguous pathway to probe interactions with NOM, allowing for the actual binding sites of these compounds to be resolved *in situ* for the first time. Compounds studied here include known persistent organic pollutants,

perfluorooctanoic acid (PFOA) and potassium perfluorooctane sulfonate (KPFOS), as well as many aromatic organofluorine compounds. Initially, these interactions were studied using dissolved humic acid, which is the alkali-soluble fraction of SOM. While itself chemically complex, humic acid is simplified relative to intact SOM and while more accessible for analytical study than a whole soil, does not necessarily reflect what the true state of this material would be in a whole, intact soil. Nevertheless, using crucial knowledge gained from several humic acid studies, a detailed molecular-level investigation of xenobiotic interactions in an intact and unmodified whole soil was made possible. A direct and *in situ* elucidation of the components in unmodified SOM that interact with small organofluorine xenobiotic molecules has been presented, allowing, for the first time, resolution of multiple interactions occurring for xenobiotics simultaneously at different sites within a whole peat soil. It was found that different components of SOM interact with dissimilar xenobiotic compounds by way of dissimilar mechanisms. This results in the observation of apparent preferences for interactions at different SOM binding sites for dissimilar organofluorine compounds, confirming the main hypothesis of this dissertation. The most notable preferences observed are for interactions at lignin- or protein-derived components of SOM.

To probe the mechanisms behind the interactions between humic acid and organofluorine compounds, various experimental parameters were varied in order to induce changes in the nature of the observed interactions. These parameters included: the molecular framework of the organofluorine compound, including the functionality, polarity, and solubility; the concentration of the organofluorine compound; the concentration of humic acid; the temperature; and the solution pH. In general, the extent to which an organofluorine compound interacts with humic acid in solution is related to its aqueous solubility or hydrophobicity (chapters 2 and 4). PFOA, which is one of the more soluble compounds studied here, is an exception to this observation as it interacts with humic acid more strongly than other compounds with similar aqueous solubility. Tetrafluoro-1,4-terephthalic acid, for example, has a comparable aqueous solubility and does not exhibit any interaction with humic acid at all (chapter 3). The reason for this divergent behaviour for PFOA is that a strong interaction occurs between PFOA and protein-derived components of humic acid (chapter 2). Aside from the protein-derived components of humic acid, PFOA exhibits no interaction with the other components of humic acid, in agreement with the solubility-based trends observed for other compounds. The observation of protein selectivity

was first noted in dissolved humic acid, where it was shown that these protein-derived sites have a limited capacity for interactions with PFOA (chapter 2), but was also later confirmed in the whole peat soil from which that humic acid was extracted (chapter 6). Using variable temperature measurements of the association between PFOA and dissolved humic acid, it was further suggested that the nature of this interaction is highly dependent upon conformational changes in the protein sites, with the extent of the interaction decreasing markedly as the temperature decreases. When conformational changes in the protein sites exclude access to PFOA, this compound prefers to be in solution rather than interact with any other components humic acid (chapter 4). All other compounds studied for temperature effects, including KPFOS, exhibit the opposite temperature dependence on their interaction with humic acid, with the extent of interaction increasing as energy is removed from the system. To a first approximation, these other organofluorine compounds interact with all humic acid components available to them.

It was shown for most of the organofluorine compounds studied here that the interactions with humic acid are primarily driven by the high energy barrier for complete aqueous solvation rather than by specific interactions with humic acid itself (chapters 3 and 4), nevertheless some preference for interactions at some sites in humic acid are observed over others (chapter 3). In addition to the exclusive interactions with PFOA at protein sites discussed above, many of the aromatic organofluorine compounds studied here exhibit a greater tendency to interact with aromatic moieties of humic acid over non-aromatic moieties of humic acid (chapters 2, 3, 5). These aromatic sites were shown to be similar in structure to lignin and exhibit a limited capacity for interactions (chapter 2). For polar compounds, the aromatic preference increases with decreasing aqueous solubility. Furthermore, the extent to which a compound exhibits preference for aromatic sites correlates well to measures of molecular polarity, particularly the molecular quadrupolar moments of the aromatic organofluorine compounds (chapter 3). Aromatic organofluorine compounds with electron donating groups on them, such as NH_2 or OH, show the strongest apparent preference for these aromatic humic acid sites, while compounds with electron withdrawing groups, such as COOH or NO_2, show little to no preference for aromatic interactions. In general, this trend also corresponds to the hydrophobicity of these compounds, with more hydrophobic compounds showing more preference for aromatic sites. Aromatic organofluorine compounds with two OH or COOH groups, interact with the aromatic sites in humic acid following the same trends observed for the other compounds, however they exhibit a

reduced interaction with the non-aromatic components given their molecular properties relative to the other organofluorine compounds (chapter 3). This observation suggests that while solubility and hydrophobic effects may drive the interactions with humic acid in general, and at aromatic sites in specific, there seems to be some avoidance of the non-aromatic humic acid sites for some compounds and that apparent aromatic preference may in fact by due to incompatibility with non-aromatic sites in humic acid rather than specific interactions at aromatic sites.

The apparent aromatic preference is found to be highly pH-sensitive: at low pH a strong aromatic preference is observed for selected compounds, however as pH increases this preference weakens and at high pH values a nearly uniform distribution of interactions at all humic acid sites is observed (chapter 5). This effect is due to a redistribution of organofluorine compounds from aromatic sites to carbohydrate sites due to conformational changes in the humic acid that increase the accessibility to non-aromatic sites in humic acid, particularly carbohydrates-like domains. At high pH, inter and intra-molecular hydrogen bonds in the carbohydrate humic acid domains weaken, resulting in an opening up of their supramolecular structure. It is suggested that at low pH, these carbohydrate sites form tightly bound hydrophobic domains with restricted access binding sites, particularly for polar aromatic compounds, whereas at high pH these restrictions are lifted by changes in the conformational structure that opens up more sites for interaction. Interactions at non-aromatic sites increase, however, once available aromatic sites become saturated (chapter 2). Non-polar aromatic compounds pass easily into the more restricted hydrophobic domains and never exhibit any preference for different humic acid sites (chapter 5). Likewise, weakly interacting compounds do not exhibit strong aromatic preferences because the smaller number of sites needed to accommodate their interactions are easily satisfied, even with many potential binding sites closed off. The possibility of specific aromatic-aromatic interactions was investigated using quantum mechanics-based computational methods, but was found to be unlikely to account for differences in observed site preference compounds for different compounds (chapters 3 and 5). A graphical overview of the investigations and observations made here into the nature of organofluorine interactions with dissolved humic acid is shown in figure 7.1.

The identification of binding sites, and the accompanying studies of interaction mechanisms with SOM were all performed initially using dissolved humic acid, which represents a simplification
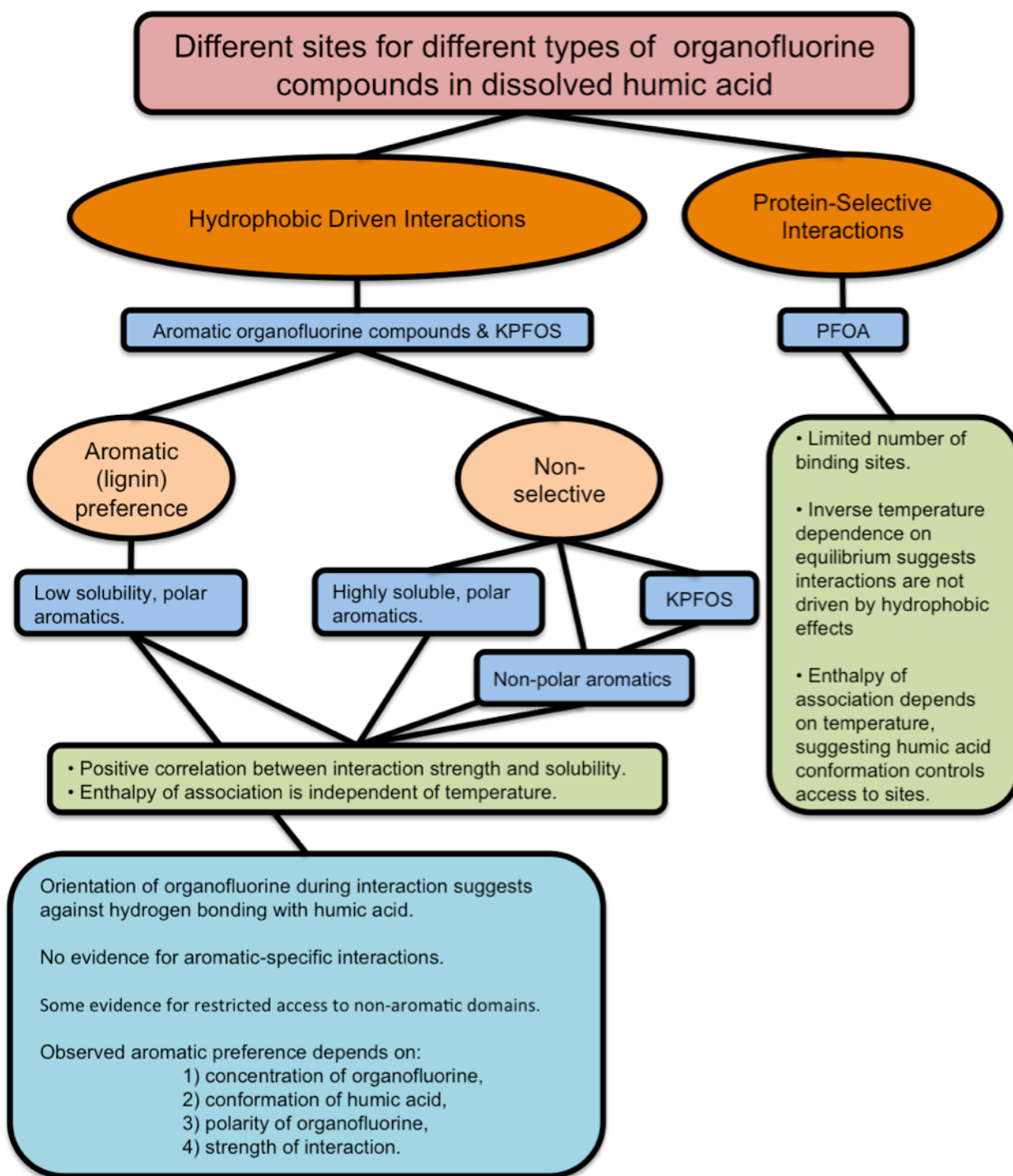
Figure 7.1   A graphical overview of the investigations and observations of the nature of organofluorine interactions with dissolved humic acid made in this dissertation.

of SOM from its form in an unmodified whole soil. The humic acid extraction process is harsh, however, and disrupts much of the organizational structure of SOM from its natural state in a soil. Furthermore, humic acid, while a major fraction of SOM, represents only part of its chemical constituency. The extrapolation of interaction mechanisms proposed from humic acid alone to whole soils should thus be treated with caution. Nevertheless, the convoluted chemical environment of a whole soil is nearly impenetrable to most modern analytical probes for intermolecular interactions,. The molecular motion of dissolved fractions of SOM, such as humic acid, permits a high-resolution analysis of the NMR spectrum of the ^{1}H nuclei within SOM from which much chemical information may be extracted. This resolution is significantly compromised in the solid-state where motion is limited and ^{1}H spectra are typically featureless due to several anisotropic effects. Magic Angle Spinning (MAS) can aid in reducing this broadening, however for ^{1}H the nuclear magnetic moments are too strong for MAS to overcome without specialized, ultra-fast-spinning solid-state probes *(1)*. Despite these limitations, an attempt to study intermolecular interaction in the murky spectral environment of a whole soil is made in the final part of this dissertation. Without knowledge of the nature of these interactions in a whole soil, extrapolations made from humic acid to the actual environment are unreliable.

In a whole peat soil, selected organofluorine compounds were sorbed and then attempts were made to elucidate the identity of their binding sites in a manner similar to that carried out previously for humic acid (chapter 6). Using a cross-polarization experiment, ^{19}F nuclei from organofluorine compounds were used to produce observable magnetization in the ^{1}H nuclei of SOM. In this way, only components of SOM in close proximity to an organofluorine compound are observed. Two compounds that exhibited dissimilar interactions profiles in humic acid, heptafluoronaphthol and perfluorooctanoic acid, also produced dissimilar interaction profiles in the whole soil confirming that in the whole soil these compounds are interacting with a different combination of SOM components relative to each other. The poor resolution of the solid-state ^{1}H spectra of the whole soils, however, limits the identification of binding sites based on chemical shift alone. This was overcome in part by using the information gained through the study of humic acid and by probing the dynamics of cross-polarization to compare the chemical nature of SOM-organofluorine interactions with those involving similar biopolymers known as binding sites from the humic acid studies. In general, identical observations were found for

humic acid and an organic rich soil in its natural state: dissimilar organofluorine compounds interact with different components of SOM. Specifically, perfluorooctanoic acid shows nearly selective preference for protein-derived components and heptafluoronaphthol interacts with all components of SOM, but preferentially with lignin-derived components. This study is the first time that the chemical nature of sorption sites in SOM has been elucidated by direct methods in a completely unmodified and intact soil. The agreement between molecular-level observations of binding sites in SOM between humic acid and a whole soil is extremely positive, as studies made using simplified fractions of SOM are often criticized for their reduced relevance to real environmental systems. Presented here is strong experimental support that studies of intermolecular interactions with fractions such as humic acid can be directly relevant.

There are limitations in the analysis presented in this thesis, however: the whole soil studied here is a high organic peat soil and as such the role soil minerals play in most soils has not been addressed. By using peat humic acid and whole peat soil, rather, the chemical nature of these binding sites was addressed without many of the complications arising from physical effects that may occur in more heterogeneous soils, such as site inaccessibility due to organic-mineral complexes. The work presented here is a giant step forwards, nonetheless, as while the sorption of organic xenobiotics into soils and sediments has been well studied, much of this work has been done at the macroscopic-level where the simultaneous occurrence of processes at different sites is obscured by differences between the magnitudes of scale for the observation and the processes themselves. Macroscopic observations of soil processes have led to the discovery of numerous unexplained phenomena, including sequestration and reduced ecotoxicity. To engage these problems fully, the creation of a molecular-level, or reductionist framework for understanding sorption phenomena in soils has been necessary and is ongoing. Nevertheless, previous molecular-level investigations aimed at resolving the origins of these phenomena have required modification of the macroscopic form of the soil, leading to uncertainty in the relevance of observations made in modified or fractionated soils and SOM. The work in this dissertation represents advancement towards the goal of a molecular-level understanding of these processes without compromising the macroscopic structure of the soil.

The original goal of the research presented here was to address a relatively simple question: do dissimilar components of soil organic matter interact with xenobiotics differently. For the small

number of organofluorine compounds studied in a peat soil, the answer is yes. Following from this, the identity of some of those sites have been determined, lignin and protein. An elucidation of the chemical nature of the mechanisms underlying these preferences has been made using the humic acid fraction of this soil. Using this work as a starting point, a full molecular-level understanding of the processes occurring within the SOM black box is closer at hand. In the next section, a short discussion of the directions this work can go is presented, including some preliminary work that has already been started.

7.2   Future Directions

7.2.1 Environmental Chemistry of Organofluorine Compounds

Aromatic organofluorine compounds featured prominently throughout most of the work in this dissertation. While these compounds are emerging as an important class of persistent organic pollutants, not much is known about their environmental properties; here these compounds were useful as structural probes for the types of binding interactions that may occur between xenobiotics and SOM, or NOM in general. Perfluorooctanoic acid and potassium perfluorooctane sulfonate, for which binding interactions were also studied, are environmentally important. From the limited work presented here, many important questions remain about the interactions between perfluoroalkyl compounds and NOM that can easily be studied using the same approaches already described. For example, it was shown that PFOA interacts only with protein-derived soil components (chapters 2 and 6): is this the same for other perfluorinated carboxylic acids? Are there any trends associated with chain length, branched isomers, or the acidic functional group? KPFOS interacts with all components of humic acid equally (chapter 4), what about perfluorooctanesulfonic acid (PFOS)? Most of these types of compounds are ionic at environmentally relevant pH, does the ionization affect their interactions? What role do cations play? Polyfluorinated alkyl compounds form micelles in solution *(2)*, what role does this play in their interactions with different forms of NOM?

7.2.2 Working Without Fluorine

Perfluorinated compounds are interesting, but they are a small set of the total number of environmentally important compounds. Furthermore, as discussed in chapter 1, the strong electronegativity of fluorine makes perfluorinated compounds 'special' with respect to most other organic compounds, and extrapolations from observations made using organofluorine to other types of xenobiotics should be approached cautiously *(3)*. Perdeuterated compounds may hold the most promise as an alternative to studying molecular-level interactions in NOM using similar approaches to those described in this dissertation. Deuteration has essentially no effect on the chemical or physical properties of any compound, however, limitations do arise from the NMR properties of ^{2}H. ^{2}H is a quadrupolar nucleus with spin 1, fortunately, the quadrupolar coupling of ^{2}H is relatively small and does not cause detection problems as is the case for many other quadrupolar nuclei. The integer spin does, however, complicate spin dynamics relative to the more common half-integer nuclei, which include ^{1}H, ^{19}F, and ^{13}C and modified approaches may be needed. Furthermore, ^{2}H is a significantly less sensitive nucleus than ^{19}F. The strength of the dipole interaction between two nuclei is proportional to the product of the square of the magnetogyric ratio of each nucleus *(4)*. Therefore, reducing the magnetogyric ratio, which is proportional to the resonance frequency, of one of those nuclei greatly reduces the strength of the dipole interaction that we wish to manipulate to observe these interactions. The NMR properties of ^{2}H relative to other environmentally relevant nuclei are illustrated in table 7-1. Overcoming this last limitation requires significantly more spectrometer time than was needed for ^{1}H/^{19}F measurements. Nevertheless, with the knowledge gained from using ^{19}F as a xenobiotic probe, studies using ^{2}H can be designed with more directed goals, as the systems and problems to be studied are already understood to a certain extent for organofluorine compounds.

Other common environmental xenobiotic nuclei that may be interesting are chlorine and bromine. Both organochlorine and organobromine compounds are important environmental xenobiotics, perhaps more so than organofluorine *(5)*. The elements chlorine and bromine both have two NMR active nuclei: ^{35}Cl and ^{37}Cl for chlorine, and, ^{79}Br and ^{81}Br for bromine. The primary limitation in the use of both of these elements in NMR studies is the strong quadrupolar nature of these nuclei, which greatly inhibits the ability to detect them in asymmetric chemical environments *(4)*. This is particularly the case when they are engaged in covalent bonding. An

Table 7-1   NMR properties of selected environmental nuclei with potential to be important for investigating xenobiotic interactions *(8)*.

Element	NMR active nuclei	Spin	Relative frequency	% Natural abundance
Hydrogen	^{1}H	1/2	100	99.9885
	^{2}H	1	15.350609	0.0115
Fluorine	^{19}F	1/2	94.09	100
Aluminum	^{27}Al	5/2	26.056859	100
Phosphorus	^{31}P	1/2	40.480742	100
Chlorine	^{35}Cl	3/2	9.797909	75.77
	^{37}Cl	3/2	8.155725	24.23
Arsenic	^{75}As	3/2	17.122710	100
Bromine	^{79}Br	3/2	25.054452	50.69
	^{81}Br	3/2	27.007026	49.31
Cadmium	^{111}Cd	1/2	21.215478	12.80
	^{113}Cd	1/2	22.193173	12.22
Tin	^{115}Sn	1/2	32.718746	0.34
	^{117}Sn	1/2	35.632256	7.68
	^{119}Sn	1/2	37.290629	8.59
Mercury	^{199}Hg	1/2	17.910323	16.87
	^{201}Hg	3/2	6.611400	13.18
Thallium	^{203}Tl	1/2	57.123200	29.524
	^{207}Tl	1/2	57.633833	70.476
Lead	^{207}Pb	1/2	20.920597	22.1

additional limitation for chlorine is its relatively low magnetogyric ratio relative to most commonly studied nuclei (see table 7-1) and requires specialized low frequency NMR equipment. The quadrupolar nature of these nuclei makes acquiring usable spectra difficult: coupling of the quadrupole moment of the nucleus to the local asymmetric electric field gradient provided by the surrounding electrons produces lineshape that may be 10's of MHz broad *(6, 7)*. Nevertheless, once acquired, these lineshapes, can provide a multitude of data about the shape of that surrounding electric field gradient *(7)*, which is influenced by the orientation of the bromine or chlorine with respect to neighbouring molecular structures. In theory, different strengths of this quadrupolar coupling will occur for organohalides interacting with different components of a soil matrix. There are techniques, such as Multiple Quantum Magic Angle Spinning (MQMAS), that can separate out the number of different quadrupolar coupling constants in a sample *(9)*, or at the least demonstrate a distribution of them *(10)*, however this will likely be very difficult for chlorine or bromine, as studies of these nuclei are still a relatively new field of NMR research *(6, 7)*. In general, ultra high magnetic fields help when coupled with CPMG based experiments that break up very broad spectra in to smaller units in such a way that the overall shape of the resonances may still be resolved *(11)*.

Nuclear Quadrupole Resonance (NQR) spectroscopy may also have promise for studying the molecular environmental surrounding organohalides. NQR uses the electric field gradient induced by the asymmetry of a quadrupolar nucleus to polarize the spin states in the same way as an external magnetic field *(12)*. In practice, NQR is NMR spectroscopy for quadrupolar nuclei in the absence of an external magnetic field. The observed resonance frequencies of a chlorine or bromine nucleus is related to the strength of the quadrupolar coupling, and thus it is possible that for organohalide compounds sorbed into different soil environments, these nuclei will have different quadrupolar couplings and thus will have different resonances in an NQR spectrum. An approach similar to this is used to detect the quadrupolar ^{14}N nuclei in landmine explosives *(13)* and there is reason to believe that a similar approach could detect organobromine or organochlorine in soils, if one knew at which frequencies to look.

Organic compounds are not the only important environmental xenobiotics for which NMR may be useful. Many main-group heavy metals are easily studied by NMR spectroscopy, including cadmium, mercury, lead, and thallium. Thallium, which is the most toxic of all heavy metals is

also one of the more sensitive NMR nuclei, as is shown in table 7-1. Thallium exhibits an incredible chemical shift dispersion of several thousand ppm in the NMR scale (compared to the 15 ppm scale of ^{1}H and the 100 ppm scale of ^{13}C) *(14)*. The ability of NMR spectroscopy to resolve the presence of different interaction sites for dissolved cadmium with dissolved forms of NOM has already been shown *(15)*. Tin has several NMR active spin ½ nuclei with easily attainable frequencies, and observations of the interactions of organotin with NOM may be possible in much the same way interactions with organofluorine were studied here. Similarly, for organophosphorus; ^{31}P is 100% abundant with a strong magnetic moment. Many other important environmental elements have quadrupolar nuclei, including aluminum and arsenic, and approaches for studying these element's interactions with NOM should be similar to those described for organohalides, if not more attainable. ^{27}Al, for example is an easily studied quadrupolar nucleus as well as an important soil element that can be related to environmental processes such as acidification *(16)* and mineral erosion *(17)*.

7.2.3 Improved Resolution of Binding Sites in Whole Soils Using ^{13}C Detection

The ^{19}F$\rightarrow$^{1}H CPMAS NMR spectra of the whole soil used in chapter 6 to elucidate preferred organofluorine binding domains have very low resolution relative to the comparable ^{1}H{^{19}F} RHSTD solution state spectra used in chapters 2 through 5. A comparison of the resolution of solution state ^{1}H and solid-state ^{1}H is illustrated in figure 7.2 using mixtures of humic acid and heptafluoronaphthol for the solution-state and the whole peat soil and heptafluoronaphthol for the solid-state. In the solid-state, the nature of the binding domains are suggested by the ^{1}H spectral profile, however further work was required to confirm the identity of the binding domains. The solid-state ^{13}C spectrum of soil organic matter exhibits greater spectral resolution than ^{1}H, and if interactions with xenobiotics could be ascertained from a ^{13}C spectrum, the identity of those binding sites would be more definitive and allow for more detailed probes of xenobiotic interaction mechanisms in whole soils. In general, this approach is limited by two factors: the low natural abundance of ^{13}C, which reduces the NMR sensitivity of ^{13}C observation relative to ^{1}H, and the rapid weakening of through-space dipole interactions as internuclear distances increase *(18)*; the ^{13}C nuclei of NOM will be further in space from the xenobiotic than
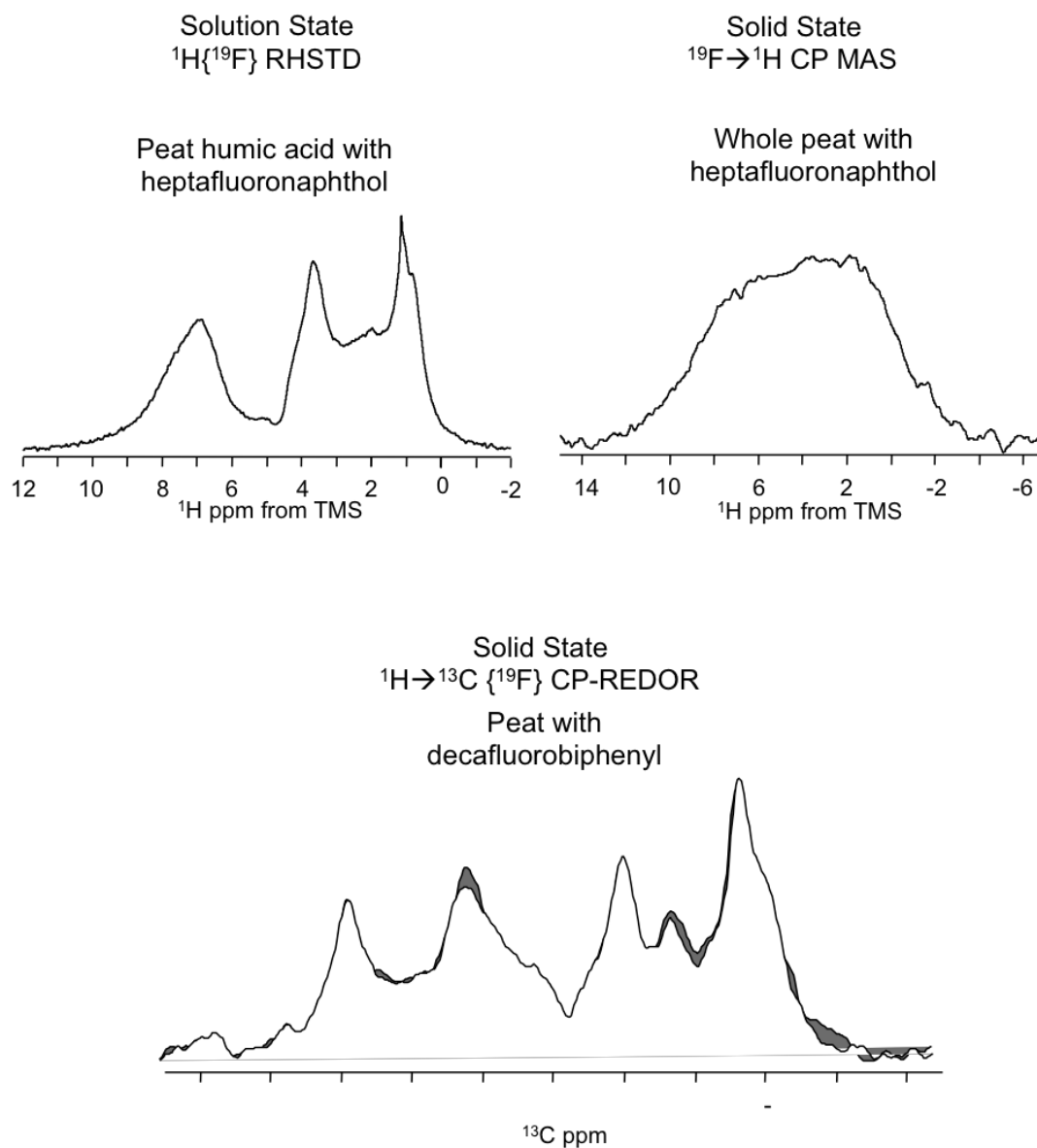
Figure 7.2 Comparison of the solid-state $^{19}F \rightarrow ^{1}H$ CP spectrum of whole soil and the $^{1}H\{^{19}F\}$ RHSTD spectrum of the humic acid extract of the same soil. In both mixtures, ^{1}H resonances are observed from SOM components in close proximity of heptafluoronaphthol. Also shown is a solid-state $^{1}H \rightarrow ^{13}C\{^{19}F\}$ CP-REDOR spectrum of the same soil mixed with decafluorobiphenyl. The REDOR spectrum shows two overlapping ^{13}C spectra: one that is quantitative, and one with components in close proximity of organofluorine which have been reduced by dipolar dephasing.

the ^{1}H nuclei are. Two possible approaches to directly observing organofluorine xenobiotic interactions at the ^{13}C nuclei of NOM are dipolar-dephasing based double-resonance experiments, and multiple cross-polarization experiments.

The dipolar-dephasing methods modulates the strength to the internuclear dipolar interaction between ^{13}C and ^{19}F, such that compared to a control spectrum, ^{13}C can be reduced in intensity relative to their spatial proximity of local ^{19}F nuclei. In this way an intermolecular interaction between NOM and organofluorine may be observed. There are several experiments designed for this sort of analysis, including Rotational-Echo Double Resonance, or REDOR *(19)*, and Transfer of Populations by Double Resonance, or TRAPDOR *(20)*. An attempt to observe such interactions using REDOR is shown in figure 7.2 for a mixture of whole peat and decafluorobiphenyl. Here, a slight loss of signal is observed for ^{13}C resonances associated with aromatic and methoxy groups, suggesting an interaction at lignin sites in agreement with the other findings reported in this dissertation. A significant limitation of the REDOR approach, however, is that these experiments are very sensitive to the fluctuating dipole moments associated with molecular motion. Whole soils consist of significant moisture content, and as such much of the organic material occurs at, or near aqueous interfaces, and a xenobiotic compound interacting with these components may not be immobile long enough for the experiment to work. Indeed, in the example shown in figure 7.2, which is a fairly poor result compared to the results from the ^{19}F→^{1}H CPMAS experiment shown in the same figure, the sample has been cooled to -35°C in order to quench molecular motion. Nevertheless, there is some promise for observing interactions at ^{13}C using this approach, and it may be worth pursuing further.

The second possible approach to observing xenobiotic interactions involves cross-polarization, similar to that reported in chapter 6. In cross-polarization, the magnetization of one set of nuclei is used to induce observable transverse magnetization in another set of nuclei. In normal cross-polarization, two types of nuclei equilibrate spin-temperatures of their respective spin-baths, which are based on the magnetogyric ratio (γ) of each nucleus. Recall from chapter 1 that a high-γ nucleus has a larger energy gap between spin-states than a low-γ nucleus. This results in greater polarization and thus a stronger NMR signal for the high-γ nucleus, which is considered to have a lower spin-temperature because transitions are less frequent, than the low-γ nucleus,

which has a hot spin-temperature because transitions are more frequent. In standard cross-polarization, the spin-temperature of these two sets of nuclei, or spin-baths, are brought into mutual equilibrium, much like mixing beakers of hot and cold water. Typically, CP is used to enhance the signal intensity from of a low-γ nucleus, such as ^{13}C, using a high-γ nucleus such as ^{1}H by cooling the spin temperature of ^{13}C. The equilibrium spin-temperature is mutual, however, and while ^{13}C will gain magnetization, ^{1}H will lose it. For the $^{13}C/^{1}H$ system, however, the ^{1}H is loss is hardly ever noted because the low natural abundance of ^{13}C ensures that the average ^{1}H nucleus never sees a ^{13}C nucleus, whereas all of the ^{13}C nuclei are close to ^{1}H.

While direct ^{19}F to ^{13}C cross polarization is not impossible as a means to observer organofluorine interactions with NOM, the larger internuclear distances between fluorine and NOM carbon compared to the short C-F bond within the organofluorine itself all but guarantees that carbon signals from the organofluorine will overpower those originating from the more distant NOM. There are two possible alternative pathways to transfer magnetic information from ^{19}F nuclei to the ^{13}C nuclei on the NOM that may resolve this problem, both of which make use of the ^{1}H nuclei as an intermediary using triple-resonance. The first approach is termed double cross-polarization, and involves two independent cross-polarization steps: first creating transverse magnetization in the ^{1}H spin-bath using ^{19}F and then using this selected ^{1}H spin-bath (only ^{1}H located near ^{19}F) to induce transverse magnetization in the ^{13}C of NOM. In this manner, ^{13}C nuclei that are located near ^{1}H that are in turn located near ^{19}F will be observed preferentially.

A slightly different approach to observe xenobiotic interactions using the ^{13}C of NOM is triple-CP *(21)*. Here, a third set of nuclei are included in the equilibrium, contributing its own spin temperature to the system in a single, grand three-way step rather than two subsequent two-ways steps as in double-CP. Rather than using ^{19}F, perhaps the most ideal xenobiotic nucleus for this experiment is ^{2}H, which has a γ smaller than ^{13}C and thus a higher relative spin temperature. Consider the ^{2}H nuclei of a perdeuterated compound interacting with the ^{1}H nuclei in soil organic matter. Because the difference in γ is large here (recall that for $^{1}H/^{19}F$ it was not), under cross-polarization conditions ^{2}H will gain a lot of signal, while the ^{1}H of NOM sites close to ^{2}H will lose a comparable amount. If one was to compare the ^{1}H spectrum of the NOM before and after the loss of magnetization to ^{2}H nuclei, those ^{1}H resonances arising from sites interacting with the perdeuterated xenobiotics will be reduced in intensity. The ^{1}H spectrum has low

resolution, however, and the results would be hard to interpret. If we include the ^{13}C nuclei of the NOM into the equilibrium of ^1H and ^2H, things may now become more informative when looking at what happens to the ^{13}C magnetization. Under standard CP conditions with ^1H, each ^{13}C resonance will be approximately 4x stronger than if it was observed on its own. This is because the γ of ^1H is 4x that of ^{13}C. Under triple-CP conditions with ^2H, however, the amount of ^1H magnetization at sites interacting with ^2H will be reduced by a significant amount. This means that ^{13}C nuclei in ^2H rich environments (i.e. near a xenobiotic) will get a much smaller signal boost from their neighbouring ^1H than ^{13}C in ^2H poor environments, which will still see the full 4x boost. Comparing ^{13}C spectra with and without ^2H cross-polarization will reveal those components of NOM interacting with perdeuterated xenobiotics. Relative to the dipolar-dephasing double resonance approach to identifying xenobiotic interactions at ^{13}C, triple-CP is less sensitive to fluctuating dipoles and thus much more likely to be useful for studying these soil interactions under natural conditions.

7.2.4 Sorption Behaviour

The justifications for studying the molecular-level processes of xenobiotic interactions in soils discussed in this dissertation focus on improving our understandings of broad and macroscopic phenomenon that have molecular-level origins, such as sequestration or bioaccessibility. The connections presented between the interactions studied here and macroscopic environmental processes have been deliberately vague, however, because those topics were not specifically studied in the research. The groundwork has been set, however, for molecular-level studies of these macroscopic phenomena. In chapter 6, the binding sites were shown for some organofluorine compounds in the SOM of a whole soil after their sorption. Some of those sites may be where sequestration occurs; others may not. The next step for this study is to extract those organofluorine compounds and then observe where the non-extractable compounds are situated. A similar approach could be applied for bioacceisblity. Studies such as these would present a clear and direct elucidation of sequestration sites, not just binding sites, and could be combined with temporal studies, or used to compare different extraction techniques for different types of compounds.

Sorption dynamics are also an important subject that can be advanced using molecular-level studies. In chapter 4 diffusion measurements were used to probe the equilibrium dynamics between bound and free states of xenobiotics in dissolved humic acid. With a comprehensive multiphase NMR probe, which has been developed specifically for studying soil environments and was employed in chapter 6, similar diffusion measurements can be made in whole soils. Preliminary work in this regard has been completed: the dynamics of hexafluorobenzene in a whole peat soil was studied and is shown in figure 7.3. Here, the apparent diffusivity of free hexafluorobenzene was measured as a function of the time allowed for diffusion. Measurements of diffusion generally assume linear diffusivity, wherein the instantaneous rate of diffusion at any moment is also the average rate of diffusion *(22)*. When exchange occurs with surfaces, however, for a certain period of a molecules life the average rate of diffusion is zero (i.e. when it is stuck to a soil particle), and a certain amount of its life is spent moving at the rate its hydrodynamic ratio allows *(22)*. By measuring how much the apparent diffusivity is affected by how long one observes the diffusion, features of the exchange between bound and free can be extracted *(23)*. In the example shown, the diffusivity in peat is compared to that in sand. In general, sand has no effect on the measured diffusivity of hexafluorobenzene, indicating that no interaction occurs here. For peat, however, the apparent diffusivity decreases with longer observation periods, and reflects how long a molecule is stuck to a soil particle before it is released. Measurements such as this may be useful for probing contaminant transport in different soil environments on a very small scale.

7.2.5 Computer Simulations

A recent issue of the journal Geoderma *(24)* was devoted to the use of computer simulations to study soil chemistry. Simulations based on quantum mechanical principles or molecular mechanics hold a great deal of promise in forming or testing hypotheses about the nature of interactions in complex molecular systems. Some attempts have been made to probe the nature of xenobiotic interactions with NOM computationally similar to the attempts made here to probe them experimentally *(25, 26)*. A limitation of computational methods, however, is the accuracy of the model because the exact structure of the binding sites in NOM or SOM for these xenobiotics have been largely unknown. Simple computer simulations were presented here in
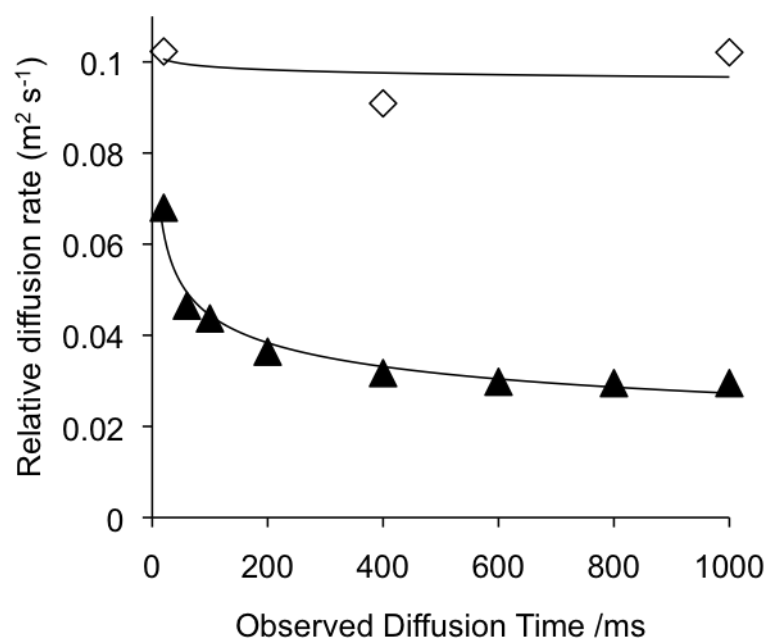
Figure 7.3   Non-linear diffusion of hexafluorobenzene in swollen peat soil.   Legend: diamonds are diffusion measurements in sand and triangles are diffusion measurements in peat soil.

chapter 5, probing the nature of the interactions between organofluorine compounds and the simplest possible fragments of humic acid: single aromatic rings. Computations made using the now out-dated concept of a humic acid monomer *(27)*, for example, have reduced relevance to real environmental systems despite the elegance of the computational work *(26)*. The work presented here has addressed this limited knowledge and it is perhaps now possible to perform complex computations using more accurate representations of binding sites and mechanisms in NOM.

7.3 References

(1) Salager, E.; Stein, R. S.; Steuernagel, S.; Lesage, A.; Elena, B.; Elmsely, L. Enhanced sensitivity in high-resolution 1H solid-state NMR spectroscopy with DUMBO dipolar decoupling under ultra-fast MAS. *Chem. Phys. Lett.* **2009**, *469* (4-6), 336-341.

(2) La Mesa, C.; Sesta, B. Micelles in perfluorinated surfactant solutions. *J. Phys. Chem.* **1987**, *91* (6), 1450-1454.

(3) Ellis, D. A.; Cahill, T. M.; Mabury, S. A.; Cousins, I. T.; Mackay, D. Partitioning of organofluorine compounds in the environment. The handbook of environmental chemistry, Vol . 3, Part N ed. A.H. Neilson, Springer-Verlag, Berlin, **2002**. pp 63-83.

(4) Slichter C.P. *Principles of Magnetic Resonance*, Third Enlarged and Updated Edition; Springer-Verlag: New York, 1989.

(5) Häggblom, M. M.; Bossert, I. D. Halogenated organic compounds-a global perspective. *Dehalogenation*, **2004** Part I, 3-29.

(6) Bryce, D. L.; Sward, G.D. Solid-state NMR spectroscopy of the quadrupolar halogens: Chlorine-35/37, bromine-79/81, and iodine-127. *Magn. Reson, Chem.* **2006**, *44* (4), 409-450

(7) Bryce, D. L.; Gee, M.; Wasylishen, R. E. High-field chlorine NMR spectroscopy of solid organic hydrochloride salts: A sensitive robe of hydrogen bonding. *J. Phys. Chem. A* **2001**, *105* (45), 10413-10421.

(8)   Harris, R. K. IN *Encyclopedia of Nuclear Magnetic Resonance*, D.M. Granty and R.K. Harris, (eds.), vol. 5, John Wiley & Sons, Chichester, UK, 1996.

(9)   Medek, A.; Harwood, J. S.; Frydman, L. Multiple-quantum MAS NMR: a new method for the study of quadrupolar nuclei in solids. *J. Am. Chem. Soc.* **1995**, 117, 12779-12787.

(10)   Karpukhina, N. K.; Werner-Zwanziger, U.; Zwanziger, J. W.; Kiprianov, A. A. Preferential binding of fluorine to aluminum in high peralkaline aluminosilicate glasses. *J. Phys. Chem. B* **2007**, *111* (35), 10413-10420.

(11)   Tang, J. A.; O'Dell, L. A.; Aguiar, P. M.; Lucier, B. E. G.; Sakellariou, D.; Schurko, R. W. Application of static microcoils and WURST pulses for solid-state ultra-wideline NMR spectroscopy of quadrupolar nuclei. *Chem. Phys. Lett.* **2008**, *466* (4-6), 227-234.

(*12)*   Bloom, M.; Hahn, E. L.; Herzog, B. Free magnetic induction in nuclear quadrupole resonance. *Phys. Rev.* **1955**, *97* (6), 1699-1709.

(13)   Ostafin, M.; Nogal, B. 14N-NQR based device for detection of explosives in landmines. *Measure. J. Inter. Measure. Conf.* **2007**, *40* (1), 43-45.

(14)   Hinton, J. F.; Metz, K. R.; Briggs, R.W. Thallium NMR spectroscopy. *Prog. Nucl. Magn. Reson.* **1988**, *20* (5), 423-523.

(15)   Otto, W. H.; Burton, S. D.; Carper, W. R.; Larive, C. K. Measurements of cadmium (II) and calcium (II) complexation by fulvic acids using 113Cd NMR. Environ. Sci. Technol. **2001**, *35* (7), 1463-1468.

(16)   Loganathan, P.; Hedley, M. J.; Grace, N. D.; Lee, J.; Grace, N. D.; Bolan, N. S.; Zanders, J. M. Fertiliser contaminants in New Zealand grazed-pasture with special reference to cadmium and fluorine: a review. *Austra. J. Soil Res.* **2003**, *41* (3), 501-532.

(17)   Lundstöm, U. S.; van Breemen, N.; Bain, D. The podzolization process. A review. *Geoderma*, **2000**, *94* (2-4), 91-107.

(18) Longstaffe J. G.; Werner-Zwanziger U.; Schneider J. F.; Nascimento M. L. F.; Zanotto E. D.; Zwanziger J. W. Intermediate-range order of alkali disilicate glasses and its relation to the devitrification mechanisms. *J. Phys. Chem. C* **2008**, *112* (15), 6151-6159.

(19) Gullion T.; Schaefer J. Rotational-echo double-resonance. NMR. *J. Mag. Reson.* **1989**, *81* (1), 196-200.

(20) van Wüllen, L. ^{1}H-^{13}C-^{27}Al triple resonance transfer of populations in double resonance experiments for the detection of ^{13}C-^{27}Al dipolar interactions. *Solid State NMR* **1998**, *13*, 123-127.

(21) Grey, C. P.; Veeman, W. S. The detection of weak heteronuclear coupling between spin 1 and spin ½ nuclei in MAS NMR; ^{14}N/^{13}C/^{1}H triple resonance experiments. *Chem. Phys. Lett.* **1992**, *192* (4), 379-385.

(22) Johnson Jr, C. S. Diffusion ordered nuclear magnetic resonance spectroscopy: principles and applications. *Prog. Nucl. Magn. Reson. Spectrosc.* **1999,** 34 (3-4), 203-.256

(23) Derrick, T. S.; Lucas, L. H.; Dimicoli, J-L.; Larive, C. K. ^{19}F diffusion NMR analysis of enzyme-inhibitor bindings. *Magn. Reson. Chem.* **2002,** 40 (13), S98-S105.

(24) Schaumann, G. E.; Thiele-Bruhn, S. Molecular modeling of soil organic matter: squaring the circle?. *Geoderma.* **2011**, *169*, 55-68.

(25) Sutton, R.; Sposito, G.; Diallo, M. S.; Schulten, H-R. Molecular simulation of a model of dissolved organic matter. Environ. *Toxicol. Chem.* **2005**, *24* (8), 1902-1911.

(26) Aquino, A. J. A.; Tunega, D.; Pasalic, H.; Schaumann, G. E.; Haberhauer, G.; Gerzabek, M. H.; Lischka, H. Study of solvent effect on the stability of water bridge-linked carboxyl groups in humic acid models. *Geoderma* **2011**, *169*, 20-26.

(27) Schulten, H-R. Three-dimensional models for humic acids and soil organic matter. *Naturwissenschaften* **1995**, *82* (11), 487-498.

APPENDIX A: Data for Chapter 2

Table A-1 Integrations of $^1H\{^{19}F\}$ RHSTD spectra of dissolved humic acid mixed with organofluorine compounds.

Organofluorine Compound	Loading/ mg	Total RHSTD Signal	Aromatic signal	Aliphatic signal	Aliphatic $(S-S_o)/S_o$	Aliphatic $(S-S_o)/S_o$
Reference	0	NA	0.19	0.32	NA	NA
Perfluorooctanoic acid	0.9	0.38				
	2.0	0.30				
	2.5	0.62				
	3.1	0.41				
	5.6	0.51				
	10.1	0.78				
	15.8	0.85				
	19.8	0.84				
	29.9	0.99				
	39.9	0.82				
	49.9	1.00				
	76.6	1.00				
Heptafluoronaphthol	1.0	0.11	0.03	0.03	0.55	-0.09
	5.2	0.31	0.10	0.09	0.79	-0.07
	14.8	0.63	0.24	0.18	0.99	-0.11
	20.0	0.79	0.29	0.21	0.91	-0.16
	30.2	0.73	0.26	0.23	0.86	-0.03
	39.8	0.86	0.31	0.26	0.91	-0.05
	49.8	1.00	0.35	0.32	0.86	0.00
	74.3	1.04	0.31	0.41	0.58	0.22

APPENDIX B: Data for Chapter 3

Table B-1 Epitope maps for selected organofluorine compounds interacting with dissolved humic acid in D_2O as determined using $^{19}F\{^1H\}$ STD NMR spectroscopy by comparing changes in relative signal intensity to that of a reference spectrum.

Organofluorine Compound	pH	HA site	Ortho (2' position, or 1' position*)			Meta (3' position, or 1' position*)			Para (4' position)		
			STD	Ref.	% diff	STD	Ref.	% diff	STD	Ref.	% diff
Pentafluoro-Benzoic acid	5.34	aromatic	1.43	1.96	72.9	1.99	2.00	99.3	1.00	1.00	100
		aliphatic	1.00	1.96	57.9	1.625	2.00	81.3	1.00	1.00	100
Tetrafluoro-1,3-benzene diol	5.63	aromatic	0.56*	1.11*	50.3	2.18	2.07	105.4	1.00	1.00	100
		aliphatic	0.61*	1.11*	54.9	1.79	2.07	86.7	1.00	1.00	100
Pentafluoro-phenol	3.87	aromatic	1.61	2.17	74.2	1.53	2.17	70.5	1.00	1.00	100
		aliphatic	2.38	2.17	109.5	1.98	2.17	90.9	1.00	1.00	100
	5.83	aromatic	1.32	1.96	67.1	1.83	2.00	91.4	1.00	1.00	100
		aliphatic	1.69	1.96	86.4	1.97	2.00	98.3	1.00	1.00	100
	6.26	aromatic	1.89	1.89	100	2.55	1.94	131.1	1.00	1.00	100
		aliphatic	1.56	1.89	82.8	1.84	1.94	94.8	1.00	1.00	100
	9.35	aromatic	1.61	1.96	82.3	2.18	2.00	108.9	1.00	1.00	100
		aliphatic	1.67	1.96	82.3	2.07	2.00	103.3	1.00	1.00	100
Pentafluoro-aniline	4.86	aromatic	*NA*	*NA*	*NA*	*NA*	*NA*	*NA*	*NA*	*NA*	*NA*
		aliphatic	1.92	2.38	80.7	2.79	2.62	106.5	1.00	1.00	100
	6.51	aromatic	1.16	1.96	59.2	1.65	1.88	87.8	1.00	1.00	100
		aliphatic	1.14	1.96	58.2	1.78	1.88	94.7	1.00	1.00	100
	7.08	aromatic	2.13	2.00	106.5	3.26	1.94	168	1.00	1.00	100
		aliphatic	1.79	2.00	89.5	2.39	1.94	123	1.00	1.00	100
	10.25	aromatic	1.06	2.04	52.0	1.89	2.04	92.6	1.00	1.00	100
		aliphatic	1.16	2.04	56.9	2.16	2.04	105.9	1.00	1.00	100

Table B-2 Ratio between the intensity of ortho and meta ^{19}F signals in $^{19}F\{^{1}H\}$ STD NMR spectra for pentafluoroaniline and pentafluorophenol as a function of pH.

Organofluorine Compound	pH	Ortho / Meta	
		Aromatic HA	Aliphatic HA
Pentafluoroaniline	4.86	0.74	0.69
	6.51	0.7	0.64
	7.08	0.65	NA
	10.25	0.56	0.54
Pentafluorophenol	3.87	1.05	1.2
	5.83	0.72	0.86
	6.26	0.74	0.85
	9.35	0.74	0.81

Heptafluoronaphthol

Tetrafluoro-1,3-diaminobenzene

Pentafluoroaniline

Pentafluorophenol

Tetrafluoro-1,3, benzene diol

Pentafluorobenzoic acid

Pentafluoronitrobenzene

Tetrafluoro-1,2-phthalic acid
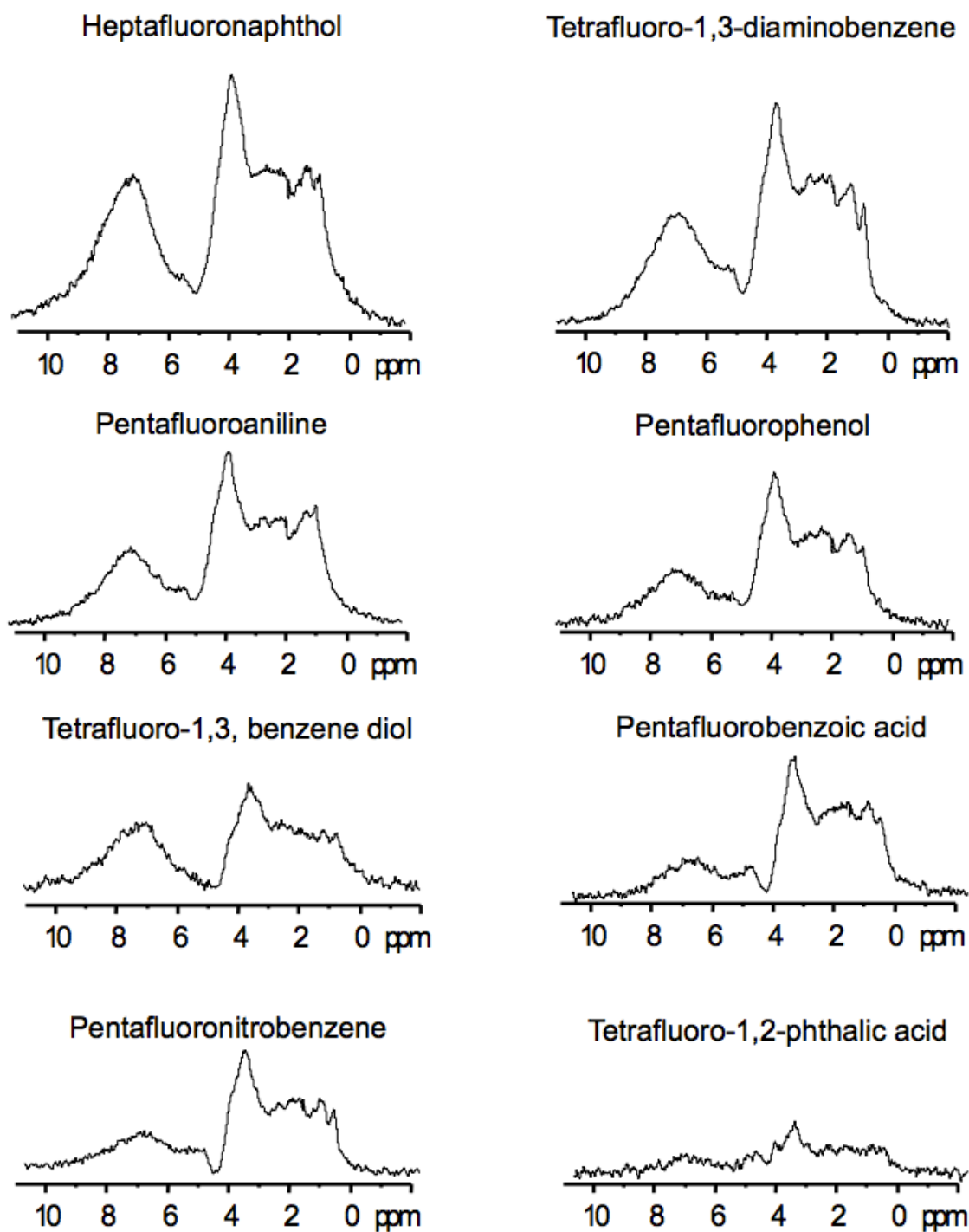
Figure B.1 $^1H\{^{19}F\}$ RHSTD spectra of dissolved humic acid mixed with selected organofluorine compounds in D_2O.

213

Table B-3   Integrations of the ^{1}H{^{19}F} RHSTD NMR spectra of dissolved humic acid mixed with organofluorine compounds in D_2O.

Organofluorine compound	Q_{zz} DÅ	Log (Sol)	Log (k_{OW})	Total signal	Aromatic signal	Non-aromatic signal	Aromatic / non-aromatic ratio	(aro/non-aro)$_{RHSTD}$ – (aro/non-aro)$_{ref}$
Tetrafluoro-diamino benzene	-11.2	-2.89	1.54	0.54	0.33	0.66	0.50	0.206
Pentafluoro-aniline	2.36	-4.03	3.14	0.40	0.28	0.72	0.37	0.092
Pentafluoro-nitrobenzene	18.8	-5.34	3.93	0.24	0.23	0.74	0.31	0.014
Pentafluoro-phenol	9.19	-4.09	3.00	0.34	0.26	0.72	0.36	0.067
Pentafluoro-benzoic acid	11.8	-4.58	4.33	0.27	0.24	0.76	0.31	0.0189
Tetrafluoro-1,3 benzene diol	3.31	-3.58	2.05	0.28	0.38	0.68	0.56	0.261
Tetrafluoro-1,4-benzene diol	3.35	-4.05	2.34	0.29	0.34	0.63	0.54	0.245
Tetrafluoro-1,2-pthalic acid	20.7	-4.90	3.50	0.11	0.26	0.64	0.44	0.151
Tetrafluoro-1,4-terepthalic acid	32.2	-5.52	3.89	~0	~0	~0	*NA*	*NA*
Heptafluoro-naphthol	*NA*	-6.08	4.67	1.00	0.36	0.64	0.56	0.267
Humic Acid Reference	*NA*	*NA*	*NA*	*NA*	0.23	0.78	0.29	*NA*

APPENDIX C: Data for Chapter 4

Table C-1 Apparent rates of self-diffusion for selected organofluorine compounds in D_2O as a function of humic acid concentration at pH* 7.2 and 298 K as measured using ^{19}F DOSY NMR spectroscopy.

Organofluorine apparent rates of self-diffusion measured using ^{19}F DOSY NMR / 10^{10} m^2 s^{-1}. Δ is calculated as the difference from the 0 mg mL^{-1} humic acid concentration.

[HA] / mg mL^{-1}	Tetrafluoro-terephthalic acid		Pentafluoro-benzoic acid		Pentafluoro-phenol		Pentafluoro-aniline		Perfluoro-octanoic acid		Potassium Perfluorooctane sulfonate	
	D	Δ	D	Δ	D	Δ	D	Δ	D	Δ	D	Δ
0	6.5696	0.0000	7.5110	0.0000	7.8596	0.0000	9.2470	0.0000	7.1072	0.0000	6.8360	0.0000
5	6.5279	0.0417	7.4268	0.0842	7.6577	0.2019	8.6896	0.5574	6.8077	0.2995	6.5208	0.3152
10	6.477	0.0926	7.3621	0.1489	7.5474	0.3121	8.2813	0.9657	6.7360	0.3713	6.0576	0.7784
20	6.4547	0.1149	7.1944	0.3165	7.2610	0.5985	7.3961	1.8509	6.1660	0.9413	5.3827	1.4533

Table C-2 Apparent rates of self-diffusion for selected organofluorine compounds and humic acid in D_2O as a function of temperature at humic acid concentrations of 20 mg mL^{-1} and solution pH* 7.2 as measured using ^{19}F and ^{1}H DOSY NMR spectroscopy.

Apparent diffusivity / 10^{-10} m^2 s^{-1}. $D_{X(free)}$ and $D_{X(obs)}$ are measured using ^{19}F DOSY NMR; $D_{(HA)}$ is measured using ^{1}H DOSY NMR. $D_{X(free)}$ is measured under identical conditions in the absence of HA.

T / K	Pentafluoroaniline			Pentafluorophenol			Perfluorooctanoic acid			Potassium Perfluorooctane sulfonate		
	$D_{X(free)}$	$D_{X(obs)}$	$D_{(HA)}$	$D_{X(free)}$	$D_{X(obs)}$	$D_{(HA)}$	$D_{X(free)}$	$D_{X(obs)}$	$D_{(HA)}$	$D_{X(free)}$	$D_{X(obs)}$	$D_{(HA)}$
279.1	4.74	3.40	0.676	4.62	3.72	0.516	3.20	2.96	0.579	3.77	2.81	
286.3	6.22	4.35	0.598	5.83	4.72	0.561	3.97	3.73	0.755		3.35	2.48
289.9		4.88	0.895							4.72		
293.4	7.45	5.78	1.04	7.53	6.03	1.06	5.56	4.90	0.946		4.65	2.84
297.0		6.93	1.16									
300.6	9.53	7.85	1.24	9.18	7.64	0.738	7.05	6.14	0.776	6.65	5.38	3.20
304.2		8.73	1.38									
307.8	1.20	9.84	1.71	11.4	9.68	2.67	9.24	7.71	1.01	8.49	6.71	4.91
311.4		10.7	1.79									
314.9	16.1	13.3	6.58	15.3	12.8	11.2	16.8	9.40	2.28		9.43	8.77

Table C-3 Equations for the apparent rates of diffusion of selected organofluorine compounds with and without humic acid, as well as humic acid, as a function of temperature as measured using DOSY NMR spectroscopy.

	Pentafluoroaniline	Pentafluoroaniline	Perfluorooctanoic acid	Potassium Perfluorooctane sulfonate
$D_{(Xfree)}$ (T)=	$4.58\times10^{-4}\, e^{0.0331\, T}$	$5.04\times10^{-4}\, e^{0.0327\, T}$	$8.73\times10^{-5}\, e^{0.0376\, T}$	$1.28\times10^{-3}\, e^{0.0285\, T}$
$D_{(Xobs)}$ (T)=	$9.44\times10^{-5}\, e^{0.0376\, T}$	$2.71\times10^{-4}\, e^{0.0341\, T}$	$3.36\times10^{-4}\, e^{0.0326\, T}$	$4.94\times10^{-4}\, e^{0.0310\, T}$
$D_{(HA)}$ (T)=	$3.68\times10^{-5}\, e^{0.0347\, T}$	$4.27\times10^{-7}\, e^{0.0496\, T}$	$1.28\times10^{-4}\, e^{0.0300\, T}$	$4.27\times10^{-7}\, e^{0.0496\, T}$

Table C-4 Calculated f_{HA} and $\ln(k_{HA-aq})$ for selected organofluorine compounds interacting with humic acid in D_2O as a function of temperature.

T /K	1000/T /K^{-1}	Pentafluoroaniline		Pentafluorophenol		Perfluorooctanoic acid		Potassium perfluorooctane sulfonate	
		f_{HA}	$\ln(k_{HA-aq})$	f_{HA}	$\ln(k_{HA-aq})$	f_{HA}	$\ln(k_{HA-aq})$	f_{HA}	$\ln(k_{HA-aq})$
279.1	3.58	0.316	-0.7724	0.205	-1.3539	0.057	-2.8139	0.4.9	-0.1225
286.3	3.49	0.289	-0.8987	0.197	-1.4037	0.096	-2.2401	0.446	-0.2151
293.4	3.40	0.262	-1.0371	0.189	-1.4557	0.134	-1.8692	0.422	-0.3133
300.6	3.33	0.223	-1.1911	0.181	-1.5099	0.169	-1.5925	0.397	-0.4180
307.8	3.25	0.203	-1.3653	0.173	-1.5667	0.203	-1.3703	0.370	-0.5306
314.9	3.18	0.173	-1.5672	0.164	-1.6262	0.234	-1.1837	0.342	-0.6527

APPENDIX D: Data for Chapter 5

D.1 Integrations of RHSTD spectra.

D.1.1 Humic acid and hexafluorobenzene.

Table D-1 Total and deconvoluted integrations of the RHSTD and reference spectra for solutions of humic acid mixed with hexafluorobenzene as a function of pH.

pH*	RHSTD				Reference			
	Total	10 – 5.7 ppm	5 – 2.9 ppm	1.7 - 0 ppm	Total	10 – 5.7 ppm	5 – 2.9 ppm	1.7 - 0 ppm
3.43	0.7492	0.1310	0.4374	0.1808	16.8589	4.2040	9.6520	3.0029
4.31	1.1933	0.3725	0.5635	0.2573	29.7518	9.0854	13.9577	6.7087
5.00	2.0339	0.6527	0.9686	0.4126	37.1809	11.8133	16.3584	9.0092
6.38	3.0935	0.9907	1.3510	0.7518	45.7907	14.993	18.5928	12.2049
7.06	3.3063	1.0989	1.4688	0.7386	46.7637	14.8871	19.3179	12.5587
10.64	5.0967	1.2823	2.0083	1.8061	54.3637	15.4795	22.5302	16.3540

Table D-2 Integrated and deconvoluted signal areas of the RHSTD spectra relative to the reference spectra for hexafluorobenzene as a function of pH. The normalized area is calculated as *(RHSTD) / (reference)* for the total signal and each region, respectively.

pH	Total	10 – 5.7 ppm	5 – 2.9 ppm	1.7 – 0 ppm
3.43	0.0444	0.0312	0.0453	0.0602
4.31	0.0401	0.0410	0.0404	0.0384
5.00	0.0547	0.0553	0.0592	0.0458
6.38	0.0676	0.0661	0.0727	0.0616
7.06	0.0707	0.0738	0.0760	0.0588
10.64	0.0938	0.0828	0.0891	0.1104

D.1.2 Humic acid and pentafluorophenol

Table D-3   Total and deconvoluted integrations of the RHSTD and reference spectra for solutions of humic acid mixed with pentafluorophenol as a function of solution pH.

pH*	RHSTD				Reference			
	Total	10 – 5.7 ppm	5 – 2.9 ppm	1.7 - 0 ppm	Total	10 – 5.7 ppm	5 – 2.9 ppm	1.7 - 0 ppm
4.94	7.4524	4.4619	1.3264	1.6641	32.9311	10.5115	15.4284	6.9912
5.90	8.6809	4.5037	2.0836	2.0936	38.1732	11.6575	17.1918	9.3239
6.84	5.0894	2.2569	1.688	1.1445	45.4964	14.0921	19.6646	11.7397
7.27	3.4288	1.391	1.2471	0.7907	45.0724	13.6989	18.6643	12.7092
8.26	3.1717	1.0643	1.2973	0.8101	46.4124	13.9189	19.7755	12.718
10.01	2.732	0.8226	1.2146	0.6948	51.7957	15.4557	21.7352	14.6048
11.92	3.0315	0.9068	1.2854	0.8393	55.0278	16.0958	23.2494	15.6826

Table D-4   Integrated and deconvoluted signal areas of the RHSTD spectra relative to the reference spectra for pentafluorophenol as a function of pH. The normalized area is calculated as (RHSTD) / (reference) for the total signal and each region, respectively.

pH	Total	10 – 5.7 ppm	5 – 2.9 ppm	1.7 – 0 ppm
4.94	0.2263	0.4245	0.0860	0.2380
5.90	0.2274	0.3863	0.1212	0.2245
6.84	0.1119	0.1602	0.0858	0.0975
7.27	0.0761	0.1015	0.0668	0.0622
8.26	0.0683	0.0765	0.0656	0.0637
10.01	0.0527	0.0532	0.0559	0.0476

D.1.2 Humic acid and pentafluoroaniline

Table D-5   Total and deconvoluted integrations of the RHSTD and reference spectra for solutions of humic acid mixed with pentafluoroaniline as a function of pH.

pH*	RHSTD				Reference			
	Total	10 – 5.7 ppm	5 – 2.9 ppm	1.7 - 0 ppm	Total	10 – 5.7 ppm	5 – 2.9 ppm	1.7 - 0 ppm
3.64	3.4914	1.8273	0.8764	0.7877	25.4102	8.3334	11.2671	5.8097
4.52	5.3681	2.7442	1.3108	1.3131	33.2753	11.2227	14.2378	7.8148
5.52	5.9571	2.9691	1.5753	1.4127	39.0938	13.1732	16.264	9.6566
5.87	6.6803	3.3069	1.7101	1.6633	43.3154	14.6881	17.9703	10.657
6.97	6.4671	2.9234	1.8996	1.6441	46.1056	15.1547	18.6569	12.294
8.14	6.8876	2.8767	2.2042	1.8067	50.3994	16.269	20.3086	13.8218
12.01	8.2806	2.5164	3.2812	2.483	66.0646	18.001	26.9285	21.1351

Table D-6   Integrated and deconvoluted signal areas of the RHSTD spectra relative to the reference spectra for pentafluoroaniline as a function of pH. The normalized area is calculated as (RHSTD) / (reference) for the total signal and each region, respectively.

pH	Total	10 – 5.7 ppm	5 – 2.9 ppm	1.7 – 0 ppm
3.64	0.1374	0.2193	0.0778	0.1356
4.52	0.1613	0.2445	0.0921	0.1680
5.52	0.1524	0.2254	0.0969	0.1463
5.87	0.1542	0.2251	0.0952	0.1561
6.97	0.1403	0.1929	0.1018	0.1337
8.14	0.1367	0.1768	0.1085	0.1307
12.01	0.1253	0.1398	0.1218	0.1175

D.2 Diffusivity data for humic acid

Table D-7   Apparent rates of diffusivity for different regions of the ^{1}H NMR spectrum of humic acid as measured using DOSY NMR as a function of solution pH.

	Apparent Diffusivity / m^{2}s^{-1}		
pH	1.31 ppm *(aliphatics)*	3.74 ppm *(carbohydrates)*	7.49 ppm *(aromatics)*
3.64	1.6255	2.5159	1.0093
5.52	1.2794	1.8026	1.0327
6.97	1.1143	1.6051	1.0471
8.14	1.0864	1.5181	1.0328

D.3 Example GAMESS Input.

The following is the input to calculate the energy of a stacked dimmer of 1,3,5-trihydroxybenzene and pentafluoroaniline spaced 3.5 Å apart using the MP2(full) 6-31+G** level of theory.   This level of theory is adequate to produce comparable relative energies, however exact energies require a more expanded basis set.   For the purposes here, relative energies are enough.   Second order Møller-Plesset perturbation theory (MP2) and additional dispersion (+) and polarization functions on the s and p orbitals (**) are required for intermolecular interaction calculations between benzene rings to account for the dispersive qualities of delocalized electrons.

Intermolecular interaction energies for a dimmer, A-B, are determined based on three independent calculations using the formula

$$E_{A-B} = E_A + E_B. \qquad\qquad (D-1)$$

In the calculation of the energies of the monomers, however, care must be taken to account for slight changes in the energy on one monomer in the presence of orbitals for the second monomer that occur when calculating the energy of the dimer.   This is the basis-set super-position error (BSSE), and is accounted for by using ghost orbitals for the non-present monomer in energy calculations for the present monomer.   This achieved in the GAMESS code by using the same Cartesian matrix as for the dimer in the monomer calculations, but changing the nuclear charge

of the absent monomer to its negative value (i.e. carbon = 6 for the monomer being calculated and -6 for the monomer that is absent). This tells the code to put in empty orbitals for the missing monomer. When calculating the energy of the dimer, all of the nuclear charges are positive.
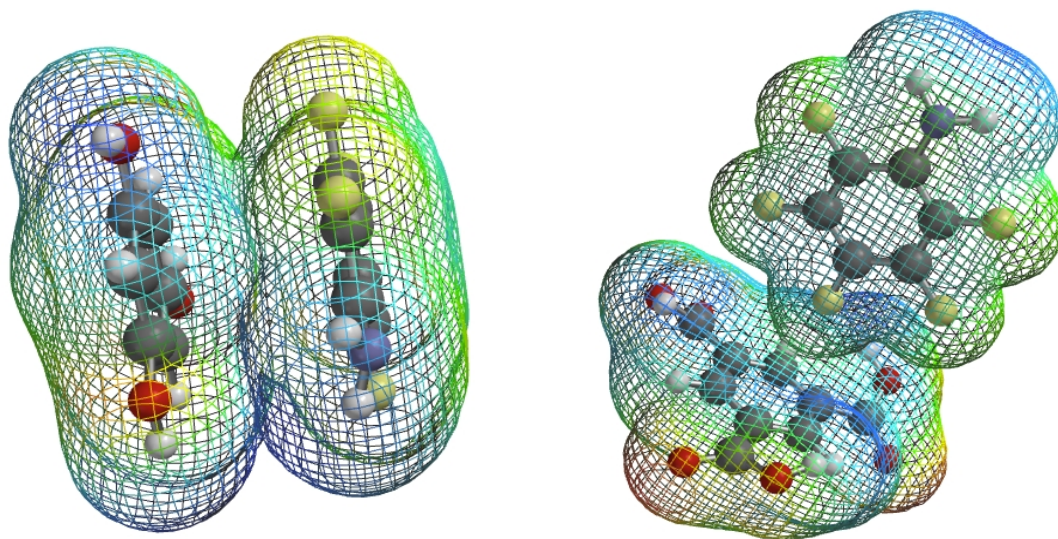
Example 1: no dummy orbitals.

```
$CONTRL SCFTYP=RHF MPLEVL=2 RUNTYP=ENERGY
    ICHARG=0 MULT=1 COORD=UNIQUE QMTTOL=1.0d-6 $END
 $SYSTEM MWORDS=30 $END
 $BASIS GBASIS=N31 NGAUSS=6 NDFUNC=1 NPFUNC=1 DIFFSP=.TRUE. $END
 $MP2 NACORE=0 $END
 $DATA
MP2(full) 6-31+G** trihydroxybenzene-pentafluoroaniline dimer 3.5 up 0 over no dummy
orbitals
C1 1
C 6 0.3411816321 -1.3409018768 0.0007436413
C 6 0.9906642733 0.9659228991 0.0007436413
C 6 -1.3318459054 0.3749789777 0.0007436413
C 6 1.3510045984 -0.3832512301 -0.0044032215
C 6 -0.3435969979 1.3616299179 -0.0044032215
C 6 -1.0074076005 -0.9783786878 -0.0044032215
H 1 -1.7658302437 -1.7500516866 -0.0012485289
H 1 2.3985043404 -0.6542280065 -0.0012485289
H 1 -0.6326740967 2.4042796931 -0.0012485289
O 8 -2.6341100362 0.8196939276 0.0016520963
O 8 0.6071792535 -2.6910531715 0.0016520963
O 8 2.0269307827 1.8713592439 0.0016520963
H 1 -3.2280960119 0.0574169468 0.0032560128
H 1 1.5643234714 -2.8243216256 0.0032560128
H 1 1.6637725405 2.7669046788 0.0032560128
C 6 0.0115812410 -1.4024048806 3.544889476
C 6 1.1939140430 -0.6583237331 3.561287180
C 6 1.1982124809 0.7288919903 3.484785865
C 6 -0.0070307950 1.4248675848 3.498758646
C 6 -1.2029542724 0.7130527054 3.483759671
C 6 -1.1804356574 -0.6739470961 3.560238263
F 9 -2.3509397046 -1.3589403258 3.558792896
F 9 -2.3783762270 1.3702004462 3.469553250
F 9 -0.0158185766 2.7702938856 3.448233993
F 9 2.3649100787 1.4014119819 3.471777953
F 9 2.3733199682 -1.3278665667 3.560871580
N 7 0.0204561924 -2.7847292789 3.674604514
H 1 -0.8172493667 -3.2389313141 3.340697490
H 1 0.8643821041 -3.2280865790 3.341749225
```

$END

example 2: dummy orbitals on 1,3,5-trihydroxy benzene

$CONTRL SCFTYP=RHF MPLEVL=2 RUNTYP=ENERGY
     ICHARG=0 MULT=1 COORD=UNIQUE QMTTOL=1.0d-6 $END
 $SYSTEM MWORDS=30 $END
 $BASIS GBASIS=N31 NGAUSS=6 NDFUNC=1 NPFUNC=1 DIFFSP=.TRUE. $END
 $MP2 NACORE=0 $END
 $DATA
MP2(full) 6-31+G** THB-PFA dimer 3.5 up 0 over dummy orbitals on THB
C1 1
C -6 0.3411816321 -1.3409018768 0.0007436413
C -6 0.9906642733 0.9659228991 0.0007436413
C -6 -1.3318459054 0.3749789777 0.0007436413
C -6 1.3510045984 -0.3832512301 -0.0044032215
C -6 -0.3435969979 1.3616299179 -0.0044032215
C -6 -1.0074076005 -0.9783786878 -0.0044032215
H -1 -1.7658302437 -1.7500516866 -0.0012485289
H -1 2.3985043404 -0.6542280065 -0.0012485289
H -1 -0.6326740967 2.4042796931 -0.0012485289
O -8 -2.6341100362 0.8196939276 0.0016520963
O -8 0.6071792535 -2.6910531715 0.0016520963
O -8 2.0269307827 1.8713592439 0.0016520963
H -1 -3.2280960119 0.0574169468 0.0032560128
H -1 1.5643234714 -2.8243216256 0.0032560128
H -1 1.6637725405 2.7669046788 0.0032560128
C 6 0.0115812410 -1.4024048806 3.544889476
C 6 1.1939140430 -0.6583237331 3.561287180
C 6 1.1982124809 0.7288919903 3.484785865
C 6 -0.0070307950 1.4248675848 3.498758646
C 6 -1.2029542724 0.7130527054 3.483759671
C 6 -1.1804356574 -0.6739470961 3.560238263
F 9 -2.3509397046 -1.3589403258 3.558792896
F 9 -2.3783762270 1.3702004462 3.469553250
F 9 -0.0158185766 2.7702938856 3.448233993
F 9 2.3649100787 1.4014119819 3.471777953
F 9 2.3733199682 -1.3278665667 3.560871580
N 7 0.0204561924 -2.7847292789 3.674604514
H 1 -0.8172493667 -3.2389313141 3.340697490
H 1 0.8643821041 -3.2280865790 3.341749225
 $END

Above: Stacked and T-shaped interactions between pentafluoroaniline and a model humic acid aromatic structure, 1,3,5-trihydroxy benzene.

APPENDIX E: Data for Chapter 6

Integrations of $^{19}F{\rightarrow}^{1}H$ Cross-Polarization spectra of organofluorine compounds mixed with peat, albumin, or lignin as a function of cross-polarization contact-time as discussed in chapter 6. Listed are the raw integrations against a common arbitrary scale, and an internal scale normalized against the contact-time with the strongest signal for each data set.

E.1 Peat mixed with perfluorooctanoic acid, heptafluoronaphthol, pentafluorophenol, or pentafluorobenzoic acid.

Table E-1 $^{19}F{\rightarrow}^{1}H$ cross-polarization signal strength as a function of contact-time for perfluorooctanoic acid mixed with peat.

Contact-Time / ms	I (raw)	I (normalized)
0.000	0.0000	0.0000
0.050	0.3464	0.2059
0.100	0.6345	0.3772
0.150	0.9010	0.5356
0.250	1.1823	0.7028
0.400	1.3926	0.8278
0.500	1.5357	0.9129
0.600	1.5821	0.9405
0.750	1.6503	0.9810
0.900	**1.6821**	1.0000
1.000	1.6514	0.9817
1.250	1.4503	0.8621
1.500	1.3072	0.7771
2.000	0.9681	0.5755

Table E-2 $^{19}F \rightarrow {}^{1}H$ cross-polarization signal strength as a function of contact-time for heptafluoronaphthol mixed with peat.

Contact-Time / ms	I (raw)	I (normalized)
0.000	0.0000	0.0000
0.050	0.6021	0.2541
0.075	0.9533	0.4024
0.100	1.6236	0.6853
0.150	2.1795	0.9200
0.200	2.2801	0.9624
0.250	**2.3690**	1.0000
0.300	2.3185	0.9786
0.350	2.2044	0.9305
0.400	2.0923	0.8831
0.500	1.9046	0.8039
0.750	1.6077	0.6786
1.000	1.2017	0.5072
1.500	0.9499	0.4009

Table E-3 $^{19}F \rightarrow {}^{1}H$ cross-polarization signal strength as a function of contact-time for pentafluorobenzoic acid mixed with peat.

Contact-Time / ms	I (raw)	I (normalized)
0.000	0.0000	0.0000
0.250	0.0787	0.7893
0.500	0.0997	1.0000
0.750	0.0942	0.9448
1.000	0.0725	0.7272

225

Table E-4 $^{19}F \rightarrow {}^1H$ cross-polarization signal strength as a function of contact-time for pentafluorophenol mixed with peat.

Contact-Time / ms	I (raw)	I (normalized)
0.000	0.0000	0.0000
0.050	0.2389	0.2770
0.150	0.7255	0.8412
0.250	0.8624	1.0000
0.500	0.6920	0.8024
0.750	0.4868	0.5644
1.000	0.3865	0.4481

E.2 Albumin mixed with perfluorooctanoic acid or heptafluoronaphthol.

Table E-5 $^{19}F \rightarrow {}^1H$ cross-polarization signal strength as a function of contact-time for perfluorooctanoic acid mixed with albumin.

Contact-Time / ms	I (raw)	I (normalized)
0.000	0.0000	0.0000
0.050	5.7467	0.2470
0.100	11.1871	0.4809
0.150	13.9562	0.6000
0.300	18.6593	0.8021
0.350	19.1863	0.8248
0.400	19.1497	0.8232
0.500	20.9255	0.8996
0.600	21.4909	0.9239
0.700	22.2132	0.9549
0.800	22.7079	0.9762
0.900	23.2616	1.0000
1.000	23.0353	0.9903
1.250	21.0663	0.9056
1.500	19.3748	0.8329
1.750	16.9816	0.7300
2.000	15.8520	0.6815
2.500	12.4904	0.5370

Table E-6 $^{19}F \rightarrow {}^{1}H$ cross-polarization signal strength as a function of contact-time for heptafluoronaphthol mixed with albumin.

Contact-Time / ms	I (raw)	I (normalized)
0.000	0.0000	0.0000
0.050	1.6438	0.2128
0.100	5.0012	0.6473
0.200	7.1329	0.9232
0.250	7.4925	0.9697
0.300	7.5672	0.9794
0.400	7.7264	1.0000
0.500	7.6720	0.9930
0.600	7.5559	0.9779
0.700	7.3929	0.9568
0.800	6.7717	0.8764
0.900	6.4069	0.8292
1.000	6.0641	0.7849
1.250	5.0322	0.6513
1.500	4.1450	0.5365
1.750	3.5148	0.4549
2.000	2.8169	0.3646
2.500	1.9067	0.2468

E.3   Lignin mixed with perfluorooctanoic acid or heptafluoronaphthol.

Table E--7 $^{19}F \rightarrow {}^{1}H$ cross-polarization signal strength as a function of contact-time for perfluorooctanoic acid mixed with lignin.

Contact-Time / ms	I (raw)	I (normalized)
0.000	0.0000	0.0000
0.250	0.9789	0.7758
0.400	1.2618	1.0000
0.900	0.7424	0.5884
1.500	0.5916	0.4689

Table E-8 $^{19}F \rightarrow {}^{1}H$ cross-polarization signal strength as a function of contact-time for heptafluoronaphthol mixed with lignin.

Contact-Time / ms	I (raw)	I (normalized)
0.000	0.000	0.0000
0.050	1.4728	0.3114
0.100	3.1440	0.6648
0.200	4.7294	1.0000
0.300	4.5740	0.9671
0.400	4.2160	0.8914
0.500	3.8478	0.8136
0.600	3.4927	0.7385
0.700	3.3148	0.7009
0.800	2.9151	0.6164
0.900	2.6475	0.5598
1.000	2.4740	0.5231
1.250	2.1437	0.4533
1.500	1.9037	0.4025
1.750	1.8185	0.3845
2.000	1.4152	0.2992
2.500	0.7563	0.1599

APPENDIX F: STD PULSE SEQUENCES

F.1 ^{19}F{^{1}H} Heteronuclear Saturation Transfer Difference (HSTD)

A saturation pulse train of selective Gaussian-shaped pulses saturates ^{1}H nuclei followed by a $\pi/2$ pulse on the ^{19}F channel where detection occurs.
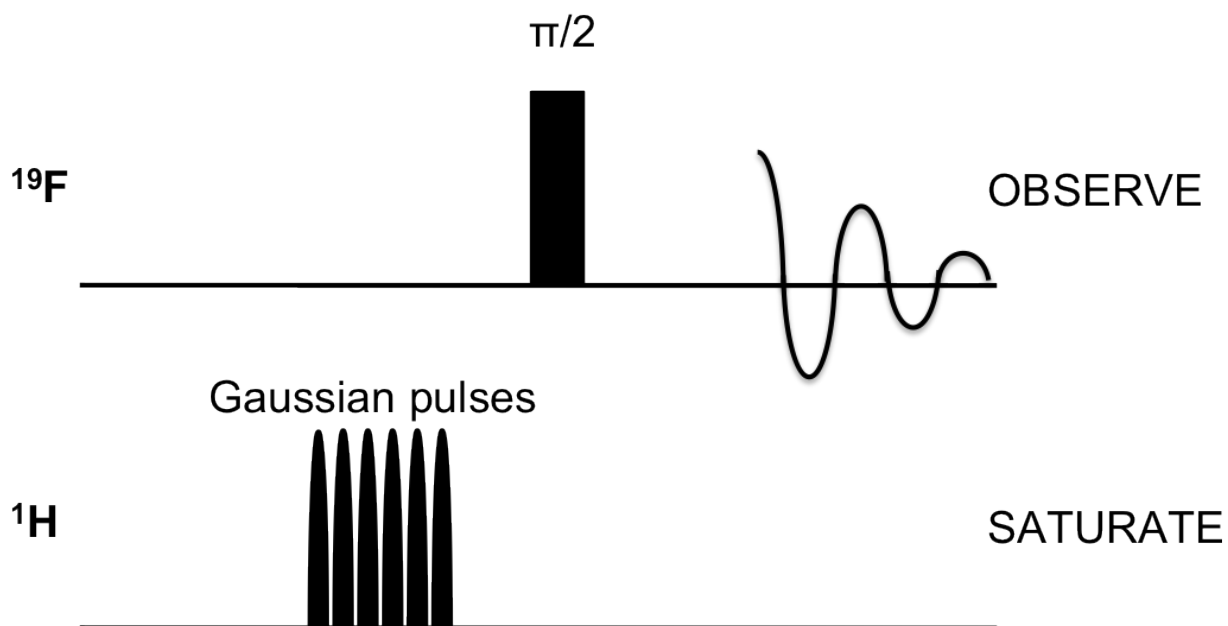

Figure F.1   The ^{19}F{^{1}H} 'forward' Heteronuclear Saturation Transfer Difference NMR pulse sequence.

F.2   ¹H{¹⁹F} Reverse Heteronuclear Saturation Difference (RHSTD)

A saturation pulse train of selective Gaussian-shaped pulses saturates ^{19}F nuclei followed by a $\pi/2$ pulse on the ^{1}H channel where detection occurs. Presaturation is used on water signals to remove them from the spectrum.
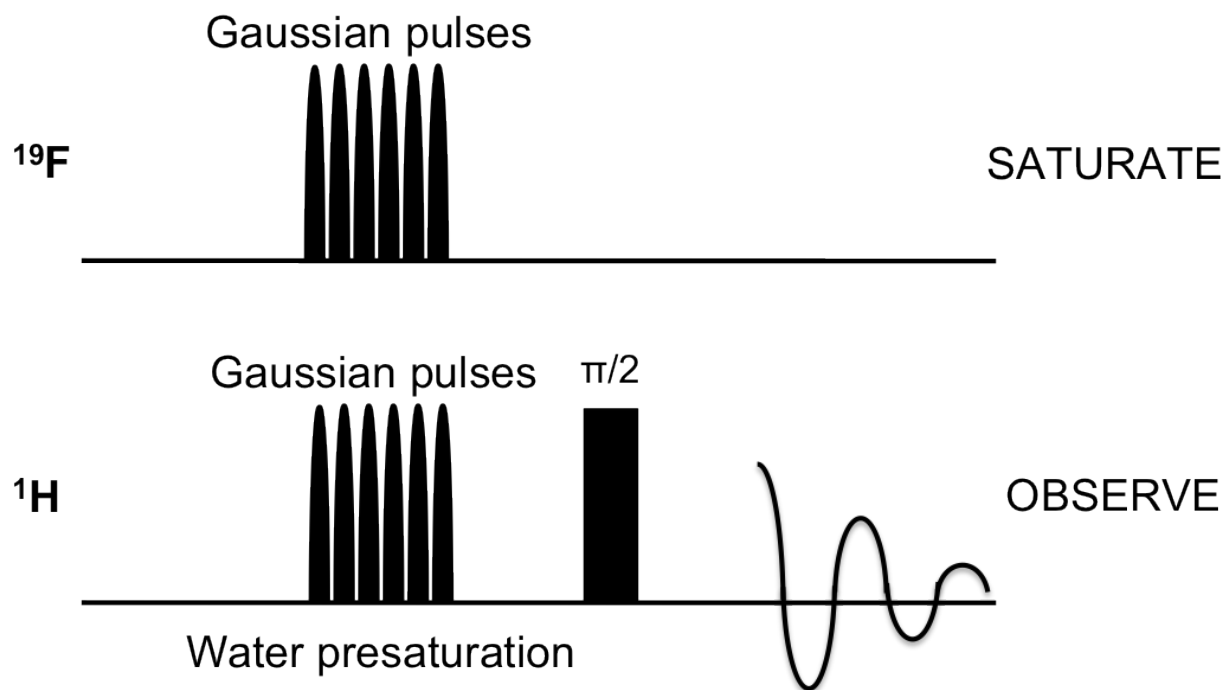

Figure F.2   The ^{1}H{^{19}F} Reverse Heteronuclear Saturation Transfer Difference NMR pulse sequence.

Appendix G: Copyright Permissions

https://s100.copyright.com/AppDispatchServlet

Copyright Clearance Center

RightsLink®

Home | Create Account | Help

ACS Publications
High quality. High impact.

Title: Identifying Components in Dissolved Humic Acid That Bind Organofluorine Contaminants using 1H{19F} Reverse Heteronuclear Saturation Transfer Difference NMR Spectroscopy

Author: James G. Longstaffe, Myrna J. Simpson, Werner Maas, and André J. Simpson

Publication: Environmental Science & Technology

Publisher: American Chemical Society

Date: Jul 1, 2010

Copyright © 2010, American Chemical Society

User ID

Password

☐ Enable Auto Login

LOGIN

Forgot Password/User ID?

If you're a copyright.com user, you can login to RightsLink using your copyright.com credentials. Already **a RightsLink user** or want to learn more?

PERMISSION/LICENSE IS GRANTED FOR YOUR ORDER AT NO CHARGE

This type of permission/license, instead of the standard Terms & Conditions, is sent to you because no fee is being charged for your order. Please note the following:

- Permission is granted for your request in both print and electronic formats, and translations.
- If figures and/or tables were requested, they may be adapted or used in part.
- Please print this page for your records and send a copy of it to your publisher/graduate school.
- Appropriate credit for the requested material should be given as follows: "Reprinted (adapted) with permission from (COMPLETE REFERENCE CITATION). Copyright (YEAR) American Chemical Society." Insert appropriate information in place of the capitalized words.
- One-time permission is granted only for the use specified in your request. No additional uses are granted (such as derivative works or other editions). For any other uses, please submit a new request.

BACK | CLOSE WINDOW

12-07-30 11:18 PM

JOHN WILEY AND SONS LICENSE
TERMS AND CONDITIONS

Sep 29, 2012

This is a License Agreement between James G Longstaffe ("You") and John Wiley and Sons ("John Wiley and Sons") provided by Copyright Clearance Center ("CCC"). The license consists of your order details, the terms and conditions provided by John Wiley and Sons, and the payment terms and conditions.

All payments must be made in full to CCC. For payment instructions, please see information listed at the bottom of this form.

License Number	2998010260719
License date	Sep 29, 2012
Licensed content publisher	John Wiley and Sons
Licensed content publication	Environmental Toxicology and Chemistry
Book title	
Licensed content author	James G. Longstaffe,André J. Simpson
Licensed content date	May 23, 2011
Start page	1745
End page	1753
Type of use	Dissertation/Thesis
Requestor type	Author of this Wiley article
Format	Print and electronic
Portion	Full article
Will you be translating?	No
Order reference number	
Total	0.00 USD
Terms and Conditions	

TERMS AND CONDITIONS

This copyrighted material is owned by or exclusively licensed to John Wiley & Sons, Inc. or one of its group companies (each a "Wiley Company") or a society for whom a Wiley Company has exclusive publishing rights in relation to a particular journal (collectively WILEY"). By clicking "accept" in connection with completing this licensing transaction, you agree that the following terms and conditions apply to this transaction (along with the billing and payment terms and conditions established by the Copyright Clearance Center Inc., ("CCC's Billing and Payment terms and conditions"), at the time that you opened your Rightslink account (these are available at any time at http://myaccount.copyright.com)

Copyright Clearance Center	RightsLink®		Account Info	Help

Title:	The pH-dependence of organofluorine binding domain preference in dissolved humic acid
Author:	James G. Longstaffe,Denis Courtier-Murias,André J. Simpson
Publication:	Chemosphere
Publisher:	Elsevier
Date:	Aug 2, 2012
	Copyright © 2012, Elsevier

Logged in as:
James Longstaffe
Account #:
3000557270

LOGOUT

Order Completed

Thank you very much for your order.

This is a License Agreement between James G Longstaffe ("You") and Elsevier ("Elsevier"). The license consists of your order details, the terms and conditions provided by Elsevier, and the payment terms and conditions.

License number	Reference confirmation email for license number
License date	Aug 04, 2012
Licensed content publisher	Elsevier
Licensed content publication	Chemosphere
Licensed content title	The pH-dependence of organofluorine binding domain preference in dissolved humic acid
Licensed content author	James G. Longstaffe,Denis Courtier-Murias,André J. Simpson
Licensed content date	2 August 2012
Number of pages	1
Type of Use	reuse in a thesis/dissertation
Portion	full article
Format	both print and electronic
Are you the author of this Elsevier article?	Yes
Will you be translating?	No
Order reference number	
Title of your thesis/dissertation	A Molecular-level Investigation of the interactions between organofluorine compounds and soil organic matter using nuclear magnetic resonance spectroscopy
Expected completion date	Sep 2012
Estimated size (number of pages)	315
Elsevier VAT number	GB 494 6272 12
Billing Type	Invoice
Billing address	23939 Amiens Rd

Copyright Clearance Center **RightsLink®**

Home   Account Info   Help

ACS Publications
High quality. High impact.

Title:	In-Situ Molecular-Level Elucidation of Organofluorine Binding Sites in a Whole Peat Soil
Author:	James G. Longstaffe, Denis Courtier-Murias, Ronald Soong, Myrna J. Simpson, Werner E. Maas, Michael Fey, Howard Hutchins, Sridevi Krishnamurthy, Jochem Struppe, Mehran Alaee, Rajeev Kumar, Martine Monette, Henry J. Stronks, and André J. Simpson
Publication:	Environmental Science & Technology
Publisher:	American Chemical Society
Date:	Sep 1, 2012
	Copyright © 2012, American Chemical Society

Logged in as:
James Longstaffe
Account #:
3000557270

LOGOUT

BACK   CLOSE WINDOW